Novel Reporter Systems to Study Semliki Forest virus Pathogenesis

Rennos Fragkoudis

A thesis submitted to The University of Edinburgh for the degree of Doctor of Philoshophy

August 2007

Table of Contents

Declaration

I declare that all the work included in this thesis is my own except where otherwise stated. No part of this work has been, or will be submitted for any other degree or professional qualification.

Kennos Fragkoudis

2007

Centre for Infectious Diseases
University of Edinburgh
Summerhall
Edinburgh
EH9 1QH

Acknowledgements

I would like to thank my supervisor **John Fazakerley** for his support and his patience with me over the course of this PhD. John was an unlimited source of knowledge and his passion for science was a strong motive throughout this project. I would also like to thank my second supervisor **Tony Nash**. Many thanks belong to **Andres Merits**, his expertise and his resourceful advices had a great contribution on many aspects of my studies.

I am very grateful to all the members (past and present) of the Fazakerley Group and especially **Cat Dixon**, **Gerald Barry**, **Lucy Breakwell**, **Clive McKimmie** and **Ricky Siu**. Their friendship and help was essential for the success of this project. Also, thanks to **Bill Smith** and **Christine Forrest** for their help and patience with my constant demands for "few extra mice". Big thanks to **Linda Sharp** for teaching me how to use the confocal microscope.

A special thanks to **Nele Tamberg**, **Kaja Kiiver**, **Ingrid Tangen** and everybody in Estonian Biocentre who made me feel welcome and made my stay in Tartu both pleasant and productive. Suur Aitäh!

Thanks to my friends **George**, **Maria**, **Alex**, **Makrina**, **Sofia** and **Vivian** who helped me maintain my sanity and tolerated my constant complaining, especially while writing-up.

Finally, I would like to seize the opportunity and express my gratitude to my parents **Menelao** and **Irini** for their love and support without which none of this would be possible.

List of Figures

Chapter 1

Chapter 3

Chapter 4

Chapter 5

List of Tables

Chapter 2

Chapter 3

Chapter 4

Abbreviations

BBB	Blood Brain Barrier
BHK-21	Baby Hamster Kidney
BSA	Bovine Serum Albumin
cc	Corpus Callosum
cDNA	complementary DNA
cg	Cingulum
CHICK	Chickungunya
CMV	Cytomegalovirus
CNPase	2',3'-cyclic nucleotide 3'-phosphodiesterase
CNS	Central Nervous System
CPE	Cytopathic Effect
CPVs	Cytoplasmic Vacuoles
CTL	Cytotoxic T-Lymphocyte
DAB	Diaminobenzidine
DAPI	4',6-diamidino-2-phenylindole dihydrochloride
D-MEM	Dulbecco's Modified Eagle's Medium
DMSO	Dimethylsulfoxide
DNA	Deoxyribonucleic Acid
dNPT	Deoxy-Nucleoside Triphosphate
dsDNA	Double Stranded DNA
DSP	Duplicated Subgenomic Promoter
DSRed	*Discosoma spp.* Red Fluorescent protein
DTT	Dithiothreitol
E.coli	*Escherichia coli*
EAV	Equine Arteritis Virus
EDTA	Ethylenediaminetetraacetic acid
EEEV	Eastern Equine Encephalitis Virus
eGFP	Enhanced Green Fluorescent Protein
EMCV	Encephalomyocarditis Virus
ER	Endoplasmic Reticulum
euCre	eukaryotic Cre Recombinase
FCS	Foetal Calf Serum
fctx	Frontal Cortex
FMDV	Foot-and-Mouth Disease Virus
GFAP	Glial Fibrillary Acidic Protein
GMEM	Glasgow's Minimal Essential Media
GrDG	Granular Dentate gyrus
H_2O	Water
HCV	Hepatitis C Virus
HEPES	4-(2-hydroxyethyl)-1-piperazineethanesulfonic acid
HI	Hyperimmune
HIV	Human Immunodeficiency Virus
HSV	Herpes Simplex Virus
ic	Inferior Colliculus

i.c.	Intracerebral
i.p.	Intraperitoneal
icDNA	Infectious Complementary Deoxyribonucleic Acid
IFN	Interferon
IMDM	Iscove's Modified Dulbecco's Medium
IPTG	Isopropyl-beta-D-thiogalactopyranoside
IRES	Internal Ribosome Entry Site
KO	Knockout
LB	Luria-Bertani
LCMV	Lymphocytic Choriomeningitis Virus
M.O.I	Multiplicity of Infection
MEFs	Mouse Embryo Fibroblasts
MHC	Major Histocompatibility Complex
MHV	Mouse Hepatitis Virus
MV	Measles Virus
NBCS	Newborn Calf Serum
nsP	Non Structural Protein
mob	Main Olfactory Bulb
OD	Optical Density
ORF	Open Reading Frame
PBS	Phosphate Buffered Saline
PBSA	Phosphate Buffered Saline Albumin
PBST	Phosphate Buffered Saline containing Tween 20
PCR	Polymerase Chain Reaction
PFU	Plaque Forming Unit
PI	Propidium Iodide
PID	Post-Inoculation Day
rp	Red Pulp
RNA	Ribonucleic Acid
RRV	Ross River Virus
RT-PCR	Reverse-Transcription Polymerase Chain Reaction
SA	Streptavidin
SFV	Semliki Forest Virus
sPBS	Sterile Phosphate Buffered Saline
sPBSA	Sterile PBS Containing Bovine Serum Albumin
STAT	Signal Transducers and Activators of Transduction
SV	Sindbis Virus
TBE	Tris borate EDTA
TLR	Toll-Like Receptor
TMEV	Theiler's Murine Encephalitis Virus
TNF	Tumour Necrosis Factor
UV	Ultra-Violet
VEEV	Venezuelan Equine Encephalitis Virus
VLPs	Virus-Like Particles
VZV	Varicella Zoster Virus
WEEV	Western Equine Encephalitis Virus
wp	White Pulp
WT	Wild-type

Abstract

Semliki Forest virus (SFV) has been much used to study the cell biology and molecular pathogenesis of RNA viruses, particularly virus encephalitis. The genome encodes nine functional proteins in two open-reading frames (ORFs). The 5' ORF carries information for synthesis of four non-structural replicase proteins (nsP1 – nsP4). The 3' third of the genome encodes the structural proteins. The aim of this study was to develop novel reporter systems to study the pathogenesis of SFV *in vivo*.

Two different types of recombinant viruses each carrying one of two foreign genes, enhanced green fluorescent protein (eGFP) or Cre recombinase, were constructed based on the SFV4 backbone. In the first type of construct the transgene was inserted in the non-structural ORF, between the coding sequences for nsP3 and nsP4, flanked by processing sites recognised by the nsP2 proteinase. In the second type of constructs the 2A sequence from foot-and-mouth disease virus was added to the C-terminus of the foreign gene and this was placed between the capsid and the p62 protein of SFV4 (structural ORF). The *in vitro* and *in vivo* phenotypes of the resulting viruses were assessed and compared to SFV4.

All recombinant viruses constructed were viable and able to replicate *in vitro*. eGFP expressing viruses reached titres similar to those of wild-type virus whereas Cre expressing viruses were slightly attenuated. For viruses with the marker gene inserted in the non-structural ORF, western blotting showed that the processing pattern of the non-structural polyprotein was similar to that of SFV4 and verified the expression of both foreign genes. *In vivo*, following intracerebral inoculation, all viruses caused encephalitis. Viruses expressing the foreign gene as a cleavable component of the structural ORF induced disease slower than SFV4 or viruses carrying the transgene in the replicase ORF. eGFP fluorescence was stronger and occurred later in infection when expressed in the structural ORF than in the replicase ORF.

eGFP expression from the replicase ORF marked only recently infected cells; a property useful in pathogenesis studies. eGFP expressing viruses demonstrated the same cell tropism as SFV4 with infection principally of neurons and

oligodendrocytes. None of the mice infected intraperitoneally with SFV4 or the recombinant viruses succumbed to infection demonstrating poor neuroinvasiveness. The powerful suppression of alphavirus replication by the interferon system was demonstrated in IFN α/β receptor knockout mice. The true tropism and the potential of SFV4 was revealed in the absence of a functional IFN system.

These studies demonstrated that foreign genes can be inserted into the non-structural or the structural ORF of SFV4 without destroying virus infectivity or major changes in phenotype. These viruses are likely to be highly valuable for *in vivo* pathogenesis studies.

Chapter: 1 Introduction

Contents

Alphaviruses: Morphology, classification, geographical distribution and disease associations

Togaviridae is a large family of enveloped, positive-strand RNA viruses. The family, which takes its name from the morphology of the virus particles (toga stands for cloak in Latin), consists of two genera, *Alphavirus*, which has 28 members, and *Rubivirus*, which has a single member, rubella virus (Strauss & Strauss, 1994). Alphaviruses are transmitted by arthropod vectors (mainly mosquitoes) with small mammals and birds serving as natural reservoirs. Occasionally, infection of dead-end hosts, including large mammals and humans, results in outbreaks of significant size. Examples include outbreaks of encephalitis in the Americas (associated with Eastern and Venezuelan equine encephalitis viruses) and of severe arthralgia in Australia and in the islands of the Indian Ocean, associated with Ross River and Chikungunya virus, respectively (Vodkin *et al.*, 1993; Lindsay *et al.*, 1996; Camara *et al.*, 2003; Schuffenecker *et al.*, 2006). The natural enzootic and epizootic (or epidemic) cycles of alphaviruses can be seen in Figure 1.1. An example of these cycles is given below using Eastern equine encephalitis virus (EEEV). Naturally, the virus is maintained in an enzootic cycle between the ornithophilic species of mosquito *Culiseta melanura* and migratory passerine songbirds (Dalrymple *et al.*, 1972). Mosquitoes of the *Aedes* species, which feed on both birds and susceptible mammals act as a bridge vector between the virus reservoir and dead-end hosts (Scott & Weaver, 1989; Mitchell *et al.*, 1992).

Alphaviruses are classified into 7 distinct antigenic complexes (based on structural polyprotein sequences) and have a worldwide and geographically distinct distribution. Members of the genus can be found in all continents except Antarctica (Powers *et al.*, 2001). Examples of alphaviruses inhabiting different continents include EEEV and Venezuelan equine encephalitis virus (VEEV) in the Americas, Sindbis virus (SV) in Europe, Semliki Forest virus (SFV) in Africa and Ross River virus in Australia. Alphaviruses have the ability to infect a wide range of hosts including insects, fish, birds, rodents, amphibians, reptiles, primates, horses and humans. In humans, alphaviruses are associated with a range of symptomatic diseases varying from a

mild febrile illness through to rash, arthritis and fatal encephalitis (Mathiot *et al.*, 1990; Rivas *et al.*, 1997; Schuffenecker *et al.*, 2006; Griffin, 2007).

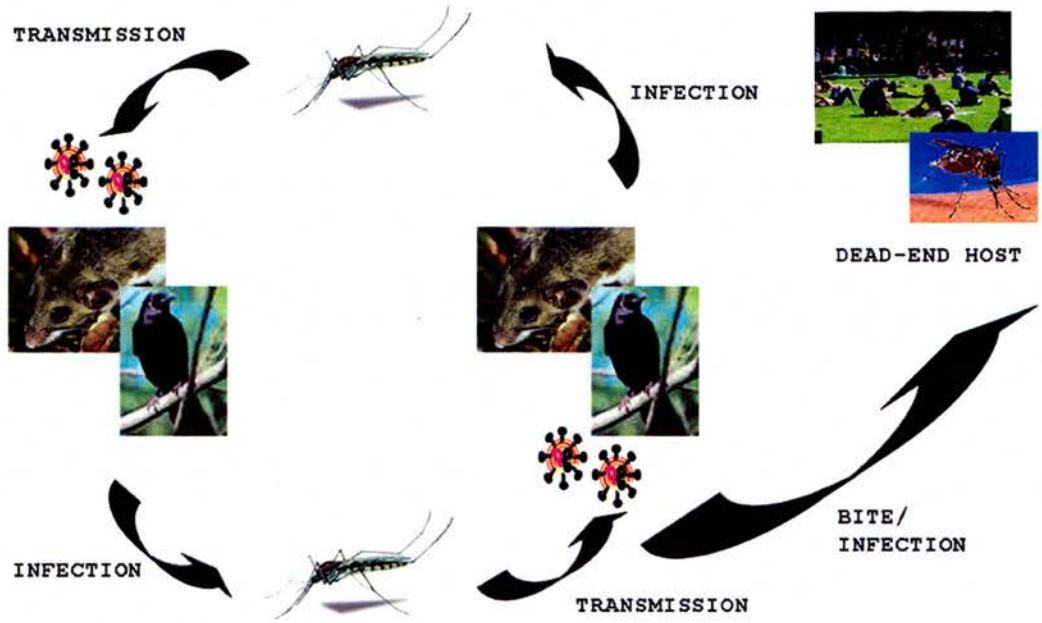

Figure 1.1. Natural enzootic cycle of alphaviruses. In nature alphaviruses circulate between mosquitoes and their natural hosts, small mammals and birds. Occasionally, and through a mosquito vector that feeds in both the natural hosts and dead-end hosts (humans and horses) alphaviruses are transmitted to individuals susceptible to disease.

Alphaviruses, also known for their use as research tools, are amongst the simplest enveloped animal viruses (Atkins *et al.*, 1999). An icosahedral capsid (T=4 symmetry) composed of 240 copies of a single capsid protein surrounds a single-stranded positive sense RNA genome with a size of approximately 11 – 13 kb. The capsid is enveloped in a lipid envelope derived from the plasma membrane of the host cell. Eighty spikes, composed of E1 and E2 glycoprotein heterotrimers cover the virion in a T=4 lattice. Alphavirus virions have a size of approximately 70 nm, depicted in Figure 1.2, (Paredes *et al.*, 1993; Strauss & Strauss, 1994; Cheng *et al.*, 1995). Alphaviruses infect their host cells via receptor-mediated endocytosis. Virus particles attach to the receptor on the cell surface through the receptor-binding domains of E2 glycoprotein (Strauss & Strauss, 1994; Smith *et al.*, 1995; Kuhn, 2007). However, the identity of the receptor which mediates viral attachment and entry remains unclear. The list of putative receptors include the class I major histocompatibility complex, laminin, heparin sulphate and C-type lectins (Helenius *et al.*, 1978; Wang *et al.*, 1992; Klimstra *et al.*, 1998; Klimstra *et al.*, 2003).

Alphaviruses, especially SV and SFV have widely been used to study the viral and immunological events of viral encephalitis, the mechanisms of viral apoptosis and the effects of interferon during viral infection. Moreover, they have been used as a model to understand the pathogenesis of both alphavirus and non-alphavirus encephalitides and provide a useful model for other central nervous system (CNS) diseases such as multiple sclerosis (Atkins *et al.*, 1999; Ryman *et al.*, 2000; Fazakerley & Allsopp, 2001; Fazakerley, 2002).

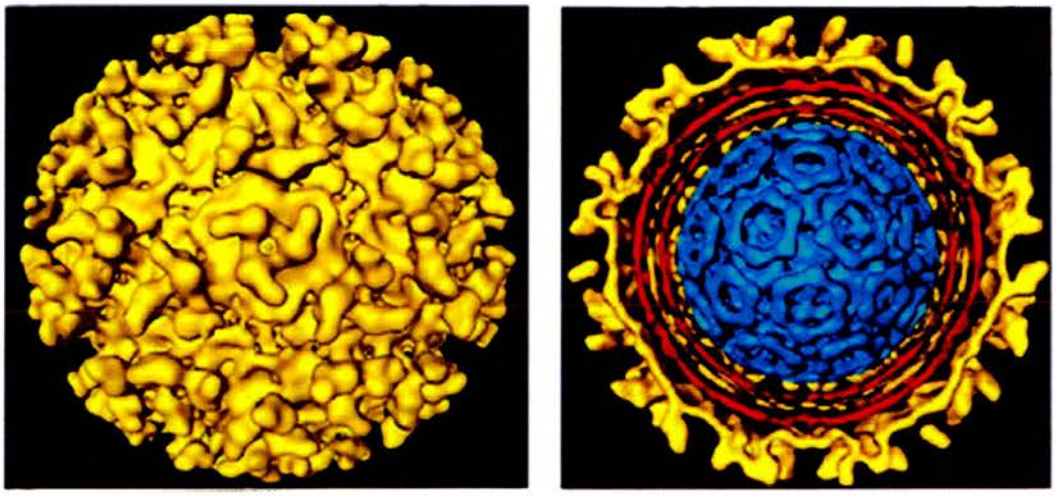

Figure 1.2. Three-dimensional structure of Sindbis virus particles. The yellow area represents the envelope with the spikes. The red area represents the nucleocapsid and blue area corresponds to the viral genome. Pictures taken with permission from: http://biochem.ncsu.edu/faculty/brown/brown.htm.

Genome structure, life cycle and replication of alphaviruses

The genome of alphaviruses is short (11.7 kb for SV and 11.5 kb for SFV) and encodes nine functional proteins from two open reading frames. The 5' end of the genome is capped and the 3' end of the genome is polyadenylated (Kaariainen & Soderlund, 1978; Hill *et al.*, 1997). Like most RNA viruses, alphaviruses express their proteins in the form of large polyproteins which are co- and post-translationally processed to form the mature viral proteins (Figure 1.3). The 5' two-thirds of the genome correspond to four non-structural proteins (nsP1 – 4) whereas the 3' third of the genome encodes five structural proteins (C, E1, E2, E3 & 6K) under the control of an internal subgenomic (26S) promoter (Ding & Schlesinger, 1989; Hardy & Strauss, 1989; Strauss & Strauss, 1994; Kuhn, 2007).

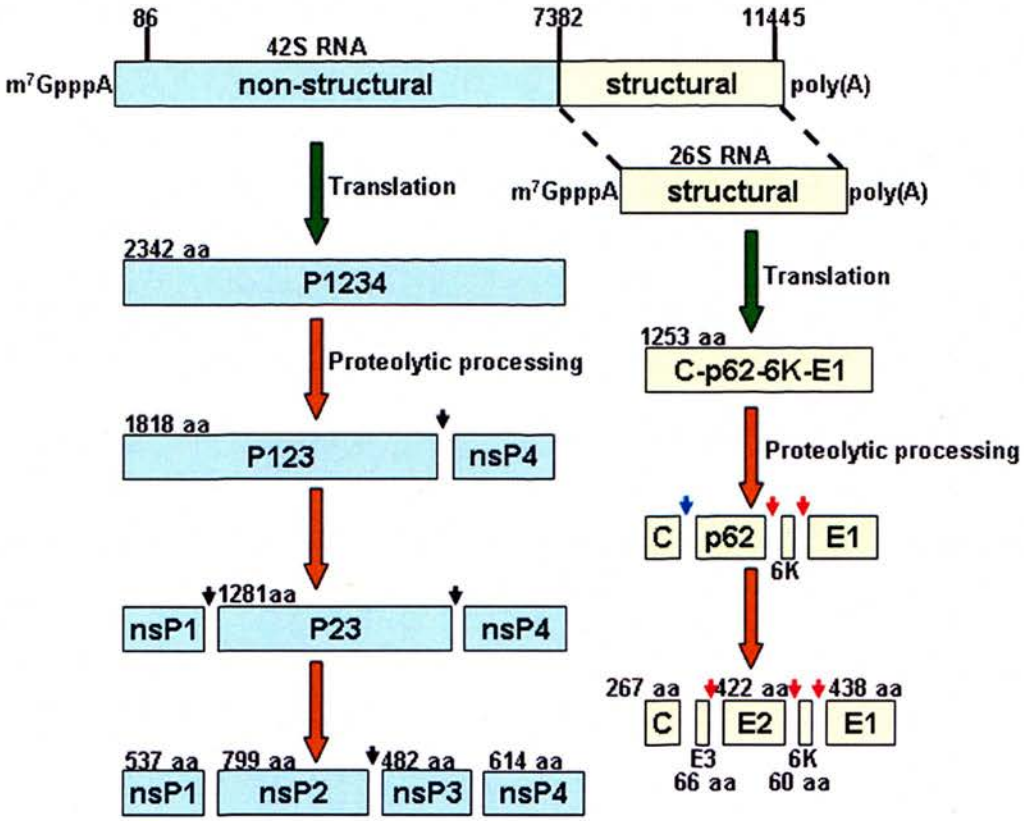

Figure 1.3. Schematic representation of SFV genome. SFV genome is 11,445 nucleotides long. The 5' two-thirds of the genome (light blue) correspond to the non-structural ORF of the virus whereas the 3' third (light yellow) encodes the structural proteins of the virus. The proteolytic processing of the viral polyproteins is shown. The black arrows highlight the position of the nsP2 protease recognition sites in the non-structural ORF. The capsid protein self-cleaves itself from the rest of the structural polyprotein (blue arrow). The proteolytic processing of the remaining proteins is mediated by the cellular enzyme signalase; positions of cleavage sites are highlighted by red arrows.

Following attachment to the cell membrane viral particles are endocytosed through a clathrin-dependent pathway (DeTulleo & Kirchhausen, 1998). The acidic environment of the endosomes alters the three-dimensional structure of the spike protein and the E1 spike protein facilitates the fusion between the virus envelope and the endosome membrane (White & Helenius, 1980; Wahlberg *et al.*, 1992; Wahlberg & Garoff, 1992; Glomb-Reinmund & Kielian, 1998). Numerous studies have shown that the presence of cholesterol is obligatory for fusion to occur (Phalen & Kielian, 1991; Lu *et al.*, 1999).

After fusion, the nucleocapsid is released into the cytoplasm. It has been suggested that the acidic conditions of the endosomes also modify the conformation of the capsid protein revealing ribosomal binding sites. Ribosomes bind to these sites, the nucleocapsid is then disassembled and the viral RNA is uncoated in the cell cytoplasm (Singh & Helenius, 1992; Wengler *et al.*, 1996). In the cytoplasm viral RNA functions as mRNA.

Upon entry and uncoating, ribosomes bind to the 5' end of the genome and the four non-structural proteins are translated either as two overlapping polyproteins (P123 & P1234) in SV or as a single polyprotein (P1234) in the case of SFV. This difference is due to the presence of an opal termination codon at the end of the nsP3 sequence of SV. Ocassionally, read-through translation (with an efficiency of 10-20%) occurs to produce full length P1234 (Strauss *et al.*, 1983; Takkinen, 1986; de Groot *et al.*, 1990; Shirako & Strauss, 1994). The polyprotein(s) is then processed into its individual components through the proteinase activity of the C-terminus of nsP2, which is a papain-like protease domain (Ding & Schlesinger, 1989; Hardy & Strauss, 1989; Merits *et al.*, 2001; Vasiljeva *et al.*, 2001).

Processing of the non-structural polyprotein is highly regulated and in turn regulates the viral replication process (Lemm & Rice, 1993b; Lemm *et al.*, 1994; Shirako & Strauss, 1994). Initially, the non-structural polyprotein is cleaved between nsP3 and nsP4 *in trans* (*in cis* for SV). The protein complex formed (P123 and nsP4) is the early replication complex responsible for the synthesis of the negative strand RNA intermediate (Lemm & Rice, 1993b; Lemm *et al.*, 1994; Shirako & Strauss, 1994; Vasiljeva *et al.*, 2003). Following cleavage between nsP3 and nsP4 the site between nsP1 and nsP2 is cleaved *in cis* and then the site between nsP2 and nsP3 *in trans*

leading to the formation of four individual proteins which remain together as a protein complex. This complex is the viral replication complex responsible for the synthesis of the positive-strand RNA. The mature replication complex is targeted to membranous structures of endosomic and lysosomic origin known as cytoplasmic vacuoles (CPVs). On the external surface of CPVs numerous invaginations called spherules can be found. Synthesis of viral RNA occurs on these spherules. During the late stages of infection this processing pattern is altered to inhibit the formation of new replication complexes and synthesis of minus-strand RNA (Grimley *et al.*, 1968; Froshauer *et al.*, 1988; Lemm *et al.*, 1994; Kujala *et al.*, 2001; Vasiljeva *et al.*, 2003; Salonen *et al.*, 2003; Kim *et al.*, 2004). The nsP2 processing site between nsP3 and nsP4 has been well characterised for SFV (Merits *et al.*, 2001; Vasiljeva *et al.*, 2003; Lulla *et al.*, 2006).

The viral structural proteins are translated as a single ORF. The capsid protein is autocatalytically released from the rest of the polyprotein. On translation of the p62 signal sequence, translation is translocated to the endoplasmic reticulum. The subsequent polyprotein is cleaved to its individual components by the cellular enzyme signalase and the glycoproteins are transported to the golgi apparatus for post-translational modifications and maturation before migrating to the cell membrane. The genomic RNA has packaging signals (in nsP1 for SV and in nsP2 for SFV) that facilitate binding and encapsidation of the RNA (Frolova *et al.*, 1997). Only the genomic RNA is packaged in alphavirus particles, the sole exception is AURA virus, which packages both the genomic and the subgenomic RNAs. The nucleocapsid then interacts with E2 through helical transmembrane segments of the cytoplasmic tail of the latter and new virus particles are released from the cell by budding. The 6K structural protein has an important role in the budding process and experiments with a 6K-deficient SFV show that the structure of the spikes was altered and the membrane fusion capacity of the virus was reduced (Melancon & Garoff, 1986; Garoff *et al.*, 1990; Strauss & Strauss, 1994; Loewy *et al.*, 1995; McInerney *et al.*, 2004; Kuhn, 2007).

Alphaviruses express a limited number of proteins many of which are multifunctional. The functions of the non-structural proteins will be discussed briefly.

nsP1 catalyses the capping of both genomic and subgenomic messages through its methyl and guanylyl transferase activities (Mi & Stollar, 1991; Laakkonen *et al.*, 1994; Ahola & Kaariainen, 1995). In addition, together with a conserved area at the 3' end of the viral genome it is involved in the initiation of the negative-strand RNA synthesis and the docking of the mature replicase complexes onto the surface of membranes (Hahn *et al.*, 1989; Peranen & Kaariainen, 1991; Ahola *et al.*, 1997). Palmitoylation of nsP1 appears to be important for membrane binding. Mutant viruses that have lost their ability to palmitoylate nsP1 are still viable but have attenuated neurovirulence (Laakkonen *et al.*, 1996; Ahola *et al.*, 2000; Zusinaite *et al.*, 2007).

nsP2 is a very interesting protein, the N-terminal domain has ATPase, GTPase as well as RNA helicase activities. Its RNA triphosphatase activity is involved in capping of viral RNA (Rikkonen *et al.*, 1994a; Gomez *et al.*, 1999; Vasiljeva *et al.*, 2000). The C-terminal domain is a papain-like protease which is exclusively responsible for the processing of the replicase polyprotein (Hardy & Strauss, 1989; Merits *et al.*, 2001). nsP2 is also involved in the regulation of subgenomic RNA synthesis and the shut-off of minus-strand RNA synthesis (Hahn *et al.*, 1989; Wang *et al.*, 1994; Suopanki *et al.*, 1998; Sawicki *et al.*, 2006). Another interesting feature of nsP2 is a nuclear localisation signal which facilitates translocation of approximately 50% of the protein to the nucleus of infected cells (Rikkonen *et al.*, 1992; Rikkonen *et al.*, 1994b). The reason for that is not entirely clear but it has been suggested that nsP2 functions as a type-I IFN suppressor (Breakwell *et al.*, 2007). In addition, nsP2 is implicated in pathogenesis and virulence both *in vitro* and *in vivo*; viruses with mutations in nsP2 are less cytopathic and have attenuated neurovirulence (Rikkonen *et al.*, 1994b; Perri *et al.*, 2000; Fazakerley *et al.*, 2002; Frolova *et al.*, 2002).

nsP3's function is not known yet. This phosphoprotein is essential for replication and studies suggest that it is involved in minus-strand and subgenomic RNA production; viruses with mutations or deletions in nsP3 produce lower amounts of RNA. Numerous studies suggest that nsP3 contains important determinants of alphavirus neurovirulence in mice (Lastarza *et al.*, 1994; LaStarza *et al.*, 1994; Wang *et al.*, 1994; Tuittila *et al.*, 2000; Vihinen *et al.*, 2001; Galbraith *et al.*, 2006).

nsP4 has catalytic activity and is the viral RNA polymerase. Interestingly, nsP4 is synthesised to considerably lower amounts compared to nsP3 and in most alphaviruses expression of nsP4 occurs only when the ribosomes read-through the opal-termination codon at the end of nsP3. Various studies have shown that nsP4 is degraded via proteasome-mediated degradation according to the N-end rule. However, the exact sequence that directs nsP4 to the proteasome compartment is not found yet (de Groot *et al.*, 1991; Merits *et al.*, 2001).

Pathogenesis of Semliki Forest virus

SFV is an arbovirus circulating in sub-Saharan Africa and it was first isolated in Uganda in 1942 from mosquitoes of the *Aedes abnormalis* species (Smithburn & Haddow, 1944). SFV is predominantly transmitted by two species of mosquitoes; *Aedes africanus* and *Aedes aegypti*. Infections of monkeys, humans and horses have been reported. In humans the virus is associated with a mild febrile illness. The symptoms of this illness include fever, myalgia (pain of muscles), arthralgia (pain of joints) and persistent headaches. SFV has proven to be the causative agent of human disease in two instances one of which was fatal. In 1987 SFV was isolated from blood samples of 22 French soldiers with symptoms of a mild febrile illness. The virus has also been associated with the death of a laboratory worker in Germany (Willems *et al.*, 1979; Mathiot *et al.*, 1990; Fazakerley, 2002).

There are numerous viral strains infecting various experimental animals including mice, rats, rabbits and guinea pigs (Bradish *et al.*, 1971; Atkins *et al.*, 1990). Two different cell lines permissive for infection are usually used for *in vitro* studies. Chicken embryo fibroblasts (CEF) and baby hamster kidney (BHK) cells but the virus has the ability to infect many other cell lines; examples include Vero cells originating from African green monkey and human lung carcinoma A549 cell line (Atkins *et al.*, 1999; Deuber & Pavlovic, 2007; Griffin, 2007). Infection of laboratory mice with SFV is a very useful model for the study of virus pathogenesis and in particular virus encephalitis (Fazakerley, 2004).

Four strains of SFV have been studied most extensively. L10 and prototype which are virulent in adult mice and A7 and A7(74) which are avirulent in adult mice. All strains of SFV (virulent and avirulent) are neuroinvasive and virulent in neonatal mice (Seamer *et al.*, 1967; Bradish *et al.*, 1971; Pusztai *et al.*, 1971).

A unique characteristic of the avirulent SFV strains is their age-related virulence. Neonatal or young suckling mice (up to 11 days old) inoculated intraperitoneally with SFV A7(74) exhibit symptoms of fulminant encephalitis and succumb to infection 48 to 96 hours post-inoculation due to widespread apoptotic neuronal cell death; from 12 days onwards the infection is avirulent (Gates *et al.*, 1984; Oliver *et al.*, 1997; Oliver & Fazakerley, 1997; Allsopp *et al.*, 1998). Studies utilising adult

athymic *nu/nu* mice and adult mice with severe combined immunodeficiency showed that the spread of SFV A7(74) in the CNS remained limited and concentrated to perivascular foci in the brain and the spinal cord suggesting that the age-related virulence is not dependent upon specific immune responses (Fazakerley *et al.*, 1993; Amor *et al.*, 1996).

All evidence to date suggests that the age-related virulence of the avirulent SFV strains is closely related to the maturation of the nervous system. During the first two weeks after birth, the mouse CNS undergoes a series of major maturational processes including synaptogenesis, gliogenesis, axonogenesis and myelination (Oliver *et al.*, 1997; Oliver & Fazakerley, 1997; Fazakerley, 2001). Upon completion of the CNS maturation, virus replication becomes restricted, especially in neurons (Fazakerley *et al.*, 1993). As mentioned earlier, replication of SFV is associated with membranes; during the early developmental stages of the murine CNS large amounts of smooth membrane vesicles are produced. The virus uses these membranes to productively replicate and spread in the immature brain and when their production is halted replication of the virus is restricted to small foci of infection (Froshauer *et al.*, 1988; Fazakerley, 2001). Furthermore, when gold compounds (aurothiolates), which stimulate the production of smooth membranes in neurons, were used to treat adult Balb/c mice, the SFV A7(74) avirulent strain spread in the mature brain to the same extent as the virulent SFV L10 strain. Notably, following treatment with aurothiolates neurons did not become susceptible to apoptosis. This finding outlines the crucial role that smooth membranes have in SFV replication in the CNS (Mehta *et al.*, 1990; Scallan & Fazakerley, 1999).

Differential susceptibility to apoptotic cell death could also explain the age-related virulence of SFV. As neurons mature, they become less susceptible to apoptosis probably as a defence mechanism to avoid destruction of vital, non-replaceable cell populations. Infection of neurons in the brain of neonatal mice by the avirulent SFV A7(74) strain results in apoptotic cell death. In contrast, infection of the mature brain with the same virus results in persistent infection, even after direct intracerebral inoculation (Fazakerley *et al.*, 1993; Allsopp & Fazakerley, 2000; Fazakerley & Allsopp, 2001). The connection between the developmental status of neuronal cells and the susceptibility to apoptotic cell death was also studied using a rat model.

Adult rats were infected with the SFV4 virulent strain. In the brains of these animals, apoptosis was observed only in the rostral migratory stream, an area of the brain along which neuronal precursors constantly renew and differentiate (Sammin *et al.*, 1999). Upregulation of anti-apoptotic genes like *bcl*-2 in the mature brain might also contribute to reduced susceptibility to apoptosis. Expression of *bcl*-2 has been previously shown to have a protective effect against alphaviral infection both *in vitro* and *in vivo* (Levine *et al.*, 1996; Scallan *et al.*, 1997).

Age-related virulence has been also shown for numerous other viruses including the very similar alphavirus; Sindbis virus. Studies using avirulent strains of SV in neonatal mice suggest that death in these animals is the result of a systemic inflammatory response characterised by high levels of expression of α, β and γ interferon, tumour necrosis factor α and other cytokines (Sherman & Griffin, 1990; Klimstra *et al.*, 1999; Trgovcich *et al.*, 1999).

Following intraperitoneal inoculation SFV has been documented to replicate in muscle tissue (skeletal, smooth and cardiac) and in lymph nodes establishing a high titre plasma viraemia (Grimley & Friedman, 1970; Amor *et al.*, 1996; Fazakerley, 2002). Subsequently, the virus infects cerebrovascular endothelial cells and enters the brain where it replicates and initiates small perivascular foci of infection. In the brain, the virus infects neurons and oligodendrocytes but not astrocytes (Pathak & Webb, 1978; Soilu-Hanninen *et al.*, 1994; Amor *et al.*, 1996; Fazakerley, 2002). Interestingly, both virulent and avirulent strains of SFV exhibit similar tropism in the CNS (Balluz *et al.*, 1993; Fazakerley *et al.*, 2006). Although astrocyte infection has not been reported *in vivo*, various alphaviruses including SFV, SV and VEEV have the ability to infect these cells *in vitro* (Brodie *et al.*, 1997; Schoneboom *et al.*, 1999; McKimmie & Fazakerley, 2005).

The progress and the outcome of the infection is mainly based on two factors; the strain of the virus and the age of the inoculated animal. In neonatal mice where the CNS is still immature, widespread neuronal death due to apoptosis is observed following infection with virulent or avirulent strains (Gates *et al.*, 1984; Oliver *et al.*, 1997; Oliver & Fazakerley, 1997; Allsopp *et al.*, 1998). In adult mice infection with a virulent strain, like SFV L10 or SFV4, leads to rapid death (72 – 96 hours after inoculation). Post-mortem examination of infected brains shows extensive neuronal

cell death due to necrosis (Fazakerley *et al.*, 1993). It is believed that virulent strains induce death because in contrast to the avirulent strains they have the ability to replicate productively and destroy a large number of mature neurons before intervention of immune responses (Atkins & Sheahan, 1982; Smyth *et al.*, 1990; Fazakerley *et al.*, 1993).

Infection of adult mice with avirulent strains is limited to small foci of infection around blood vessels. Infectious virus is cleared from the brain 7 to 10 days post-inoculation and lesions of demyelination scattered throughout the brain are apparent at approximately 14 days post-inoculation (Amor *et al.*, 1996; Donnelly *et al.*, 1997; Fazakerley, 2002). Responsible for this demyelination are activated $CD8^+$ T lymphocytes which destroy virally infected oligodendrocytes. Further studies using *nu/nu* and SCID mice outline the importance of cellular immune responses in induction of lesions of demyelination (Subak-Sharpe *et al.*, 1993; Amor *et al.*, 1996).

The ability of SFV to induce demyelination has made SFV infection of the laboratory mouse a valuable model for multiple sclerosis a human demyelinating disease (Mokhtarian *et al.*, 1994; Atkins *et al.*, 1999).

Another interesting pathogenic complication of infection with avirulent strains of SFV is that these viruses can cross the placenta in pregnant mice and can either induce abortions or have a teratogenetic effect on the foetuses (Atkins *et al.*, 1982; Mabruk *et al.*, 1989).

Immune responses to Semliki Forest virus

Both humoural and cellular immune responses are required to control SFV infection of the CNS. In the absence of specific immune responses the avirulent strains of the virus have the ability to persist in the CNS for long periods of time without any obvious cytotoxic effect (Fazakerley *et al.*, 1993; Amor *et al.*, 1996; Fazakerley, 2002).

Following intraperitoneal inoculation with SFV A7(74) a high level plasma viraemia which peaks at 24 hours post-inoculation is established. Infectious virus is cleared from the periphery and from the brain by day 3 and day 8 post-inoculation respectively (Fazakerley *et al.*, 1993). In athymic *nu/nu* mice, which produce IgM antibodies but cannot class switch to produce IgG, viraemia is cleared in an identical

manner to wild-type Balb/c mice but infectious virus in the brain persists for long periods of time. This suggests that IgM antibody alone can clear the viraemia but it is unable to control virus in the brain (Suckling *et al.*, 1982; Amor *et al.*, 1996). In SCID mice, which do not produce antibodies or T-cells, persistent viraemia and persistent infection of the CNS is established. Transfer of serum from infected *nu/nu* mice to infected SCID mice resulted in clearance of the viraemia but not of the brain virus. When serum from infected Balb/c was used to perform the same experiment the infectious virus was cleared from both the blood and the brain. However, the effect of the serum transfer was transient suggesting that T-cell responses are required for sterilising immunity (Amor *et al.*, 1996; Dixon, 2007 PhD Thesis). The role of antibody in clearance of infectious virus was further highlighted using μMT mice, which lack antibodies but have an intact T-cell response. These animals were not able to clear infectious virus from their blood or their brain and SFV RNA was detectable in their brain for up to 12 weeks post-infection (Rennos Fragkoudis, manuscript in preparation). Similar studies with Sindbis virus have shown the important role that antibody plays in infectious virus clearance and prevention of reactivation (Byrnes *et al.*, 2000; Burdeinick-Kerr *et al.*, 2007).

Although infectious virus is cleared from the brain, viral RNA persists for long periods of time (Levine & Griffin, 1992; Donnelly *et al.*, 1997). Cells that contain viral RNA possibly are cleared by cytotoxic T-cell responses. However, $CD8^+$ T-cells have been shown to be responsible for brain histopathology (mononuclear infiltrates are mostly $CD8^+$) and the appearance of lesions of demyelination following inoculation with avirulent strains of SFV (Subak-Sharpe *et al.*, 1993; Mokhtarian *et al.*, 2003).

Even though antibody and T-cell responses are important for clearance of infectious virus and prevention of reactivation the mice would not survive long enough to benefit from these specific immune responses without type-I interferons (interferon α/β). Mice with impaired type-I IFN responses succumb to infection after the administration of low doses of virulent or avirulent strains of SFV. In early studies on the protective effect of interferon it had been shown that administration of IFN derived from mice infected with West Nile virus had a protective effect against virulent strains of SFV (Finter, 1966). In this and subsequent studies, the extent of

protection was clearly dependent upon the virus strain, dose and time of administration (Smillie *et al.*, 1973; Bradish & Titmuss, 1981). When α-IFN antibodies were administered, SFV avirulent infection became highly virulent (Fauconnier, 1971). Levels of type-I IFN directly correlate to the levels of infectious virus in the blood (Bradish *et al.*, 1975). Muller *et al.* (1994) have shown that genetically modified mice which lack a functional type-I interferon system succumb much more rapidly to SFV infection (with either a virulent or an avirulent strain) compared to immunocompetent mice. Administration of an avirulent strain of SFV prior to challenge with a virulent strain like SFV L10 or SFV V13 has also been shown to have a protective effect (Smillie *et al.*, 1973). The type-I interferon system has also been demonstrated to be crucial for the protection of mice from nominally avirulent strains of other alphaviruses including Venezuelan equine encephalitis and Sindbis viruses (Grieder & Vogel, 1999; Ryman *et al.*, 2000). Interestingly, the action of type-I interferon determines the tropism of the virus by strongly curtailing virus spread in many cell types in many tissues, for example meningeal cells in the brain but it is not responsible for the restricted replication of SFV A7(74) in mature neuronal cells (Ryman *et al.*, 2000; Fragkoudis *et al.* manuscript submitted).

Alphaviral vectors

The idea of using a viral vector for therapeutic purposes (gene therapy) or as a vaccine has been around for quite a long time. Both RNA and DNA viruses have been used as expression systems for the expression and the delivery of foreign genes. A successful vector suitable for applications in humans should include the following features:

- High level of biological safety.
- High level transient heterologous protein expression.
- Ability to carry large inserts.
- Lack of pre-existing immunity.
- Broad host range and tissue/cell tropism
- Ability to induce adequate levels of humoural and cellular immunity.

Expression vectors based on alphavirus are highly successful because they encompass all the above mentioned characteristics (Frolov *et al.*, 1996; Lundstrom *et al.*, 2001). Construction of alphavirus-based expression vectors required the development of infectious cDNA (icDNA) clones. Such clones have been developed for several alphaviruses; the viruses used most extensively for the construction of expression vectors include SFV, SV and VEEV (Rice *et al.*, 1987; Davis *et al.*, 1989; Liljestrom & Garoff, 1991). To express non-viral genes using an alphavirus, two different types of vectors have been constructed, replication competent and replication deficient vectors.

Replication-deficient vectors

For vaccination and gene therapy applications the replication deficient system is preferred because it offers a very high level of biosafety. As already mentioned the genome of alphaviruses has two ORFs, one encoding for the non-structural proteins and one encoding for the structural proteins. In this approach, the part of the genome corresponding to the structural proteins is replaced by the gene of interest, which is placed under the control of the subgenomic promoter. The subgenomic promoter, which is very powerful due to the presence of a translational enhancer found in the capsid protein, can be duplicated and consequently two proteins can be expressed concurrently (Sjoberg *et al.*, 1994; Frolov & Schlesinger, 1994b; Frolov *et al.*, 1996; Ehrengruber, 2002). Figure 1.4 diagrammatically shows the alphavirus vector system.

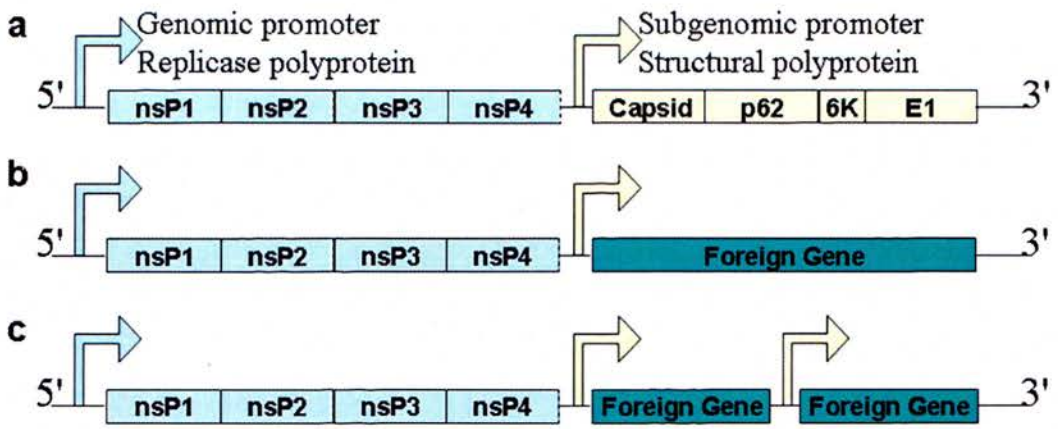

Figure 1.4. Alphavirus replicon system. (a) Alphavirus genome; light blue area corresponds to the non-structural genes. The light yellow area corresponds to the structural genes. **(b)** In the replicon system the structural protein coding region is replaced by a foreign gene (dark blue). **(c)** The subgenomic promoter can be duplicated and two foreign genes can be inserted and expressed. In some vectors, the foreign gene is preceded by part of the capsid sequence which contains the translation enhancer.

To mobilise alphaviral vectors three different strategies have been applied to date. The first approach, and possibly the most efficient utilises suicidal viral particles known as virus-like particles (VLPs) capable of only one round of replication. To generate VLPs, the structural genes are provided *in trans* either as separate RNA messages lacking packaging signals, (called helper) or in packaging cell lines (Polo *et al.*, 1999; Karlsson & Liljestrom, 2003). In the early studies the structural genes were provided as a single RNA message. This was proven problematic because recombination between the replicon and the helper RNA leading to the production of infectious virus was often observed (Berglund *et al.*, 1993; Pushko *et al.*, 1997). To circumvent that problem, systems where the structural genes are provided as two separate RNA messages were developed. In these systems, known as two-helper or split-helper system, the capsid and glycoprotein genes are separated and expressed by two individual RNAs. To further increase biosafety, mutations were incorporated in the structural genes (Pushko *et al.*, 1997; Smerdou & Liljestrom, 1999; Fayzulin *et al.*, 2005). The split-helper system used to produce SFV VLPs can be seen in Figure 1.5.

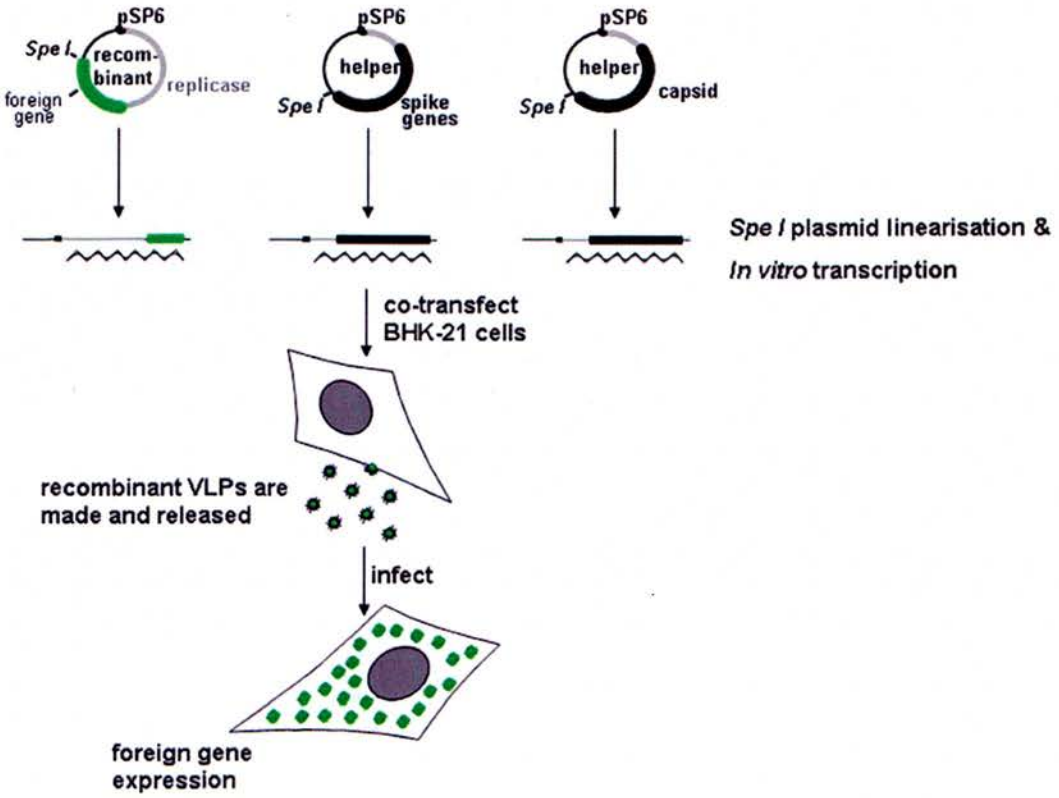

Figure 1.5. The split-helper system of SFV replicons. Three plasmids coding for the replicon with the foreign gene of interest, the glycoprotein genes and the capsid gene are linearised using *Spe I* and following *in vitro* transcription the RNAs are used to co-transfect BHK-21 cells. Recombinant VLPs are made and released and following titration they can be used to infect cells into which high-level transient expression of the foreign gene occurs.

In a different system, naked DNA encoding for the replicase genes and one or more foreign genes (under the control of the 26S subgenomic promoter) are placed under the control of a eukaryotic promoter like the CMV – IE promoter (cytomegalovirus immediate-early) and the constructs are transfected into cells. This vector system is known as layered DNA/RNA vector. The system provides strong transient expression of the gene of interest. Additionally, the production is easier and more cost effective compared to VLP production because *in vitro* transcription is not required (Dubensky, Jr. *et al.*, 1996; Berglund *et al.*, 1998). Finally, *in vitro* transcribed RNA encoding the replicon (replicase genes and gene of interest) can be directly transfected into cells (Karlsson & Liljestrom, 2003).

All three strategies described above have been proven efficient to carry, deliver and express proteins (genes up to 5 kb can be inserted) at high levels over extended periods of time (Xiong *et al.*, 1989; Morris-Downes *et al.*, 2001; Graham *et al.*, 2006). Vaccines based on alphavirus vectors are very appealing because replication occurs in the cytoplasm and thus there is no risk of integration of genes into the host cell genome. In addition, alphavirus replicons induce apoptosis in the host cell. Other advantageous characteristics of alphaviral systems include lack of pre-existing immunity and a broad range of susceptible cells (Morris-Downes *et al.*, 2001; Karlsson & Liljestrom, 2003). Various studies have shown that alphaviruses induce adequate immune responses and have the potential to be used as vaccines for bacterial, parasitic and viral diseases. Examples include HIV, influenza, and malaria (Tsuji *et al.*, 1998; Nordstrom *et al.*, 2005).

Since alphaviruses have a tropism for the CNS, especially for neurons, they appear to be good candidates for gene therapy in the brain (Frolov *et al.*, 1996; Ehrengruber, 2002). Also a study using SFV replicons showed that SFV induces p53-independent apoptosis in tumour cells suggesting a potential use in tumour therapy (Glasgow *et al.*, 1998).

Even though alphaviral vectors have excellent properties their use in humans is hampered due to their cytotoxicity *in vitro* and *in vivo*. More specifically, after infection by an alphavirus, the host cell transcriptional and translational machinery is shut down and eventually the cell dies (Frolov & Schlesinger, 1994a; Lundstrom *et al.*, 2003; Graham *et al.*, 2006). nsP2 appears to play a critical role in alphavirus-

mediated cytotoxicity. During infection 50% of the synthesised nsP2 migrates to the nucleus (Peranen *et al.*, 1990). Mutation of a single amino acid in the nuclear localisation signal of nsP2 results in the production of a virus with reduced virulence (Fazakerley *et al.*, 2002). Much work has been conducted in order to produce alphaviral vectors with reduced cytotoxicity. Through these studies vectors with reduced cytotoxicity which are able to persistently infect the host cell have been produced. Most of the less cytotoxic vectors carry mutations in their nsP2 protein; such vectors have been described for SFV, SV and VEEV (Dryga *et al.*, 1997; Lundstrom *et al.*, 2003; Kim *et al.*, 2004; Petrakova *et al.*, 2005). Interestingly, although mutations in nsP2 usually result in decreased viral RNA synthesis the expression levels of the foreign gene are increased. This possibly happens because host cell protein synthesis is not affected to such extent in cells infected with mutant replicons compared to cells infected with wild-type replicons (Lundstrom *et al.*, 2003; Kim *et al.*, 2004; Petrakova *et al.*, 2005). During studies for less cytotoxic replicons, temperature-sensitive mutations in the non-structural genes have been identified. These mutations offer a means to control expression of foreign genes by shifting the temperature, from the non-permissive temperature to the permissive and vice versa (Boorsma *et al.*, 2000; Lundstrom *et al.*, 2003). Cells persistently infected with alphavirus replicons could be used for the screening of antiviral compounds or for expression of recombinant proteins.

In vivo, in the CNS of rodents (mice and rats) non-replicating alphavirus vectors have the ability to express foreign genes at high levels and for prolonged periods of time. Most studies to assess the efficiency of gene transfer in neuronal cells have been performed using replicons expressing enhanced green fluorescent protein (eGFP). Both SV and SFV packaged vectors have the ability to infect neurons and readily produce fluorescence (Gwag *et al.*, 1998; Ehrengruber *et al.*, 2001; D'Apuzzo *et al.*, 2001; Jeromin *et al.*, 2003). In most studies mentioned above eGFP-positive cells were detectable for 5 – 9 days after intracerebral inoculation. Graham *et. al.* (2006) showed that stereotaxic inoculation of eGFP-expressing SFV VLPs into the substantia nigra, an area of the brain damaged in patients with Parkinson's disease, resulted in eGFP expression in dopaminergic neurons for up to 12 weeks. However, dopaminergic neurons of the substantia nigra showed signs of apoptosis and

axonopathy indicative of the cytopathic effect that SFV VLPs have. In contrast to SV, SFV has the ability to infect oligodendrocytes. To study the interactions between this particular cell type eGFP-expressing VLPs were used (Fazakerley *et al.*, 2006).

The examples mentioned above highlight the potential applications of SFV in therapeutic and experimental procedures. However, the use of replication deficient vectors in *in vivo* pathogenesis studies is limited because they can only undergo a single round of replication and therefore cannot spread far from the point of inoculation. For that purpose, propagating vectors are required.

Replication-competent vectors

Replication-competent vectors have been constructed from many members of the alphaviruses including SV, SFV, VEEV and Chickungunya virus (CHICK). Traditionally, to construct a replication-competent vector the foreign gene of interest is inserted under the control of a duplicated subgenomic promoter. The duplicated subgenomic promoter can be inserted either into the 3' non-translated region of the genome or into the short non-translated region between the replicase and the structural ORF (Raju & Huang, 1991; Hahn *et al.*, 1992; Caley *et al.*, 1999; Vaha-Koskela *et al.*, 2003; Vanlandingham *et al.*, 2005). The possible ways to insert a second subgenomic promoter and a foreign gene can be seen in Figure 1.6.

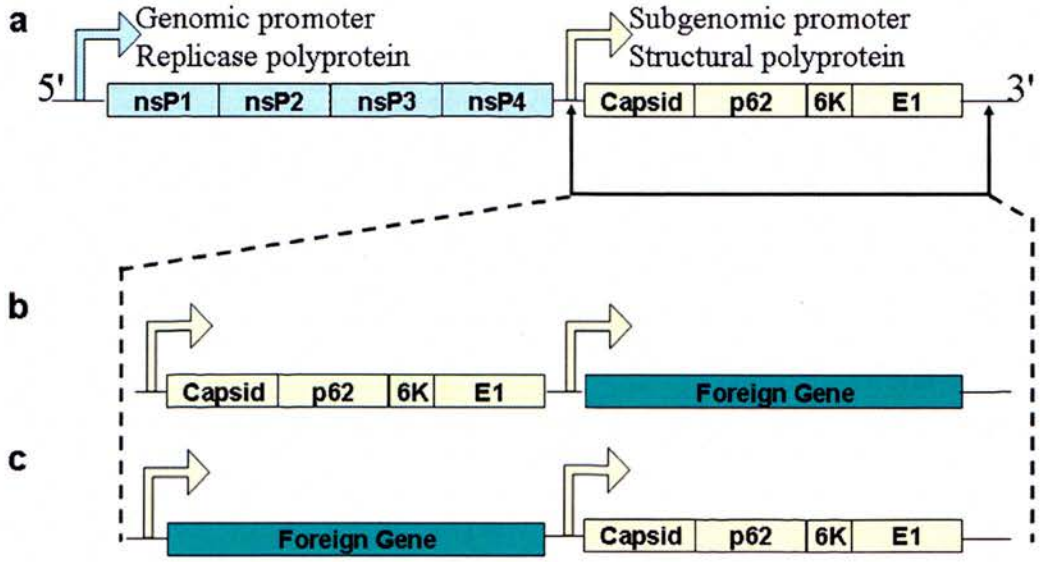

Figure 1.6. Alphavirus replication-competent vectors. (a) Schematic representation of alphaviral genome; light blue area corresponds to the replicase ORF and light yellow area to the structural ORF. **(b)** Insertion of the second 26S promoter at the 3' end of the structural polyprotein. **(c)** Insertion of the second 26S promoter at the 5' end of the structural polyprotein.

The position of insertion (upstream, 5', or downstream, 3', the structural ORF), the length and the nature of the inserted sequence appear to be crucial for the levels of transgene expression and the genetic stability of these vectors (Pugachev *et al.*, 1995; Higgs *et al.*, 1999; Vanlandingham *et al.*, 2005). Most studies to date suggest that expression is stronger if the foreign gene is inserted downstream from the structural ORF. This has been shown in numerous studies; examples include SV duplicated subgenomic vectors expressing eGFP and Japanese encephalitis sequences, VEEV vectors expressing the MA/CA domain of HIV gag protein and CHICK vectors expressing eGFP (Pugachev *et al.*, 1995; Caley *et al.*, 1999; Pierro *et al.*, 2003; Vanlandingham *et al.*, 2005). However, according to the study by Pugachev *et al.* (1995) levels of expression are not different when long sequences are inserted in either the 5' or the 3' position.

In terms of genetic stability, constructs having the second subgenomic promoter and the foreign gene of interest inserted at the 5' of the structural ORF are in general more stable compared to those carrying insert at the 3' of the same region of the genome (Pugachev *et al.*, 1995; Caley *et al.*, 1999; Pierro *et al.*, 2003; Vanlandingham *et al.*, 2005). The length and the nature of the transgene are important determinants of genetic stability; viruses expressing long sequences (3 – 4 kb) are less stable than constructs carrying shorter genes (1 – 2kb) and have the ability to reach titres similar to those of the parental virus strain (Hahn *et al.*, 1992; Chen *et al.*, 1995; Caley *et al.*, 1999). Constructs with duplicated subgenomic promoter have been used to express many genes; examples include influenza haemagglutinin, *bcl-2*, eGFP, luciferase, antisense RNAs (Hahn *et al.*, 1992; Levine *et al.*, 1996; Johnson *et al.*, 1999; Cook & Griffin, 2003; Vaha-Koskela *et al.*, 2003). These constructs have been extensively used in mammalian and insect systems for *in vitro* and *in vivo* applications. However, these viruses exhibit high levels of genetic instability probably because the inserted sequences are incorporated as separate transcription units that do not provide any selective advantage to the virus. This instability has been attributed to a slower replication rate; viruses that eliminate the inserted sequences replicate faster. Recombination between the duplicated subgenomic promoters is another possibility (Pugachev *et al.*, 1995; Pugachev *et al.*, 2000; Thomas *et al.*, 2003; Vaha-Koskela *et al.*, 2003; Gehrke *et al.*, 2005).

To construct replication-competent vectors with increased genetic stability several alternative approaches have been employed. Pugachev *et al,* (2000) constructed a recombinant rubella virus expressing foreign genes under the control of an IRES (internal ribosomal entry sequence) from encephalomyocarditis virus (EMCV; picornavirus). This virus was capable of stable expression of the transgene following several passages in tissue culture.

More recently, recombinant viruses expressing foreign genes as components of the natural expression units, the replicase or the structural ORF, of the virus have been constructed. Using this method recombinant SV expressing eGFP, and firefly luciferase in fusion with nsP2 or nsP3 non-structural proteins have been produced (Bick *et al.*, 2003; Zhimin Liang and Guangpu Li, 2005; Frolova *et al.*, 2006; Atasheva *et al.*, 2007). Additionally, a similar virus expressing eGFP and cherry red in fusion with nsP2 and nsP3 proteins respectively has been constructed. This virus, although it replicated to lower levels compared to its parental strain was viable and capable of expressing both proteins. An interesting finding of this study was that insertions in the N-terminal domain of nsP2 had a negative effect on the cleavage of the nsP2/nsP3 site. This supports the hypothesis that the N-terminal region of nsP2 has a possible function as a protease co-factor (Vasiljeva *et al.*, 2003; Atasheva *et al.*, 2007).

A different strategy was employed by Thomas *et al.* (2003). In their vector, foreign proteins are cloned into the structural ORF as a cleavable component. The transgene is released by the autocatalytic activity of the capsid protein at its 5' – end and by the autoprotease activity of the 2A peptide from foot-and-mouth disease virus (FMDV) at its 3' – end (Donnelly *et al.*, 2001a; Thomas *et al.*, 2003). This virus has increased genetic stability compared to duplicated subgenomic promoter constructs and additionally it offers high levels of transgene expression since the foreign gene is under the control of the powerful 26S promoter. It is important to mention that as with other studies, this study showed that genetic stability is dependent on the size and nature of the inserted sequences.

All the replication-competent vectors mentioned above have their advantages and disadvantages as discussed. However, they all share a common disadvantage; the icDNA plasmids appear to be toxic for *E. coli* cells and this makes purification of these plasmids a difficult procedure. It is believed that in SFV, this is due to the presence of cryptic *E. coli* promoters in nsP2, which drive the expression of the viral structural proteins and these proteins are toxic for the bacterial cells (personal communication with Professor Andres Merits). A possible solution for this problem would be the use of low-copy number plasmids as described for VEEV and EEEV recombinant viruses (Petrakova *et al.*, 2005).

Marker genes in virology

Marker genes are very valuable tools for various studies in virology. Applications of marker genes will be discussed below.

Viruses tagged with marker genes have been widely used to study virus life cycle, replication, protein localisation and cell-to-cell spread as well as virus interactions with cellular components. The most widely used marker protein is eGFP because it is easy to detect and most standard fluorescent microscopes have a filter suitable for its visualisation.

In recent studies investigating replication complex formation of alphaviruses, nsP2 and nsP3 non-structural proteins of SV have been tagged with eGFP or cherry red. This facilitated visualisation and isolation of replication complexes at early and late time-points post-infection. In addition using α-eGFP antibodies it was possible to isolate the complexes of cellular proteins associated with the nsP3-eGFP fusion protein and study their role in the formation of alphaviral replication complexes (Frolova *et al.*, 2006; Atasheva *et al.*, 2007). Visualisation of replication complexes by tagging non-structural proteins with eGFP has been demonstrated for a number of other viruses including hepatitis C virus (HCV) and equine arteritis virus (EAV). In these studies eGFP was fused to the 5A and upstream of nsP1 or nsP2 non-structural proteins respectively (Moradpour *et al.*, 2004; van den Born *et al.*, 2007).

eGFP has also been used to study the localisation and the function of numerous proteins. It is known that during alphaviral replication approximately 50% of nsP2 protein is translocated to the nucleus. Using nsP2-eGFP fusion protein it was feasible

to observe that distribution without the need of an immunostaining (Atasheva *et al.*, 2007; Breakwell *et al.*, 2007). In another study eGFP was used to study the localisation and the function of the L protein (RNA-dependent RNA polymerase) of measles virus (Duprex *et al.*, 2002). To examine the role of the NS2B-NS3 protease precursor of dengue virus in induction of apoptosis, NS2B-NS3 was fused to eGFP (Shafee & AbuBakar, 2003).

Virus entry into permissive cells and spread of viruses from one cell to another, both *in vivo* and *in vitro*, is another field in which eGFP-tagged viruses have been used successfully. Examples include herpes simplex virus, measles virus and rabies virus (Foster *et al.*, 1998; Duprex *et al.*, 1999; Finke *et al.*, 2004).

During development of viral vectors for protein expression, vaccine production or gene therapy the use of marker genes is a very valuable tool in order to assess the levels of expression that the candidate vector provides, its genetic stability and its cytotoxicity. eGFP and luciferase are usually the markers of choice due to the ease in their detection. Most studies for alphavirus vector development, both replication-deficient and replication-competent, utilise eGFP to assess the length and the strength of expression (Lundstrom *et al.*, 2003; Jeromin *et al.*, 2003; Frolova *et al.*, 2006). Luciferase and eGFP have also been used to assess the suitability of mouse hepatitis virus and of poliovirus respectively as expression vectors (Mueller & Wimmer, 1998; de Haan *et al.*, 2005). Viral vectors expressing eGFP have also been used for the screening of antiviral compounds like morpholino oligomers and for their potential in gene therapy against various diseases like Parkinson's disease and in tumour therapy in melanoma (van den Born *et al.*, 2005; Vaha-Koskela *et al.*, 2006; Graham *et al.*, 2006).

Probably, the most important contribution of marker viruses is their use for *in vivo* pathogenesis studies. The examples of neurotropic marker viruses used for such studies are multiple. SV expressing luciferase under the control of a duplicated subgenomic promoter has been used to study the progress of infection following peripheral infection in living animals (Cook & Griffin, 2003). Various strains of SFV and SFV replicons expressing eGFP have also been used to examine the spread of the virus in the brain as well as its cell tropism and its ability to establish persistent infections (Vaha-Koskela *et al.*, 2003; Fazakerley *et al.*, 2006). Similar studies on

virus spread and persistence have been performed for measles virus, SARS coronavirus and mouse hepatitis virus (Duprex *et al.*, 2000; Sims *et al.*, 2005; Schubert *et al.*, 2006).

Viruses carrying marker genes have also been constructed for several plant viruses like tobacco etch potyvirus, and other members of the potyvirus genus to investigate their replication and the distribution in susceptible species of plants. For the labelling of these viruses eGFP and DSRed proteins have been used (Dolja *et al.*, 1993; Dietrich & Maiss, 2003).

Marker viruses have a tremendous impact on virology studies. The ease of detection and the high sensitivity compared to traditional immunohistochemistry methods make them a very powerful tool for various studies on the field.

Aims of the project

The aims of this project were:

- To construct SFV-based recombinant viruses expressing marker genes.
- To characterise these viruses.
- To assess their suitability for *in vivo* pathogenesis studies.

Chapter 2: Materials and Methods

Contents

Viruses and Virus-Like Particles (VLPs)

Viruses and Virus Propagation

Various strains of Semliki Forest virus (SFV), existing and newly made were utilised in this project (Table 2.1).

Virus Strain	Backbone	Modification
SFV4	n/a	Virus derived from SFV4 cDNA clone (prototype strain of virus).
A7(74)	n/a	None, naturally occurring strain of SFV
SFV L10	n/a	None, naturally occurring strain of SFV
SFV4(3H)-eGFP virus is annotated SFV(3H)-eGFP in Tamberg *et. al.* (2007)	SFV4	Insertion of enhanced green fluorescent protein (eGFP) gene between nsP3 and nsP4, designed for fast processing of foreign gene from the non-structural polyprotein.
SFV4(3L)-eGFP	SFV4	Insertion of eGFP gene between nsP3 and nsP4, designed for slower processing of foreign gene from the non-structural polyprotein.
SFV4(3H)-euCre	SFV4	Insertion of cre recombinase gene between nsP3 and nsP4, designed for fast processing of foreign gene from non-structural polyprotein.
SFV4(3L)-euCre	SFV4	Insertion of cre recombinase gene between nsP3 and nsP4, designed for slower processing of foreign gene from the non-structural polyprotein.
SFV4-steGFP	SFV4	Insertion of eGFP gene between the capsid gene and the pE2/3 gene (structural area of the genome).
SFV4-steuCre	SFV4	Insertion of cre recombinase gene between the capsid gene and the pE2/3 gene (structural area of the genome).
SFV4-RDR-steGFP	SFV4-RDR	Same as SFV4-steGFP but backbone has a mutation at the nuclear localisation signal of nsP2 that makes the virus less virulent.
SFV4-RDR-steuCre	SFV4-RDR	Same as SFV4-steuCre but backbone has a mutation at the nuclear localisation signal of nsP2 that makes the virus less virulent.

Table 2.1 List of all viruses used in this project.

All recombinant viruses were constructed in the Estonian Biocentre, University of Tartu, Tartu, Estonia by Professor Andres Merits. Viruses were safely transported back to Edinburgh in the form of infectious plasmid cDNA (icDNA). icDNA was used to transform XL-10 Gold *Escherichia coli* (*E. coli*) Ultracompetent cells according to the protocol described in this chapter. Following growth of bacteria icDNA plasmid was extracted and quantified. Two μg of icDNA were then linearised using *Spe*I restriction endonucleases and transcribed *in vitro*. The *in vitro* transcript was electroporated into baby hamster kidney (BHK-21) cells; the contents of an approximately 80% confluent 175 cm^2 tissue culture flask was electroporated. Electroporated cells were put in a fresh 175 cm^2 tissue culture flask together with 20 ml of 10% GMEM culture medium and incubated at 37°C in a humid environment enriched with 5% CO_2. Supernatant containing virus was collected 24 hrs after electroporation, centrifuged at 450 x g for 5 minutes to remove any cell debris and aliquoted into 1 ml aliquots in cryovials and stored at – 80°C.

To further propagate recombinant or natural occurring viruses, approximately 80% confluent 175 cm^2 tissue culture flasks of BHK-21 cells were infected with the virus to be propagated at a multiplicity of infection (M.O.I) of 0.1 for 1 hour at room temperature. Twenty ml of 2% GMEM culture medium were added and cells were incubated for 24 hours at 37°C, 5% CO_2. Virus containing supernatant was collected and stored at – 80°C. All viruses were titrated using standard plaque assay.

Virus-Like Particles (VLPs)

The split-helper system developed by Smerdou and Liljeström (Smerdou & Liljestrom, 1999) was used for the production of VLPs carrying the gene for cre recombinase. Briefly, pSFV1-euCre and pSFV-helper (containing the genes coding for the structural proteins of the virus) plasmids were linearised using *Spe I* restriction endonuclease and after purification were *in vitro* transcribed to produce RNA. The RNAs were mixed and electroporated into 1 x 10^7 BHK-21 cells. The cells were then placed into a 175 cm^2 tissue culture flask with 35 ml of pre-warmed medium. The flask was incubated at 33°C, 5% CO_2. When cytopathic effect was observed (approximately 48 hours after electroporation), the supernatant was collected and clarified by centrifugation, three times for 30 minutes each at 27000 x

g. Fifteen ml of 20% (w/v) sucrose in sterile TNE buffer (pH 7.4) was added to each ultracentrifugation tube and 17.5 ml of clarified supernatant was layered on top of the sucrose cushion using a 20 ml sterile syringe. Tubes were placed in the holder and balanced. The holders were then attached to the rotor and ultracentrifuged at 84,600 x g for 90 minutes. Supernatants were decanted and the VLP containing pellets resuspended in 100 µl TNE buffer for 2 hours. Pellets were collected and the tubes were rinsed with an additional 50 µl TNE buffer. Aliquots of 50 µl were prepared, snap frozen in liquid nitrogen and stored at – 80°C. VLPs expressing eGFP, SFV1-eGFP, were used in one experiment. These VLPs were kindly donated by Mr Gerald Barry.

In vitro Transcription

Approximately 1.66 µg of plasmid DNA or icDNA was linearised using *Spe I* restriction endonuclease and was *in vitro* transcribed to synthesise capped transcripts. The reagents shown in Table 2.2 were added to an eppendorf tube at room temperature (except SP6 polymerase) in the order listed.

Reagent	**Quantity**
Spe I cut plasmid	1.66 µg
10X SP6 buffer	5.0 µl
10 mM M^7 G (5')ppp (5') G (cap analog)	5.0 µl
50 mM DL Dithiothretiol (DTT)	5.0 µl
rNTP mix (10 mM ATP, CTP and UTP, 5 mM GTP	5.0 µl
Recombinant RNasin Ribonuclease Inhibitor (60 U)	1.5 µl
SP6 RNA Polymerase (75 U)	1.5 µl
Nuclease-free H_2O	to 50 µl

Table 2.2 Reagents used for *in vitro* transcription

The reaction was incubated for an hour at 37°C to produce capped transcripts. Synthesis of RNA was verified using a 1% agarose gel. *In vitro* transcripts were stored at – 80°C.

Animal Experiments

Mice

Various strains of mice were used (Table 2.3). Mice were maintained in the Centre for Infectious Diseases animal unit at the University of Edinburgh under pathogen-free conditions, with environmental enrichment, a 12 h light/dark cycle and food and water supplied at *libitum*. Most mice used were between 3 and 6 weeks of age. A small number of neonatal mice (8 days old) were used. All experiments were approved by the University of Edinburgh ethical review process and were carried out under the authority of a UK Home Office license.

Strain	Description	Background	Source
Balb/c			Harlan
wt129			On site
A129	IFN α/β receptor knockout	wt129	B&K
ROSA26	eGFP inserted at the ROSA26 locus	C57Bl/6	On site
ROSA26-EYFP	EYFP inserted into the ROSA26 locus	C57Bl/6	On site
sGFP7	Random insertion of eGFP expressing cassette	C57Bl/6	On site
sGFP97	Random insertion of eGFP expressing cassette	C57Bl/6	On site

Table 2.3 List of mouse strains used.

Infection of Mice

Two different routes of infection were used.

I. **Intra-cerebral infection (i.c.)**: Mice were anaesthetised using halothane mixed with O_2 and 20 µl of 5 x 10^4 PFU/ml of virus in 0.75% PBSA (phosphate buffered saline containing 0.75% of bovine serum albumin (BSA)) were inoculated directly into the brain using a 28 G needle.

II. **Intra-peritonial infection (i.p.)**: Mice were immobilised and 100 µl of virus in 0.75% PBSA were given i.p to each mouse using a 20 G needle. Two

different doses of virus were used. The intraperitoneal route was also used for administration of hyperimmune serum (HI-serum).

All virus inoculation stocks were titrated prior to their use to make sure the doses of virus given were correct.

Tissue Sampling

Mice were euthanised by CO_2 overdose according the Home Office legislation. To collect blood and internal organs the abdominal region of the animal was opened using surgical scissors and using a pasteur pipette two drops of heparin were added to the thoracic cavity. The right auricle of the heart was cut and blood was collected into eppendorf tubes and centrifuged at 500 x g in a standard bench top centrifuge for 5 minutes to separate the cellular fraction of blood from serum. Serum samples were stored at – 80°C. After collection of blood, the internal organs of the animal were collected and placed into bijoux tubes containing 4% neutral buffered formaldehyde. Heart, lung, liver, kidney, spleen and pancreas were collected and processed for histology. Subsequently, the skull of the mouse was carefully opened, the spinal cord was cut and the brain was bisected sagitally down the midline. Half of the brain was placed into 4% neutral buffered formaldehyde and processed for histology. The other half of the brain was either snap frozen using dry ice to be used for virus titration or was submerged immediately in 2 ml RNA*later* RNA a reagent, which inhibits RNases (RNA-degrading enzymes) and preserves RNA in tissue samples to be used for RNA extraction. RNA*later* stabilised samples were stored at 4°C.

Histology

Processing of Tissues and Cryosectioning

After sampling, tissues intended to be used for histology studies were kept for at least 24 hours (maximum 48 hours) into 4% neutral buffered formaldehyde. Then the tissues were processed through graded sucrose solutions to 25% sucrose (5% (w/v) for 1 hour, 10% (w/v) for 1 hour and 25% (w/v) overnight), embedded into OCT cryoprotection medium and frozen using isopentane. Tissue containing OCT blocks

were then stored at – 80°C. Using a cryomicrotome tissues were sectioned into 12 - 14 μm thick sections and placed on polysine coated slides to ensure optimal adhesion. Slides were stored at – 80°C.

Immunostaining

Cryosections of brain tissue were immunostained using antibodies targeting various viral and cellular epitopes. Initially, slides were removed from – 80°C, placed in front of a fan and allowed to dry for approximately 30 minutes at room temperature. Two different methods were used in order to increase permeability of cell membranes in the sections; sections were either treated with 0.3% Triton-X100 for 15 minutes at room temperature or with proteinase K (20 μg/ml) for 15 minutes at 37°C followed by a 5 minute inactivation step using EDTA/Glycine/PBS. Following membrane permeabilisation the slides were placed on a staining rack and washed in PBS 3 times for 10 minutes constant shaking. Excess PBS was removed and tissue sections were treated with CAS block for 30 minutes at room temperature inside a humid chamber. Blocking solution was removed and the primary antibody was diluted to the desired concentration in CAS block and added to the sections. Sections were covered using parafilm, placed into a humid chamber and incubated overnight with primary antibody. The following day parafilm was removed carefully, excess primary antibody solution was drained from the slides and the slides were washed 3 times, for 15 minutes each, with PBS. The secondary antibody was diluted using CAS block and added to the sections which were then incubated for a further 3 hours at room temperature. All secondary antibodies were biotinylated. After incubation with secondary antibody sections were washed 3 times, for 15 minutes each, with PBS. Streptavidin (SA) conjugated Alexa Fluor 594 (excitation 590 and emission 617 nm) was diluted 1:1400 in H_2O and added to the sections for 45 minutes at room temperature. The slides were washed 3 times, for 15 minutes each, with PBS and then mounted. The mounting media contained DAPI (4'-6-Diamidino-2-phenylindole) to allow visualisation of nuclei. In some cases sections were incubated with TO-PRO 3 nuclear marker solution before mounting with fluorescence mounting medium (without DAPI). Coverslips were then permanently sealed around

the perimeter using nail varnish and stored in a dark box at 4°C. Sections of non-infected brain or sections of infected brain where no primary or no secondary antibody was added were used as controls. Systematic optimisation was performed and optimum conditions for all antibodies used were established. In Table 2.4 the antibodies used are shown together with their optimal dilutions.

Name	Type	Host	Isotype	Source	Optimum Dilution
anti-nsP3	Primary	Rabbit	Polyclonal	Tero Ahola	1:800
anti-SFV	Primary	Rabbit	Polyclonal	In house	1:500
anti-GFAP	Primary	Rabbit	IgG	Sigma	1:750
anti-NeuN	Primary	Mouse	IgG1	Chemicon	1:400
anti-CNPase	Primary	Rabbit	Polyclonal	Wistar Institute	1:400
anti-F4/80	Primary	Rat	IgG2b	Abcam	*
anti-Cre	Primary	Mouse	IgG1	Abcam	*
anti-Rabbit IgG biotinylated	Secondary	Goat	IgG	Vector Labs	1:500
anti-Mouse IgG biotinylated	Secondary	Sheep	IgG	Diagnostics	1:500
anti-Rat Ig biotinylated	Secondary	Rabbit	Polyclonal	Abcam	*
SA-Alexa Fluor 594	Tertiary	-	-	Invitrogen	1:1400

Table 2.4 List of antibodies used for immunostainings.

Microscopy of Animal Tissues

Sections of various tissues on polysine coated slides were submerged in PBS, excess liquid was drained and slides were mounted as described above (some slides were mounted using mounting medium containing propidium iodide (PI) as a nuclear marker). Standard histology stains such as eosin and haematoxylin were not used because they mask the fluorescence signal. Sections were screened for fluorescence using a standard Zeiss Axioskop2 microscope with filters suitable for visualisation of eGFP (green), Alexa Fluor 594 (red) and DAPI (UV) or a Zeiss Axioskop confocal microscope using 3 different lasers; an argon laser (488 nm) suitable for visualisation of eGFP, a Helium/Neon laser (He/Ne 1, 543 nm), suitable for visualisation of Alexa Fluor 594 and PI and a Helium/Neon laser (He/Ne 2, 633 nm), suitable for visualisation of To-Pro3 (far red side of the spectrum).

Cell Lines

BHK-21 cells

BHK-21 (clone 13) cells were used to propagate and titrate viruses and to determine the infectious virus titre of various samples. Cells were maintained in 175 cm^2 tissue culture flasks using Glasgow's minimum essential medium (GMEM) containing 10% new born calf serum (NBCS), 10% tryptose phosphate broth, antibiotics (penicillin/streptomycin – 100U/ml and 100 µg/ml, respectively) and L-glutamine (2 mM) at 37°C and in a humidified environment containing 5% CO_2. When cells were confluent, culture medium was removed and the cell monolayer rinsed with 0.02% versene. After versene was removed 5 ml of 0.25% trypsin/EDTA was added and the cells were incubated at room temperature until dislodged from the plastic. Following that, 10 ml of 10% GMEM was added to neutralise the trypsin and the cell suspension was centrifuged for 5 minutes at 450 x g. The supernatant was discarded and the cells were resuspended in 10 ml medium. Ten µl of the cell suspension was diluted into 90 µl of trypan blue and using a glass haemocytometer the number of cells was calculated. Three to five million cells were seeded into 175 cm^2 tissue culture flasks with 25 – 30 ml of 10% GMEM and kept at 37°C with 5% CO_2. Cells were passaged about 30 times after that their growth was very slow.

ROSA26 Mouse Embryonic Fibroblasts (MEFs)

To produce MEFs from ROSA26 Cre reporter mice a 13.5 days pregnant mouse was sacrificed by cervical dislocation. The animal was swabbed with absolute ethanol and the abdomen was dissected. The uterine horns were removed and placed into a petri dish with sterile phosphate buffered saline (sPBS) to remove blood. The amniotic sac was then removed and placed in another petri dish with sPBS. Embryos were released from the amniotic sac and placed in a petri dish with sPBS. Neuronal tissue was removed by decapitation. Following that the liver was removed and the embryos were grinded using a blade into 1 ml trypsin/EDTA. Ground tissue was incubated at 37°C for 10 minutes. A further 2 ml of trypsin/EDTA were then added

and the tissue was incubated for a further 10 minutes. Digested tissue was transferred to a universal tube and allowed to settle. The supernatant containing cells was placed into a fresh universal tube and following the addition of fresh Dulbecco's modified eagle's medium (D-MEM), containing 10% of foetal calf serum (FCS), antibiotics (100 U/ml penicillin and 100 μg/ml streptomycin) and L-glutamine, the cells were centrifuged for 5 minutes at 450 x g. The pellet was resuspended in 10 ml of medium and centrifuged again. The medium was decanted and cells were resuspended in fresh medium and added into a 80 cm^2 tissue culture flask along with 15 ml of fresh medium. Cells were incubated for approximately 2 days at 37°C in humidified environment containing 5% CO_2. After 2 days dead cell debris was removed, fresh medium was added and cells were incubated until 90% confluent. Then the cells were passaged into 175 cm^2 flasks and maintained as described above for BHK-21 cells. Before passage 2 vials of cells were frozen and stored in liquid nitrogen.

C6/36 Mosquito Cells

C6/36 cells are mosquito larvae cells derived from *Aedes albopictus*. Cells were purchased from European Collection of Cell Cultures. C6/36 cells were maintained using L-15 medium (Leibovitz) containing 10% FCS, 10% tryptose phosphate broth, and L-glutamine (2mM) in 175 cm^2 tissue culture flasks. Tissue culture flasks containing cells were kept at 28°C without additional CO_2. To passage the cells, old medium was removed from the tissue culture flask and the cell monolayer was rinsed with 5 ml of fresh L-15 medium. To dislodge the cells, medium was removed, and a cell scraper was used. Following that 10 ml of L-15 medium was added and the suspension containing the cells was transferred into a universal tube. The suspension was centrifuged at 450 x g for 5 minutes. The supernatant was discarded and the cells were resuspended in 10 ml of medium. Cells were counted using a haemocytometer as previously described and 175 cm^2 flasks were seeded with 5 x 10^6 cells.

K562 and K562-DSRed[EGFP] cell lines

K562 and K562-DSRed[EGFP] cells were kindly provided by Dr Peter Ponsaerts, University of Antwerp. Briefly, K562 cells were cultured in Iscove's modified Dulbecco's medium (IMDM) containing 10% foetal calf serum (FCS), 2 mM L-glutamine, 100 U/ml penicillin and 100 μg/ml streptomycin. To maintain K562-DSRed[EGFP] cells the culture medium described above was used but G418 (geneticin sulphate) was supplemented at a concentration of 0.5 mg/ml to avoid elimination of the DSRed[EGFP] insert. Cells were cultured in suspension and maintained at 37°C in a humidified environment with 5% CO_2. In order to maintain cells in logarithmic phase growth, when the desired confluency was reached cells were passaged into fresh culture media in a 1:3 or 1:5 ratio.

Rat Hippocampal Neurons

Rat hippocampal neurons were kindly provided by Colin Rickman, Centre for Integrative Physiology, University of Edinburgh. Cells were isolated from rat pup brain and plated in 6 well plates onto poly-D-lysine coated coverslips (optimal plating density ~150 cells/mm^2). Cells were maintained using neurobasal-A/B-27 growth medium containing 10% horse serum, L-glutamine (0.5 mM), B-27 supplement (1 ml of 50X per 50ml), penicillin and streptomycin (125 U/ml). Plates were maintained in a humidified environment with 5% CO_2. The cells were given enough time to transform to mature neurons (approximately 3 weeks) and were then infected with virus.

Infection of Cultured Cells

All adherent cell lines (BHK-21, ROSA26 MEFs, C6/36 mosquito cells and rat hippocampal neurons) were infected as described in the plaque assay protocol. For the infection of K562 and K562-DSRed[EGFP] cells, the cell suspension was centrifuged for 5 minutes at 450 x g and resuspended in 10 ml of fresh culture medium. Cells were counted and diluted to the desired density using serum-free

culture medium. Virus was added (at the appropriate M.O.I) and cells were incubated for 1 hour at room temperature with constant shaking. Following infection cells were centrifuged at 450 x g for 5 minutes and the virus containing supernatant was decanted, cells were washed for one more time using serum-free culture medium and transferred to tissue culture flasks containing complete media. The same protocols were used for infection using virus like particles (VLPs).

Transfection of Cultured Cells by Electroporation

Nucleic acids were transfected into BHK-21 cells, ROSA26 MEFs and K562/K562-DSRed[EGFP] cells using a BioRad Gene Pulser Xcell electroporator. On the day of the experiment cells were collected, counted and resuspended in ice-cold phosphate buffered saline (PBS) at a concentration of 6.25 x 10^6 cells per ml. Plasmid DNA or *in vitro* transcribed RNA were mixed with 800 µl of cell suspension. Four hundred µl of cells/nucleic acid mixture were added to a 0.4 cm electroporation cuvette and cells were pulsed twice using a square wave of 140 volts for 25 mseconds. Electroporated cells were transferred to suitable containers (6 well plates or 175 cm^2 tissue culture flasks) and appropriate tissue culture media added. Plates or flasks were incubated at 33 or 37°C (depending on the application) with 5% CO_2.

Microscopy of Infected and Transfected Cells

Infected cells were examined for cytopathic effect and/or presence of eGFP fluorescence using a Nikon inverted microscope. Given that multiple layers of plastic, distort the UV light it was not always possible to obtain good images using this microscope. For this reason cells were cultured on chamber slides, infected, fixed, mounted and examined using either a standard Zeiss Axioskop2 microscope or a Zeiss Axioskop confocal microscope.

Freezing and Thawing Cell lines

To ensure adequate amounts of cells were always available frozen stocks of all cell lines mentioned above (sole exception being the rat hippocampal neurons) were

prepared. Briefly, 5 x 10^6 cells were resuspended in 1 ml of FCS containing 10% dimethylsulfoxide (DMSO) and cells were put into vials suitable for deep freezing (cryovials). Cryovials were put into a cell freezer containing isopropanol and the cell freezer was placed in – 80°C overnight. The next morning the cells were transferred to liquid nitrogen. To grow the cells from frozen stocks, cryovials were removed from liquid nitrogen and kept in dry ice. Then the cells were thawed rapidly using a 37°C water bath and slowly mixed with 10 ml of pre-warmed culture medium. Cell suspension was centrifuged at 450 x g and the supernatant was decanted. Ten ml of fresh medium were added and cells were transferred into a 25 cm^2 tissue culture flask and incubated in a humidified environment at 37°C with 5% CO_2.

It is important to note that all the tissue culture procedures described above were carried out in a class II hood under aseptic conditions to avoid microbiological contamination.

Plaque Assay

Plaque assay was used to detect and titrate infectious virus in the brains of infected mice and in infected cell supernatants. Six well plates were seeded with 2 ml 10% GMEM containing 3 x 10^5 BHK-21 cells and incubated at 37°C and in a humidified environment containing 5% CO_2. During incubation GMEM containing 2% NBCS was prepared and half brain samples were thawed and homogenised immediately in 1.35 ml of sPBS. It is estimated that the mass of a half brain is ~0.15 g, homogenisation in 1.35 ml therefore gives a final volume of 1.5 ml and a 1 in 10 weight to volume homogenate. Ten-fold serial dilutions of brain homogenates/cell supernatants/animal blood were prepared using 0.75% PBSA. When the monolayers were approximately 80% confluent, growth medium was removed, monolayers were washed with sPBS and 400 µl of each dilution were added to duplicate wells starting with the most dilute sample. The plates were incubated for 1 hour at room temperature inside a humid box. GMEM containing 2% NBCS was mixed with 4% agar (10:3 ratio) and 2 ml of the mixture was used to overlay each well. The plates were then incubated for 48-72 hours (depending on the phenotype of the viral strain) at 37°C in 5% CO_2. After incubation, the plates were fixed with 3 ml of 4% neutral

buffered formaldehyde for 1 hour at room temperature. The fixative and the agar plug were then removed and the monolayers stained with 0.1% toluidine blue for 30 minutes. Finally, the plates were washed and the plaques counted. To calculate the pfu per ml content of each sample the following formula was used: (average number of plaques/amount of inoculum) x dilution factor.

Plaque Assay-Limit of Detection

The limit of detection of the plaque assay was determined for each one of the animal tissues and the cell supernatants. Limit of detection is the threshold below which the assay was unable to detect any infectious virus. The formula shown above was used to calculate the titre if the most concentrated dilution used in each assay produced a single plaque. When brain homogenate was used the 10^{-1} dilution was the highest dilution used. Because the brain homogenate was already a 1 in 10 dilution of the original material the 10^{-1} dilution used in the plaque assay was actually a 10^{-2}. Applying the formula mentioned above it works out that if this dilution was used if would give a titre 250 PFU/ml. The logarithm of that is 2.397(~2.4) Log_{10} PFU/ml. In an identical manner, the limit of detection of the plaque assay using animal blood or cell supernatants was calculated to be 1.397(~1.4) Log_{10} PFU/ml.

Plaque Purification of Viruses

To purify viruses from plaques the virus containing cell supernatant/brain homogenate was first titrated according to the protocol described above. Following that, fresh 6 well plates were seeded with BHK-21 cells and the virus containing cell supernatant/brain homogenate was diluted in 0.75% PBSA so as approximately 20 PFU were contained in 400 µl and the suspension was used to infect 80% confluent monolayers of BHK-21 cells. The plates were covered with agar as described above and incubated for 48-72 hours at 37°C in 5% CO_2. After this, an extra ml of GMEM containing 2% NBCS mixed with 4% agar (10:3 ratio) and 0.02% neutral red was added to each well in order to facilitate visualisation of plaques. The plates were incubated for another 24 hours. In the meantime, 24 well plates were seeded with 2 ml of 10% GMEM containing 1 x 10^5 BHK-21 cells and incubated at 37°C and in an

environment containing 5% CO_2. The following day, sterile pipette tips were used to pick individual plaques and each plaque was then added to a separate well of a 24 well plate. The plates were incubated further at 37°C in 5% CO_2 until cytopathic effect was observed.

One-Step Growth Curves

To obtain One-Step growth curves BHK-21 cells monolayers were infected at an M.O.I of 10 in triplicate. Briefly, 6 well plates were seeded with BHK-21 cells and incubated at 37°C with 5% CO_2. When the monolayers reached the desired confluency the growth medium (GMEM with 10% NBCS) was removed and the cells were washed with sPBS and infected with the required amount of virus diluted in 400 μl of 0.75% PBSA. Infection was 1 hour long and took place in a humid chamber at room temperature with constant gentle shaking. After 1 hour the monolayers were washed three times using 0.75% PBSA to remove any unbound virus. Two ml of pre-warmed 10% GMEM were added. That was time-point zero. Two hundred μl of supernatant were collected every 2 hours for the next 12 hours in sterile eppendorf tubes and the samples were stored at – 80°C. All samples were titrated according to the protocol described above and one-step growth curves were constructed.

Western Blotting

BHK-21 cells were grown in 6 well plates until approximately 80% confluent. Cells were infected as previously described. Following that, and at various time-points depending on the strain of virus used, culture medium was removed and cells were lysed using 300 μl Laemmli sample buffer. Lysates were transferred to an eppendorf tube and heated at 100°C for 5 minutes. BioRad's Mini-Protean II apparatus was used for protein electrophoresis. Briefly, the gel casting apparatus was assembled and filled with resolving gel containing 10% acrylamide to a level just below the bottom of the comb. A layer of isobutanol was added and the gel allowed to set for approximately 20 minutes. Isopropanol was removed with filter paper and stacking gel containing 4% acrylamide was added, the combs were inserted and the gel

allowed to set for approximately 20 minutes. The combs were removed, the gel was assembled in the electrophoresis tank of the Mini-Protean II apparatus and the chambers of the apparatus were filled with running buffer (BioRaD 10x Tris/Glycine/SDS Buffer). Ten µl of each sample was added to the wells and the gel electrophoresis was performed by applying 170 V for 1 hour (electrophoresis was stopped when blue dye band reached the bottom of the resolving gel). Nitrocellulose membrane was soaked in distilled H_2O for 3 minutes and then in transfer buffer (Tris base 5.8 g, glycine 2.9 g, SDS 0.37 g, ethanol 200 ml and H_2O to a final volume of 1 L) for 10 minutes. The gel was also soaked in transfer buffer for 5 minutes. A sandwich consisting of 3 MM Whatman paper (x3) cut in the size of the gel and soaked into transfer buffer, nitrocellulose membrane, SDS gel and another 3 pieces of 3 MM Whatman paper. The proteins were transferred to the membrane by applying a current of 25 V for 30 minutes. Nitrocellulose membrane was blocked overnight at 4°C using blocking solution containing 5% non-fat milk in PBS containing 0.1% Tween 20. Primary antibody was diluted in blocking solution and added to the membrane for approximately 1 hour at room temperature. The membrane was washed 3 times for 15 minutes each using wash buffer (50 ml 1M Tris pH 7.5, 30 ml 5M NaCl, 1 ml Tween 20 and H_2O to a final volume of 1 lt). Secondary antibody was diluted in blocking solution and added to the membrane for 45 minutes at room temperature. The membrane was washed 3 more times for 10 minutes each. The reagents of the ECL detection kit were mixed (1:1) and added to the membrane for 1 minute. Nitrocellulose membrane was wrapped using cling film, put into exposure cassette and taped in place. X-ray film was exposed to the membrane, time varied between 1 minute and 1 hour, developed and dried. Optimal concentrations of all antibodies used for western blotting can be seen in Table 2.5.

Name	Type	Host	Isotype	Source	Optimum Dilution
anti-nsP1	Primary	Rabbit	Polyclonal	Tero Ahola	1:10000
anti-nsP2	Primary	Mouse	Monoclonal	Tero Ahola	1:6000
anti-nsP3	Primary	Rabbit	Polyclonal	Tero Ahola	1:10000
anti-nsP4	Primary	Rabbit	Polyclonal	Tero Ahola	1:4000
anti-capsid	Primary	Rabbit	Polyclonal	Andres Merits	1:10000
anti-eGFP	Primary	Rabbit	IgG1	Molecular Probes	1:1000
anti-Cre	Primary	Mouse	IgG1	Abcam	1:500
anti-Rabbit IgG peroxidase	Secondary	Goat	IgG	Sigma	1:10000
anti-Mouse IgG peroxidase	Secondary	Goat	IgG	Sigma	1:10000

Table 2.5 List of antibodies used for western blotting.

RNA Extraction

From Cultured Cells

Total RNA was extracted from virally infected cells using the Qiagen RNeasy Mini kit according to the manufacturer's instructions. Briefly, 1 x 10^6 infected cells were lysed using 350 µl of RLT buffer containing 1% β-mercaptoethanol. Cell lysate was transferred to a 1.75 ml sterile RNase-free eppendorf tube and passed at least 10 times through a 21 gauge needle to ensure complete lysis. Three hundred and fifty µl of 70% molecular grade ethanol was added to the lysate and the mixture mixed by pippeting. Seven hundred µl of suspension were added in an RNeasy mini column and the column centrifuged for 15 seconds at 8,000 x g in a table top centrifuge. The column was then washed by adding 350 µl of RW1 buffer and centrifuging at 8,000 x g for 15 seconds. Eighty µl of RNase-free DNase was then added directly onto the membrane of the column and the column was incubated for 15 minutes at room temperature. Another 350 µl of RW1 buffer were added and the column was centrifuged. The column was then transferred to a new collection tube and 500 µl of buffer RPE was added to the column in order to precipitate the RNA. After centrifugation at 8,000 x g for 15 seconds another 500 µl of buffer RPE was added and the column was centrifuged for 3 minutes at maximum speed to ensure all

residual ethanol was removed. Thirty µl of RNase-free water was passed twice through the column to elute the RNA.

From Brain Samples

All brain samples were stored in RNA*later* stabilisation reagent, which inhibits RNAses and preserves RNA in tissue samples. Total RNA was extracted using the RNeasy Lipid kit according to the manufacturer's instructions. Briefly, 100 mg of brain tissue was homogenised with 1 ml of QIAzol lysis reagent using a disposable RNase-free plastic homogeniser. The homogenate was passed through a 20 gauge needle at least 20 times and was then incubated for 5 minutes at room temperature to promote dissociation of nucleoprotein complexes. Then 200 µl of chloroform was added and the homogenate was shaken vigorously. After a 3 minute incubation at room temperature the sample was centrifuged at 12000 x g for 15 minutes at 4°C. Following centrifugation three separate layers were formed; the upper aqueous phase was transferred to a new RNase-free eppendorf tube and 70% ethanol was added (1:1 ratio). The subsequent steps of the protocol are identical to the ones described above.

Nucleic Acid Quantification and Qualification

All RNA samples were quantified using a NanoDrop ND-1000 spectrophotometer and the quality of the RNA was assessed using the Agilent Bioanalyser. Briefly, 1 µl of each RNA sample was placed in the NanoDrop ND-1000 spectrophotometer and the RNA concentration was measured (range 2 ng/µl-3 µg/µl). After this 1 µl of each sample was diluted using RNase-free water to obtain samples within a range of 50-250 ng/µl. All samples were heat-denatured (70°C for 2 minutes) and placed immediately on ice. Finally, samples were loaded to the Agilent RNA 6000 Nano assay chip (12 samples per chip) following the manufacturer's instructions and the chip was analysed using the Agilent 2100 Bioanalyser. At the end of the assay the analysis software provides information about the integrity of the RNA. This data can then be used to assess if the RNA samples are suitable for downstream procedures. All DNA samples were quantified using the NanoDrop ND-1000 spectrophotometer in a similar manner to the RNA samples.

First-Strand cDNA Synthesis by Reverse Transcription

Reverse transcription was performed into 0.2 ml thin-walled PCR tubes. The reaction mixture had a volume of 20 µl and contained the following: 1 µl of Oligo $(dt)_{15}$ primer, 2 µg total RNA, 1 µl of 10 mM dNTPs and DNase/RNase-free water to a volume of 12 µl. The mixture was heated for 5 minutes at 65 °C and then chilled on ice for a minute. The tubes were kept on ice and 4 µl of 5X First-Strand buffer, 2 µl of 0.1 M DTT and 1 µl of RNasin recombinant ribonuclease inhibitor were added. The tubes were then incubated at 42°C for two minutes. Following that, 1 µl of SuperScript II RNase H^- reverse transcriptase enzyme (from Moloney Murine leukaemia virus) was added and the reaction was incubated for an hour at 42°C. A final incubation of 15 minutes at 70°C was performed and the cDNA was stored at -20°C.

Polymerase Chain Reaction (PCR)

Polymerase chain reaction (PCR) was utilised for the amplification of nucleic acids. Two different thermostable polymerases were used depending on the downstream application for which the amplified fragment would be used. If the amplified fragment was intended to be used for blunt-end cloning and subsequent sub-cloning into SFV replicons and/or full length SFV icDNA Platinum *Pfx* DNA polymerase, which also provides high fidelity amplification, was used. The reaction mixture had a volume of 50 µl and contained the following: 5 µl 10X *Pfx* amplification buffer, 1.5 µl of 10 mM dNTPs, 1 µl of 50 mM $MgSO_4$, 1 µl of each primer (50 pM), 2 µl of template DNA, 1 U of Platinum *Pfx* DNA polymerase and DNase/RNase-free water to a final volume of 50 µl. The reactions were incubated in a thermal cycler using the following protocol: an initial denaturation step of 3 minutes at 94°C followed by 30 cycles of three steps; denaturation at 94°C for 15 seconds, annealing at 55°C for 30 seconds and extension at 68°C for 1 minute 30 seconds. Then a final extension step was performed at 72°C for 15 minutes. A non-template (H_2O) control was used in every PCR run to test possible contamination of the reagents. The PCR products

were analysed using gel electrophoresis (1% agarose gel) and stored at – 20°C for further experiments.

For diagnostic PCR and to use the amplified fragments for sequencing standard *Taq* DNA polymerase was used. The reaction mixture had a volume of 20 µl and contained the following: 2 µl of 10X PCR buffer containing 15 mM $MgCl_2$, 0.4 µl of 10 mM dNTPs, 0.5 µl of each primer (50 pM), 0.3 µl of *Taq* DNA polymerase and DNase/RNase-free water to a final volume of 20 µl. The reactions were incubated in a thermal cycler using the following protocol: an initial denaturation step of 5 minutes at 95°C followed by 27 cycles of three steps; denaturation at 94°C for 30 seconds, annealing at 55°C for 30 seconds and extension at 72°C (time varied depending on the size of the amplified fragment. Then a final extension step was performed at 72°C for 15 minutes. A non-template (H_2O) control was used in every PCR run to test for possible contamination of the reagents. Suitable positive controls were also included when diagnostic PCR was performed The PCR products were analysed using gel electrophoresis (1% agarose gel) and stored at – 20°C for further experiments. A list of all primers used is shown in Table 2.6.

Name	**Primer Sequence 5'→3'**
eGFP-Apa	TATAGGGCCCATGGTGAGCAA
eGFP-Bam	TATGGATCCTGATCTAGAG
euCre-Apa	TATGGGCCCATGACAGGAGAACCACCAT
euCre-Bgl	TATAGATCTGCTAATCGCCATCTTC
CreRec-for	TATAGATCTACAGGAGAACCACCAT
CreRec-rev	TATCCCGGGGCTAATCGCCATCTTC
nsP3-4973	ATACCATGTAGATGGGGTGCAGAAGGT
nsP4-5646	TGCGGTCCAGGAGGAGAAAATGTACC
St-for	ACGTGAAAGGAGTCATCGAC
St-rev	GGTGGCTACCTTCAAAGATG

Table 2.6 List of primers used for PCR amplification.

Agarose Gel Electrophoresis

DNA and RNA were analysed by agarose gel electrophoresis. Briefly, 0.7 – 2% agarose gels were prepared using 0.5 M Tris borate (TBE) buffer with 0.5 μg/ml ethidium bromide to enable visualisation of DNA or RNA under UV light. Samples were mixed with 6X loading buffer and loaded in the wells of the agarose gel. Electric current was then applied to the gel (100 – 130 volts depending on the percentage of the gel) for approximately 1 hour in order to separate different fragments of nucleic acid. As a size marker, two different DNA ladders were used; 1 Kb and 100 bp DNA ladder. Using a UV transilluminator nucleic acid fragments were visualised.

DNA Extraction from Agarose Gel

DNA fragments were extracted from agarose gel using the QIAquick Gel Extraction Kit according to the manufacturer's instructions. Briefly, DNA fragments were separated by electrophoresis and long wavelength UV light was used to visualise the fragments. Using a sterile blade the fragment was excised from the agarose gel and weighed. Three volumes of Buffer QG were added and the sample was incubated at 50°C until completely dissolved. One volume of isopropanol was then added and the sample mixed. The sample was applied to a QIAquick column and centrifuged for 1 minute at 17900 x g to bind the DNA onto the silica membrane. Flow-through was decanted and 500 μl of QG Buffer was added to remove any traces of agarose. The column was spun again and 750 μl of PE Buffer was applied, the column was allowed to stand for 5 minutes and centrifuged for 1 minute at 17900 x g. To ensure complete removal of residual ethanol, the QIAquick column was centrifuged for an additional minute. To obtain increased yield of DNA 30 μl of DNase-free H_2O were added to the column and the column was allowed to stand for 1 minute. Finally, the column was centrifuged for 1 more minute and the samples were stored at – 20°C for further experiments.

Molecular Cloning

TOPO Cloning

Zero Blunt® TOPO® PCR cloning was used for cloning of blunt-ended PCR fragments. The cloning reaction contained; 2 µl fresh PCR product, 1 µl salt solution, 2 µl molecular grade H_2O and 1 µl of pCR®-Blunt II-TOPO® vector. The reaction was incubated at room temperature for 15 minutes. Then 2 µl of the ligation reaction were used to transform One Shot® DH5α–T1 chemically competent *E. coli* cells.

pGEM-T Easy Cloning

PCR fragments were cloned into the pGEM®-T Easy vector according to the manufacturer's instructions. Briefly, 5 µl of 2X Rapid Ligation buffer, 1 µl (50 ng) of pGEM®-T-Easy Vector, 1 – 3 µl PCR product (depending on the size of the fragment), 3 Weiss units of T4 DNA ligase (1 µl) and molecular grade H_2O to a final volume of 10 µl. The reaction was incubated for approximately 16 hours at 4°C to maximise number of transformants. Following incubation 3 µl of the ligation reaction were used to transform subcloning efficiency DH5α chemically competent *E. coli* cells.

pSFV1 Vector Cloning

pSFV1 vector was kindly provided by Professor Peter Liljeström, Karolinska Institute, Sweeden. The vector has a multiple cloning site, which facilitates the insertion of foreign genes. For the insertion of a foreign gene the vector was digested using *Bam*HI and *Sma*I restriction endonucleases; because these two enzymes exhibit their maximum activity in different buffers sequential digestions were performed. One hour before the end of the second digestion calf-intestinal alkaline phosphatase (CIAP, 1U/µg of plasmid DNA) was added to the reaction in order to dephosphorylate the vector and avoid religation. The digested dephosphorylated vector was then purified using a Jetquick kit according to the protocol described

below. The insert was sequentially digested using *Bgl*II and *Sma*I restriction endonucleases and it was purified using a QIAquick PCR purification kit according to the protocol described below. Both the linearised vector and the insert were run on a 0.7% agarose gel to verify their size. Subsequently, ligation reactions using a 1:1, 1:3 and 3:1 molar ratio of vector:insert DNA were prepared. Each ligation reaction had a final volume of 10 µl and contained 1 µl ligase 10X buffer, 1 µl of T4 DNA ligase, and H_2O to make up the final volume. The amount of vector and insert varied according to the vector:insert ratio. To calculate the amounts of insert and vector required for each reaction the following formula was used: ((ng of vector x kb size of insert)/kb size of vector) x insert:vector molar ratio) = ng of insert. The reactions were incubated overnight at 4°C. Five µl of the ligation reaction were then used to transform subcloning efficiency DH5α chemically competent *E. coli* cells.

Bacterial Techniques

Bacterial Culture

Various laboratory strains of *E. coli* were used. These were grown in Luria-Bertani (LB) medium or on LB plates with 1.5% agar. Media was sterilised and agar melted by autoclaving. Media was supplemented with appropriate antibiotics (100 µg/ml ampicillin or 50 µg/ml kanamycin) prior to use. LB agar was poured into 10 cm diameter Petri dishes. Bacteria were plated on the surface of LB agar by spreading with a glass spreader and plates were incubated, inverted, at 37°C for approximately 16 hours. Single colonies from agar plates were used to inoculate liquid medium. Liquid cultures were incubated for approximately 16 hours with constant shaking at 225 rpm in an orbital shaker at 37°C. All bacterial procedures were performed under aseptic conditions.

Transformation of One Shot® DH5α - T1 and DH5α Chemically Competent cells

One Shot® DH5α – T1 chemically competent cells were transformed with the products of the TOPO cloning reaction. In brief, a vial of competent cells was

thawed on ice. Two µl of the cloning reaction were added to the cells and mixed gently. The vial was then incubated on ice for 30 minutes. Cells were then heat-shocked for 30 seconds at 42°C and 250 µl of pre-warmed SOC medium was added. The vials were incubated for 1 hour at 37°C with constant shaking at 225 rpm in an orbital shaker. Fifty or 100 µl of the transformation reaction was then plated on LB agar plates supplemented with 50 µg/ml kanamycin and the plates were incubated, inverted, for approximately 16 hours at 37°C.

To transform subcloning efficiency DH5α chemically competent cells, a vial of cells was thawed on ice and cells were aliquoted into 50 µl aliquots in 1.5 ml sterile eppendorf tubes. Three µl of the pGEM-T easy ligation reaction or 5 µl of the pSFV1 ligation reaction were added to the cells and the mixture was incubated for 30 minutes on ice. Cells were then heat-shocked for 20 seconds at 37°C and 950 µl of pre-warmed SOC medium was added. The vials were incubated for 1 hour at 37°C with constant shaking at 225 rpm in an orbital shaker. Fifty and 150 µl of the transformed cells was plated on LB agar plates supplemented with 100 µg/ml ampicillin and the plates were incubated, inverted, for approximately 16 hrs at 37°C. pGEM-T Easy vector allows blue/white colony screening to facilitate the selection of colonies carrying recombinant plasmids (insertion of a PCR fragment disrupts the coding sequence of β-galactosidase and colonies appear white on indicator plates) . Indicator plates were made by spreading 100 µl of 100 mM IPTG (isopropyl-beta-D-thiogalactopyranoside) and 20 µl pf 50 mg/ml X-Gal on the surface on LB agar plates supplemented with ampicillin. Plates were allowed to absorb IPTG/X-Gal for 30 minutes at 37°C. To allow development of colour these plates were incubated, inverted, for at least 17 hours at 37°C.

Transformation of XL 10-Gold Ultracompetent cells

Efficiency of transformation of DH5α cells by large constructs, like icDNA of the recombinant viruses, is low. For this reason XL 10-Gold ultracompetent cells, which are suitable for the transformation of large DNA molecules with high efficiency were used. Ultracompetent cells were chilled on ice and 100 µl were aliquoted into 15 ml pre-chilled Falcon tubes. Four µl of β-mercaptoethanol were added to the cells and

the cells were incubated for 10 minutes on ice; mixed gently every 2 minutes. Approximately 200 ng of plasmid DNA was added to the cells and the tubes were incubated for 30 minutes on ice. Cells were then heat-shocked for 30 seconds at 42°C and placed on ice for 2 more minutes. Pre-warmed SOC medium was added to a final volume of 1 ml and the tubes were incubated for 1 hour at 37°C with constant shaking at 225 rpm in an orbital shaker. Two hundred µl of the transformation mix was plated on LB agar plates supplemented with 50 µg/ml ampicillin and the plates were incubated, inverted, at 37°C for 24 hours.

Plasmid DNA extraction for Diagnostic Purposes (Miniprep)

The QIAprep Spin Miniprep Kit was used, according to the instructions given by the manufacturer, to isolate small amounts of plasmid DNA for diagnostic purposes (sequencing and restriction digestions). A single fresh colony was isolated from an LB agar plate and placed into 5 ml of LB broth supplemented with either 100 µg/ml ampicillin (50 µg/ml for XL 10-Gold ultracompetent cells) of 50 µg/ml kanamycin in universal tubes. Tubes were incubated overnight at 37°C at 225 rpm in an orbital shaker. After overnight incubation tubes were centrifuged at 1,500 x g for 6 minutes. Pelleted bacterial cells were resuspended in 250 µl Buffer P1 and transferred to a microcentrifuge tube. Lysis Buffer P2 was added (250 µl) and the tube was mixed by gentle inversion. Lysis was allowed to proceed for 5 minutes and 350 µl of buffer N3 was added and the tube was mixed gently and centrifuged at 17,900 x g for 10 minutes. The supernatant was transferred to a QIAprep Spin column and the column was centrifuged for 1 minute at 17,900 x g to bind the DNA to the silica-gel membrane. The column was washed by adding 500 µl of Buffer PB and centrifuged at 17,900 x g for 1 minute. An additional wash wish 750 µl of Buffer PE was performed followed by another centrifugation step. Column was centrifuged for an additional minute to remove residual wash buffer. To elute DNA 50 µl of DNase-free H_2O was added directly onto the silica-gel membrane, the column was allowed to stand for 1 minute and centrifuged for one minute at 17,900 x g. DNA samples were quantified and checked for quality as described elsewhere in this chapter and stored at – 80°C.

Large Scale Plasmid DNA Extraction (Maxiprep)

For the extraction of large amounts of high quality plasmid DNA the Qiagen EndoFree Plasmid Maxi Kit was used. A single colony was isolated from an LB agar plate and used to inoculate a starter culture of 2 ml LB medium containing the appropriate antibiotic, 100 μg/ml ampicillin (50 μg/ml for XL 10-Gold Ultracompetent cells) or 50 μg/ml kanamycin. The starter culture was incubated for 6-8 hours at 37°C in an orbital shaker (225 rpm). Five hundred μl of the starter colony was inoculated in 250 ml of LB medium supplemented with the appropriate antibiotic. The culture was grown for 14-16 hours at 37°C with constant shaking. Bacterial cells were harvested by centrifugation at 6,000 x g for 15 minutes at 4°C. Ten ml of Buffer P1 was used to resuspend the bacterial pellet and following the addition of 10 ml of Buffer P2 the mixture was gently mixed and lysis was allowed to proceed for no more than 5 minutes. Chilled Buffer P3 (10 ml) was added to the lysate and the lysate was poured into the barrel of the QIAfilter Cartridge and incubated for 10 minutes at room temperature. Cell lysate was then filtered into a 50 ml tube and 2.5 ml of Buffer ER was added; the tube was inverted 10 times to mix the contents and incubated on ice for 30 minutes. A QIAGEN-tip 500 was equilibrated by applying 10 ml Buffer QBT; Buffer was allowed to flow through by gravity flow. The filtered lysate was added to the equilibrated QIAGEN-tip and allowed to enter the resin. QIAGEN-tip was washed twice with 30 ml of Buffer QC, which was allowed to move through the tip by gravity flow. Fifteen ml of Buffer QN was used to elute the DNA. DNA was precipitated by the addition of 0.7 volumes of room temperature isopropanol and the mixture was centrifuged at 15,000 x g for 30 minutes at 4°C. The pellet containing the DNA was washed with 5 ml of 70% ethanol and centrifuged at 15,000 x g for 10 minutes. The supernatant was removed; the pellet air-dried for approximately 10 minutes and resuspended with 300 μl of DNase-free H_2O. Samples were stored at – 80°C.

Preparation of Frozen Stocks of Transformed Bacteria

A single colony was isolated from an LB agar plate and used to inoculate 5 ml of LB medium containing the appropriate antibiotic. The culture was grown for approximately 16 hours at 37°C in an orbital shaker (225 rpm). Bacteria were pelleted by centrifugation (6 minutes at 1,500 x g) and the pellet was resuspended using 1 ml of 50% glycerol in H_2O. The sample was transferred to sterile eppendorf tubes and snap frozen using dry ice. Tubes were stored at – 80°C.

Plasmid DNA Restriction Digestion

Restriction endonucleases were used to digest plasmid DNA. Various restriction endonucleases were used for the purposes of this project. In general, digestion reactions had a final volume of 20 µl and the reaction mixture contained: 2 µl of digestion buffer, 2 µl of 10X BSA, 1 µl of restriction endonucleases, plasmid DNA (volume varied according to the required amount of plasmid DNA) and DNase-free H_2O to the final volume. The reactions were then incubated for 2 – 4 hours at the optimum temperature for each restriction endonuclease and the products were purified as described below and analysed using agarose gel electrophoresis.

Purification of Restriction Digestion Products

To purify DNA fragments from restriction digestion reactions two different kits were used. For fragments up to 10 kb the QIAquick PCR purification Kit was used. In brief, 5 volumes of buffer PB were added to 1 volume of the digestion reaction and mixed by pippeting. To bind the DNA the sample was applied to the QIAquick column and the column was centrifuged for 1 minute at 17900 x g. Flow-through was discarded and 750 µl of Buffer PE were added followed by a 1 minute centrifugation. An additional centrifugation of one minute was performed to remove any residual ethanol. DNA was eluted using 30 µl of DNase-free H_2O as previously described and samples were stored at – 20°C. For fragments larger than 10 kb the Jetquick (Genomed) kit was used. The volume of the digestion restriction reaction was

adjusted to 100 µl with DNase-free H_2O and 400 µl of solution H1 were added. The mixture was loaded onto the provided column and centrifuged for 1 minute at 12000 x g. The flow-through was discarded and 500 µl of solution H2 were added and the centrifugation step was removed twice to ensure complete removal of ethanol. DNase-free H_2O was heated at 65-70°C and 30 µl were added directly onto the silica matrix. The column was allowed to stand for 1 minute and then centrifuged for 1 more minute. Eluted nucleic acid was stored at – 20°C.

Sequencing of Plasmid DNA and Sequence Analysis

In order to verify that the gene of interest was amplified and cloned successfully into the pCR®-Blunt II-TOPO® vector, approximately 5 µg of multiple plasmid DNA samples were sent to the departmental sequencing facility and were sequenced using M13 forward and reverse primers. For sequencing of PCR fragments cloned into the pGEM®-T-Easy Vector, 2 µg of multiple plasmid DNA samples were sent to MWG-Biotech and were sequenced using M13 forward and reverse primers. Sequences were analysed using BLAST (http://www.ncbi.nlm.nih.gov/BLAST) and the BioEdit software package.

Details about the manufacturers of kits used in this project and recipes of common solutions can be found in Appendix I.

Chapter 3: Insertion of eGFP in the non-structural ORF

Contents

Introduction

Heterologous gene expression from RNA viruses or viral vectors has potential applications in biotechnology (recombinant protein production, vaccines and therapeutics) as well as in basic research (examples include virus replication studies and *in vivo* pathogenesis studies). The development of infectious cDNA (icDNA) clones for many RNA viruses, both positive and negative strand, has simplified the process of manipulating the genomes of these viruses and allowed researchers to introduce various genes.

Alphavirus-based vectors are currently amongst the most widely used expression vector systems. icDNA clones and expression vectors have been developed for most alphaviruses including Semliki Forest virus (SFV), Sindbis virus (SV) and Chikungunya virus (Rice *et al.*, 1987; Liljestrom & Garoff, 1991; Vanlandingham *et al.*, 2005). In order to express non-viral genes using these systems two different types of vectors have been constructed. Replication-deficient vectors, also known as replicons, and replication competent vectors.

Replication-deficient vectors are ideal for *in vitro* studies on virus replication and are potential candidates for vaccines and therapeutics applications. They have an ability to carry large inserts and have good biosafety (Smerdou & Liljestrom, 1999). However, these vectors have a major disadvantage which does not allow their use for *in vivo* pathogenesis studies; they lack the structural ORF of the virus and therefore can only undergo a single cycle of infection (Frolov *et al.*, 1996).

To create replication-competent vectors a duplicated subgenomic 26S promoter was inserted into either the 3' non-translated region of the genomic 42S RNA or the short non-translated region between the non-structural and the structural ORF (Raju & Huang, 1991; Hahn *et al.*, 1992; Vanlandingham *et al.*, 2005). An alternative strategy employed by Pugachev *et al.* (2000) expressed the foreign gene using an internal ribosomal entry site element (IRES) from a picornavirus in the genome of rubella virus (also a member of the *Togaviridae* family). Double-subgenomic promoter replicating vectors carrying a variety of foreign genes including marker genes (for example eGFP and luciferase) have been constructed and used in animal studies (Cook & Griffin, 2003; Vaha-Koskela *et al.*, 2003). Although very useful, double-

subgenomic promoter viruses have generally proved to be genetically unstable. That is somehow expected since inserted genes are incorporated as separate transcription units that do not provide any selective advantage to the virus (Pugachev *et al.*, 1995; Caley *et al.*, 1999; Pugachev *et al.*, 2000).

Alphavirus vectors with increased genetic stability have been constructed by applying an alternative approach. The foreign gene of interest was inserted into the non-structural (replicase) ORF. Using this method SV with marker genes (eGFP and firefly luciferase) inserted in the replicase ORF (in fusion with nsP2 or nsP3 proteins) have been constructed (Bick *et al.*, 2003; Frolova *et al.*, 2006; Atasheva *et al.*, 2007).

In the present study, replication-competent SFV vectors carrying eGFP were generated and characterised. The eGFP gene was inserted in the non-structural ORF of SFV4 between nsP3 and nsP4. The novelty of these newly made marker viruses was based on their ability to express eGFP as a cleavable component of the replicase polyprotein. The complete *in vitro* and *in vivo* characterisation of these two newly made replicating vectors is described in this chapter.

Objectives

The objectives of this study were:

- To investigate if insertion of eGFP in the replicase ORF alters the replicase polyprotein processing or the replication efficiency of the virus.
- To test if levels of eGFP expression are adequate for detection using a standard fluorescent microscope.
- To examine the effect of the eGFP insertion on the *in vitro* and *in vivo* virulence of SFV4.
- To assess the phenotypic and genotypic stability of recombinant viruses *in vitro* and *in vivo*.
- To evaluate the suitability of the recombinant viruses for *in vivo* pathogenesis studies.

Construction of recombinant viruses

Recombinant viruses used for this project were constructed by Professor Andres Merits at the Estonian Biocentre. Initially, a vector annotated pSFV4(3F) designed to express foreign proteins fused to the C-terminus of nsP3 was constructed. To facilitate the insertion of foreign genes in this vector, a short polylinker incorporating *Apa*I and *Bam*HI restriction sites was inserted (Tamberg *et al.*, 2007). Enhanced green fluorescent protein (eGFP) was amplified from pEGFP-N1 plasmid (Clontech) with primers incorporating *Apa*I and *Bam*HI adapter sites (shown in materials and methods chapter) and cloned in-frame into the C-terminus of nsP3 (amino acid 452). The resulting construct (pSFV4(3F)-eGFP) was used to produce infectious virus (SFV4(3F)-eGFP) as described by Liljestrom *et al.* (1991) (Fig 3.1a). Characterisation of SFV4(3F)-eGFP showed that although the virus was viable, able to infect cells and express an nsP3-eGFP fusion protein, it was genetically highly unstable. SFV4(3F)-eGFP has potential use as a tool to investigate the expression of SFV replicase genes and the formation of SFV replicase complexes *in vitro* but is not suitable for *in vivo* pathogenesis studies due to its genetic instability (Tamberg *et al.*, 2007).

To construct a replicating vector able to express eGFP as a separate protein (not fused to nsPs) pSFV4(3F) was engineered further. The native C-terminus of nsP3 was restored by duplication of its last 30 amino acids (aa 453-482) and one of two optimised artificial nsP2 protease recognition sites was inserted between the C-terminus of nsP3 and eGFP. The two artificial protease recognition sites were designated L and H, standing for low and high respectively, indicating the efficiency by which these sites are cleaved by nsP2 protease. In both L and H the first amino acid residue (P1') after the cleavage was mutated from a tyrosine (Y) to a glycine (G) for two reasons: glycine is a stabilising amino acid according to the N-end rule (Varshavsky, 1996) and nsP2 protease cleaves more efficiently with glycine in that position (Lulla *et al.*, 2006). In the case of the H recognition site, amino acid residues 2-7 from the N-terminus of nsP4 were inserted after glycine to enhance the cleavage efficiency. The additional proline inserted at the end of the H and L nsP2 recognition sites originates from the ApaI restriction site. The resulting vectors were annotated

pSFV4(3L) and pSFV4(3H). eGFP was amplified and cloned into these vectors as described above and infectious viruses designated SFV4(3L)-eGFP and SFV4(3H)-eGFP were obtained from their icDNA clones (Fig 3.1b). The recombinant viruses described in this thesis and the Tamberg *et. al.* (2007) publication are identical. The differences in the clone names are due to different annotation systems used in Edinburgh and Tartu, respectively. SFV4(3F)-eGFP is annotated SFV(3F)4-eGFP and SFV4(3H)-eGFP is annotated SFV(3H)4-eGFP in Tamberg *et. al* (2007).

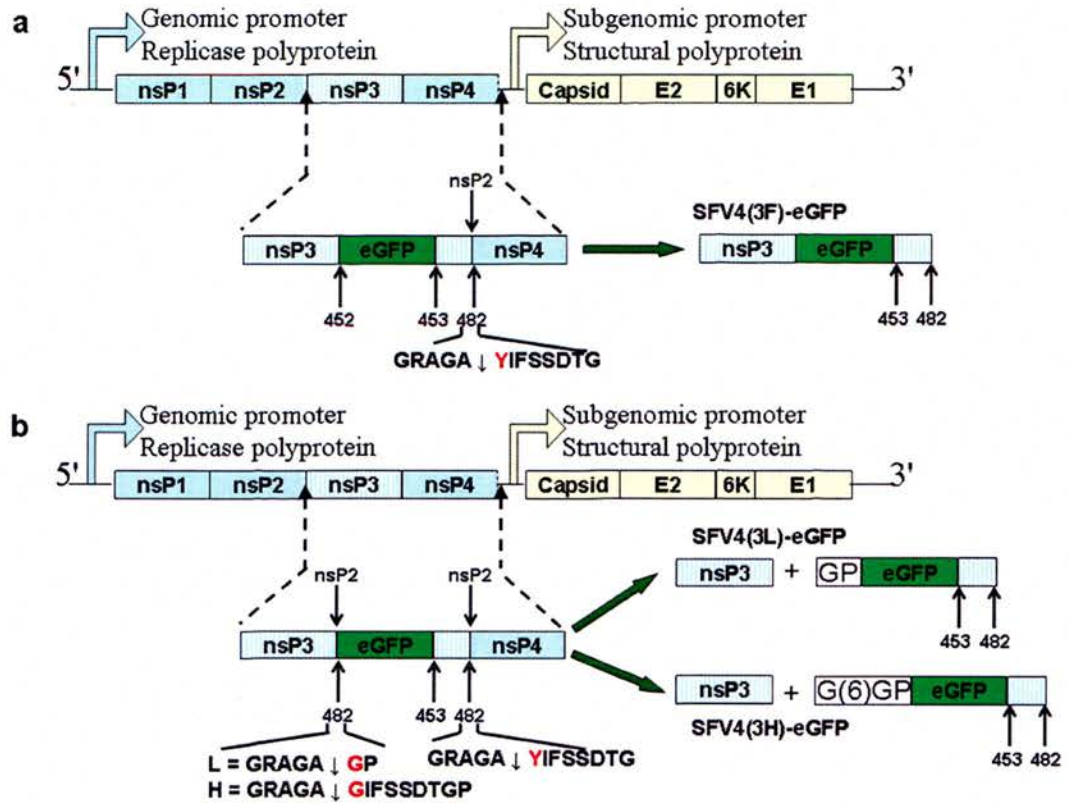

Figure 3.1. Schematic representation of eGFP expressing replicating vectors. (a). SFV4(3F)-eGFP, construction and predicted processing of the non-structural polyprotein. The amino acid sequence, the position of the native nsP2 protease recognition site between nsP3 and nsP4 and the 30 amino acids (453-482) from the C-terminus of nsP3 which were fused at the C-terminus of eGFP are shown. Tyrosine residue at position P1' is shown in red. **(b).** SFV4(3L)-eGFP and SFV4(3H)-eGFP, construction and predicted processing of the non-structural polyprotein. The amino acid sequence, the position of both the artificial and the native nsP2 protease recognition sites and the 30 amino acids (453-482) from the C-terminus of nsP3 which were fused at the C-terminus of eGFP are shown. Tyrosine residue in the native cleavage site and glycine residue in the artificial sites are shown in red. In the predicted processing of SFV4(3H)-eGFP, (6) corresponds to the IFSSDT sequence. The proline (P) residue at the end of both L and H constructs is the result of the insertion of *Apa*I restriction site.

Assessment of the expression levels of a marker gene (eGFP) as part of the replicase ORF and the effect of this insertion on virus viability and replication.

Experimental design

To assess the effect of eGFP insertion on virus viability and replication efficiency, BHK-21 cells were infected with SFV4, SFV4(3H)-eGFP and SFV4(3L)-eGFP at a multiplicity of infection (M.O.I) of 10 in triplicate and virus replication was compared in a one-step growth curve. Two hundred µl of virus containing supernatant were collected and replaced with an equal amount of fresh medium every 2 hours for 12 hours. All samples were then titrated using standard plaque assay. In addition, to determine whether or not eGFP was expressed to adequate levels to be detected using a standard fluorescent microscope and to determine the kinetics of eGFP expression, cultures of BHK-21 cells were infected with SFV4(3H)-eGFP and SFV4(3L)-eGFP at an M.O.I of 10 and were monitored for expression of eGFP every hour for the first 12 hours post-infection and every 4-6 hours thereafter. The ability of these viruses to induce a cytopathic effect (CPE) was determined by infection of parallel cultures of BHK-21 cells.

One-step growth curves

One-step growth curves (Figure 3.2a) demonstrated that insertion of eGFP into the replicase polyprotein did not have a major effect on the viability and replication efficiency of SFV. Both SFV4(3H)-eGFP and SFV4(3L)-eGFP were able to infect BHK-21 cells and replicated to similar levels to SFV4. However, there were minor differences, at 4 hours post-infection SFV4(3H)-eGFP and SFV4(3L)-eGFP had significantly lower titres than SFV4 ($P<0.05$). At 6 hours post-infection SFV4(3H)-eGFP had similar titres to SFV4 (no significant difference, $P>0.05$), whereas SFV4(3L)-eGFP still had significantly lower titres ($P<0.05$). From 8 hours post-infection until the end of the experiment (12 hours post-infection) all viruses had similar titres (no significant differences, $P>0.05$). Titres at each time-point were

compared using a paired t-test. Titration of the supernatant samples showed that on BHK-21 cells, SFV4(3H)-eGFP and SFV4(3L)-eGFP produced plaques with size similar to SFV4 (data not shown).

eGFP expression and development of CPE in BHK-21 cells

Following infection of BHK-21 cells with SFV4, SFV4(3H)-eGFP and SFV4(3L)-eGFP cells were monitored at regular intervals for eGFP fluorescence and CPE. For the cultures infected with the eGFP marker viruses, fluorescent signal was detected as early as 2 hours post-infection, a representative example of eGFP fluorescence early during infection can be seen in Figure 3.2b. The intensity of the fluorescence signal increased until about 6 hours post-infection and then rapidly decreased. Late in infection cells had a dull green fluorescent signal. Prior to approximately 16-20 hours post-infection with all three viruses, cells had the typical elongated morphology of BHK-21 cells and no sign of CPE was observed (Figure 3.2b). Between 16-20 hours post-infection CPE was first apparent (Figure 3.2c). Cells rounded up and their nuclei condensed suggesting that cells were dieing. At 36 hours post-infection almost all the cells were detached. Infection progressed in an identical manner with all three viruses demonstrating that insertion of eGFP had no significant effect on the *in vitro* outcome of infection.

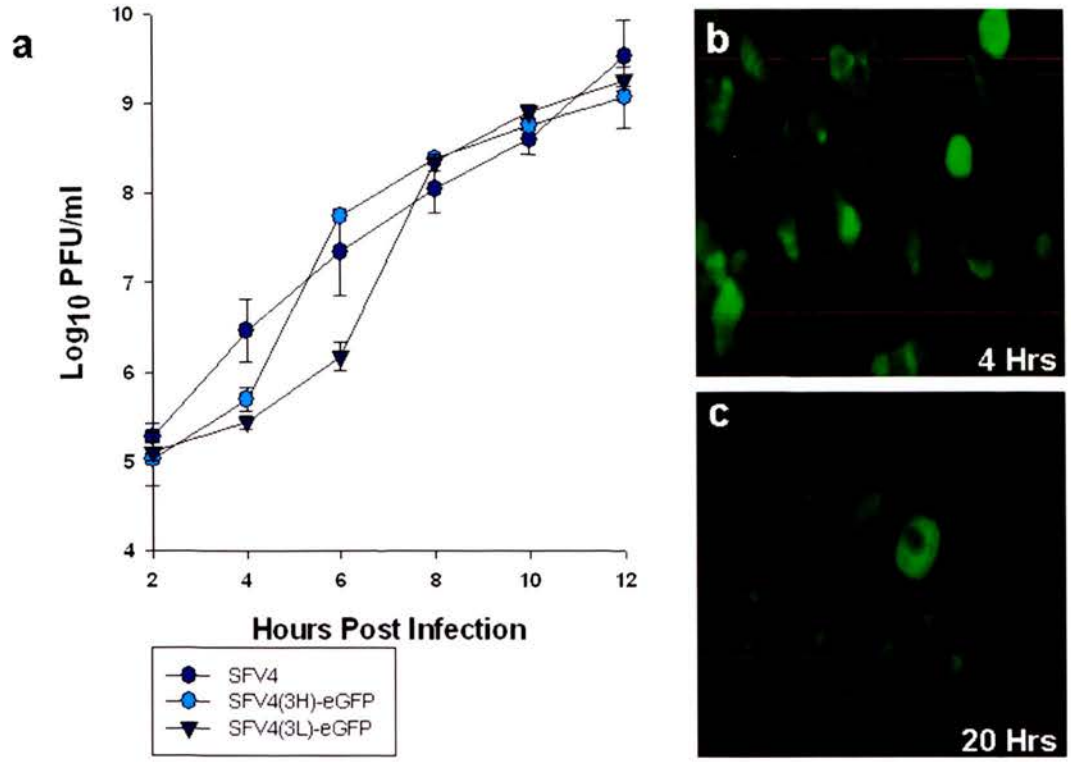

Figure 3.2. Growth curves and expression of eGFP in BHK-21 cells. (a) Monolayers of BHK-21 cells were infected in triplicate with SFV4 (dark blue circles), SFV4(3H)-eGFP (light blue circles) or SFV4(3L)-eGFP (inverted dark blue triangles) at an M.O.I of 10. Supernatant samples were collected every 2 hours for 12 hours and titrated for infectious virus. Each point represents the mean of 3 samples. The bar represents the standard deviation (SD). **(b)** and **(c)**. All growth curves shown in this thesis were performed in parallel. The data for SFV4 presented in this figure is identical to that in Figures 4.2a and 5.3a allowing comparison of the growth of all recombinant viruses. Images of BHK-21 cells infected with SFV4(3H)-eGFP virus at an M.O.I of 10 taken 4 and 20 hours post-infection, respectively. Panel **(b)** shows the typical morphology of BHK-21 cells observed early in infection whereas panel **(c)** shows the characteristic morphology of cells dying at the late stages of infection. No difference on eGFP expression or development of CPE was observed when SFV4(3L)-eGFP was used to infect BHK-21 cells. Pictures acquired with Zeiss Axioskop microscope.

Expression and stability of the replicase complex and eGFP proteins in eGFP expressing viruses

Experimental design

To investigate if insertion of eGFP between nsP3 and nsP4 altered the pattern of expression of the four non-structural proteins and to study the stability of the viral non-structural proteins and of eGFP, two experiments were performed.

Experiment I) BHK-21 cells were infected with SFV4(3H)-eGFP or SFV4(3L)-eGFP at an M.O.I of 20. PBSA was used as a negative control to mock-infect cells. After 6 hours, cells were lysed and samples corresponding to 100,000 cells were separated on an SDS-PAGE gel and proteins were transferred to a nitrocellulose membrane. Antibodies recognising specific epitopes on nsP1, nsP2, nsP3, nsP4 and eGFP were used (see methods) to detect SFV non-structural proteins and eGFP.

Experiment II) To investigate the stability of eGFP, BHK-21 cells were infected at an M.O.I of 100 with SFV4, SFV4(3H)-eGFP or SFV4(3L)-eGFP for 3 hours. Using [^{35}S]methionine and [^{35}S]cysteine, cells were metabolically labelled and chased for 1, 3, 8 or 24 hours. nsP1, nsP3 and eGFP antibodies were used to immunoprecipitate the respective labelled proteins in cell lysates. This experiment was performed by my colleague Mrs Nele Tamberg at Estonian Biocentre according to the method described in Tamberg *et al.* (2007).

Expression of eGFP & of the replicase proteins of SFV4(3H)-eGFP and SFV4(3L)-eGFP in BHK-21 cells

As it can be seen in Figure 3.3a, all non-structural proteins and eGFP were expressed from both recombinant viruses. All proteins had correct molecular weights (migrated to the expected position) on the SDS-PAGE gel. The artificial cleavage sites inserted between nsP3 and eGFP appeared to be cleaved very efficiently; no band corresponding to an nsP3-eGFP fusion protein was visible. In contrast, an eGFP-nsP4 fusion protein was detected when anti-nsP4 and anti-eGFP antibodies were used. Comparison of the density of the bands corresponding to eGFP-nsP4, nsP4 and

eGFP proteins for both recombinant viruses shows that the amounts of eGFP-nsP4 fusion protein were considerably lower than the amounts of individual nsP4 and eGFP proteins. The results of this experiment indicate that insertion of eGFP as a cleavable protein between nsP3 and nsP4 does not interfere with the expression of the non-structural proteins of SFV. The western blotting analysis (Figure 3.3a) suggested that both SFV4(3H)-eGFP and SFV4(3L)-eGFP produced similar amounts of non-structural proteins and eGFP at 6 hours post-infection; however the one-step growth curves (Figure 3.2a) at this same time-point showed that more SFV4(3H)-eGFP infectious virus was produced than SFV4(3L)-eGFP. This inconsistency could, for example, be related to differences in the release of infectious virus particles between SFV4(3H)-eGFP and SFV4(3L)-eGFP, perhaps as a result of slower replication of the virus resulting from slower processing of the replicase polyprotein. Another possibility is that SFV4(3L)-eGFP produced more DI particles than SFV4(3H)-eGFP.

Stability of eGFP & of the non-structural proteins of SFV4(3H)-eGFP and SFV4(3L)-eGFP in BHK-21 cells

The intensity of the eGFP fluorescence signal in BHK-21 cells dramatically decreased late in infection (from 6 hours onwards). The eGFP used in these constructs normally has a half-life of approximately 24 hours in BHK-21 cells (personal communication with Clontech technical support). One explanation would be an increased instability of eGFP. Following shut-off of the replicase gene translation, which starts a few hours after infection, fluorescence intensity can be taken as a measure of eGFP stability. Rapid loss of fluorescence after 6 hours indicates high instability of eGFP. The results of the pulse-chase experiment (Figure 3.3b) showed that nsP1 and nsP3 were stable throughout the 24 hours of the experiment, only a minor decrease in nsP3 was observed. It is important to note that this result was very similar for both the recombinant viruses and SFV4. In contrast, eGFP was detectable only for up to 8 hours and was thereafter below the limit of detection. This finding is in accordance with the findings obtained from microscopic examination of infected BHK-21 cells and again suggests that rapid degradation of eGFP is responsible for the low intensity and short duration of the fluorescent signal.

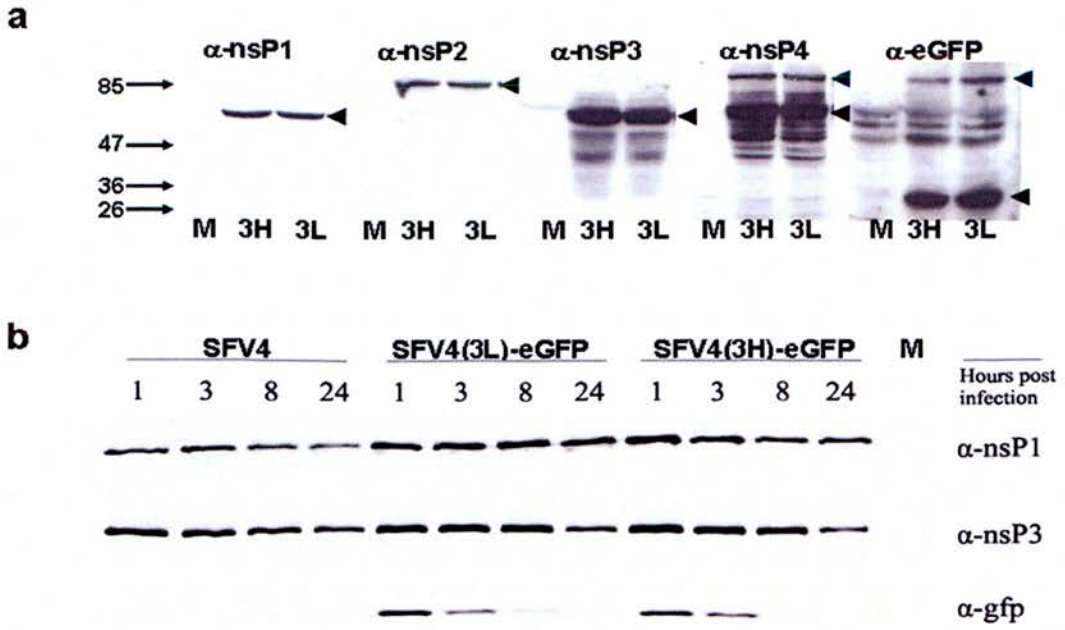

Figure 3.3. Expression and stability of the replicase complex and eGFP proteins in eGFP expressing viruses. (a) Western blotting of cell lysates of BHK-21 cells inoculated with SFV4(3H)-eGFP (**3H**), SFV4(3L)-eGFP (**3L**) (M.O.I 20) or PBSA (mock-infection **M**). Specific bands of the appropriate molecular weight for nsP1, nsP2, nsP3, nsP4 non-structural proteins and for eGFP are shown with a black arrowhead. The blue arrowheads on the panels corresponding to nsP4 and eGFP indicate an eGFP-nsP4 fusion protein. **(b)** BHK-21 cells were infected with SFV4, SFV4(3L)-eGFP, SFV4(3H)-eGFP (M.O.I 100) or PBSA (**M**). Synthesised protein was labelled with [^{35}S]methionine and [^{35}S]cysteine at 3 hours post-infection and chased for 1, 3, 8 or 24 hours. Cell lysates were immunoprecipitated with nsP1, nsP3 and eGFP specific antibodies. Picture for **3.3(b)** was kindly provided by Mrs Nele Tamberg.

Distribution of eGFP and nsP3 non-structural protein in BHK-21 cells infected with SFV4(3H)-eGFP and SFV4(3L)-eGFP

Experimental design

SFV RNA replication complexes consisting of the 4 fully processed non-structural proteins are known to associate with cellular membranes, especially the cytoplasmic surface of endosomes and lysosomes (Froshauer *et al.*, 1988; Salonen *et al.*, 2005). It has been also shown that free eGFP is distributed throughout the cell cytoplasm and the nucleus. Recent studies using replicating Sindbis virus vectors expressing eGFP in fusion with nsP3 show that eGFP and nsP3 co-localise in the cytoplasm of infected cells (Frolova *et al.*, 2006). In order to examine if eGFP was released free from the replicase complex in SFV4(3H)-eGFP and SFV4(3L)-eGFP infected cells, cultures of BHK-21 cells on glass slides were infected at an M.O.I of 10 and at 6 hours, fixed and stained with anti-nsP3 antibody.

Distribution of eGFP and nsP3 in BHK-21 cells

In BHK-21 cells infected with SFV4(3H)-eGFP (Figure 3.4a) or SFV4(3L)-eGFP (Figure 3.4d) distribution of eGFP was very similar; fluorescence was observed throughout the cytoplasm and the nucleus of the infected cells. SFV replication and eGFP protein synthesis occur in the cytoplasm of the cell. Due to its small size, eGFP, can also diffuse through the nuclear pores and localise in the nucleus (passive transfer). Interestingly, eGFP fluorescence was more intense in the nuclei of infected cells than in the cytoplasm. On the other hand, nsP3 was detected only in the cytoplasm of infected cells with both viruses (Figure 3.4b and Figure 3.4e). During infection, after the replicase polyprotein is processed by the viral protease (nsP2), individual proteins assemble to form replication complexes (Lemm & Rice, 1993a; Kujala *et al.*, 2001; Salonen *et al.*, 2003). The punctate, predominantly perinuclear, cytoplasmic staining for nsP3 most probably corresponds to the location of these replication complexes. The absence of co-localisation between eGFP and nsP3

suggest, as also observed by western blotting (Figure 3.3a), that eGFP was cleaved efficiently from the replicase polyprotein.

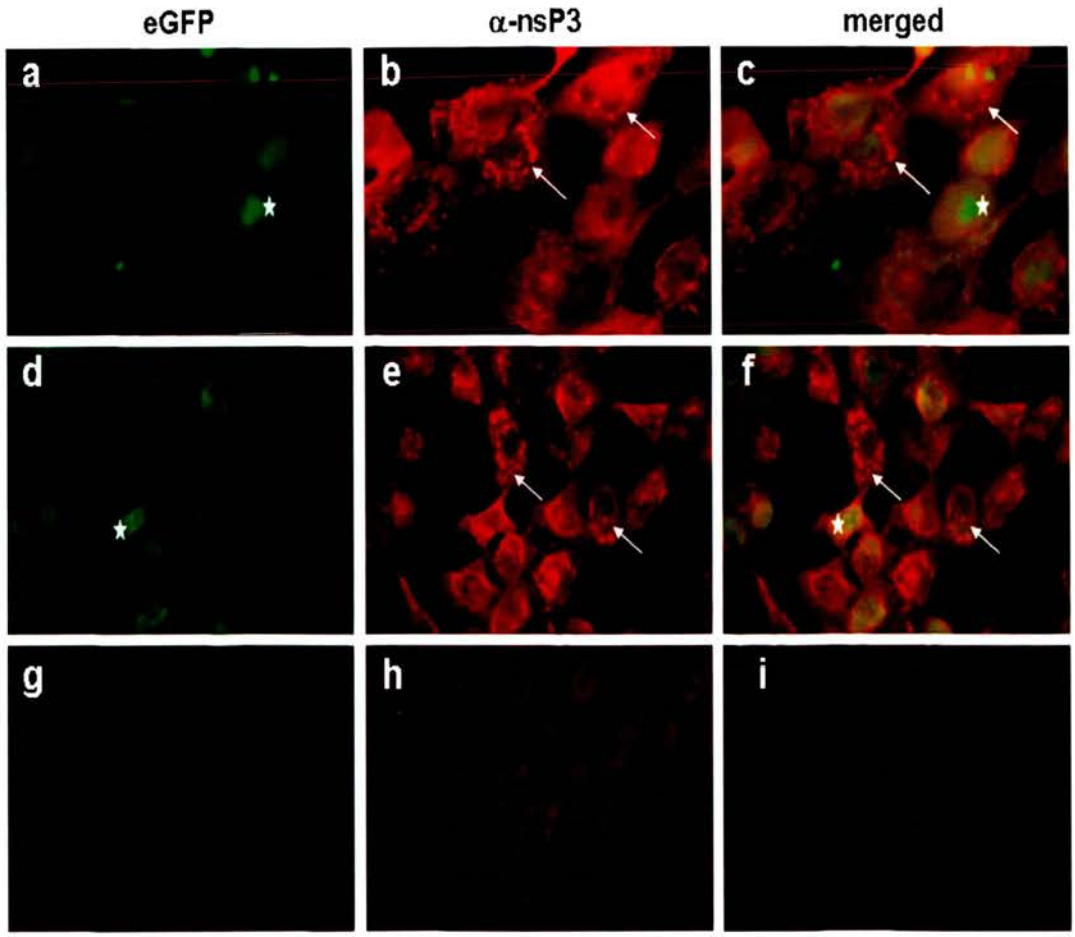

Figure 3.4. Distribution of eGFP and nsP3 in BHK-21 cells. Confocal microscopy images of BHK-21 cultures infected with SFV4(3H)-eGFP [**(a)**, **(b)** and **(c)**] or SFV4(3L)-eGFP [**(d)**, **(e)** and **(f)**] at an M.O.I of 10. Mock- infected (PBSA) control culture can be seen on panels **(g)**, **(h)** and **(i)**. Cells marked with an asterisk show the characteristic distribution of eGFP in BHK-21 cells, where eGFP stains the cytoplasm of the cell and also diffuses to the nucleus. Arrows point to cells exhibiting punctate nsP3 staining; the staining is consistent with the distribution of virus replication complexes formed by fully processed non-structural proteins on the surface of cytoplasmic membranes.

In vitro phenotypic and genotypic stability of SFV4(3H)-eGFP and SFV4(3L)-eGFP in BHK-21 cells

Experimental design

To examine whether the recombinant viruses maintained their ability to express eGFP or if the inserted gene was eliminated after several passages *in vitro*, SFV4(3H)-eGFP and SFV4(3L)-eGFP were passaged 5 times in BHK-21 cells at an M.O.I of 0.01 (low M.O.I increases the possibility to detect changes). Figure 3.5 outlines the experimental design used to investigate the *in vitro* stability of eGFP expressing viruses.

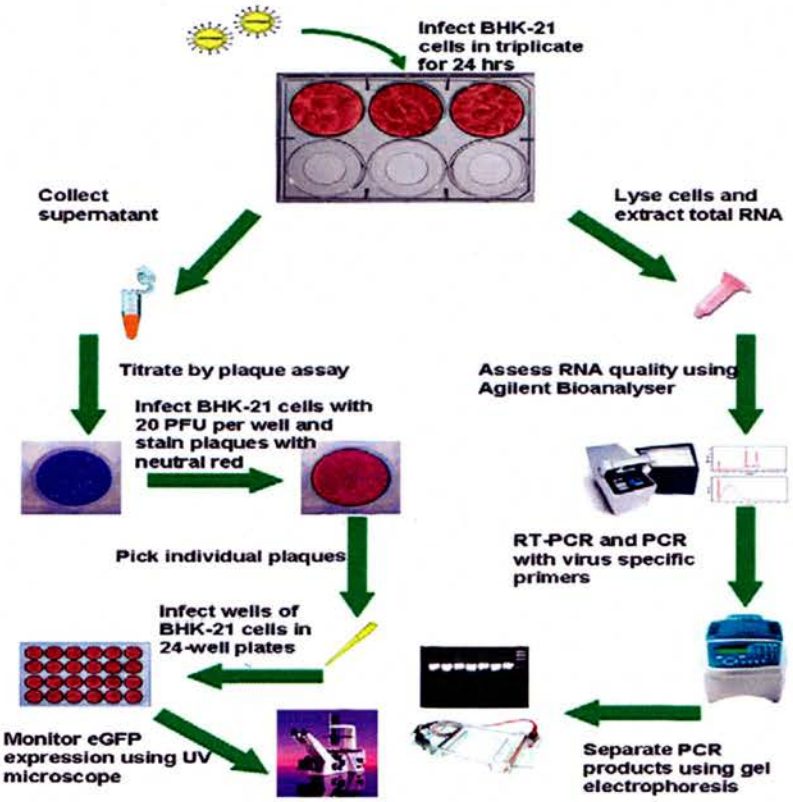

Figure 3.5. Experimental design to investigate *in vitro* phenotypic and genotypic stability. In triplicate, monolayers of BHK-21 cells were infected with recombinant viruses. Supernatant was collected at 24 h and total RNA was extracted from the cells and analysed by RT-PCR for virus RNA. Each supernatant was passaged four more times through BHK-21 cells. Supernatants after each passage were then titrated and used to infect (20 PFU) fresh BHK-21 cells. These monolayers were overlayed with agar and 96 plaques were purified; individual plaques were transferred to 24-well plates and each well was analysed for eGFP expression.

Phenotypic stability of SFV4(3H)-eGFP & SFV4(3L)-eGFP

Viruses from 96 plaques purified from each of 5 *in vitro* passages were used to infect BHK-21 cells and eGFP expression was determined by fluorescent microscopy. For the first two passages, 100% of plaque purified viruses for both recombinant viruses were eGFP positive. After 3 passages 98.9% of SFV4(3H)-eGFP and 94.5% of SFV4(3L)-eGFP plaque purified viruses maintained their ability to express the marker gene. These percentages went down to 95.2% and 68.75% respectively after the 4th passage. At the 5th passage 93.6% of SFV4(3H)-eGFP and 50% of SFV4(3L)-eGFP plaque purified viruses were expressing eGFP (Figure 3.6a).

Genotypic stability of SFV4(3H)-eGFP & SFV4(3L)-eGFP

After removal of the supernatants from the BHK-21 cells for the assessment of phenotypic stability, RNA was extracted from these cells. The RNA was quantified, its quality was tested using an Agilent Bioanalyzer and 2 μg were reverse-transcribed to cDNA. Primers flanking the area of the eGFP insertion were used for amplification. If the intact insert was present a product with a size of approximately 1,500 bp would be produced. If the insert was eliminated the expected product would have a size of approximately 670 bp. The results obtained (Figure 3.6b) indicate that the amount of product (and consequently of eGFP negative viruses) of ~670 bp gradually increased between the 2nd and 5th passage for both recombinant viruses. The increase was considerably greater for SFV4(3L)-eGFP and at the 4th and 5th passage the amount exceeded that of the product corresponding to the eGFP positive virus. In contrast, the levels of product corresponding to eGFP negative virus did not increase much when SFV4(3H)-eGFP was passaged and did not exceeded the eGFP positive virus.

As can be seen on the panel of Figure 3.6b corresponding to the 5th passage; numerous bands appear between the band corresponding to the product containing the eGFP insert and the band of the product where the insert was eliminated (especially for SFV4(3H)-eGFP; lanes 1-3). These bands together with the ~1,500 bp and the ~670 bp bands were extracted from the gel and sub-cloned into

the pGEM-T Easy vector which was amplified and sent off for commercial sequencing. Sequencing was carried out from both ends of the cloned insert and the consensus sequences are shown in Appendix II. The obtained sequences were aligned to SFV4 and to SFV4(3H)-eGFP or SFV4(3L)-eGFP using the BioEdit software. The ~1,500 bp product contained the complete inserted sequence. The ~670 bp product had a complete elimination of the inserted sequence. The intermediate sized bands contained in-frame deletions varying in size from 75 nucleotides to 843 nucleotides (Appendix II). Interestingly, in most of these recombinants deletion started at the inserted nsP2 protease recognition site upstream of eGFP. This site is located directly after the C-terminus of nsP3, the 30 amino acids of which are repeated downstream from eGFP. This suggests that recombination may have occured between the duplicated nsP3 C-terminal sequences. The genotypic stability analysis is consistent with the phenotypic stability; SFV4(3L)-eGFP produces more eGFP negative viruses than SFV4(3H)-eGFP.

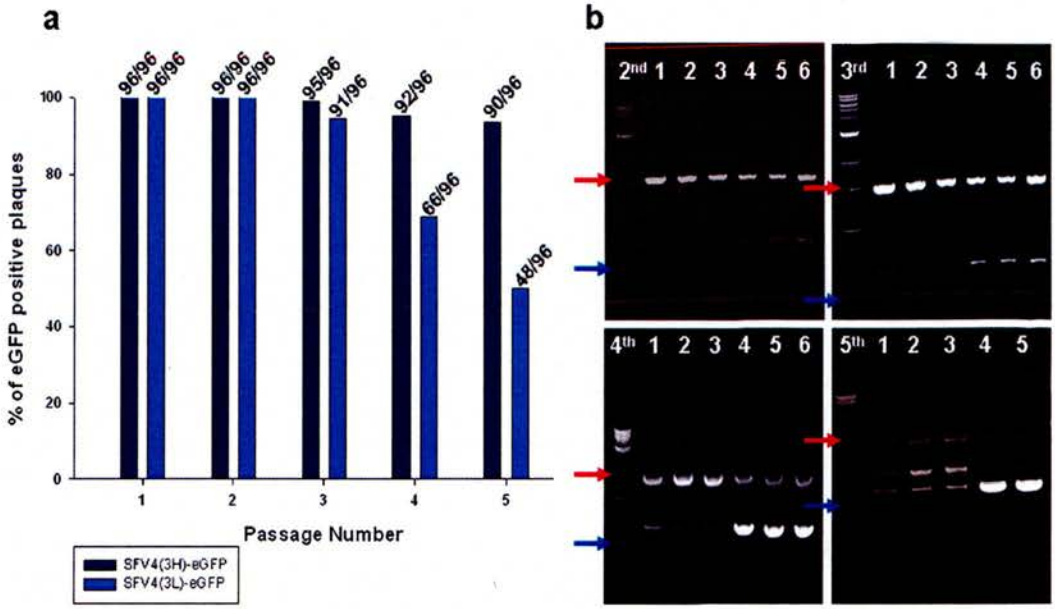

Figure 3.6. *In vitro* phenotypic and genotypic stability of SFV4(3H)-eGFP and SFV4(3L)-eGFP. (a) percentage of eGFP positive plaque purified viruses after serial passaging; dark blue is SFV4(3H)-eGFP and light blue is SFV4(3L)-eGFP. **(b)** RT-PCR genotyping of virus RNA using nsP3 – nsP4 primers on RNA samples isolated from BHK-21 monolayers at passages 2, 3, 4 and 5; the passage number is indicated at the top left of each panel. In all panels, lanes 1 – 3 are the triplicate passages of SFV4(3H)-eGFP and lanes 4 – 6 are the triplicate passages of SFV4(3L)-eGFP (except in bottom right panel where there is no lane 6). The red arrow corresponds to the 1.5 kb band of the DNA ladder and the blue arrow corresponds to the 0.5 kb band of the DNA ladder.

Cell tropism of recombinant viruses *in vitro*

Experimental design

SFV is a neurotropic virus transmitted by mosquitoes, to determine if the insertion of eGFP had any effect on the ability of the virus to infect mosquito cells and cells of the vertebrate nervous system, cultures of C6/36 cells from *Aedes albopictus* and of rat hippocampal neurons were infected with SFV4(3H)-eGFP. Only SFV4(3H)-eGFP was used in these studies as the previous *in vitro* experiments had shown that it had higher genetic stability compared to SFV4(3L)-eGFP. eGFP expression was monitored using fluorescence microscopy. Infected C6/36 cells were immunostained with anti-nsP3 antibody to determine if the distribution of eGFP and nsP3 were the same as in BHK-21 cells. C6/36 cells were infected at an M.O.I of 10. Rat hippocampal neurons were plated at their optimal density (150 cells/mm^2 on 22x22 mm coverslips) and infected at an M.O.I of 10.

In vitro cell tropism

SFV4(3H)-eGFP was able to infect C6/36 cells and express eGFP (Figure 3.7a & 3.7d). The distribution and the intensity of the eGFP signal were similar to those observed in BHK-21 cells; eGFP stained both the cytoplasm and the nucleus of the infected cells. When the infected cells were immunostained with anti-nsP3 antibody the nsP3 staining was cytoplasmic and exhibited the characteristic punctate distribution observed in BHK-21 cells (Figure 3.7b and 3.7e). Merging the green (eGFP) and red channels (Alexa Fluor 594; anti-nsP3 immunostaining) it was observed that some eGFP-positive cells (marked with an asterisk in Figure 3.7f) were not positive for nsP3. The cells were fixed and stained 16 hours after addition of virus (M.O.I of 10). It is possible that these eGFP-positive nsP3-negative cells were recently infected and that nsP3 had not accumulated to adequate amounts to be detected by immunostaining. Additional experiments would be required to investigate this. C6/36 cultures infected with SFV4 and SFV4(3H)-eGFP were also monitored for the presence of CPE; none was observed over 5 days of study.

Given that eGFP expression was detectable in both BHK-21 and C6/36 cells for at least 20 hours, neuronal cultures were examined after overnight infection with SFV4(3H)-eGFP (approximately 16 hours), at that time no eGFP was detectable. Due to the shortage of neuronal cultures, the experiment was not repeated. The CPE induced by both SFV4 and SFV4(3H)-eGFP was taken to indicate that both viruses infected vertebrate neurons and that the recombinant virus had not lost this property. Cells looked healthy for up to 48 hours post-infection, after which widespread cell death was observed. All cells were dead by 4 days post-infection. Parallel cultures infected with SFV4 showed the same pattern on the development of CPE whereas mock-infected cultures remained viable throughout the study.

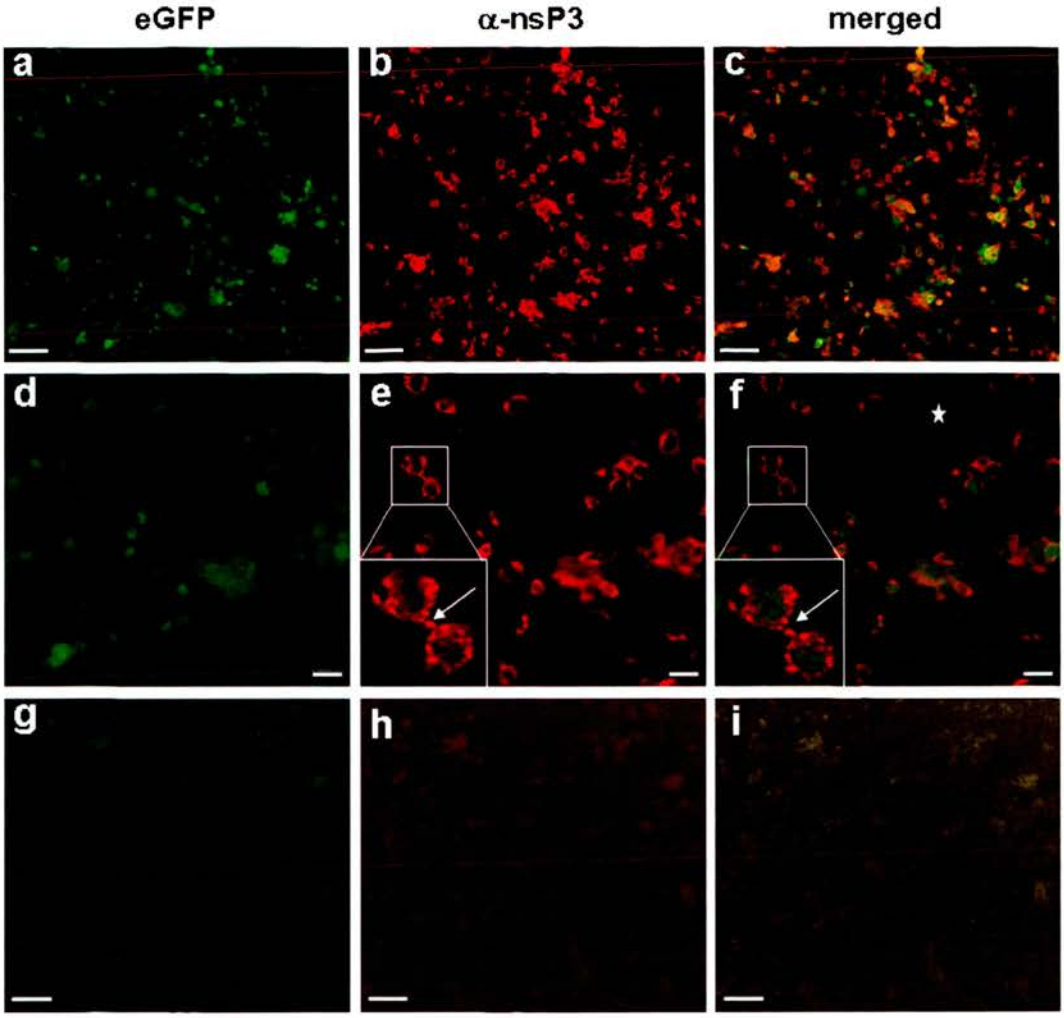

Figure 3.7. Infection of C6/36 cells from *Aedes albopictus* with SFV4(3H)-eGFP. Panels **(a)** and **(d)** show eGFP expression in C6/36 cells infected with SFV4(3H)-eGFP at an M.O.I of 10 for 16 hours. Panels **(b)** and **(e)** show immunostaining of the same monolayer with anti-nsP3 antibody. Inset of panel **(e)** demonstrates the characteristic punctate cytoplasmic staining at high magnification. Merged images shown on panels **(c)** and **(f)**. The asterisk on **(f)** marks an area with cells which expressed eGFP but were negative for nsP3. Non-infected control culture is shown in panels **(g)**, **(h)** and **(i)**. Bars in all panels correspond to 100 μm. All images were acquired with a Zeiss confocal microscope.

Virus pathogenesis following intraperitoneal inoculation

To investigate the course of recombinant virus infection *in vivo* following intraperitoneal (i.p.) infection and compare it with SFV4 infection three experiments were performed.

Experiment I-Assement of virulence

Experimental design

Groups (n=10) of adult (4-5 week old female) Balb/c mice were inoculated i.p. with 5 x 10^3 PFU of SFV4, SFV4(3H)-eGFP, SFV4(3L)-eGFP, SFV L10 (virulent strain of SFV) or mock-infected with PBSA. Weight-loss is indicative of clinical disease and mice were weighed daily for the first 4 days post-infection (PID). On PID 4, five mice from each group (except the group infected with SFV L10) were euthanised and their brains were sampled. Half of each brain was snap frozen and used for infectious virus titration. The other half was processed for frozen sections to examine eGFP expression. The remaining mice from each group were kept for 10 days and monitored daily for symptoms of viral encephalitis. The data was used to construct survival curves.

Results

Infected and mock-infected mice were weighed daily (Figure 3.8a). Mice infected with SFV4, SFV4(3H)-eGFP or SFV4(3L)-eGFP gained weight over the first four days of the infection (average change of +2%). However, this increase was approximately 5 times lower than the control group mock-infected with PBSA (change of +9.7%). In contrast, mice infected with SFV L10 showed a weight-loss of -13.3%. On PID 2 all mice in the L10 group had symptoms of severe encephalitis (ataxia and paralysis) and, after measuring their weight, were euthanised. On PID 4, five mice from each of the remaining groups were sampled; half brain for virus titration and half for histological study, as described previously. None of these mice exhibited symptoms of viral encephalitis. Mice were sampled at this time as previous

studies have shown that the highest levels of infectious virus are detectable in the brain 3-4 days after i.p. inoculation (Fazakerley *et al.*, 1993). However, previous studies were performed with SFV A7(74) and the efficiency of SFV4 to cross the blood-brain barrier and replicate in the brain has not previously been characterised. All PID 4 brain samples titrated for infectious virus were below the limit of detection of the assay (2.4 Log_{10} PFU/g) suggesting that the virus did not cross the blood-brain barrier or, at least that it had not done so by PID 4. Examination of frozen sections (12 μm thick) of brain tissue (6 slides per brain sample, 3 sections per slide) of all the mice infected with SFV4(3H)-eGFP or SFV4(3L)-eGFP and sampled on PID 4 showed no eGFP expression. This result is consistent with the absence of detectable infectious virus.

Data on the survival of the infected mice was used to plot survival curves (Figure 3.8b). In contrast to the SFV L10 infected group in which 100% of the animals were dead or had reached clinically defined terminal end-points by PID 3, 100% of the animals infected with SFV4, SFV4(3H)-eGFP or SFV4(3L)-eGFP survived the infection without any clinical signs. According to other researchers using SFV4 (personal communication), neuroinvasion of SFV4 appears to be dose dependent but once the virus is in the brain it confers lethal neurovirulence. Therefore the experiment was repeated using a higher dose of virus (5×10^5 PFU) and mice were monitored for 10 days for signs of viral encephalitis. The results obtained were identical to the results of the first experiment, with no clinical evidence of brain infection by the SFV4 viruses (data not shown).

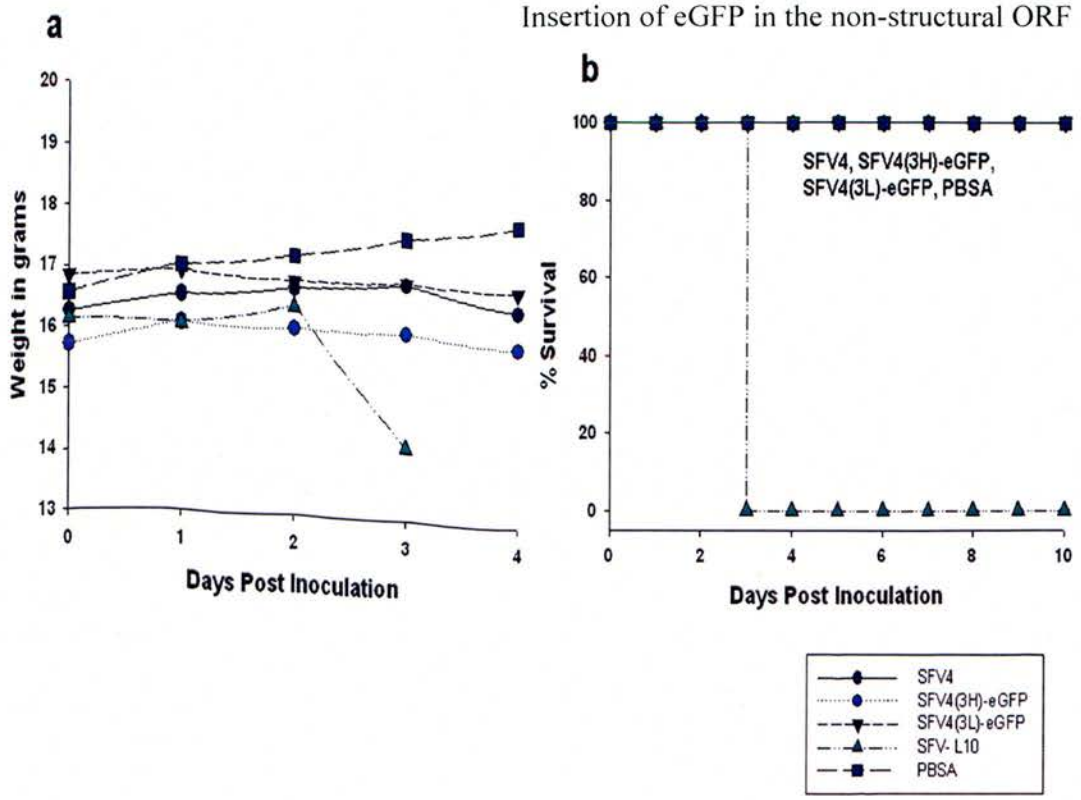

Figure 3.8. Changes in body weight and survival rates of Balb/c mice following i.p. inoculation with SFV. (a). Average body weight of i.p. infected mice (n=10). At the end of the experiment (PID4), SFV4-infected animals had a 2.7% weight increase. For SFV4(3H)-eGFP and SFV4(3L)-eGFP-infected animals this increase was 2.2% and 1.1%, respectively. Animals infected with SFV L10 had a 13.3% weight decrease. In contrast the animals mock-infected with PBSA had a 9.7% weight increase **(b).** Survival rates of mice (n=5) following i.p. inoculation.

Experiment II-Determination of viraemia

Experimental design

To examine if the recombinant viruses were able to establish a peripheral infection (viraemia), groups of 6 adult Balb/c mice were inoculated i.p. with 5 x 10^3 PFU of SFV4, SFV4(3H)-eGFP, SFV A7(74), SFV L10 or mock-infected with PBSA. SFV A7(74) is an avirulent strain, in adult mice, known to be neuroinvasive following extraneural inoculation,(Bradish *et al.*, 1971; Pathak & Webb, 1978). Twenty-four hours post-infection mice were euthanised and heparinised blood was collected and titrated for infectious virus.

Results

It was hypothesised that SFV4 and SFV4-based constructs expressing eGFP failed to infect the brain of Balb/c mice following i.p. inoculation because they did not replicate to high enough titres in the periphery. To test this hypothesis groups of mice were infected, as described above, with SFV4, SFV4(3H)-eGFP, SFV L10 or mock-infected with PBSA and virus titres in the blood were determined at 24 hours. SFV4(3L)-eGFP was excluded since it appears to be no different to SFV4(3H)-eGFP and the *in vitro* characterisation of the viruses showed that it loses its ability to express eGFP fairly quickly.

Titration of blood samples at 24 hours post-infection showed that 5 out of 6 mice infected with SFV4 and 4 out of 6 mice infected with SFV4(3H)-eGFP had detectable levels of infectious virus. On the other hand, all mice infected with SFV A7(74) or SFV L10 (6/6) were positive. SFV4 infected mice had an average titre of 3.7 Log_{10} PFU/ml (SD: 1.4) and SFV4(3H)-eGFP an average titre of 3.3 Log_{10} PFU/ml (SD: 1.6). Statistical analysis using paired t-test showed no significant difference between the two viruses ($P>0.05$). In contrast, SFV A7(74) infected mice had an average titre of 7.2 Log_{10} PFU/ml (SD: 0.4) and mice infected with SFV L10 had an average titre of 6.6 Log_{10} PFU/ml (SD: 0.7). Using paired t-test the values of the titres for SFV A7(74) and SFV L10 were not statistically different ($P>0.05$).

However, the titres of both these viruses were significantly higher than those of SFV4 and SFV4(3H)-eGFP ($P<0.05$) (Figure 3.9a). As expected, all mice mock-infected with PBSA had no detectable infectious virus. Comparison of the plaque sizes (on BHK-21 cells) produced by these viruses showed that SFV4 and SFV4(3H)-eGFP produced plaques with a very similar size (0.5-1 mm), Figure 3.9b, which were smaller than the plaque size produced by SFV A7(74) (1.5-3 mm), Figure 3.9c. These results suggest that insertion of eGFP in the non-structural ORF did not attenuate SFV4 since SFV4(3H)-eGFP had the same phenotype as SFV4 following intraperitoneal inoculation. However, titres of SFV4 and SFV4(3H)-eGFP were significantly lower than those of SFV A7(74) and SFV L10 (approximately 3 logs) and the plaque sizes were smaller, indicating that SFV4 virus and viruses derived form it, replicate less efficiently *in vitro* and *in vivo* than SFV A7(74) or SFV L10. This probably explains why SFV4 and SFV4-based recombinant viruses failed to infect the brain after i.p. challenge.

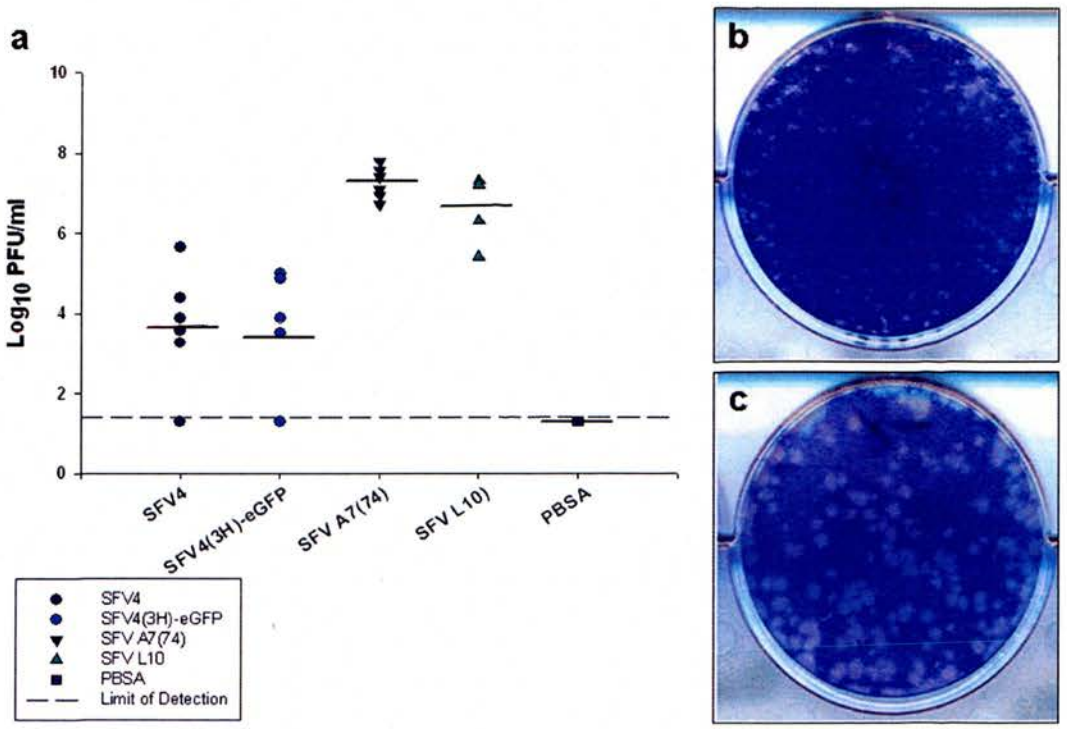

Figure 3.9. Comparison of levels of viraemia and of plaque size caused by various SFV strains. (a) SFV4 (dark blue circle) and SFV4(3H)-eGFP (light blue circle) had significantly lower titres than SFV A7(74) (inverted dark blue triangle) or SFV L10 (green triangle) ($P<0.05$; paired t-test). SFV4 and SFV A7(74) were not significantly different to SFV4(3H)-eGFP and SFV L10 respectively ($P>0.05$; paired t-test). Mock-infected mice (PBSA, dark blue square) had no infectious virus in the blood as expected. All samples were collected at 24 hours post-infection. Plaques produced by SFV4 and SFV4(3H)-eGFP had a similar size; representative plaques can be seen on **(b.** The plaques produced by SFV A7(74) **(c)** were larger. Monolayers of BHK-21 cells shown on **(b)** and **(c)** were infected with heparinised blood; sampled from mice infected with SFV4(3H)-eGFP and SFV A7(74), respectively. Cells were fixed 2 days post-infection and stained with toluidine blue.

Experiment III-Virus spread in wt mice and mice deficient in type-I interferon responses

Since the SFV4 icDNA was originally derived from the SFV prototype strain which is related to SFV L10, the difference between SFV4 and SFV L10 is surprising. Most likely some changes were introduced into the SFV4 as a result of this cloning process. These could have affected one of more aspects of the virus life-cycle, but changes in receptor binding or interaction with host defences are two important factors of infection which could be responsible for the difference between SFV4 and SFV L10. To investigate the role of the IFN system the following experiment was performed.

Experimental design

Type-I interferon is an important factor affecting the outcome of viral infections (Isaacs & Lindenmann, 1957). To study the spread of the infection in the absence of type-I interferon, groups (n=3) of adult (4-5 week old, female) IFN α/β receptor knock-out mice (A129) (Muller *et al.*, 1994) and wt129 mice were infected with 5 x 10^3 PFU of SFV4 or SFV4(3H)-eGFP. One mouse from each group was sampled at 24 hours post-infection and the remaining mice were sampled on PID 2. Heparinised blood was collected to determine the amount of infectious virus present. In SFV4(3H)-eGFP infected mice; spleen, pancreas, heart, lung, kidney, and brain were sampled and processed for frozen sections. Sections were examined for eGFP expression.

Results

Blood samples from A129 (IFN α/β $R^{0/0}$) and wt129 mice infected (i.p.) with SFV4 or SFV4(3H)-eGFP were titrated and the results are summarised in Table 3.1. SFV4 and SFV4(3H)-eGFP infected wt129 mice had similar titres on PID 1 (0.15 Log_{10} PFU/ml difference). All wt129 mice sampled on PID 2 had no detectable virus in the blood. As expected A129 mice, which lack type-I interferon responses, were not able to control the infection and had much higher titres of virus in the blood. On PID 1

SFV4 and SFV4(3H)-eGFP had a viral load of 8.5 and 7.9 Log_{10} PFU/ml respectively (0.6 Log_{10} PFU/ml difference). On PID 2 both remaining mice infected with SFV4 were found dead. SFV4(3H)-eGFP infected mice had an average titre of 8.3 Log_{10} PFU/ml. It is not possible to draw any firm conclusions, due to the small number of animals used per time-point, however the results suggest that in the absence of active type-I interferon responses, insertion of eGFP had a slight attenuating effect on SFV4. A129 mice infected with SFV4(3H)-eGFP had lower titres of infectious virus in the blood at PID 1 and survived longer than A129 mice infected with SFV4. A study with a larger number of animals is required to obtain results with statistical significance. These results also illustrate that the type-I interferon system very effectively limits SFV4 infection; blood virus titres at 24 hours were increased in the order of 10,000-fold in the absence of an intact type-I interferon system. Other data from this laboratory indicates that titres of SFV A7(74) also increased in the absence of type-I interferon response but not to the same extent suggesting that SFV4 either generates more interferon or is more sensitive to it than SFV A7(74).

Virus	**PID 1 wt129**	**PID 2 wt129**	**PID1 A129**	**PID2 A129**
SFV4	4.4 (1/1)	<1.4 (2/2)	8.5 (1/1)	-
SFV4(3H)-eGFP	4.2 (1/1)	<1.4 (2/2)	7.8 (1/1)	8.3 (2/2)

Table 3.1. Levels of viraemia in A129 and wt129 mice. All values are expressed as Log_{10} PFU/ml of blood. On PID 2 both mice infected with SFV4 were found dead (-).

Frozen sections of several different tissues from wt129 mice sampled on PID 1 were examined for eGFP expression. For each tissue, six slides each with 3 sections of spleen (12 μm thick), pancreas (14 μm thick), heart (12 μm thick), lung (12 μm thick), kidney (12 μm thick), and brain (12 μm thick) were examined for eGFP expression using a Zeiss Axioskop microscope. None of these tissues was eGFP-positive.

Sections of the same tissues from A129 mice sampled on PID 1 or 2 were also examined for eGFP expression. Heart, lung, kidney and brain tissues showed no sign of eGFP expression at any time-point (6 slides per tissue with 3 sections per slide). In

contrast, pancreas (Figure 3.10a - 3.10f) and spleen (Figure 3.10g-3.10i) had eGFP expression. Interestingly, in the pancreas only cells of the exocrine pancreas had eGFP expression. The infected cells found in the spleen were predominantly cells at the marginal zone between the red pulp and the white pulp; probably macrophages. Haematoxylin and eosin staining masked the fluorescent signal, so it was not possible to undertake a detailed analysis of the pathology in these tissues.

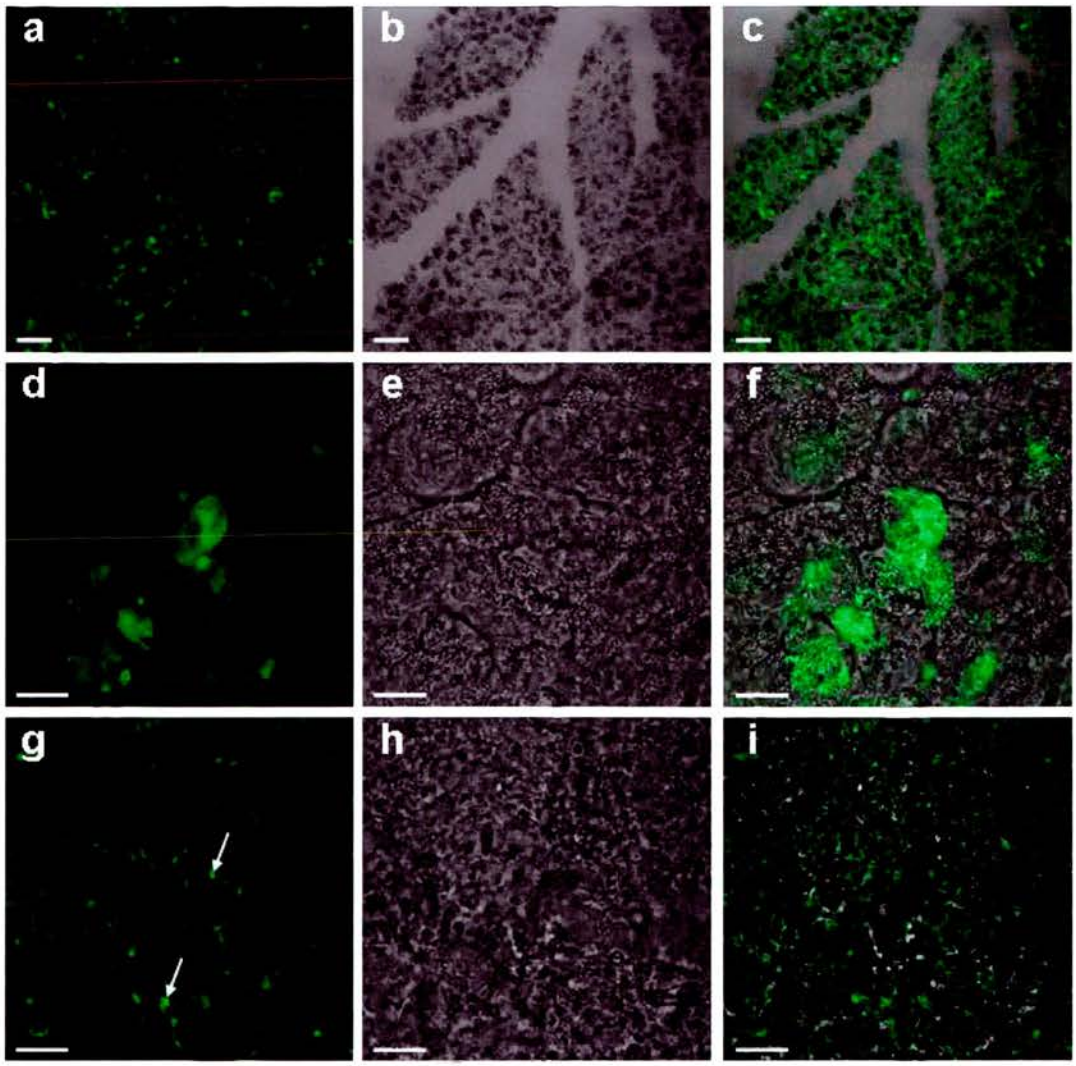

Figure 3.10. Distribution of SFV4(3H)-eGFP in the absence of type-I interferons. (a) low magnification image of eGFP expression in pancreatic tissue. **(b)** bright field image of the same section. **(c)** merged image of **(a)** and **(b)** Bars represent 100 μm in all panels. **(d)** high magnification image of a focus of infection in pancreatic tissue. **(e)** bright field image of the same section. **(f)** merged image of **(d)** and **(e)**. Bars represent 20 μm in all panels **(g)** high magnification image of infected splenic cells at the marginal zone, arrows point at representative cells. **(h)** bright field image of the same section. **(i)** merged image of **(g)** and **(h)**. Bars represent 20 μm in all panels. All tissues are from a A129 mouse sampled on PID 2.

Virus pathogenesis following intracerebral inoculation

As SFV4 and the two recombinant viruses expressing eGFP as a cleavable component of the replicase polyprotein did not efficiently spread to the brain of Balb/c mice following intraperitoneal inoculation it was decided to administer these viruses directly into the brain (intracerebral inoculation; i.c.) to investigate if the recombinant virus was able to replicate efficiently in the brain.

Experiment I-Virulence following direct brain inoculation

Experimental design

To determine the efficiency of replication and virus virulence following i.c. inoculation, groups (n=6) of adult (4-5 week old, female) Balb/c mice were infected i.c. with 1,000 PFU of SFV4, SFV4(3H)-eGFP, SFV4(3L)-eGFP, or mock-infected with PBSA. Mice were monitored at regular intervals for clinical end-points of viral encephalitis. All animals exhibiting substantial clinical signs of disease were euthanised and their brains were snap frozen for virus titration.

Results

Direct inoculation of SFV4, SFV4(3H)-eGFP and SFV4(3L)-eGFP in the CNS led to the development of severe encephalitis in all animals. In particular, at approximately 24 hours post-infection, mice had reduced motility and piloerection. By 48 hours 100% (6/6) of the infected animals had reached clinically defined terminal end-points indicative of substantial disease and were killed. In contrast, mock-infected animals (PBSA) were healthy for the 10 days that the experiment lasted (Figure 3.11a). All mice infected with SFV4, SFV4(3H)-eGFP or SFV4(3L)-eGFP developed clinical signs at the same time post-inoculation. The brains from SFV4, SFV4(3H)-eGFP and mock-infected animals were titrated to determine infectious virus titres. As expected, 100% of virus inoculated animals had high levels of infectious virus in the brain. SFV4 infected mice had an average infectious virus titre of 9.5 Log_{10} PFU/g of brain (SD: 0.11). SFV4(3H)-eGFP infected mice had an average titre of 9.7 Log_{10} PFU/g

of brain (SD: 0.15). Paired t-tests showed no significant difference between the brain titres of SFV4 and SFV4(3H)-eGFP infected animals ($P>0.05$). Mock-infected mice had no detectable infectious virus (Figure 3.11b).

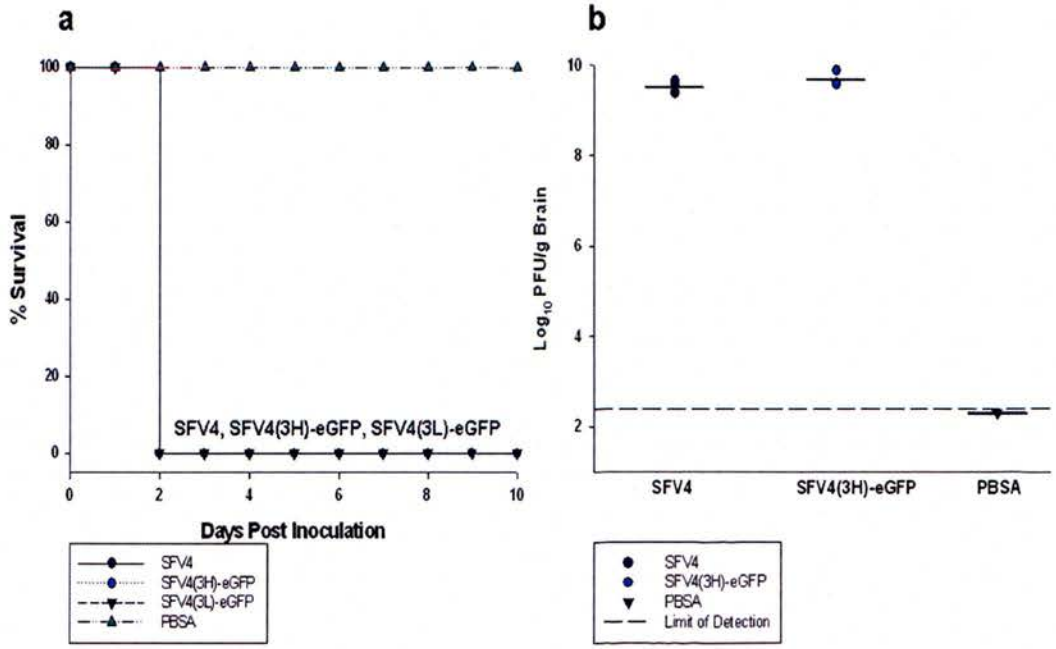

Figure 3.11. Survival rates and brain virus titres in Balb/c mice following i.c. inoculation. (a) Survival rates of Balb/c mice inoculated i.c. with SFV4, SFV4(3H)-eGFP, SFV4(3L)-eGFP or mock-infected with PBSA. **(b)** Infectious virus titres of SFV4 and SFV4(3H)-eGFP in the brains of Balb/c mice inoculated i.c. with 1,000 PFU. Each group had 6 mice. Mice were sampled on PID 2. Values are expressed as Log_{10} PFU/g of brain tissue. The two groups were compared using paired t-test and were not statistically different ($P>0.05$).

Experiment II-eGFP expression and distribution

Experimental design

To determine whether eGFP was expressed in the brain following i.c. inoculation, groups (n=6) of adult (4-5 week old, female) Balb/c mice were inoculated i.c. with 1,000 PFU of SFV4(3H)-eGFP. On PID 2 the mice were killed and their brains sampled and processed for frozen sections (12 μm thick). In addition, to study the expression of eGFP at different stages of infection, sections of brain tissue were stained with anti-nsP3 and anti-structural protein antibodies. Also, to find out if the insertion of eGFP altered the cell tropism of SFV4 in the CNS, antibodies against cell-specific markers of neurons, astrocytes and oligodendrocytes were used.

Results

Six out of six mice inoculated (i.c.) with SFV4(3H)-eGFP developed signs of severe encephalitis approximately 48 hours post-inoculation and the animals were sampled. Frozen sections of brain tissue from all animals were examined using a Zeiss Axioskop and a Zeiss confocal microscope. Expression of eGFP was evident in areas of white and gray matter. Figure 3.12a. shows infected cells at the alveus hippocampus (alv), a white matter tract below the corpus callosum (cc); the cc is the major white mater tract of the brain. On the same panel a cell of the granular dentate gyrus (GrDG) (gray matter) is expressing eGFP. Figure 3.12b and 3.12c show higher magnification images of the same field acquired with a standard and a confocal microscope respectively. Cells with low (asterisk) or high (arrow) intensity of eGFP signal were detected. The morphology of these cells and their anatomical position strongly suggests that these were oligodendrocytes. It is likely that the intensity of the fluorescent signal is related to the stage of infection of the cell. A cell at the early stages of infection, when expression of non-structural proteins is very active will, be brighter than a cell at the late stages of infection, when the levels of expression of non-structural proteins (and consequently of eGFP) are reduced. Multiple foci of

infection were found scattered around the cortex of the brain in areas of gray matter (Figure 3.12d & e) and in areas of white matter (Figure 3.12f).

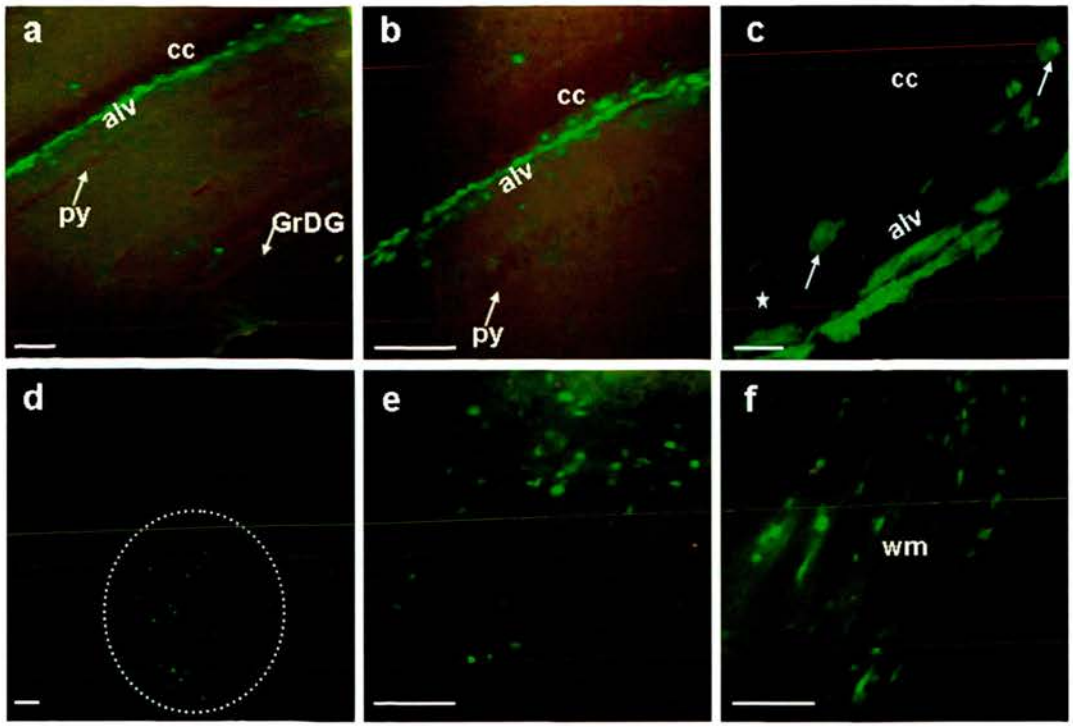

Figure 3.12. eGFP expression and distribution following i.c. inoculation of Balb/c mice with SFV4(3H)-eGFP. (a & b) GrDG: granular dentate gyrus; cc: corpus callosum; py: pyramidal cell layer of the hippocampus probably CA1-2 of Ammon's horn; alv: alveus hippocampus white matter, bar represents 100 μm. **(c)** Arrows and asterisk mark cells exhibiting high and low eGFP fluorescence, respectively. The anatomic position of these cells and their morphology suggests that they are oligodendrocytes, bar represents 20 μm. **(d)** A focus of infection in the brain cortex is shown inside the dotted circle, bar represents 100 μm **(e)** Large focus of infection found in the brain cortex. Different levels of eGFP fluorescence are observed, bar represents 100 μm. **(f)** The lighter areas correspond to myelinated tracts (white matter:wm), these tracts contain many eGFP-positive cells, these are most likely oligodendrocytes. Bar represents 100 μm. All tissue sections shown here were cut from brains sampled on PID 2. Images on panels **(a), (b), (e)** and **(f)** were acquired using a Zeiss Axioskop. Images on panels **(c)** and **(d)** were acquired by confocal microscopy.

eGFP expression vs nsP3 non-structural protein expression

Although green fluorescence was readily detectable in the brains of all infected animals, the number of positive (green) cells was smaller than expected. Since SFV4(3H)-eGFP was as virulent as SFV4 (survival rates; Figure 3.11a) and reached titres similar to those of the wild-type SFV4 virus (Figure 3.11b) and because the half-life of eGFP in BHK-21 cells was short (Figure 3.3b) frozen sections were immunostained using an anti anti-nsP3 antibody to investigate the hypothesis that infection was actually widespread, as was expected with SFV4, but that due to the short half-life of eGFP this was not apparent from the number of green cells.

The results verified this hypothesis; nsP3-positive cells (red fluorescent signal, Figure 3.13) outnumbered eGFP-positive cells. Counting nsP3 and eGFP-positive cells, it was found that the ratio varied between 3:1 and 5:1 depending on the area of the brain (at least 6 slides with 3 sections per slide were examined). As expected, the vast majority (approximately 100%) of eGFP-positive cells also stained positive for nsP3. Only rare were eGFP-positive, nsP3-negative cells observed. Representative images of double-labelled cells are shown on Figure 3.13, panel **(a)-(f)**. At the top left of panel **(c)** marked with an asterisk, the CA3 zone of pyramidal neurons of Ammon's horn is shown. Although, many cells presumably neurons, in this area stained positive for nsP3 protein, none was eGFP-positive at the same time. Interestingly, numerous small cells in close proximity to the nsP3-positive cells were eGFP-positive (Figure 3.13c and inset). The position and morphology of these small eGFP-positive cells is consistent with satellite oligodendrocytes. Perhaps, these cells were infected later than the adjacent pyramidal neurons or these two cells differ in their interaction with this virus. The characteristic punctate staining observed when infected BHK-21 cells were immunostained with an anti-nsP3 antibody was also apparent in the frozen brain tissue sections stained with this antibody (Figure 3.13e inset & Figure 3.14c). On Figure 3.14, the hypothetical progress of infection *in vivo* based on eGFP vs nsP3 expression is shown. Early in infection, eGFP is visible throughout the cytoplasm and the nucleus of infected cells and nsP3 is located in the outer areas of the cytoplasm (panel **a**). Later in infection (panel **b**) the intensity of eGFP signal declines and punctate, cytoplasmic nsP3 is prominent. At the very late

stage of infection (panel **c**) eGFP is not detectable and nsP3-specific staining is found in abundance and is punctate and cytoplasmic. As discussed earlier, the distribution of the punctate nsP3 staining is consistent with the known distribution of SFV replication complexes.

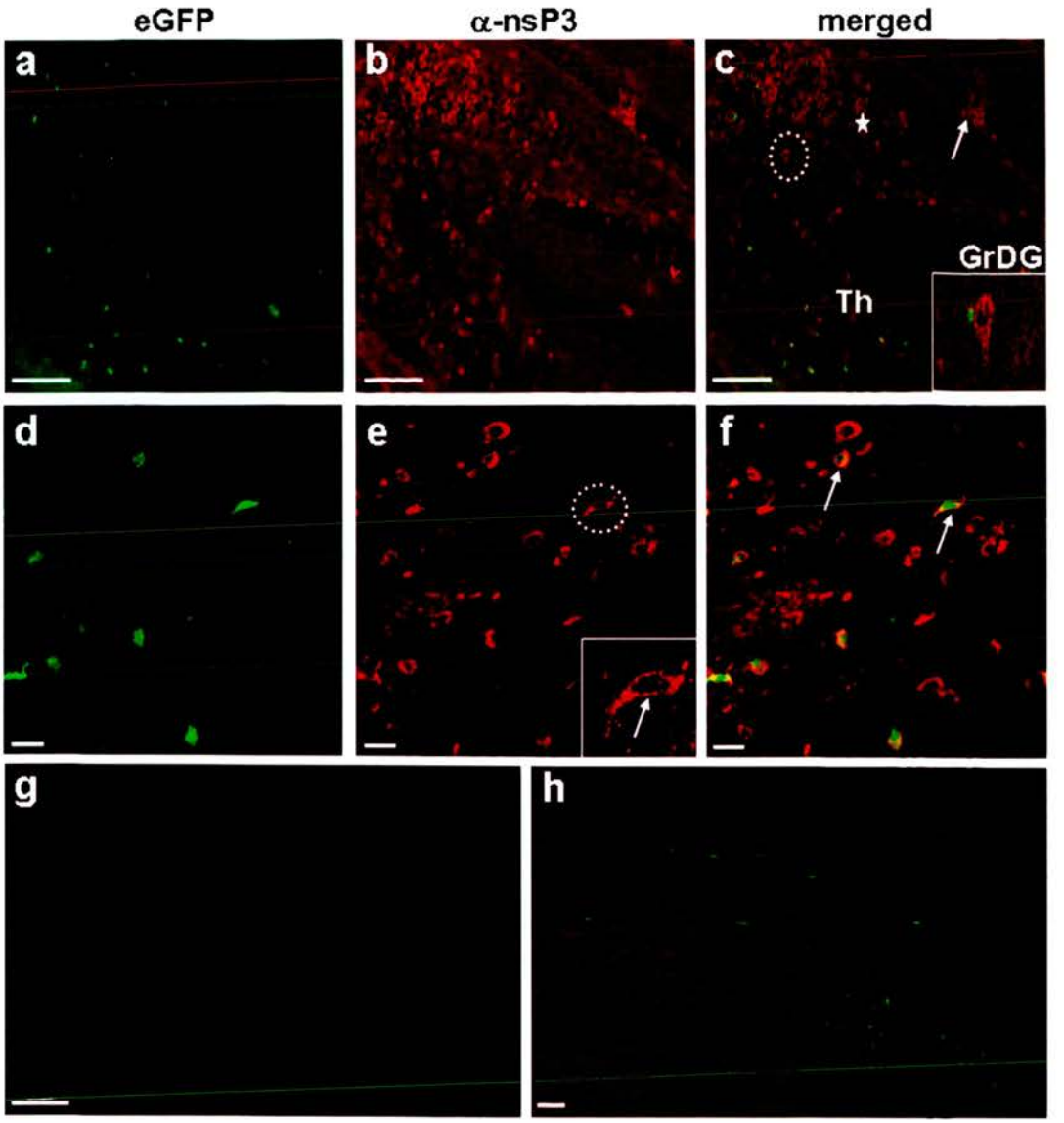

Figure 3.13. eGFP expression and nsP3 expression in the brains of SFV4(3H)-eGFP infected mice. (a) low power magnification showing several scattered eGFP-positive cells. **(b)** low power magnification of nsP3-specific staining on the same section showing many more nsP3-positive cells. **(c)** merged image of **(a)** and **(b)**, GrDG: granular dendate gyrus, Th: thalamus, asterisk marks the CA3 zone of pyramidal cell layer of the Ammon's horn. Arrow points at a focus of infection on the GrDG. The area in the dotted circle is shown in high magnification in the inset. The eGFP-positive cell proximal to the nsP3-positive cell is most probably a satellite oligodendrocyte. Bar in panels **a-c** represents 100 μm. **(d)** eGFP expression in a focus of infection in the brain cortex. **(e)** nsP3-specific staining on the same section; the cell surrounded by the dotted circle is shown in high magnification in the inset, the arrow points at the punctate distribution of nsP3 staining. **(f)** merged image of **(d)** and **(e)**, arrows mark examples of double-labelled cells. Bar in panels **d – f** represents 20 μm. Non-infected and no secondary antibody controls are shown on **(g)** and **(h)**,

respectively; bar in both represents 100 μm. All tissue sections shown here were cut from brains sampled on PID 2. All images were acquired with a Zeiss confocal microscope.

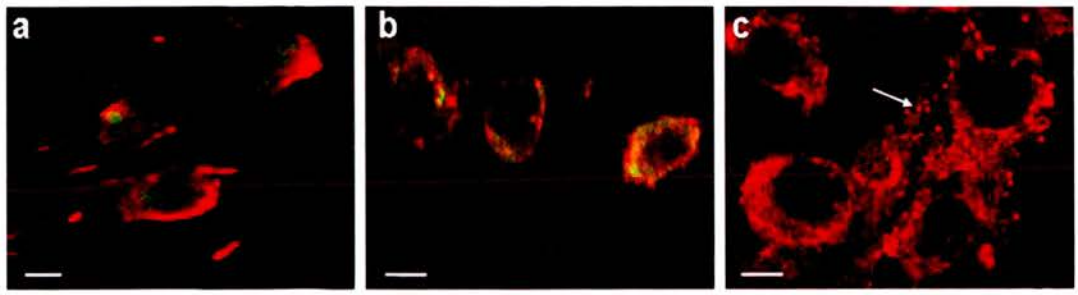

Figure 3.14. eGFP expression and nsP3 expression *in vivo*. Hypothetical progress of infection. (a) double-labelled cells at the early stages of infection. **(b)** double-labelled cells later in infection; note the reduction in eGFP signal. **(c)** nsP3 stained cells at the very late stage of infection. Arrow points at the punctate staining. Bar in panels **a – b** represents 20 μm. All images were from the same section. All tissue sections were from a brain sampled on PID 2. All images were acquired with a Zeiss confocal microscope.

eGFP expression vs SFV structural protein expression

Frozen sections of infected brain tissue were also immunostained using an antibody recognising the structural viral proteins. The results obtained verified the findings of the nsP3-specific immunostaining; infection was widespread as determined by immunostaining of virus structural proteins but only a small percentage of these cells were eGFP-positive. However, in contrast to the nsP3 staining where approximately 100% of eGFP-positive cells were also nsP3-positive, only a small fraction (1-5%; different areas of the brain examined, at least 6 slides with 3 sections per slide) of eGFP-positive cells were positive for SFV structural proteins (Figure 3.15f). In most instances, SFV structural protein-positive cells were distinct from the eGFP-positive cells. A representative example is shown on panels **(a)-(c)** of Figure 3.15; the vast majority of the eGFP-positive cells (green) are on the right hand-side of the field of vision whereas most of the SFV structural protein positive cells (red) are on the left hand-side. This would be consistent with infection having started from the left hand-side and spread towards the right hand-side. In foci of infection where eGFP-positive cells and cells positive for SFV structural proteins were in close proximity, a few double-labelled cells were found (Figure 3.15f). On Figure 3.16, the hypothetical progress of infection *in vivo* based on eGFP and structural protein expression is shown. Early in infection, eGFP is expressed throughout the cytoplasm and the nucleus of infected cells but SFV structural proteins are not detected (panel **a**). Later in infection (panel **b**) and while eGFP is still present, viral structural proteins are detected. Cells like the one shown here were very rare. At later stages of infection (panel **c**) eGFP signal is no longer detectable whereas structural protein staining is still present. The distribution of the structural proteins was as expected; proteins were found on the outer area of the cytoplasm, most probably associated with the cell membrane.

The percentage of double-labelled cells (eGFP/nsP3-positive vs eGFP/structural-positive) is different but is as expected given that the two viral promoters (genomic (42S and subgenomic 26S) are active at different stages post-infection and the half-life of eGFP was short. The findings of the immunostainings using anti-nsP3 and anti-structural antibodies suggest that SFV4(3H)-eGFP has potential application for

in vivo pathogenesis studies. This virus may be useful to distinguish cells in which the replicase polyprotein is being synthesised from those in which the synthesis of this particular polyprotein has been terminated.

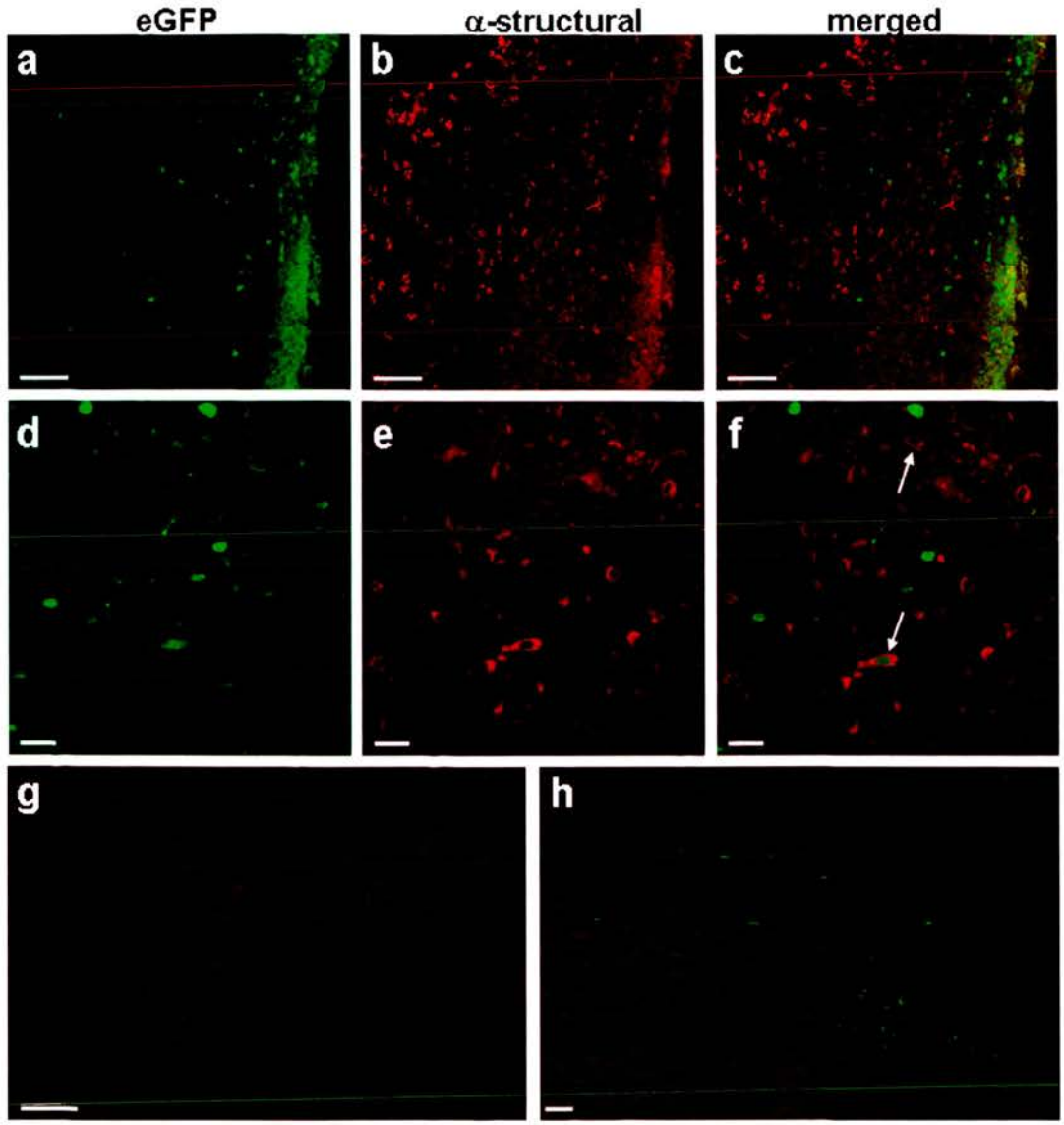

Figure 3.15. eGFP expression and viral structural protein expression in the brain of SFV4(3H)-eGFP infected mice. (a) low power magnification showing several scattered eGFP-positive cells. **(b)** low power magnification of structural proteins specific staining on the same section showing many more virus positive cells. **(c)** merged image of **(a)** and **(b)**. Bar in panels **a-c** represents 100 μm. **(d)** eGFP expression in a focus of infection on the brain cortex. **(e)** viral structural protein specific staining on the same section **(f)** merged image of **(d)** and **(e)**, arrows mark double-labelled cells, most cells are not double labelled. Bar in panels **d-f** represents 20 μm. Non-infected and no secondary antibody controls are shown on **(g)** and **(h)**. Bar in both represents 100 μm. All tissue sections shown here were cut from brains sampled on PID 2. All images were acquired with a Zeiss confocal microscope.

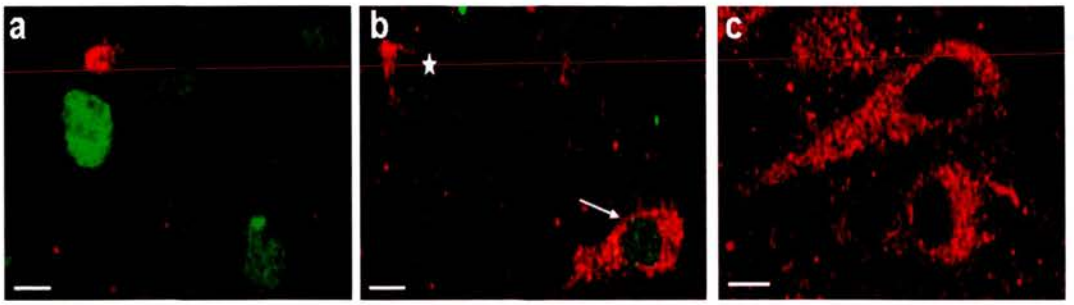

Figure 3.16. eGFP expression and viral structural protein expression *in vivo*. Hypothetical progress of infection. (a) eGFP positive cells at the early stages of infection. **(b)** double-labelled cells later in infection. The asterisk marks two adjacent cells, one eGFP-positive but negative for virus structural proteins and one which exhibits the opposite. **(c)** Cells at the later stages of infection stained positive for virus structural proteins; eGFP was not detectable. Bar in panels **a** – **c** represents 20 μm. All images were from the same section. All tissue sections shown here were cut from a brain sampled on PID 2. All images were acquired with a Zeiss confocal microscope.

Cell tropism of SFV4(3H)-eGFP in the CNS

One of the major advantages of a virus expressing a marker gene is the ability to study its *in vivo* tropism, and the effect of tropism on virulence, without the requirement for double-immunostaining. Traditionally, to study the tropism of a virus *in vivo*, it has been necessary to immunostain for viral protein, or hybridise for viral nucleic acid and also to immunostain for a cell-specific marker. Using a virus like SFV4(3H)-eGFP the need for the detection of viral protein or nucleic acid is eliminated simplifying the whole procedure.

SFV has previously been described to infect neurons and oligodendrocytes but not astrocytes (Fazakerley *et al.*, 2006). To examine if the insertion of eGFP altered the tropism of SFV in the CNS, sections of SFV4(3H)-eGFP infected brains were stained with antibodies against neurons (NeuN). This antibody specifically recognizes the DNA-binding, neuron-specific protein NeuN, which is present in the nuclei and perikarya of most CNS neurons. An antibody against 2'3'-Cyclic nucleotide 3'-phosphohydrolase (CNPase) was used as a specific marker for oligodendrocytes. Finally, an antibody against glial fibrillary acidic protein (GFAP) a member of the intermediate filament family, found exclusively in astroglial cells, was used as a marker for astrocytes.

Surprisingly, although the NeuN immunostaining worked extremely well, it was not possible to detect eGFP-positive NeuN-positive cells (Figure 3.17). This is consistent with the observation (see also Figure 3.13) that SFV4(3H)-eGFP did not result in eGFP-positive cells which were anatomically and morphologically clearly neurons (Figure 3.13c). Whereas it is possible that neurons with eGFP fluorescence might not be efficiently recognised by the anti-NeuN antibody, there were numerous neurons in the cortical area of the brain which stained positive for NeuN but none of these was eGFP-positive. When frozen sections were stained with anti-nsP3 antibody, numerous cells in areas of the brain known to be rich in neurons stained positively (Figure 3.13a – c). Yet, no eGFP-positive cells were detected in these areas. It can be hypothesised that neurons have the ability to switch off the 42S genomic promoter controlling the expression of non-structural proteins and eGFP and because eGFP has short half-life it was not detected. However, a double immunostaining with anti-nsP3

and anti-NeuN antibodies is required to determine with certainty if NeuN-positive neurons can be infected with SFV4(3H)-eGFP; certainly cells that are morphologically and anatomically neurons can be infected by this virus.

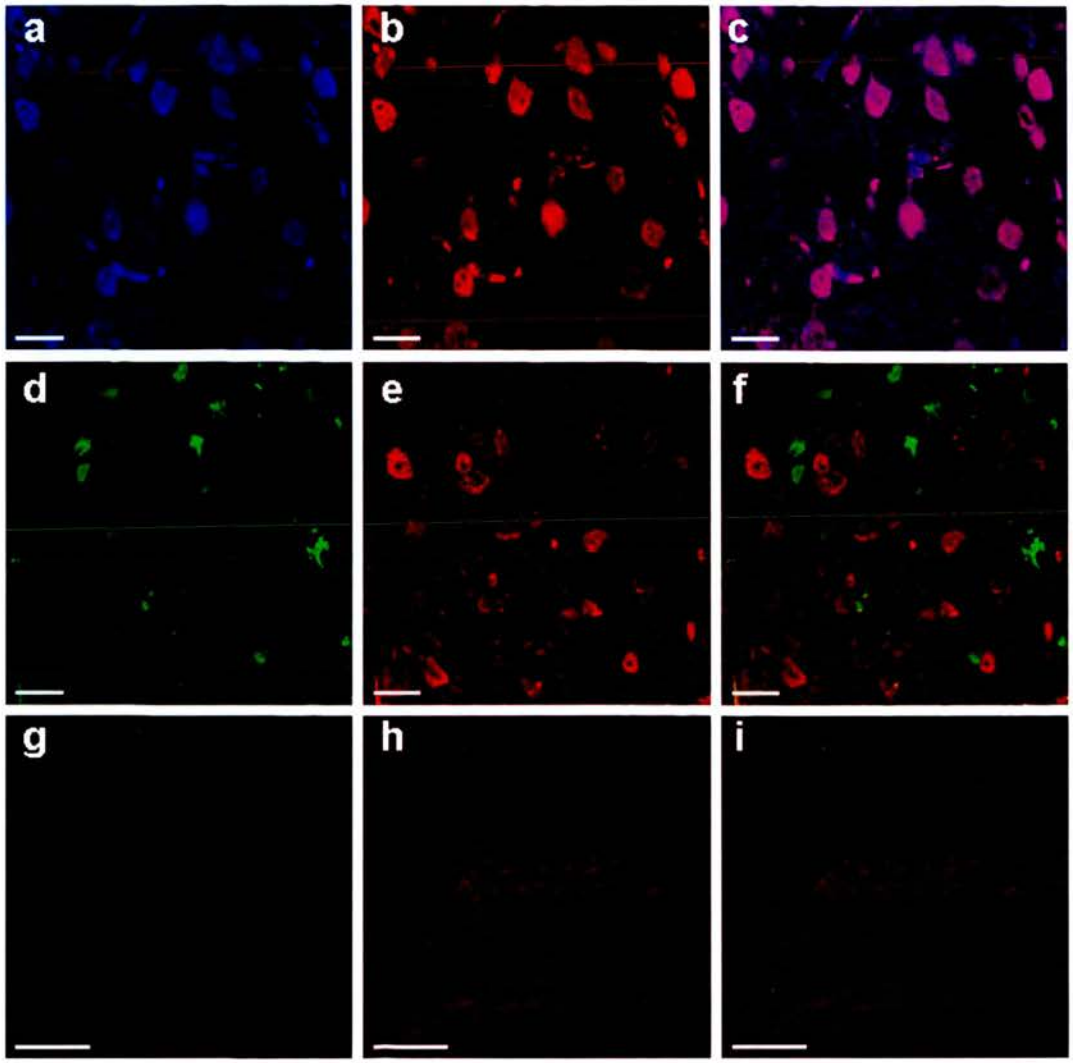

Figure 3.17. Immunostaining using NeuN neuronal marker on brain sections from Balb/c mice infected i.c. with SFV4(3H)-eGFP. (a) Positive nuclei stained by To-Pro3 nuclear marker. **(b)** Positive nuclei stained by NeuN neuron-specific antibody. **(c)** merged image of **(a)** and **(b)**, signals from the nuclear marker and the neuron-specific immunostaining co-localise. Bars represent 20 μm in all panels. **(d)** eGFP positive cells on a 12 μm thick frozen brain tissue section. **(e)** NeuN specific staining on the same section. **(f)** merged image of **(d)** and **(e).** No co-localisation was observed; at least 6 slides with 3 sections per slide were examined. Bars represent 20 μm in all panels. Panels **(g) (h)** and **(i)** show the green channel, red channel, and merged image of both channels respectively on a control non-infected brain section. Sections were immunostained with NeuN antibody but secondary antibody was not included. Bars represent 100 μm in all panels. All other tissue sections shown here were cut from brains sampled on PID 2. All images were acquired with a Zeiss confocal microscope.

SFV4(3H)-eGFP has the ability to infect areas of white and gray matter. Oligodendrocytes can be found in both areas but are far more abundant in white matter tracts where they perform their main function, synthesis and maintenance of the myelin sheaths around axons. Previous studies using SFV4 have shown that SFV has the ability to infect oligodendrocytes (Atkins & Sheahan, 1982; Balluz *et al.*, 1993). Oligodendrocytes are the predominant cell type infected when the avirulent A7(74) strain of SFV is inoculated intracerebrally (Fazakerley *et al.*, 2006).

Figure 3.18a shows a focus of infection which spreads between the corpus callosum (cc), the major white matter tract of the brain and the cingulum (cg) another white matter tract located on the top of the corpus callosum. Oligodendrocyte-specific staining (anti-CNPase; Figure 3.18b) showed numerous positive cells (red colour) scattered in the gray matter area surrounding the area of pyramidal neurons of the hippocampus. As expected, the number of oligodendrocytes detected was much greater in the white matter area defined by the corpus callosum and the cingulum (greater intensity of red signal). The area surrounded by the dotted circle in Figure 3.18c is shown in higher magnification in panels **(d)** to **(f)** of the same figure. Most infected cells (indicated by the green colour) in this field of vision appeared to be oligodendrocytes (CNPase positive; red colour). Representative double-labelled cells are marked with white arrows on panel **(d)**. This indicates that insertion of eGFP in the replicase ORF did not interfere with the ability of SFV4 to infect oligodendrocytes.

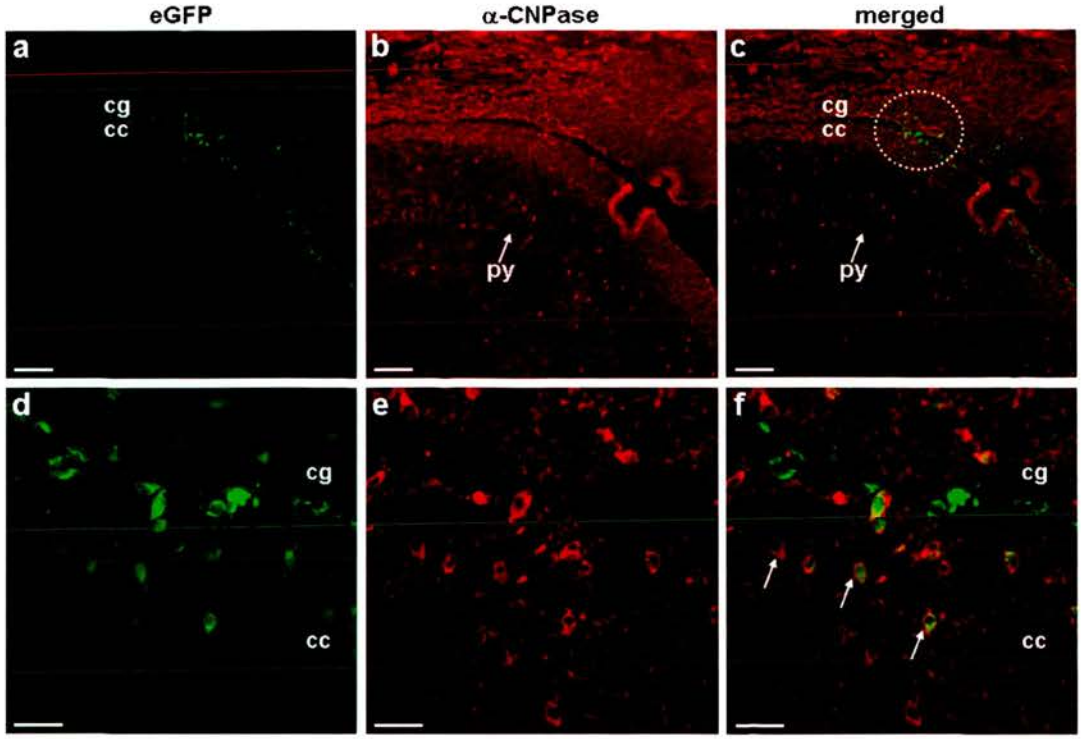

Figure 3.18. Immunostaining using CNPase as oligodendrocyte marker on brain sections from Balb/c mice infected i.c. with SFV4(3H)-eGFP. (a) Focus of infection in by the major white matter tract of the brain, the corpus calossum (cc) and another white matter tract, the cingulum (cg). **(b)** CNPase-positive cells (oligodendrocytes) scattered on the same section; py corresponds to the layer of the pyramidal neurons of the hippocampus. **(c)** merged image of **(a)** and **(b).** Bars represent 100 μm in all panels. **(d)** The area of panel **(c)** surrounded by the dotted circle is shown in higher magnification. Different levels of eGFP intensity can be observed. **(e)** CNPase specific staining of the same section. **(f)** merged image of **(d)** and **(e)**. Representative double-labelled cells marked with white arrows. Bars represent 20 μm in all panels. Same secondary antibody as the one used for anti-nsP3 and anti-structural immunostaining was used; therefore negative controls can be seen in Figure 3.13 or 3.15. All sections shown here were cut from brains sampled on PID 2 and had a thickness of 12 μm. All images were acquired with a Zeiss confocal microscope.

Astrocytes provide physical and biochemical support for neurons and are activated in infected or damaged areas of the brain. Previous studies by this laboratory (on SFV A7(74)) and others (on SFV4) have shown that SFV does not infect astrocytes. To verify that this remained the case for SFV4(3H)-eGFP, sections of SFV4(3H)-eGFP infected brain tissue were immunostained with an anti-GFAP antibody. On Figure 3.19a a focus of infection can be seen; note that the astrocyte-specific staining is concentrated in and around the focus of infection (Figure 3.19b & 3.19c); this is as expected since astrocytes get activated by the infection. Six slides with 3 sections per slide were examined for co-localisation of eGFP and GFAP-specific staining. No double-labelled cells were observed after thorough microscopic examination of many different areas on each section. Astrocytes appeared to be around infected cells (Figure 3.19f). The characteristic star-like shape of astrocytes can be seen in the inset of panel f.

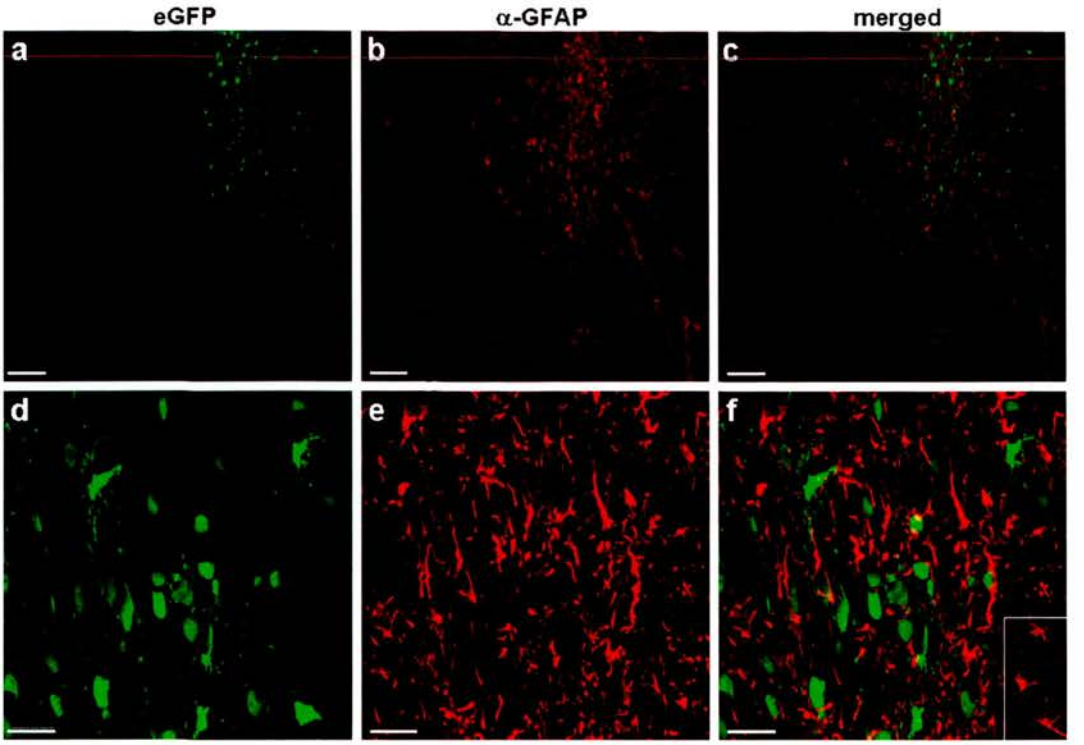

Figure 3.19. Immunostaining using GFAP as astrocyte marker on brain sections from Balb/c mice infected i.c. with SFV4(3H)-eGFP. (a) Focus of infection in the brain cortex **(b)** GFAP-positive cells (astrocytes;red signal). **(c)** merged image of **(a)** and **(b).** Astrocytes are around and within the focus of infection. Bars represent 100 μm in all panels. **(d)** Higher magnification of **(a)** Different levels of eGFP intensity can be observed. **(e)** GFAP specific staining of the same section. **(f)** merged image of **(d)** and **(e)**. Bars represent 20 μm in all panels. Same secondary antibody as the one used for anti-nsP3 and anti-structural immunostainings was used; therefore negative controls can be seen in Figure 3.13 or 3.15. All sections shown here were cut from brains sampled on PID 2 and had a thickness of 12 μm. All images were acquired with a Zeiss confocal microscope.

In vivo phenotypic and genotypic stability of SFV4(3H)-eGFP in Balb/c mice

Experimental design

To determine the genetic stability of SFV4(3H)-eGFP after several passages *in vivo* the virus was passaged 5 times in Balb/c mice and examined for phenotypic and genotypic changes after each passage. Figure 3.20 outlines the experimental design used to investigate the *in vivo* stability.

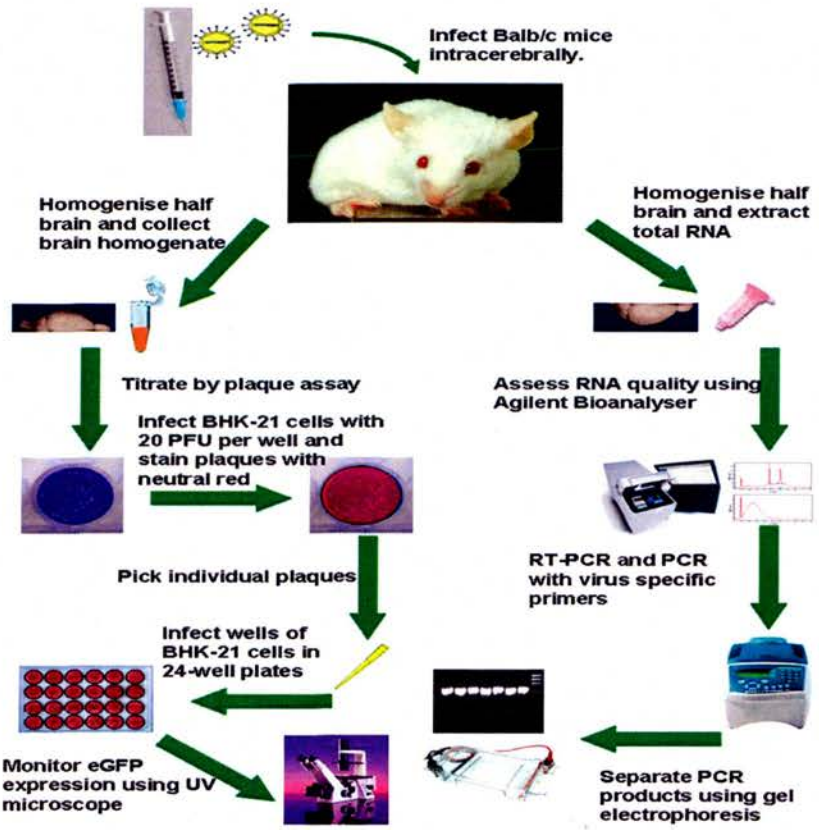

Figure 3.20. Experimental design to investigate *in vivo* phenotypic and genotypic stability. Two Balb/c mice were inoculated i.c with 20 µl of 5 x 10^4 PFU/ml virus stock. At PID 2 their brains were sampled, half of each brain was homogenised and titrated and half was used for extraction of total RNA, which was analysed by RT-PCR. One brain homogenate was passaged into the brains of another two Balb/c mice and also used to infect (20 PFU) fresh BHK-21 cells. These monolayers were overlayed with agar and 96 plaques were purified; individual plaques were transferred to 24-well plates and each well was analysed for eGFP expression. The passaging procedure was repeated four more times.

Phenotypic stability of SFV4(3H)-eGFP in vivo

In an identical manner to the one applied to assess the *in vitro* stability of recombinant viruses, 96 plaques were purified from each of the 5 *in vivo* passages. Each mouse was infected with 1,000 PFU and the brain was removed on PID 2; by this time all infected mice had symptoms of severe encephalitis. SFV4(3H)-eGFP exhibited remarkable phenotypic stability *in vivo*. All 96 isolated plaques were found to produce eGFP-positive viruses for the first 4 passages through the mouse brain. Of the 96 plaques isolated from the material obtained after the 5^{th} passage, only one plaque was found to be eGFP negative; 98.96% plaques were positive (Figure 3.21a).

Genotypic stability of SFV4(3H)-eGFP in vivo

One half of the brain from each infected mouse at each passage was stored in RNA*later*, an RNA stabilising reagent, and total RNA was extracted and used for RT-PCR to detect the absence or presence of the eGFP insert. If the eGFP insert was absent a PCR product with a size of ~670 bp was expected. If the eGFP insert was present a PCR product with a size of ~1,500 bp would be produced. Figure 3.21b shows the results obtained from each of the 5 *in vivo* passages as well as the product obtained when total RNA from brains of animals infected with SFV4 was amplified using RT-PCR. Between passage 1 through 4 no eGFP-negative virus was detectable. Minor amounts were detected after passage 5. These results are in agreement with the phenotypic stability analysis by plaque purification of viral clones. Since no intermediate bands were observed no sequence analysis was performed.

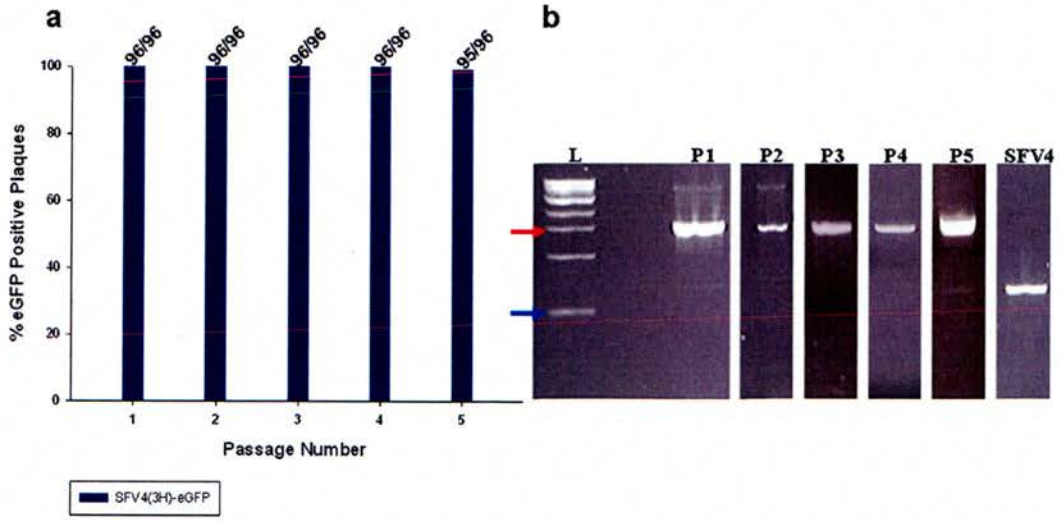

Figure 3.21. *In vivo* phenotypic and genotypic stability of SFV4(3H)-eGFP. (a) percentage of eGFP positive plaque purified viruses after serial passaging. **(b)** RT-PCR genotyping of SFV4(3H)-eGFP using nsP3 – nsP4 primers on RNA samples extracted from infected brain material. Passage number is indicated across the top of each strip. The red arrow corresponds to the 1.5 kb band of the DNA ladder and the blue arrow corresponds to the 0.5 kb band of the DNA ladder.

Summary of Findings

Summary of in vitro analysis of SFV4(3H)-eGFP and SFV4(3L)eGFP

- Insertion of eGFP in the non-structural ORF of SFV4 resulted in the production of viable viruses (SFV4(3H)-eGFP and SFV4(3L)-eGFP) which were able to replicate in BHK-21 cells to levels similar to SFV4. Both recombinant viruses were slightly slower in their replication compared to SFV4. eGFP was expressed to adequate levels for detection using a standard fluorescent microscope. However, the intensity of the eGFP signal quickly decreased and late in infection cells had a dull green colour. In terms of development of cytopathic effect (CPE) both recombinant viruses induced CPE in an identical manner to SFV4.
- All viral non-structural proteins and eGFP were expressed and processed properly. Minor amounts of an eGFP-nsP4 fusion protein were detected but most protein was released free indicating that both H and L processing sites were functional. A pulse-chase experiment suggested that eGFP is degraded soon after infection. This resulted in low levels of eGFP fluorescence late in infection.
- In infected BHK-21 cells, eGFP was present in both the cell cytoplasm and the nucleus. In some instances the eGFP signal was stronger in the nucleus than in the cytoplasm. The ability of eGFP to spread throughout the cytoplasm and the nucleus again suggests that processing of the polyprotein was efficient and eGFP was released free. The nsP3-specific staining was punctate and strictly cytoplasmic. The staining probably corresponds to the position of the virus replication complexes.
- After 5 passages in BHK-21 cells, 93.6% of plaque purified SFV4(3H)-eGFP was able to express eGFP. In contrast only 50% of SFV4(3L)-eGFP plaque purified viruses maintained that ability after 5 passages. RT-PCR showed the presence of recombinant viruses with complete or partial deletions of eGFP. Sequencing of some of these viruses showed large in-frame deletions of eGFP.

- SFV4(3H)-eGFP was able to infect C6/36 cells from *Aedes albopictus* and eGFP was expressed in these cells. Virus was used to infect rat hippocampal neurons but eGFP was not detected in these cells. However, CPE developed in these cells at the same time as in cells infected with SFV4.

Summary of in vivo analysis of SFV4-steGFP

- Following intraperitoneal inoculation of SFV4(3H)-eGFP or SFV4(3L)-eGFP in Balb/c mice 100% of the mice remained asymptomatic and survived the infection. In contrast to groups of control mice infected with SFV L10 or mock-infected with PBSA, which lost and gained considerable amounts of body weight respectively, mice infected with SFV4, SFV4(3H)-eGFP and SFV4(3L)-eGFP did not lose or gain weight. SFV4(3H)-eGFP reached similar levels of viraemia to SFV4 (no statistical difference) but considerably lower levels (statistically significant) than SFV L10 and SFV A7(74).
- SFV4(3H)-eGFP virus was used to infect IFN α/β receptor knock-out mice. This virus had slightly lower titres than SFV4 in the blood of infected mice but all animals succumbed to infection at the same time (PID 2). In wt129 mice (background strain of IFN α/β knock-out mice used as control) SFV4(3H)-eGFP had similar titres to SFV4. eGFP-positive cells were observed in the acinar cells of the exocrine pancreas and in cells in the marginal zone of the spleen.
- Intracerebral inoculation of Balb/c mice with SFV4(3H)-eGFP and SFV4(3L)-eGFP caused lethal encephalitis in 100% of the mice. Symptoms and death occurred at the same time for all groups of mice infected with the recombinant viruses and SFV4. Titres of SFV4(3H)-eGFP in the brain were not different to those of SFV4.
- eGFP expression was evident in both white and gray matter in the brains of mice infected with SFV4(3H)-eGFP. eGFP-positive cells were not as widespread as expected and frozen sections of infected brain tissue were immunostained using anti-nsP3 and anti-SFV antibodies. The infection was much more widespread when immunostaining was used. The reason for this

is probably rapid degradation of eGFP. All eGFP-positive cells stained positive for nsP3 as expected. In contrast, very rarely, eGFP-positive cells were also positive for viral structural proteins.

- *In vivo* SFV4(3H)-eGFP had impressive genetic stability. After 5 passages in the brain of Balb/c mice approximately 99% of plaque purified viruses were able to express eGFP. Minor amounts of recombinant viruses which managed to completely eliminate the eGFP insert were detected by RT-PCR.

Discussion

Alphaviruses have short genomes expressing large polyproteins which are then processed into individual proteins by the activity of virus encoded proteinases (ten Dam *et al.*, 1999). Increasing the size of the genome of such a virus by insertion of a heterologous gene affects the production of infectious particles (packaging constraints due to the compact icosahedral nucleocapsid). In addition, the size of the inserted sequence is an important factor for the genetic stability of recombinant viruses; viruses with smaller inserts appear to be more stable than viruses with large inserts (Hahn *et al.*, 1992; Frolov *et al.*, 1996). Recombinant alphaviruses carrying foreign sequences under the control of a duplicated subgenomic promoter appear to eliminate the inserted genes. This genome instability has been shown for SV (Pugachev *et al.*, 1995; Pugachev *et al.*, 2000), SFV (Vaha-Koskela *et al.*, 2003) and VEEV (Caley *et al.*, 1999). The mechanism of elimination has not been clarified but it has been suggested that recombination occurs between the duplicated subgenomic promoters (Thomas *et al.*, 2003).

Initially, a virus expressing eGFP as a fusion protein inserted in-frame at the C-terminus of nsP3 was constructed; SFV4(3F)-eGFP. Similar SV nsP3-fusion constructs expressing luciferase in a temperature sensitive manner (Bick *et al.*, 2003) and eGFP (Zhimin Liang and Guangpu Li, 2005; Frolova *et al.*, 2006) have been previously described. Data on both SV and SFV has shown that large in-frame deletions of the hypervariable C-terminus of nsP3 (12 – 159 amino acids for SV and 50 amino acids for SFV) can be tolerated and the resulting viruses are viable and able to replicate (Lastarza *et al.*, 1994; Vihinen *et al.*, 2001). SFV4(3F)-eGFP was viable and a nsP3-eGFP fusion protein was expressed. eGFP and nsP3 proteins co-localised in cytoplasmic structures (punctate staining) and had the typical distribution of nsP3 protein observed in cells infected with SV or SFV (Froshauer *et al.*, 1988; Kujala *et al.*, 2001). These structures are most probably the virus replication complexes (Frolova *et al.*, 2006; Tamberg *et al.*, 2007). The major disadvantage of SFV4(3F)-eGFP was its genetic instability, which can probably be attributed to problematic formation and function of the virus replication complexes. The data obtained is in agreement with that of Frolova *et. al.* (2006); the position of the eGFP insertion

affects the genetic stability. SFV4(3F)-eGFP (like its SV analogues) is therefore useful for *in vitro* studies on replication complex formation, replicase proteins interaction with host cell proteins and host cell transcriptional/translational shut-off but not for *in vivo* pathogenesis studies (Ryman *et al.*, 2005; Ventoso *et al.*, 2006; Frolova *et al.*, 2006; Cristea *et al.*, 2006). Recently, similar fusion constructs in which eGFP was inserted in the coding sequence of nsP2 have been described for SV (Atasheva *et al.*, 2007).

For SFV the nsP2 protease processing sequence between nsP3 and nsP4 has been well characterised (Merits *et al.*, 2001; Vasiljeva *et al.*, 2001; Lulla *et al.*, 2006). To circumvent the problems caused by the fusion of eGFP to nsP3, the eGFP-insert was flanked by two different nsP2-protease processing sites. The resulting recombinant viruses (SFV4(3H)-eGFP and SFV4(3L)-eGFP) had a slight delay in their replication compared to SFV4 *in vitro*. This data is not directly comparable to data on SV expressing eGFP as a fusion to nsP3 since the eGFP gene is inserted as a cleavable component of the non-structural ORF in the viruses used in the present study but some interesting trends can be observed. SV recombinant constructs having eGFP inserted at position 389 (amino acid) of nsP3 were engineered by two different groups. According to the results of Liang & Li (2005), insertion of eGFP at this particular position results in a delay in replication. However, this is in contrast to the data published by Frolova *et. al.* (2006), which suggests that replication efficiency of SV is not affected by insertion of eGFP after amino acid 389. A recombinant SV which is very similar to SFV4(3H)-eGFP and SFV4(3L)-eGFP was described by Frolova *et. al.* This virus had eGFP fused to amino acid position 549, the last amino acid of SV nsP3. In the recombinant viruses used in the present study eGFP was inserted after the last amino acid of SFV nsP3 (amino acid 482). As with SFV4(3H)-eGFP and SFV4(3L)-eGFP, SIN/549 was slower in BHK-21 cells but later in infection, 10 – 12 hours, it caught up with the wild-type Toto1101. SFV4(3H)-eGFP and SFV4(3L)-eGFP were also slower to replicate in BHK-21 cells than SFV4 but they caught up with the wt titres more rapidly. The delay in the replication of both recombinant SV and SFV can be attributed to the larger size of the replicase ORF or to delayed/defective formation of viral replication complexes. In alphaviruses, nsP3 is associated with viral RNA synthesis, of the minus-strand intermediate in particular,

and viruses with deletions in nsP3 produce lower amounts of viral RNA in BHK-21 cells (LaStarza *et al.*, 1994; Lemm *et al.*, 1994; Wang *et al.*, 1994; Galbraith *et al.*, 2006). Insertion of eGFP at the C-terminus of nsP3 might therefore slow down the production of the minus-strand RNA and delay viral replication. Most recently, a SV expressing eGFP as a fusion protein with nsP2 has been constructed. This virus has even slower replication than the nsP3 fusion viruses. This is not surprising since nsP2 is the protease responsible for processing of the replicase polyprotein and alphaviruses with even single amino acid mutations in nsP2 replicate less efficiently (Rikkonen, 1996; Dryga *et al.*, 1997).

BHK-21 cells infected with SFV4(3H)-eGFP and SFV4(3L)-eGFP showed only a transient eGFP expression. eGFP has been used extensively as a marker protein expressed by alphavirus vectors with expression detectable over long periods of time (Kim *et al.*, 2004; Graham *et al.*, 2006). Transient expression of eGFP has never been reported for alphavirus vectors expressing this protein. The pulse labelling study showed that the eGFP was rapidly degraded. It can be hypothesised that the instability of eGFP is due to the additional virus derived sequences at the N and C-termini. Following processing of the replicase polyprotein and release of eGFP, its N-terminus has a glycine residue, which according to the N-end rule is one of the most stabilising amino acids (Varshavsky, 1996). It is therefore logical to assume that the destabilising sequence is located at the C-terminus of eGFP, which is the C-terminal sequence of nsP3 (amino acid residues 453 – 482). Further experiments done by our Estonian colleagues using plasmids expressing eGFP fused to different lengths of the C-terminal sequence of nsP3 have verified this assumption and suggest that degradation is most efficient when the last 70 amino acids (residues 413 – 482) are fused to the C-terminus of eGFP (unpublished data). These results suggest that this nsP3 sequence contains a degron signal which in its native location has a different function or its effect is inhibited by interactions with one or more of the other non-structural proteins (Tamberg *et al.*, 2007). Further experiments (currently in progress) are required to clarify the role of this sequence, to see if its effect is exclusive in fluorescent molecules like eGFP or more generic. Fluorescence was more intense in the nucleus of infected BHK-21 cells; that could result from the more

rapid proteasome-mediated degradation in the cytoplasmic compartment, a phenomenon observed with cellular proteins (Doherty *et al.*, 2002).

Genetic stability of replication-competent alphavirus vectors has been previously investigated by assessing their ability to express marker genes *in vitro* (Thomas *et al.*, 2003) and *in vivo* (Cook & Griffin, 2003). The methods used in both these studies are not very sensitive and detect only relatively large changes in the virus population. In the present study, the method employed to assess the genetic stability of SFV4(3H)-eGFP and SFV4(3L)-eGFP was also simple but was more sensitive allowing direct assessment of the appearance and proportion of eGFP-negative genomes. For unknown reasons SFV4(3L)-eGFP was less stable than SFV4(3H)-eGFP *in vitro*. In the late *in vitro* passages some truncated genomes, possibly resulting from RNA recombination between the duplicated sequences of nsP3, were detected by RT-PCR. Sequencing of some of these genomes showed large in-frame deletions. This was expected since if the deletion was not in-frame the translation of the replicase polyprotein would be halted and therefore virus would not be viable. The very similar SV (SIN/549) demonstrated low but detectable levels of genetic instability (Frolova *et al.*, 2006). Only the stability of SFV4(3H)-eGFP was assessed *in vivo*. The results indicate that the virus is remarkably stable *in vivo* and thus suitable for pathogenesis studies. SFV4(3H)-eGFP was apparently more stable *in vivo*. A possible explanation for this is that fewer virus particles were used for each *in vivo* passage compared to the amount of infectious virus passaged in each *in vitro* passage. No animal experiments were performed using SIN/549 thus no data for comparison is available. Alphaviruses have the ability to replicate in a variety of vertebrate and insect cells (Kaariainen & Soderlund, 1978; Strauss & Strauss, 1994). In infected cells, alphaviruses induce the formation of cytoplasmic membranous structures known as cytoplasmic vacuoles (CPVs). Froshauer *et. al.* (1988) have shown that CPVs are modified endosomes and lysosomes, which have non-structural proteins (nsP3 and nsP4) on their surfaces (Peranen & Kaariainen, 1991). On the external surface of CPVs numerous invaginations called spherules can be found. According to several studies these spherules are the sites of RNA synthesis during viral replication (Grimley *et al.*, 1968; Kujala *et al.*, 2001). Replication complexes consisting of the 4 mature non-structural proteins are targeted to the endosomal compartment. Two non-

structural proteins, nsP1 and nsP3, are known to facilitate the anchoring of the replication complexes on the surface of cellular membranes (Salonen *et al.*, 2003; Galbraith *et al.*, 2006). In numerous studies, antibodies against the non-structural viral proteins have been employed to investigate the location of the viral replication complexes. The results of the present study are coherent with those of previous studies (Peranen & Kaariainen, 1991; Salonen *et al.*, 2003; Frolova *et al.*, 2006). The punctate pattern observed in infected cells immunostained using anti-nsP3 antibody marks the location of the replication complexes. In cells infected with fusion viruses like SFV4(3F)-eGFP and the SV constructs described by Frolova *et. al.* (2006) and Atasheva *et. al.* (2007) the staining for non-structural proteins co-localises with the eGFP signal. In contrast, when SFV4(3H)-eGFP or SFV4(3L)-eGFP was used, eGFP was released free from the replication complex (Tamberg *et al.*, 2007). Similar distributions of non-structural proteins have been reported for other viruses including hepatitis C virus (HCV) and equine arteritis virus (EAV) (van der Meer *et al.*, 1998; Yamaga & Ou, 2002). The use of viruses expressing marker proteins like eGFP facilitates studies on the replication mechanisms and on the interaction between viral and cellular proteins.

The recombinant viruses were based on SFV4, a virus derived from the prototype SFV strain. Although SFV4 has been used extensively for *in vitro* studies, knowledge on its neuroinvasive efficiency and its *in vivo* pathogenesis is incomplete. One of the important parameters that should be taken under consideration when performing *in vivo* pathogenesis studies simulating a natural arboviral infection is the amount of virus transmitted. Various studies have estimated the virus content of mosquito saliva to be between 40 and 200,000 infectious units (reviewed in Weaver, 2006) but it has been shown that mosquitoes transmit much less virus (Collins, 1963; Mellink, 1982). To mimic the natural infection a fairly low dose of virus was used in the present study. It appears that SFV4 virulence is dose-dependent. In studies by two different groups, 10^6 PFU of SFV4 were used to infect Balb/c mice intraperitonially. Studies by the Atkins group showed that this dose of virus killed approximately 60% of the animals (Glasgow *et al.*, 1991; Tarbatt *et al.*, 1997). A more recent study showed that 90% of mice died after intraperitoneal inoculation of the same amount of virus (Tuittila *et al.*, 2000). In the present study, 200-fold less

virus was used for *in vivo* pathogenesis studies (5 x 10^3 PFU). This has been shown to be enough to produce high levels of viraemia and encephalitis with SFV L10 (the prototype strain from which SFV4 is derived) and SFV A7(74). When Balb/c mice were given this dose intraperitoneally none of the animals succumbed to infection. This was also observed by other studies in this laboratory (Breakwell, PhD thesis, 2006).

Brains of animals infected via the intraperitoneal route were sampled on PID 4 which according to other studies is when the virus reaches its maximum titre in the brain. No infectious virus was found in the brain of any of the animals sampled at this time-point post-infection. Studies by other members of the laboratory using Balb/c and wt129 mice have also shown that SFV4 is poorly neuroinvasive; an average of 21% of animals infected had detectable virus in the brain and the titres were very low (Kim Roberts, BSc dissertation 2003 and Breakwell, PhD thesis 2006). It can be concluded that neuroinvasiveness and subsequent neurovirulence of SFV4 is dose-dependent.

The inability of SFV4 and the two eGFP-expressing recombinants (SFV4(3H)-eGFP and SFV4(3L)-eGFP) to invade the brain was attributed to the low level plasma viraemia. SFV4 and SFV4-based viruses had approximately 3.5 Log_{10} PFU/ml lower titres in the blood that the virulent L10 and the avirulent SFV A7(74) strains. Tuittila *et. al.* (2000) showed that if a high dose of virus is given intraperitoneally both SFV4 and SFVA7(74) reach similar titres in the blood. Notably, the levels of SFV A7(74) were very similar between our studies and the Tuittila study exhibiting the efficiency of that particular virus to replicate in the periphery.

Type-I interferon has been shown to protect mice following infection by alphaviruses. Infection of mice lacking an intact type-I interferon system by either virulent or avirulent strains of alphavirus causes lethal disease. This has been shown for many alphaviruses including SFV, SV and Venezuelan equine encephalitis virus (Grieder & Vogel, 1999; Ryman *et al.*, 2000; Fazakerley, 2004). There are two possibilities related to interferon which could explain the inability of SFV4 and SFV4(3H)-eGFP to produce a high titre plasma viraemia. Either SFV4 induces more type-I interferon than SFV L10 and SFV A7(74) or SFV4 is more sensitive to interferon.

The first hypothesis seems unlikely. Previous studies in our laboratory have shown that *in vitro* (in L929 cells) SFV4 and SFV A7(74) induce very similar levels of interferon as determined by bioassay (Breakwell, 2006). This was also shown for SFV L10 and the avirulent strain SFV V42 (Deuber & Pavlovic, 2007). The situation could be different *in vivo* but a recent study on a mouse model of Eastern equine encephalitis, another alphavirus, has shown that strains of virus with different virulence induce similar levels of IFN α/β suggesting that differences in virulence are not due to differential induction of type-I IFN (Aguilar *et al.*, 2005). It has been shown that many viruses are able to suppress the interferon response. In alphaviruses, nsP2 may be involved in the suppression of type-I IFN production (Frolova *et al.*, 2002; Breakwell *et al.*, 2007). The results of the present study suggest that during *in vivo* infection by SFV4, antagonism of the IFN response is weak or non-existent. Higher sensitivity of SFV4 to IFN would explain the lack of high levels of plasma viraemia following intraperitoneal inoculation. Variation in the sensitivity of viruses to IFN has been shown for alphaviruses as well as for other viruses. More specifically SFV L10 is less sensitive to IFN than SFV V42 (Deuber & Pavlovic, 2007). Also the attenuated stain TC-83 of VEEV induces less IFN than the virulent strains (Anishchenko *et al.*, 2004). SFV4 is generally considered to be a virulent strain, as it was derived from the virulent prototype strain and it is virulent when inoculated i.c., may be more sensitive to IFN than the avirulent A7(74) strain. The results from IFN α/β knockout mice indicate that IFN is responsible for the inability of SFV4 to replicate efficiently in the periphery since in the absence of type-I IFN responses virus rapidly replicates to high titres. However, there must be other factors that control the ability of the virus to replicate more efficiently because SFV A7(74) produces approximately 1 log more virus in the same strain of mice (Breakwell, PhD 2006). Perhaps when SFV4 was derived from L10 changes introduced by cloning affected the ability of the virus to replicate in the periphery and thus invade the CNS. Although the neuroinvasiveness of SFV4 and SFV4(3H)-eGFP is limited the virus is highly neurovirulent when even small doses of virus are administered directly into the brain via the intracerebral or the intranasal route. All animals given SFV4 and SFV4-based viruses through these two routes succumbed to infection. In contrast animals given SFV A7(74) directly into the CNS did not exhibit clinical signs of

encephalitis and survive. Virulent strains of SFV cause lethal encephalitis because they replicate very rapidly and efficiently in neurons before intervention of the immune system (Atkins & Sheahan, 1982; Gates *et al.*, 1985). The avirulent strains either replicate less efficiently like the M9 strain or their replication is totally restricted in neurons like the A7(74) strain (Smyth *et al.*, 1990; Fazakerley *et al.*, 1993). Virulence of SV, EEE and VEE is associated with their ability to replicate in neurons (Lustig *et al.*, 1988; Griffin, 1995; Charles *et al.*, 1995; Del Piero *et al.*, 2001).

Determinants of neurovirulence on SFV are located in both the structural and the non-structural ORF as well as on the 5' and 3' non-translated regions. Comparison of the sequence of SFV4 with SFV A7(74) showed numerous amino acid differences in the non-structural proteins (Tuittila *et al.*, 2000). The structural proteins, especially E2 also appear to play important role in SFV neurovirulence (Glasgow *et al.*, 1991; Santagati *et al.*, 1995). Nevertheless, multiple studies suggest that the most important determinants of neurovirulence lie on the non-structural region and possibly in the 5' non-translated region (NTR). When the 5' NTR and the non-structural ORF of A7(74) were replaced by those of SFV4 the resulting virus was highly virulent, a reciprocal virus (SFV4 with A7(74) structural ORF) was avirulent (Tuittila *et al.*, 2000). Also it has been reported that deletions in nsP3 affect the neurovirulence of SFV (Galbraith *et al.*, 2006). Most studies on the identification of SV neurovirulence determinants suggest that those are found in the E1 and E2 structural proteins (Lustig *et al.*, 1988; Tucker *et al.*, 1997). Neurovirulence of SV is also affected by mutations in nsP1, nsP3 and the 5' and 3' NTR (Kuhn *et al.*, 1992).

The cell tropism of SFV4(3H)-eGFP in the mouse CNS is not altered relative to that of the parental SFV4. The virus infects neurons, and oligodendrocytes but not astrocytes. This is coherent with other studies that have shown that the tropism of both virulent and avirulent strains of SFV is very similar (Balluz *et al.*, 1993; Fazakerley *et al.*, 2006). As already mentioned SV is able to infect neurons *in vivo* but no reports for infection of other cell types can be found in the literature. EEEV and VEEV can also infect neurons and it has been reported that they also infect oligodendrocytes and astrocytes (Schoneboom *et al.*, 1999; Del Piero *et al.*, 2001).

Surprisingly, although cells morphologically and anatomically known to be neurons were infected by SFV4(3H)-eGFP (as assessed by immunostaining for nsP3) no double-labelled neurons were observed when the NeuN specific neuronal marker was used for immunostaining. Neurons may switch off the 42S genomic promoter more rapidly that other cell types, for example oligodendrocytes. Possibly something similar happens in peripheral tissues as well since in IFN α/β receptor knockout mice, green cells were observed only in certain organs (spleen and pancreas) and only in certain cell types (for example pancreatic acinar cells), although it is known from other studies that both SFV4 and SFV A7(74) can infect most of the peripheral tissues in these mice (see Chapter 4).

Overall, SFV4(3H)-eGFP does not differ much to SFV4 and can be useful for *in vivo* pathogenesis studies as eGFP is only expressed in cells in which the genomic promoter is active. Therefore the rapid eGFP degradation observed is a useful property and this virus can be used to distinguish between cells infected at the early and the late stages of infection.

Chapter 4: Insertion of eGFP in the structural ORF

Contents

Introduction

Alphavirus replication is rapid and very efficient leading to the production of high numbers of infectious virus particles. In addition, alphaviruses have a broad range of susceptible host cells and organisms including vertebrates (mammals and birds) and invertebrates (insects) (Strauss & Strauss, 1994). These properties together with the ability to produce high levels of foreign proteins have made alphaviruses very appealing vector systems for protein expression (Frolov *et al.*, 1996; Lundstrom, 1997; DiCiommo & Bremner, 1998).

The 26S subgenomic promoter which drives the expression of the viral structural proteins in alphaviruses is very potent (Tubulekas *et al.*, 1997). In all alphavirus-based vector systems, this property has been exploited and the viral structural proteins have been replaced by foreign genes of interest including various marker genes like eGFP. Expression of foreign genes is rapid, high level and prolonged (Jeromin *et al.*, 2003; Graham *et al.*, 2006). These vectors, also known as replicons, cannot be packaged unless the viral structural proteins are provided *in trans* either as a separate RNA or in packaging cell lines (Polo *et al.*, 1999; Karlsson & Liljestrom, 2003). As already mentioned, these vectors can only undergo a single cycle of infection and this limits their applications especially for *in vivo* studies.

To take advantage of the strong, prolonged expression properties of the subgenomic promoter without sacrificing the ability of the virus to replicate productively, constructs expressing the foreign gene of interest under the control of a duplicated subgenomic promoter have been constructed and utilised in various studies. Such replication-competent vectors have been described for several alphaviruses including SFV, SV and Chikugunya viruses (Raju & Huang, 1991; Hahn *et al.*, 1992; Vaha-Koskela *et al.*, 2003; Vanlandingham *et al.*, 2005).

The genetic instability of viruses with double-subgenomic promoter and the inability of replicon vectors to undergo multiple rounds of replication are the major limiting factors for the use of both these expression systems for *in vivo* pathogenesis or for virus persistence studies. Replication-competent vectors with increased genetic stability have been constructed by insertion of foreign genetic material in the non-structural ORF of alphaviruses as detailed in Chapter 3 (Bick *et al.*, 2003; Frolova *et*

al., 2006; Tamberg *et al.*, 2007; Atasheva *et al.*, 2007). Although insertion into the non-structural ORF has enhanced the genetic stability of replicating vectors, expression of the foreign gene is not as strong and prolonged as it would be if the insertion was under the control of the 26S subgenomic promoter. Late in alphavirus replication the fully processed replicase enzyme complex exclusively synthesises the subgenomic message and stops transcribing the full-length genomic message (Strauss & Strauss, 1994; Kao *et al.*, 2001).

As an alternative to a duplicated subgenomic promoter or insertion into the non-strtuctural ORF, Thomas *et. al.* (2003) constructed SV vectors expressing foreign proteins (GFP and VP7 protein of bluetongue virus) as a cleavable component of the structural ORF. In the present study, a similar SFV vector carrying eGFP was constructed, fully characterised *in vitro* and *in vivo* and its suitability for *in vivo* pathogenesis study was evaluated.

Objectives

The objectives of this study were:

- To examine whether the insertion of eGFP as a cleavable component of the structural ORF of Semliki Forest virus (SFV) has an effect on the replication efficiency of the virus.
- To investigate if insertion of eGFP in the structural ORF has an impact on the *in vitro* and *in vivo* virulence of SFV4.
- To assess the *in vitro* and *in vivo* phenotypic and genotypic stability of the recombinant virus expressing eGFP as a component of the structural ORF.
- To test if the insertion of eGFP at this position affected the cell type tropism of SFV4 both *in vitro* and *in vivo*.
- To use the recombinant marker virus in a pathogenesis study in order to determine its usefulness.

Construction of a recombinant virus expressing eGFP as a cleavable component of the structural ORF

A novel replicating vector, annotated pSFV4-st, was designed to express a foreign gene as a cleavable component of the structural ORF. The construction of this vector was based on a similar sindbis virus (SV) vector designed by Thomas *et. al.* (2003). pSFV4-st was constructed by Professor Andres Merits at the Estonian Biocentre. As with the recombinant viruses described in Chapter 3, pSFV4 (Liljestrom & Garoff, 1991) was used as the backbone of this virus. For the insertion of foreign sequences in this vector, a polylinker containing *Apa*I and *Bam*HI restriction sites followed by the sequence for the foot-and-mouth disease virus (FMDV) 2A peptide were inserted between the regions encoding the capsid and the p62 protein. The efficiency of the 2A peptide is affected by the presence of the amino acids at its N-terminal and C-terminal regions (Ryan *et al.*, 1991). The 16 amino acids comprising the 2A peptide were therefore flanked by three amino acids from the C-terminus of the FMDV 1D protein and the proline from the N-terminus of the FMDV 2B protein. Previous studies indicate that the proteolytic activity of capsid protein is independent of downstream sequences (Sjoberg *et al.*, 1994; Frolov *et al.*, 1996). However, to ensure proper processing of the capsid protein from the rest of the structural polyprotein, the first three amino acids of the p62 protein (serine, alanine, proline) were duplicated between the capsid and the polylinker sequence. As described previously, enhanced green fluorescent protein (eGFP) was amplified with primers incorporating *Apa*I and *Bam*HI restriction sites (shown in the materials and methods chapter). Both the pSFV4-st vector and the eGFP insert were digested with these two restriction endonucleases and ligated using T4 DNA ligase. This construct was designated pSFV4-steGFP and was used to produce infectious virus (SFV4-steGFP) according to the method described by Liljestrom *et al.* (1991) (Fig 4.1).

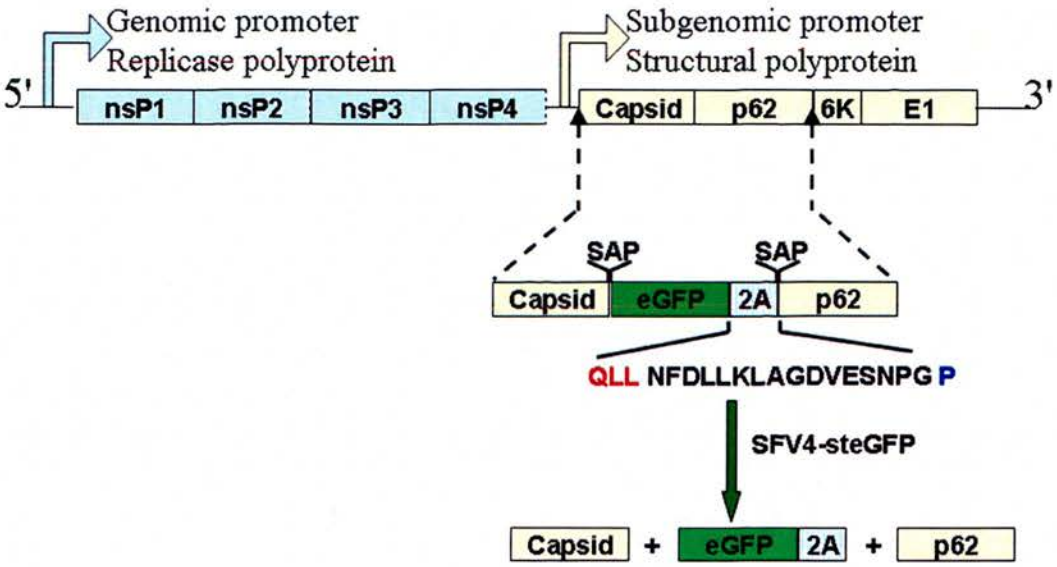

Figure 4.1. Schematic representation of the construction of SFV4-steGFP virus. SFV4-steGFP construction and predicted processing of the structural polyprotein; the three N-terminal amino acids (SAP) of p62 protein (E2 & E3) were duplicated upstream of the eGFP gene. The 2A peptide from FMDV flanked by three amino acids (red) from the C-terminus of FMDV 1D protein and the N-terminal proline (blue) from FMDV 2B protein was inserted after eGFP. Following expression of the structural ORF, all structural proteins and eGFP with 2A fused to its C-terminus were expected to be released free.

Assessment of the expression levels of eGFP as part of the structural ORF and the effect of this insertion on virus viability and replication.

Experimental design

To assess the impact that eGFP insertion in the structural ORF had on virus viability and replication efficiency, monolayers of BHK-21 cells were infected with SFV4 and SFV4-steGFP at a multiplicity of infection (M.O.I) of 10 in triplicate. Two hundred µl of virus containing supernatant were collected and replaced with an equal amount of fresh medium every 2 hours for 12 hours. All samples were titrated using standard plaque assay as previously described. To investigate the dynamics of eGFP expression *in vitro*, cultures of BHK-21 cells were infected with SFV4-steGFP at an M.O.I of 10 and were monitored for expression of eGFP every hour for the first 12 hours post-infection and every 4-6 hours thereafter until 48 hours post infection. Simultaneously, cultures were monitored for the development of cytopathic effect (CPE). For comparison, parallel cultures of BHK-21 cells were infected with SFV4.

One-step growth curves

The results obtained from the one-step growth curves (Figure 4.2a) suggest that insertion of eGFP into the structural ORF did not have any major effect on virus viability and replication since SFV4-steGFP was able to infect BHK-21 cells and replicated to similar levels to SFV4. However, the insertion reduced the replication rate of the virus relative to wild-type SFV4. Statistical analysis using a paired t-test showed that at 4 and 6 hours post-infection SFV4-steGFP had significantly lower titres than SFV4 ($P<0.05$). From 8 hours onwards, SFV4-steGFP had similar titres to SFV4 (no significant difference, $P>0.05$). SFV4-steGFP produced plaques with a similar size to SFV4 (data not shown).

eGFP expression and development of CPE in BHK-21 cells

Following infection of BHK-21 cells with SFV4-steGFP, cells were observed at regular intervals to determine when eGFP fluorescence and CPE were evident. eGFP fluorescence was first visible 5–6 hours post-infection. The eGFP signal reached its peak between 10 and 12 hours post-infection and remained high throughout the rest of the experiment (48 hours). Figure 4.2b shows eGFP expression in BHK-21 cells 20 hours post-infection with SFV4-steGFP. In contrast to SFV4, where CPE was initially observed between 16-20 hours after infection, cells infected with SFV4-steGFP exhibited the first signs of CPE at approximately 36 hours post-infection. Until that time-point cells appeared to be healthy (no CPE observed) and maintained the characteristic morphology of BHK-21 cells (Figure 4.2b and 4.2b inset). Typical morphology of cells undergoing cell death was observed at approximately 36 hours post-infection. Cells were rounded and the eGFP signal that until that point was mainly cytoplasmic was able to diffuse to the nucleus. This could have resulted from a loss of integrity of the nuclear membrane. By 48 hours all cells had this morphology (Figure 4.2c and 4.2c inset). Shortly after, the cell monolayer completely detached. The delay on the development of CPE, as well as the delay between first signs of CPE and cell death (compared to SFV4) suggests that the insertion of eGFP in the structural ORF of SFV does have an attenuating effect on the virus *in vitro*.

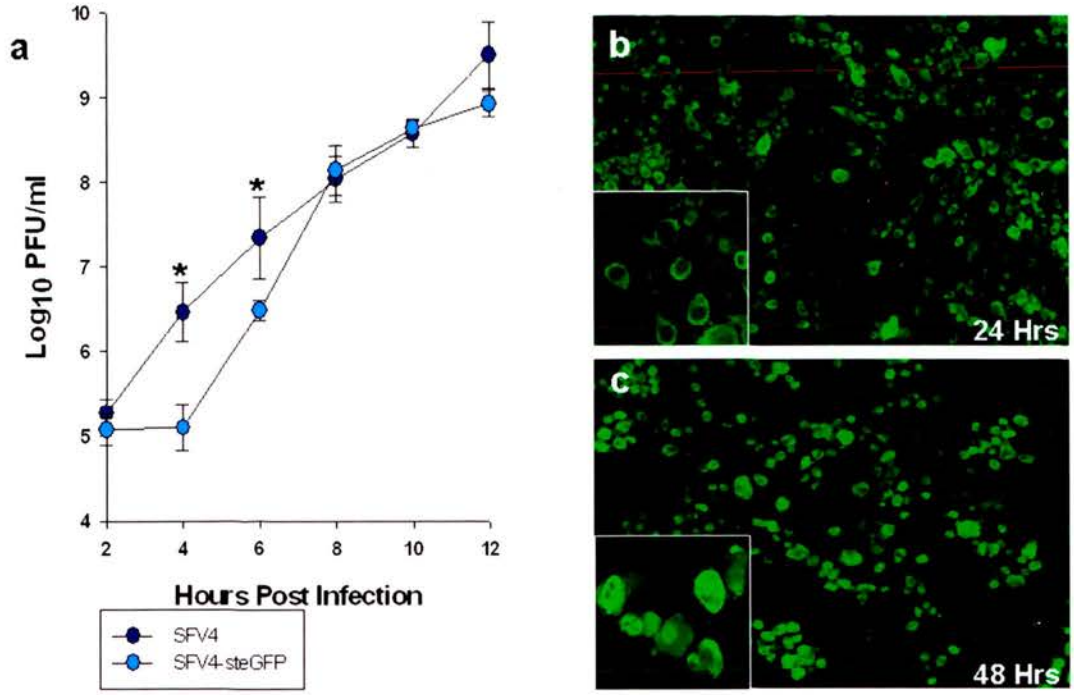

Figure 4.2. Growth curves and expression of eGFP in BHK-21 cells. (a) Monolayers of BHK-21 cells were infected in triplicate with SFV4 (dark blue circles) or SFV4-steGFP (light blue circles) at an M.O.I of 10. Each point represents the mean of 3 samples; the bar represents the standard deviation (SD). The values at each time-point were compared using paired t-test, asterisk (*) indicates statistically significant difference. All growth curves shown in this thesis were performed in parallel. The data for SFV4 presented in this figure is identical to that shown in Figures 3.2a and 5.3a allowing comparison of the growth of all recombinant viruses. **(b)** and **(c)** Images of BHK-21 cells infected, with SFV4-steGFP virus at an M.O.I of 10 taken 24 and 48 hours post-infection, respectively. Levels of eGFP expression were consistently high even at late time-points. The inset in panel **(b)** shows the morphology of BHK-21 cells prior to the development of CPE. On the inset in panel **(c)** cells with a morphology indicative of CPE can be seen. Note that at this stage eGFP expression is strong in the nucleus. Pictures were acquired with a Zeiss Axioskop microscope.

Expression of the replicase complex, capsid and eGFP proteins in SFV4-steGFP virus

Comparison of the expression of capsid, eGFP & of the replicase proteins of SFV4, SFV4(3H)-eGFP and SFV4-steGFP in BHK-21 cells

To determine whether eGFP insertion in the structural ORF of SFV had any effect on the correct processing of the non-structural or the structural proteins of the virus, BHK-21 cells were infected with SFV4, SFV4(3H)-eGFP or SFV4-steGFP at an M.O.I of 20 for 6 hours. PBSA was used as a negative control to mock-infect cells. The samples were analysed by western blotting. Briefly, 6 hours post-infection, cells were lysed and samples corresponding to 100,000 cells were separated on a 10% SDS polyacrylamide gel. Proteins were transferred to a nitrocellulose membrane. Antibodies recognising specific epitopes on nsP1, nsP2, nsP3, nsP4, capsid and eGFP were then used to detect the respective proteins.

SFV4-steGFP expressed all the non-structural proteins and capsid protein as expected with no size differences between SFV4 and SFV4(3H)-eGFP (Figure 4.3). Note that western blotting for nsP1 (black arrowhead) and capsid (blue arrowhead) was performed on a single membrane since the two proteins have different molecular weights allowing easy differentiation. As expected, no eGFP protein was detectable in the lysate of cells infected with SFV4. In contrast, eGFP was detectable in the lysates of cells infected with SFV4(3H)-eGFP or SFV4-steGFP. The eGFP protein expressed from SFV4(3H)-eGFP (black arrow) had a slight size difference to the eGFP expressed from SFV4-steGFP. This is as expected since for SFV4(3H)-eGFP 30 amino acids from the C-terminal area of nsP3 had been fused to the C-terminus of eGFP to re-create the natural nsP3/4 nsP2 protease processing site between eGFP and nsP4. In SFV4(3H)-eGFP infected cells an eGFP containing band with a higher molecular weight than eGFP can also be seen. The origin of this band remains unclear, it was not previously observed when this antibody was used for western blotting (Chapter 3). That a second band is seen in Figure 4.3 is inconsistent and the explanation is not clear. However, both experiments (described in Chapter 3 and Chapter 4) are correct. Since these experiments were not performed on the same day,

possible explanations for the presence of the additional band include differences in BHK-21 cells confluence and differences in processing of the samples, for example the activity of protease inhibitors in lysis buffer. In the previous western blot of SFV4(3H)-eGFP infected cells, Chapter 3, Figure 3.3a, a band corresponding to an eGFP-nsP4 fusion protein was detected with both the anti-nsP4 and anti-eGFP antibodies. In the present blot (Figure 4.3) an eGFP-nsP4 fusion protein was detected only with the anti-nsP4 antibody (blue arrow). In Figure 3.3a, the amount of eGFP-nsP4 fusion protein is much lower than the amounts of processed eGFP and nsP4 proteins. Perhaps in Figure 4.3 the amount of the eGFP-nsP4 fusion protein, was below the limit of detection of the eGFP antibody. An eGFP-2A-p62 fusion protein was detectable when the same (anti-eGFP) antibody was used with the lysate of SFV4-steGFP infected BHK-21 cells (red arrow). The band above this is most probably another fusion protein of eGFP and p62. These bands suggest that the 2A sequence was not 100% efficient. Due to time constraints, the western blots were not repeated. Further studies are required to fully characterise the processing of the structural proteins. These would require antibodies recognising epitopes on the p62 and E1 proteins; at the time of completion of this project these antibodies were not available.

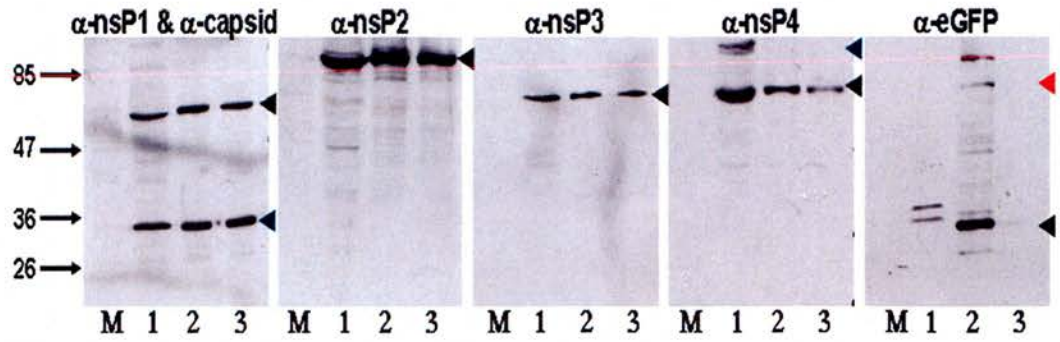

Figure 4.3. Expression of the replicase complex, capsid and eGFP proteins in SFV4, SFV4(3H)-eGFP and SFV4-steGFP infected BHK-21 cells. Western blotting of cell lysates of BHK-21 cells infected with SFV4(3H)-eGFP (**1**), SFV4-steGFP (**2**) or SFV4(**3**) (M.O.I 20) and PBSA (mock-infection **M**). Specific bands of the appropriate molecular weight for nsP1, nsP2, nsP3, nsP4 non-structural proteins and eGFP are shown with black arrowheads. Bands corresponding to the capsid protein are highlighted with a blue arrowhead. The blue arrowhead on the panel corresponding to the western blot for nsP4 protein points at an eGFP-nsP4 fusion protein (only for SFV4(3H)-eGFP, lane 1). The red arrowhead on the panel corresponding to the western blotting for eGFP highlights an eGFP-2A-p62 fusion protein. It appears that nsP1 of SFV4(3H)-eGFP has slightly smaller size. This difference is not real and it can most probably be attributed to the loading of the sample and the way the gel was ran.

Distribution of eGFP and nsP3 non-structural protein in BHK-21 cells infected with SFV4-steGFP

Experimental design

To investigate the distribution of eGFP and nsP3 proteins in BHK-21 cells following infection with SFV4-steGFP, cells were grown on glass slides with culture chambers until approximately 80% confluent and then infected with SFV4-steGFP (M.O.I of 10). As a control, virus-like particles (VLPs) expressing eGFP, previously described in Graham *et. al.* (2006) were used to infect parallel cultures. Sixteen hours post-infection, cells were fixed and immunostained with anti-nsP3 antibody. This time-point was chosen to give plenty of time for eGFP to be expressed to high levels; as shown previously nsP3 is detectable for at least 24 hours (Figure 3.3b).

Distribution of eGFP vs distribution of nsP3 in BHK-21 cells

The distribution of eGFP in BHK-21 cells infected with SFV4-steGFP was different to the distribution observed when these cells were infected with either viruses expressing eGFP as part of their non-structural ORF (SFV4(3H)-eGFP & SFV4(3L)-eGFP) (Figure 3.4) or SFV virus-like particles (VLPs) expressing eGFP from the subgenomic promoter. In BHK-21 cells infected with SFV-eGFP VLPs, eGFP expression was distributed throughout the cytoplasm and the nucleus of the infected cells (Figure 4.4a). Punctate nsP3 staining, probably corresponding to the position of the virus replication complexes, was visible in the cytoplasm of the infected cells (Figure 4.4b & 4.4c).

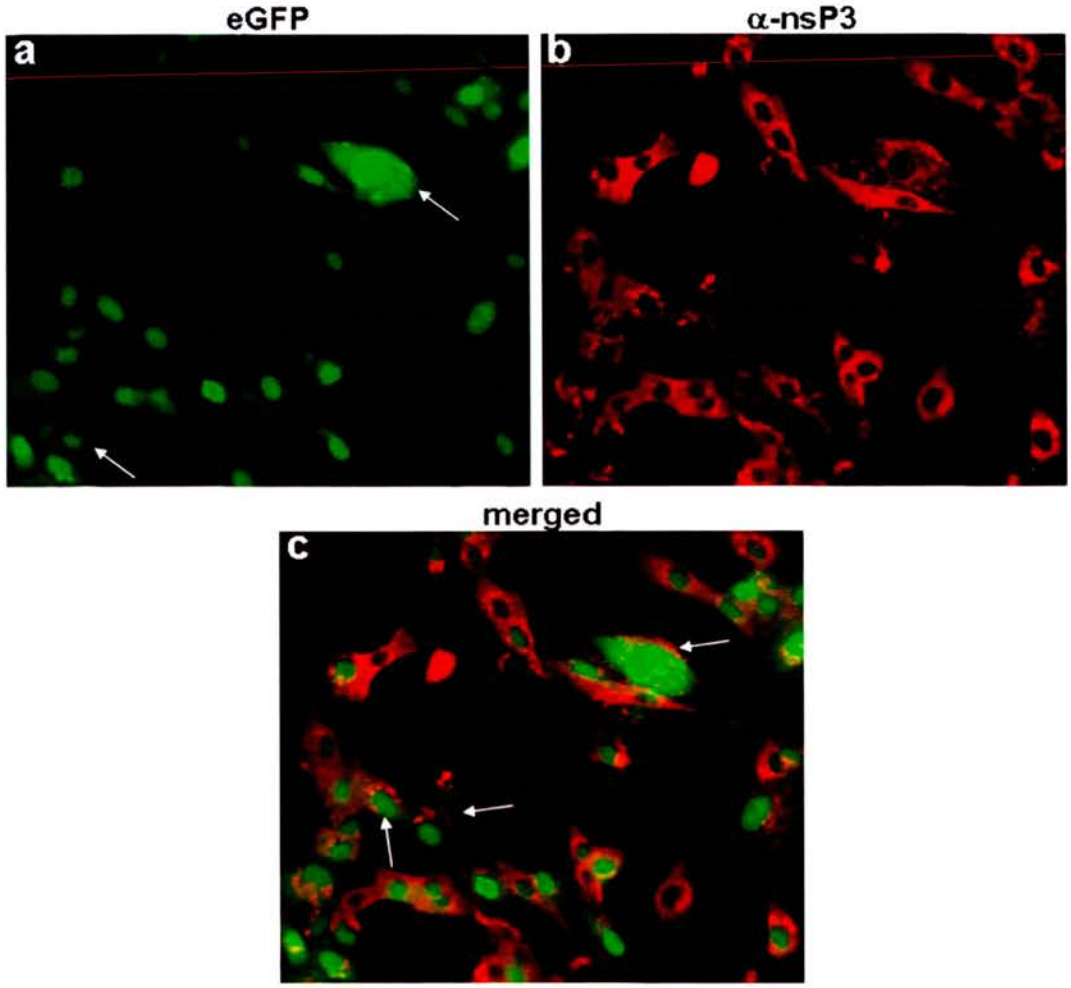

Figure 4.4. Distribution of eGFP and nsP3 in BHK-21 cells infected with SFV-eGFP VLPs. (a) Distribution of eGFP 16 hours post-infection with VLPs at an M.O.I of 10. Fluorescence is visible in the cytoplasm and in the nucleus of infected cells. Notably, the fluorescent signal is stronger in the nucleus. Arrows point at cells with characteristic distribution of eGFP. Cells were fixed and stained with a anti-nsP3 antibody. **(b)** nsP3-specific staining was as expected, cytoplasmic and punctate. This can be best seen in panel **(c)** where arrows point at cells with a typical distribution of nsP3-specific staining. A non-infected control was performed and very low levels of background fluorescence were observed (as was observed previously, Figure 3.4). All images were acquired with a Zeiss microscope.

In BHK-21 cells infected with SFV4-steGFP, the vast majority of the eGFP fluorescence was localised in the cytoplasm particularly around the nuclei of the infected cells (Figure 4.5a, 4.5d and 4.5g). This distribution was unexpected and the experiment was repeated 3 more times and gave the same result. This finding was also verified by our Estonian collaborators (A. Merits, personal communication). Punctate, cytoplasmic, nsP3-specific staining was visible in approximately 100% of cells. The distribution of nsP3-specific staining was identical for all viruses and virus-like particles irrespective of whether eGFP was expressed as a cleavable part of the non-structural or the structural ORF. Typical nsP3-specific staining is shown in Figures 4.5b, 4.5e and 4.5h. A small percentage of cells were positive for nsP3 but eGFP-negative. These were probably the cells most recently infected with virus. Examples of such cells are shown in Figure 4.5d – f and g – i (white arrows). Cells with characteristic distribution of both eGFP and nsP3-specific staining are highlighted by an asterisk in all panels of Figure 4.5. In the inset of panels a – c of the same figure, a cell with punctate nsP3-specific staining, which has a large number of very bright eGFP-containing vacuoles can be seen. These vacuoles may be the remains of an adjacent cell that died and was phagocytosed. The eGFP distribution, although different to the one observed in cells infected with viruses expressing eGFP as part of their non-structural ORF or in cells infected with VLPs expressing eGFP alone from the subgenomic promoter, is not totally unexpected and will be further discussed later in this chapter. It is important to note that although both eGFP and nsP3 staining were cytoplasmic no co-localisation was observed; as expected.

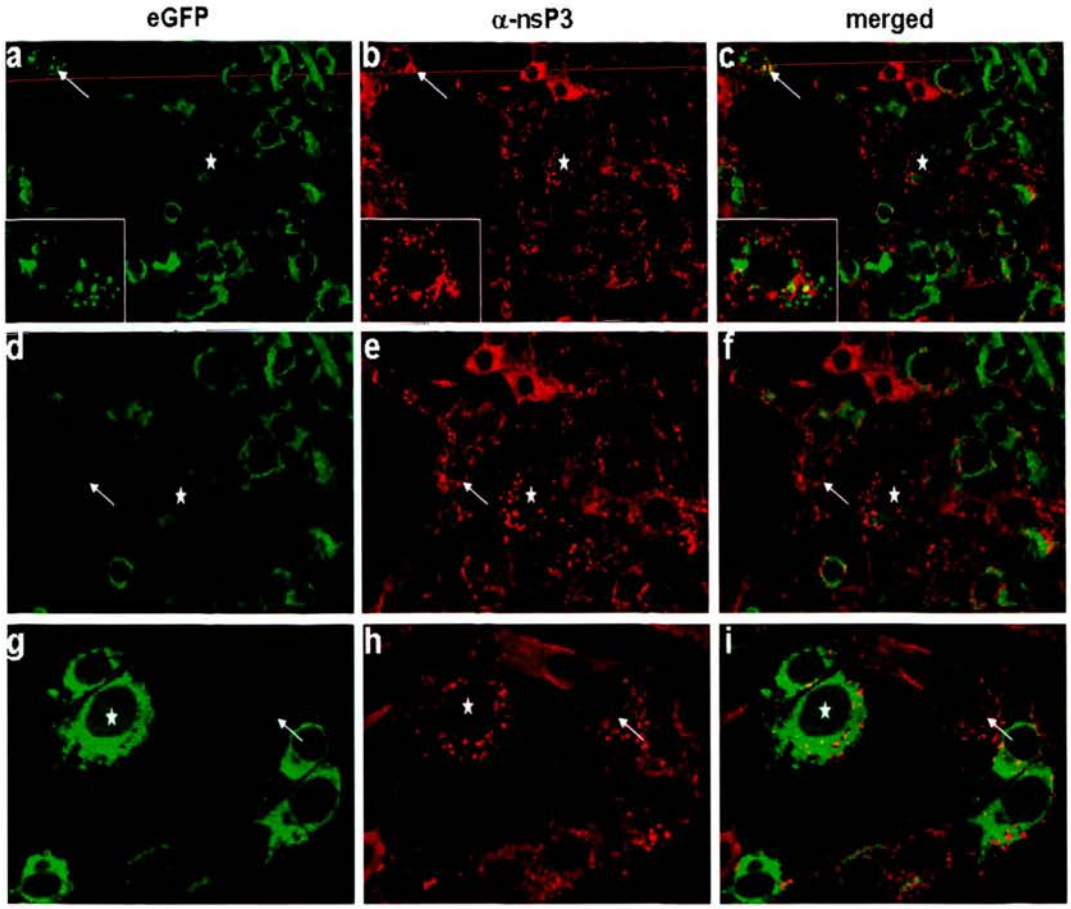

Figure 4.5. Distribution of eGFP and nsP3 in BHK-21 cells infected with SFV4-steGFP. At 16 hours post-infection cultures were fixed and stained with anti-nsP3 antibody. **(a)** eGFP fluorescence had high levels of intensity and was mostly localised in the cytoplasm especially around the nucleus. The white arrow points to a cell with multiple eGFP-containing vacuoles. **(b)** nsP3-specific staining of the same field of vision. Typical punctate staining can be seen. **(c)** merged image of **(a)** and **(b)**, the asterisk indicates a cell with characteristic eGFP and nsP3-specific staining.**(d)** Infected cells exhibiting cytoplasmic and perinuclear eGFP expression. **(e)** Typical distribution of nsP3-specific staining in the same cells. **(f)** merged image of **(d)** and **(e)**, the asterisk indicates a cell with characteristic eGFP and nsP3-specific staining. The white arrow points at a cell which is stained positive for nsP3 but does not express eGFP. **(g)**, **(h)** and **(i)**. High power images of a different field of vision. Again the white arrow points at a cell which stained positive for virus (nsP3) but was eGFP-negative. The asterisk highlights a cell with typical eGFP and nsP3 distributions. Controls for immunostaining were included; results were identical to those previously observed (Figure 3.4). All images were acquired with a Zeiss confocal microscope.

Distribution of eGFP and SFV structural proteins in BHK-21 cells infected with SFV4-steGFP

Distribution of eGFP vs distribution of SFV structural proteins in BHK-21 cells

Since SFV4-steGFP expresses eGFP as a cleavable part of the structural ORF an experiment comparing the distribution of eGFP to that of the virus structural proteins was performed. The experiment was identical to the one described above, which was used to investigate the distribution of eGFP and nsP3 non-structural protein. The only difference was that after fixation cells were immunostained using a α-SFV polyclonal antibody. VLPs expressing eGFP were not included in this experiment since they lack the viral structural proteins.

The eGFP distribution was as described previously (Figure 4.6a and 4.6d). The intensity of the green fluorescent signal was variable. Most probably this resulted from cells at different stages of infection (with dull green indicating early stages of infection and bright green late stages of infection respectively). Viral structural proteins were found exclusively in the cytoplasm (Figure 4.6b & 4.6e). This was as expected as the location of the viral structural proteins is known from previous studies and this particular antibody has been used by other members of the laboratory with identical results. In panel f of figure 4.6 it can be seen that the structural protein specific staining co-localises with the eGFP staining (indicated by the orange colour). Rare cells stained positive for viral structural proteins but were eGFP-negative (white arrows in the same panel). These cells are probably, like cells that stained positive for nsP3 but were eGFP-negative, the most recently infected cells of the culture. Alternatively, both eGFP-negative/nsP3-positive and the eGFP-negative/structural-positive could result from infection with virus that has eliminated (even partially) the eGFP insert. Interestingly, although approximately 100% of the monolayer was infected (as determined by the eGFP signal) only 15-20% of these eGFP-positive cells were positive for viral structural proteins (Figure 4.6c). This was unexpected; the experiment was repeated two more times with very similar results. The possible explanations for this finding will be discussed later in this chapter.

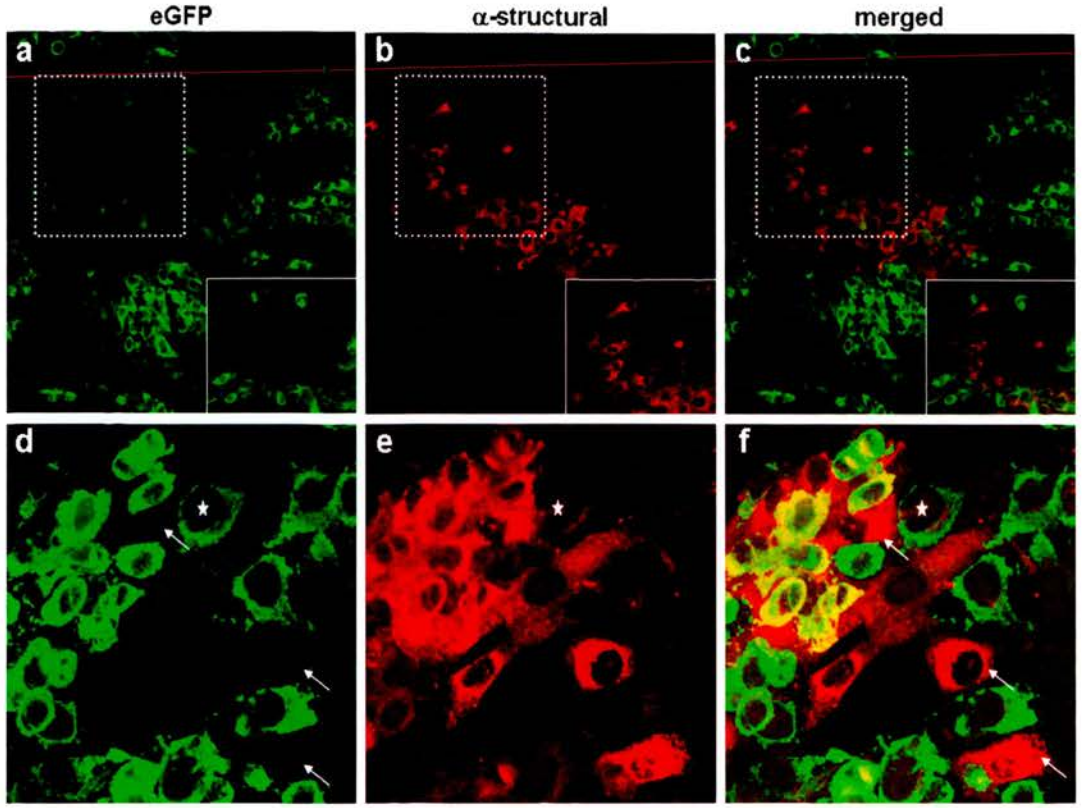

Figure 4.6. Distribution of eGFP and SFV structural proteins in BHK-21 cells infected with SFV4-steGFP. At 16 hours post-infection cultures were fixed and stained with anti-SFV antibody. **(a)** and **(d)** eGFP expression; cells with variable levels of fluorescent signal can be observed. Differences in eGFP signal intensity are possibly because cells were at different stages of the infection (early/late). **(b)** and **(e)** SFV-specific staining (for structural proteins). The staining had the expected distribution; exclusively cytoplasmic. This can be seen more clearly on panel **(e)**.From panels a – c it is clear that there are many double-labelled cells. However, it appears that there are also bright green cells which are not red and some red cells that are not green. The area denoted by the dotted box is shown in the lower right with increased brightness; again there are cells that are only red and cells that are only green. This is confirmed by the high power images (d – f). In the high power image **(f)** double-labelled cells, indicated by orange colour can be seen. White arrows indicate cells that have stained positive for SFV structural proteins (red colour) but were eGFP-negative. Asterisk indicates a cell that is clearly eGFP-positive but apparently structural-protein-negative. All images were acquired with a Zeiss confocal microscope.

In vitro phenotypic and genotypic stability of SFV4-steGFP in BHK-21 cells

Experimental design

In an identical manner to that described in Chapter 3 (Figure 3.5), the ability of SFV4-steGFP to maintain eGFP expression and an intact eGFP gene after several passages *in vitro* was assessed. Six-well plates were seeded with BHK-21 cells. SFV4-steGFP was passaged 5 times in BHK-21 cells (M.O.I 0.01). Between each passage the virus was titrated using a standard plaque assay. The passage sample was then diluted to give approximately 20 plaques per well and ninety-six plaques were picked from each of the 5 *in vitro* passages and were used to infect BHK-21 cells in 24-well plates. eGFP expression in each well was determined by fluorescent microscopy.

Phenotypic stability of SFV4-steGFP

The results show that 100% of plaque purified viruses were eGFP positive after the first passage. This percentage went down to 96.9% after the 2nd passage and 78.6% after the 3rd passage. During the last two passages SFV4-steGFP lost its ability to express eGFP. More specifically, only 2% of the plaque purified viruses were eGFP-positive after the 4th passage. No positive clones were detected after the last (5th) passage (Figure 4.7a).

Genotypic stability of SFV4-steGFP

Following removal of the virus-containing supernatant, after each passage RNA was extracted from the infected cells. As previously, 2 μg of RNA were reverse-transcribed to cDNA. Primers flanking the area of the eGFP insertion in the structural ORF were designed and used for amplification. If the insert was present a product with a size of approximately 1,650 bp was expected. If the insert was eliminated the expected product would have a size of approximately 826 bp. Figure 4.7b shows the results of the amplification for passages 2 – 5. The red and blue arrows in each panel correspond to the 1,500 bp and 1,000 bp bands of the DNA marker respectively. The experiment was done in triplicate for each passage.

After the 2nd passage, when the majority of plaque purified viruses were still eGFP-positive, most of the amplified product had a size of ~ 1,650 bp. A faint band with a size of ~ 850 bp was visible. This band had a slightly bigger size to the band corresponding to the product of PCR amplification of material originating from cells infected with SFV4, which was expected to be 826 bp in size (lane 4). After the 3rd passage, the amount of PCR product corresponding to viruses with the eGFP coding sequence in their genome was reduced and the amount of PCR product corresponding to viruses which had eliminated the eGFP insert was increased. The amplicon band produced from viruses which maintained the eGFP sequence was barely visible after the 4th passage and was totally absent after the 5th passage. In all panels of figure 4.7b it can be seen that as the passage number increased bands with sizes smaller than the ~ 1,650 bp expected appeared (especially after 2nd, 3rd & 4th passage). These bands probably correspond to viruses with large in frame deletions of eGFP (as shown previously by sequencing of passaged SFV4(3H)-eGFP and SFV4(3L)-eGFP viruses). The predominant deletion product however had a size of ~ 850 bp and was slightly bigger than the amplicon produced when SFV4-infected material was used. This finding suggests that the deletion of the inserted sequences was not complete and some sequences remained in the viral genome.

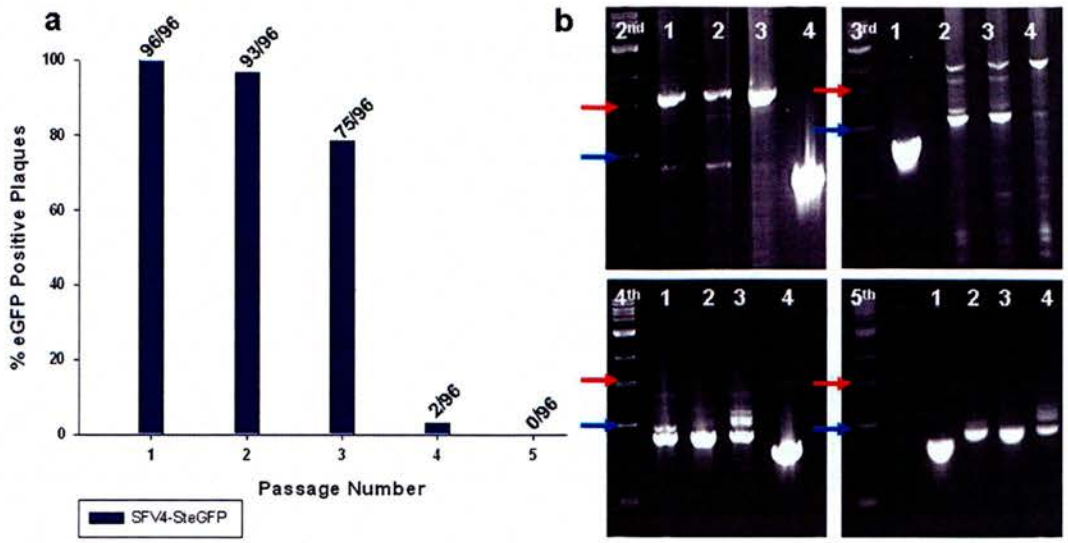

Figure 4.7. In vitro phenotypic and genotypic stability of SFV4-steGFP. (a) Percentage of eGFP positive plaque purified viruses after serial passaging. **(b)** RT-PCR genotyping of SFV4-steGFP using capsid – E3 primers on RNA samples isolated from BHK-21 monolayers at passages 2, 3, 4 and 5; the passage number is indicated at the top left of each panel. In the panels corresponding to 2nd and 4th passage lanes 1 – 3 are the triplicate passages of SFV4-steGFP. Lane 4 in the same panels shows the PCR product obtained from the amplification of SFV4-infected material (positive control). In the panels corresponding to the 3rd and 5th passage lanes 2 – 4 are the triplicate passages of SFV4-steGFP. Lane 1 in the same panels shows the PCR product obtained from the amplification of SFV4-infected material (positive control). Note that the viruses carrying eGFP deletions have a slightly larger amplicon size indicating incomplete deletion. Passage number is indicated at the left top side of each panel. The red and blue arrows correspond to the 1.5 kb and the 1 kb band of the DNA marker, respectively.

Cell tropism of SFV4-steGFP *in vitro*

SFV4-steGFP was able to infect BHK-21 cells and express eGFP in these cells. To determine whether the insertion of eGFP into the structural ORF of the virus altered the tropism of SFV4 *in vitro*; its ability to infect mosquito cells (natural virus vector) and neurons (important target of alphaviruses *in vivo*) was investigated. SFV4-steGFP was used to infect cultures of C6/36 cells from *Aedes albopictus* and of rat hippocampal neurons. The cultures were infected at an M.O.I of 10, as previously described. Cells were then monitored for eGFP expression using a fluorescent microscope. To assess the efficiency of the infection on C6/36 cells, infected monolayers were fixed at 16 hours post-infection and stained using anti-nsP3 antibody. Parallel cultures were infected with SFV4 or SFV4-steGFP and monitored at regular intervals for presence of CPE for up to 5 days. In rat hippocampal neurons the infection was allowed to progress until the death of the cells, no immunostaining was performed.

C6/36 cells infected with SFV4-steGFP expressed eGFP to high levels (Figure 4.8a, 4.8d & 4.8g). In contrast to BHK-21 cell infection, eGFP was distributed throughout the cell cytoplasm and nucleus. Notably some of the nuclei were brighter than the cytoplasm surrounding them. The range of intensity of the eGFP fluorescence was variable as observed in BHK-21 cells. The intensity of the signal probably reflects the stage of the infection; bright cells are at the late stages of infection whereas less bright cells are the most recently infected ones. Cells having numerous vacuoles containing large amounts of eGFP, like the one indicated by the white arrow in panel **(d)** of figure 4.8, and in higher magnification in the inset of the same panel, were found scattered throughout the SFV4-steGFP infected cultures.

When C6/36 cells infected with SFV4-steGFP were immunostained for nsP3 non-structural protein, approximately 100% of the cells stained positive (Figure 4.8b, 48e & 4.8h). The distribution of the nsP3-specific staining was cytoplasmic and in many instances showed the characteristic punctate pattern observed previously. Typical nsP3 staining is shown in the inset of Figure 4.8i (high magnification of the cell marked with an asterisk). Occasional nsP3-positive/eGFP-negative cells were observed, there cells were probably at the early stages of infection and eGFP had not

reached detectable levels, or were infected by a virus which had eliminated the eGFP insert, an example is highlighted with a white arrow in panels g – i. C6/36 cells infected with SFV4 or SFV4-steGFP were monitored frequently using microscopy to investigate if cytopathic effect (CPE) would develop. No signs of CPE were observed over the 5 days of this study.

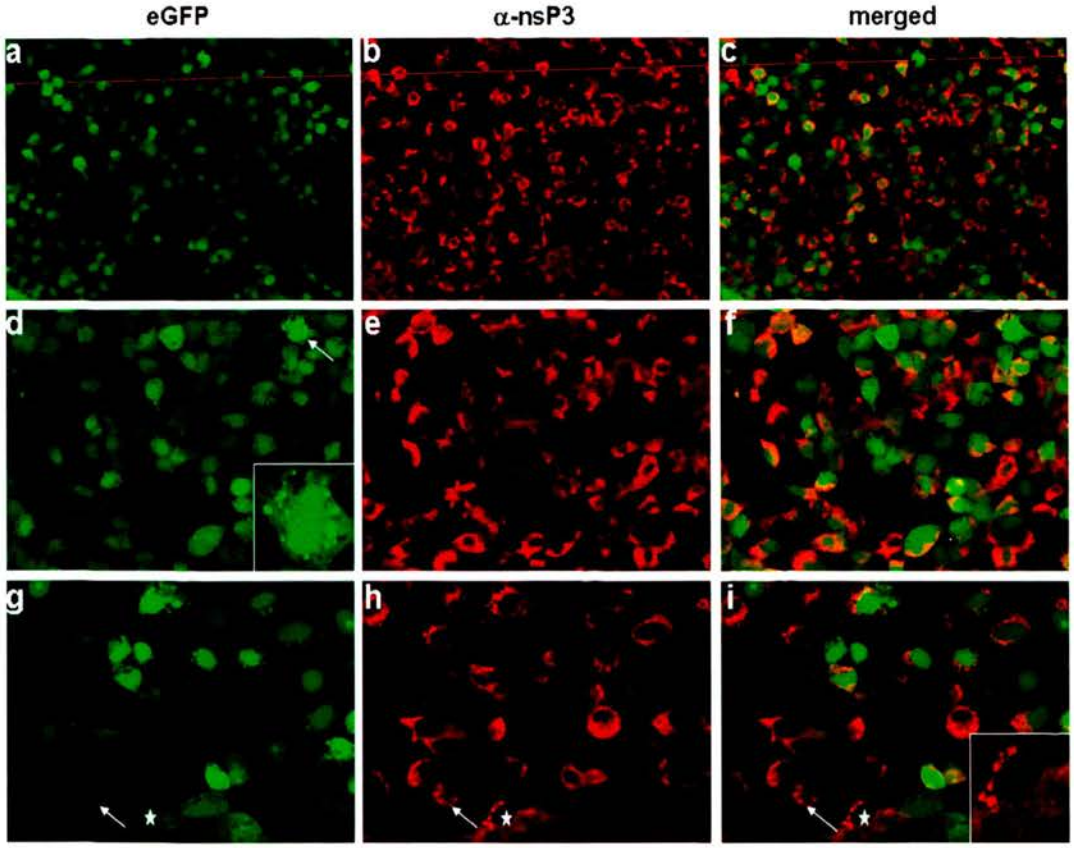

Figure 4.8. Infection of C6/36 cells from *Aedes albopictus* with SFV4-steGFP. (a) (d) & (g) Cells were infected with SFV4-steGFP (M.O.I of 10) and fixed at 16 hours post-infection. Cells with different levels of eGFP expression, probably indicative of different stages in infection can be seen. In some cells, fluorescence was more intense in the nucleus. **(d)** The white arrow indicates a cell with numerous vacuoles containing large amounts of eGFP, a high magnification image of this cell is shown in the inset. Immunostaining with anti-nsP3 antibody can be seen in **(b) (e)** and **(h)**. Merged images are shown in panels **(c) (f)** & **(i)**; the vast majority of eGFP-positive cells were also nsP3-positive. A cell with typical nsP3 staining is marked with an asterisk in panels **(g) – (i)**. In the same panels the white arrow indicates a cell stained positive for nsP3 which was eGFP-negative. Negative controls were performed and were identical to the ones shown in Figure 3.7. All images were acquired with a Zeiss confocal microscope.

Rat hippocampal neurons infected with SFV4-steGFP exhibited high levels of eGFP fluorescence (Figure 4.9). eGFP was distributed evenly throughout the cytoplasm and the nucleus of the infected cells. In addition, eGFP was able to spread to the axonal processes of the neurons (seen in panels a, g, h & i). These primary cultures contain many cell types, but principally neurons and oligodendrocytes. Oligodendrocytes are a known target of SFV (Fazakerley *et al.*, 2006). In these rat hippocampal neuron cultures, cells with oligodendrocyte morphology were infected by SFV4-steGFP. Some of these cells (pointed by white arrows or found inside the encircled area in figure 4.9a – 4.9c) appear to be in close proximity to axonal processes. Studies have shown that oligodendrocyte precursors or mature oligodendrocytes have the ability to myelinate rat hippocampal neurons *in vitro* (Rubio *et al.*, 2004; Kang *et al.*, 2007). These putative oligodendrocytes may be myelinating the adjacent axons.

Infection of rat hippocampal neurons with SFV4-steGFP resulted in death of the cultures by 4 days. After 24 hours, the cells looked perfectly healthy (Figure 4.9a, 49b & 4.9c). Forty eight hours after infection most cells looked normal but some started developing CPE and some cells had the characteristic morphology of cells undergoing apoptosis; condensed nuclei and blebbing (Figure 4.9d, 4.9e &4.9f). Widespread cell death was evident from 72 hours onwards; however, some cells were still surviving at this point (Figure 4.9g, 4.9h & 4.9i). All cells were detached 4 days after infection. The infection progressed in an identical way in cells infected with SFV4.

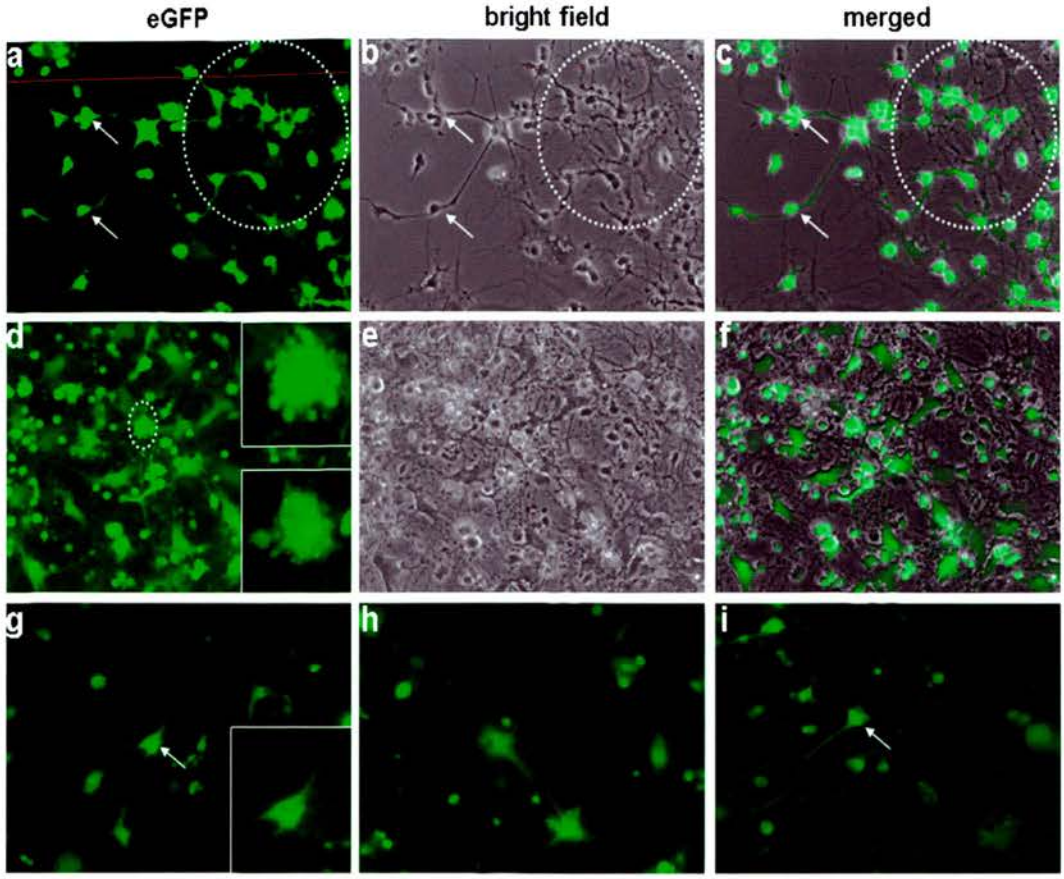

Figure 4.9. Infection of rat hippocampal neurons with SFV4-steGFP. (a), **(b)** and **(c)** In the middle of the field of vision an infected neuron with multiple long processes can be seen. White arrows indicate cells with oligodendrocyte morphology that are in close proximity to the axons of this infected neuron. The dotted circle marks an area rich in processes (best seen in the bright field image), which also contains multiple infected cells with oligodendrocyte morphology. All images acquired 24 hours after infection; no signs of CPE were obvious at this time. **(d)**, **(e)** and **(f)** Images taken 48 hours after infection; most cells looked normal but some showed evidence of CPE and death by apoptosis. In panel **(d)** two cells which show condensed nuclei (bottom inset) and blebbing (dotted circle and top inset) can be seen. Later in infection (72 hours) widespread death was observed in the infected cultures, a few cells were still surviving and had normal morphology. Examples can be seen in panels **(g)**, **(h)** and **(i)**. All images were acquired with a Nikon inverted microscope.

In vivo pathogenesis following intraperitoneal inoculation

Assessement of virulence and determination of viraemia

To assess the virulence of SFV4-steGFP, groups (n=10) of adult (4 – 5 week old, female) Balb/c mice were infected i.p. with 5 x 10^3 PFU of SFV4-steGFP or mock-infected with PBSA. To minimise the number of animals used no animals were infected with SFV4 or SFV L10 since these experiments had been done previously (Figure 3.8b). Infected animals were maintained for 10 days and monitored daily for symptoms of viral encephalitis. In addition, to determine the plasma viraemia following extraneural inoculation six adult (4 – 5 week old) Balb/c mice were inoculated i.p. with 5 x 10^3 PFU of SFV4-steGFP. Twenty-four hours later the animals were euthanised and heparinised blood was collected and titrated using a standard plaque assay.

Results

In the previous experiments using SFV4 (Figure 3.8b) mice did not succumb to the infection, it was expected therefore that the same would happen following infection with SFV4-steGFP. None of the SFV4-steGFP inoculated mice showed any clinical signs of disease throughout the 10 day period that the experiment lasted. The heparinised blood collected from the SFV4-steGFP infected animals was titrated and 100% (6/6) of the samples were below the limit of detection of the assay. Insertion of eGFP in the structural ORF therefore had an attenuating effect on the *in vivo* replication efficiency of SFV4 following inoculation via the intraperitoneal route since SFV4 was able to establish a viraemia at 24 hours post-infection (Figure 3.9a).

Virus spread in wt mice and mice deficient in type-I interferon responses

Type-I interferon (IFN) appears to play a very crucial role in limiting virus replication and determining the outcome of infection (Isaacs & Lindenmann, 1957). To determine whether SFV4-steGFP was being suppressed by the IFN system, the course of infection in the absence of an intact type-I IFN response was investigated. Groups (n=3) of adult (4-5 week old, female) IFN α/β receptor knock-out mice (A129) (Muller *et al.*, 1994) and wt129 mice were infected i.p. (at the same time using the same vial of virus) with 5 x 10^3 PFU of SFV4-steGFP. One mouse from each group was sampled 24 hours post-infection. The remaining mice from the control group (wt129) were sampled on PID 2, whereas a mouse from the A129 group was sampled on PID 2 and the last mouse from this group was sampled when symptoms of viral encephalitis developed on PID 4. To titrate the infectious virus in the peripheral blood, heparinised blood was collected. Numerous tissues from SFV4-steGFP infected mice including: spleen, pancreas, heart, lung, kidney, and brain were also sampled. The removed tissues were directly observed for fluorescence using a Zeiss stereomicroscope and were then processed into frozen sections. To facilitate visualisation of the tissue structure, tissue sections were incubated with diaminobenzidine (DAB) to obtain a light background staining. Sections were then examined microscopically for eGFP expression.

Results

The results obtained from the titration of the heparinised blood samples are shown in Table 4.1. For comparison the results previously obtained (Table 3.1) from SFV4 infected animals are also shown. In contrast to the SFV4-infected wt129 mouse which had detectable levels of infectious virus on PID 1, the mouse infected with SFV4-steGFP had no detectable infectious virus at this time. On PID 2 none of the wt129 mice infected with either SFV4 or SFV4-steGFP had infectious virus in the blood. In contrast, in A129 mice, infected with SFV4-steGFP, a viraemia was established. However, on PID 1, the titre of SFV4-steGFP was 6.3 Log_{10} PFU/ml, 2.2 Log_{10} PFU/ml lower than that of SFV4. On PID 2 the titre of SFV4-steGFP had

increased slightly (6.7 Log_{10} PFU/ml). Since the A129 mice were not exhibiting signs of encephalitis it was decided to keep the third mouse until signs of encephalitis (including limb paralysis and ataxia) developed. On PID 4 this mouse was moribund and was euthanised. Infectious virus in the blood had a titre of 6 Log_{10} PFU/ml. Given that on PID 1 and PID 2, 3/3 wt129 infected mice had no detectable viraemia and 2/2 A129 mice had high titre viraemia, it can be concluded that as with SFV4, the IFN system very efficiently controls SFV4-steGFP replication, at least in extraneural tissues. Based on the virus titres and the delay in the development of clinical symptoms it can be suggested that insertion of eGFP in the structural ORF of SFV attenuated the virus in mice lacking an intact type-I IFN system following i.p. inoculation. Only a small number of mice were used for these experiments; a breeding colony of A129 mice was not available at the departmental animal unit. Due to the small number of animals it is not possible to perform any statistical analysis on the data and ideally these studies should be repeated with more mice.

Virus	**PID 1 wt129**	**PID 2 wt129**	**PID 1 A129**	**PID 2 A129**	**PID 4 A129**
SFV4	4.3 (1/1)	<1.4 (2/2)	8.5 (1/1)	-	N/A
SFV4-steGFP	<1.4 (1/1)	<1.4 (2/2)	6.3 (1/1)	6.7 (1/1)	6.0 (1/1)

Table 4.1. Infectious virus titres in the blood of A129 and wt129 mice infected with SFV4-steGFP. All values are expressed as Log_{10} PFU/ml of whole blood. On PID 2 both A129 mice infected with SFV4 were found dead (-).

Although no infectious virus was detected on PID 1 in the blood samples of the wt129 mice infected with SFV4-steGFP it was decided to examine the tissue sections for eGFP expression. Slides with tissue sections of brain, heart, lung, liver, pancreas, kidney and spleen tissue were prepared; the thickness of the tissue sections was the same for all tissues (12 μm) except for pancreatic tissue (14 μm). Six slides with 3 sections on each slide were examined microscopically for eGFP expression. No eGFP fluorescence was observed in any of these tissues.

For A129 mice, all removed tissues were fixed and examined using a stereoscopic fluorescent Zeiss microscope. Only the brain of the A129 mouse sampled on PID 4 showed evidence of high levels of eGFP expression (Figure 4.10a). The infected

areas of this brain included the inferior colliculus (ic), a midbrain nucleus of the auditory system with high metabolic activity (Gross *et al.*, 1987), the main olfactory bulb (mob), an area of the brain associated with the perception of odours (Davison & Katz, 2007) and the frontal cortex (fctx). Foci of infection in close proximity to blood vessels were apparent, however, it is not possible to determine if these were definitely associated with the blood vessels because the depth of the eGFP signal could not be determined.

Following gross examination, frozen sections were cut from all tissues (same thickness as for the wt129 mice). Again, multiple slides were examined using a Zeiss Axioskop confocal microscope. Infected (eGFP-positive) cells were apparent in several tissues. Throughout the brain, SFV4-steGFP infected meningeal cells (Figure 4.10b) and neurons. In Figure 4.10c several infected neuronal populations including pyramidal neurons of the hippocampus (CA3 field of Ammon's horn), neurons of the granular dentate gyrus (GrDG), of the polymorph layer of the dentate gyrus (PoDG) and of the thalamus can be seen. In heart tissue many cells were infected in the valves (Figure 4.10d &4.10e) whereas, very few infected cells were seen in the myocardium (heart muscle; Figure 4.10f). In the spleen (Figure 4.10g & 4.10h), the majority of the infected cells were located in the marginal zone (mz) between the red pulp (rp) and the white pulp (wp). This area of the spleen is known to be rich in macrophages so there is a high probability that the infected cells were macrophages. In the pancreas (Figure 4.10i) many eGFP expressing cells, were observed. Interestingly, the infected cells were acinar cells of the exocrine pancreas; no infected cells were observed in the endocrine pancreas despite examination of many sections (at least 6 slides with 3 sections per slide). Cells in the kidney glomeruli were infected as were smooth muscle cells surrounding the ureter (ur) (Figure 4.10j). Adipose tissue was heavily infected (Figure 4.10k). Foci of infection were also observed in cells lining the alveoli in the lungs (Figure 4.10l). It is important to point-out that SFV4-steGFP showed a preferential cellular tropism in most tissues examined; for example cells of the heart valves in the heart, acinar cells of the exocrine pancreas in the pancreas and cells of the marginal zone of the spleen (most probably macrophages).Using SFV4-steGFP it was possible to show the spread of

the infection in the absence of a functional type-I IFN response system without the need for immunostaining.

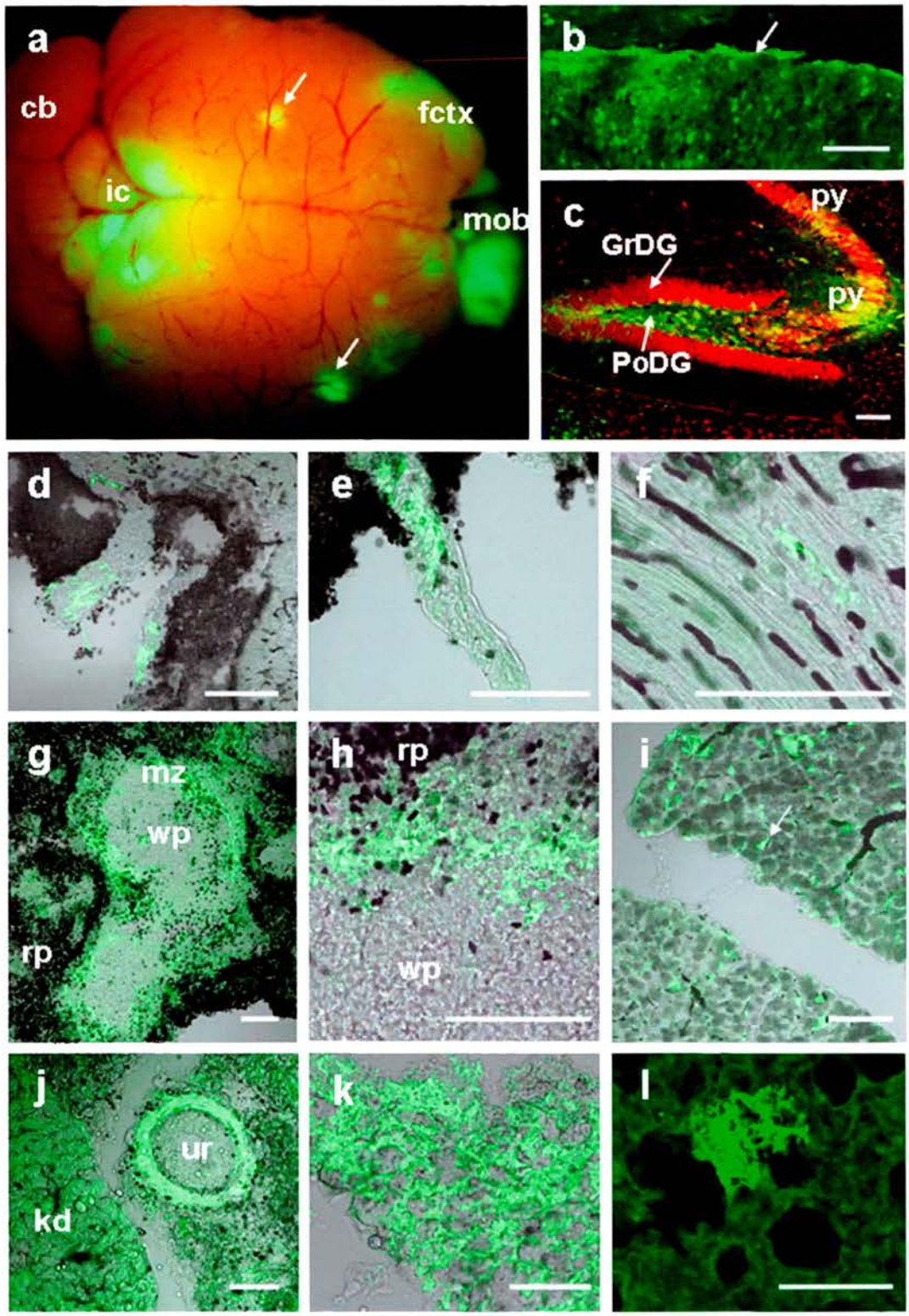

Figure 4.10. Distribution of SFV4-steGFP in the absence of type-I interferons. **(a)** Picture of the dorsal surface of the brain taken with a Zeiss stereomicroscope. Foci of infection were observed in the inferior colliculus (ic), the frontal cortex (fctx)

and the main olfactory bulb (mob). Arrows point to two foci of infection that appear to be associated with blood vessels. The depth of the image shown is unknown so it is not possible to definitely determine the association of these foci of infection with their adjacent blood vessels. **(b)** Section of the same brain exhibiting infection of meningeal cells (white arrow). **(c)** Infected neuronal populations in: the CA3 field of Ammon's horn of the pyramidal layer of neurons in the hippocampus (py). The granular dentate gyrus (GrDG) and the polymorph layer of the dentate gyrus (PoDG). A focus of infection can also be observed below the line that separates the dentate gyrus from the thalamus (bottom left-hand side of the panel). To make observation easier nuclei were stained with PI (red). **(d)** and **(e)** Sections of heart tissue showing infection of the heart valves in low and high magnification respectively **(f)** High magnification image of myocardial tissue showing SFV4-steGFP infected cells. **(g)** Section of spleen tissue, infection had a circular distribution in the marginal zone (mz) between the red pulp (rp) and the white pulp (wp). This area of the spleen is known to be rich in machrophages. **(h)** High magnification image of infected cells at the same area. **(i)** Section of pancreas with numerous infected cells. Interestingly only acinar cells of the exocrine pancreas (example shown with white arrow) were infected. **(j)** Kidney cells including cells in the glomeruli were infected (kd). The smooth muscle surrounding the ureter (ur) was found to be heavily infected. **(k)** Adipose tissue exhibiting high levels of eGFP fluorescence. Adipose tissue was one of the most heavily infected. **(l)** Focus of infection in the lung. Bars represent 100 μm in all panels. All tissues are from a mouse sampled on PID 4. Tissues shown in panel D – L were incubated shortly with DAB to give a light staining allowing better visualisation of the tissue structure. As mentioned earlier haematoxylin staining quenches the eGFP signal and for that reason it was not used. All images except **(a)** were acquired using a Zeiss confocal microscope.

Virus pathogenesis following intracerebral inoculation

Except in mice with a deficient type-I IFN system, *in vivo* replication of SFV4 and SFV4-based recombinant viruses was limited following extraneural administration of the virus and caused no clinical signs in mice. To observe events in the brain of wt mice, SFV4-steGFP was inoculated intracerebraly (i.c.). Two experiments were performed.

Assessment of virus virulence

To assess virus virulence and titres of virus in the brain following direct inoculation in the brain; groups (n=6) of adult (4-5 week old, female) Balb/c mice were infected i.c. with 1,000 PFU of SFV4-steGFP or mock-infected with PBSA. Data for i.c. infection of this dose of SFV4 was already available (Figure 3.11b) and was not repeated. Mice were monitored at regular intervals for clinical signs of viral encephalitis. All animals exhibiting substantial clinical signs were euthanised and their brains removed and snap frozen for virus titration.

Results

Initial signs of viral encephalitis, including pilar erection and reduced motility, appeared approximately 24 hours post-infection in the group of mice infected with SFV4. The mice infected with SFV4-steGFP reached the same end-point approximately 24 hours later (48 hours post-infection). All (6/6) SFV4 infected animals were sick on PID 2 with signs of fulminant encephalitis. SFV4-steGFP infected mice developed indistinguishable symptoms 24 hours later, on PID 3. The mock-infected animals (PBSA) remained asymptomatic until PID 10 when the experiment was terminated (Figure 4.11a).

All animals infected with SFV4 or SFV4-steGFP had high levels of infectious virus in their brains. More specifically, SFV4 infected mice had an average infectious virus titre of 9.5 Log_{10} PFU/g of brain (SD: 0.11) on PID 2. The brains of SFV4-steGFP infected mice had an average titre of 8.4 Log_{10} PFU/g of brain (SD: 0.34) on

PID 3. The time-points at which the two groups of mice were sampled were different because it was decided to sample the mice when they exhibited signs of terminal disease. Statistical analysis using paired t-test showed that for mice with clinical encephalitis, SFV4 reached statistically significant higher brain virus titres than SFV4-steGFP ($P<0.05$). As expected, all mock-infected (PBSA) animals were negative for infectious virus (Figure 4.11b). These results indicate that neither SFV4 nor SFV4-steGFP were attenuated in their ability to replicate and spread in the brain. This is in stark contrast to their poor replication outside the CNS. Insertion of eGFP into the structural ORF did have an attenuating effect on the *in vivo* pathogenesis of SFV4 following i.c. infection; signs of encephalitis developed with a 24 hour delay and SFV4-steGFP reached significantly lower titres in the brain.

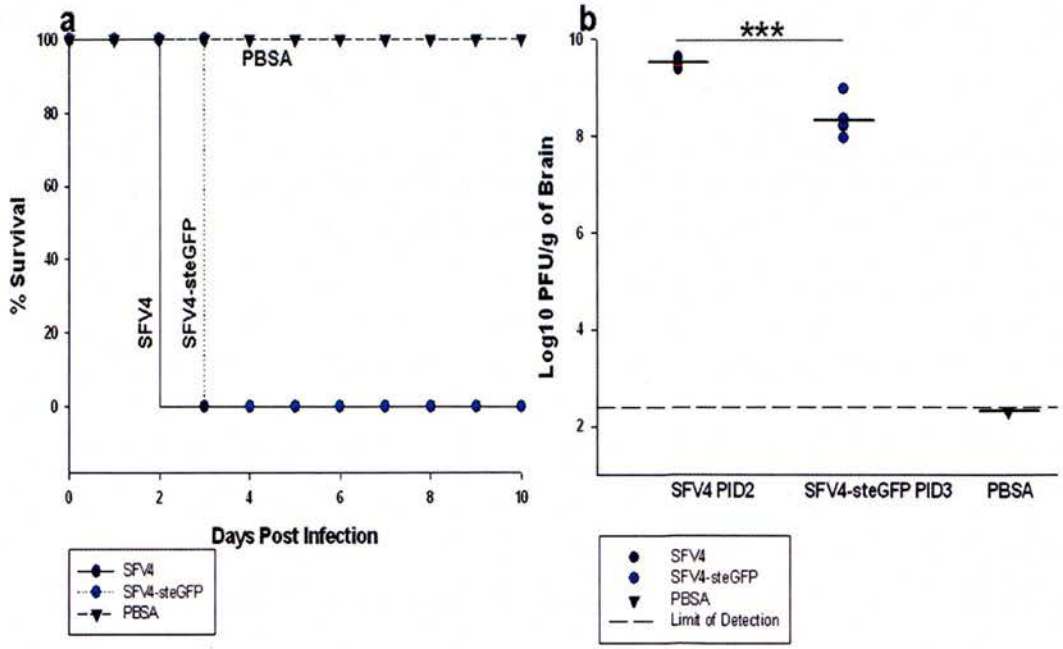

Figure 4.11. Survival rates and brain virus titres in Balb/c mice following i.c. inoculation with SFV4, SFV4-steGFP or PBSA. (a) Survival rates in Balb/c mice. Groups (n=6) of adult female Balb/c mice were inoculated i.c. with 1,000 PFU of virus or PBSA (mock). **(b)** Infectious virus titres in the brains of Balb/c mice inoculated i.c. with 1,000 PFU. Mice were sampled on PID 2 and PID 3 for SFV4 and SFV4-steGFP, respectively. The two groups were compared using paired t-test and found to be statistically different ($P<0.05$).

eGFP expression and distribution

To examine eGFP expression and distribution in the brain, groups of (n=6) adult (4-5 week old, female) Balb/c mice were inoculated i.c. with 1,000 PFU of SFV4-steGFP. On PID 3 the mice were euthanized and their brains removed, fixed and processed for frozen sections (12 μm thick). These were used to assess eGFP expression. To compare the expression of eGFP to that of viral non-structural proteins and viral structural proteins, brain sections were immunostained with antibodies targeting epitopes on nsP3 and viral structural proteins. The cell tropism of SFV4-steGFP in the CNS, was studied using antibodies recognising cell-specific markers of neurons, astrocytes and oligodendrocytes.

Results

Brains of all mice infected with SFV4-steGFP sampled on PID 3 were processed and frozen sections cut. Multiple sections from each brain were microscopically examined for eGFP expression using a Zeiss Axioskop confocal microscope. In total, 6 slides with 3 sections each were examined from each brain. Infection with SFV4-steGFP was widespread and large foci of infection were scattered throughout the brain. A representative image showing the spread of the infection and the intensity of the eGFP signal can be seen in Figure 4.12a. SFV4-steGFP was present in areas of white matter including the corpus callosum (cc) and in areas of gray matter including for example, the layer of pyramidal neurons of the hippocampus (py) and the cerebral cortex (asterisk). The area enclosed by the dotted circle is shown in higher magnification in Figure 4.12b. In the inset of that panel, a chain of cells with typical oligodendrocyte morphology was observed in the corpus callosum, an area known to be rich in oligodendrocytes. In putative oligodendrocytes most of the eGFP fluorescence was concentrated in the cytoplasm. This was similar to the eGFP distribution observed in BHK-21 cells *in vitro* but in contrast to that in rat hippocampal neurons. In the latter eGFP was evenly distributed in the cytoplasm and nucleus (Figure 4.9). A large focus of infected cells located in the cortex of the brain is shown in Figure 4.12d. In SFV infection, foci of infection in the CNS are usually

perivascular. eGFP was present throughout the neuronal cell body and the axons of infected neurons (Figure 4.12e & 4.12g). Different levels of eGFP expression were observed. The brighter cells are probably the ones infected for longest and the less bright cells the ones most recently infected. Axons of infected cells can be seen in detail in panel f of the same figure. The encircled area is magnified in the inset image; multiple neurite varicosities, most probably caused by the infection were observed. To verify that eGFP was distributed in both the cytoplasm and the nucleus of infected cells, sections were incubated with To-Pro3 nuclear marker. In panel i, the merged image of eGFP (4.12g) and To-Pro3 (4.12h) is shown. In the cells in which this confocal optical section cuts through the nucleus, the blue signal from the nuclear marker overlaps with the green signal produced by eGFP verifying the presence of eGFP in the nucleus of infected cells as well as in the cytoplasm.

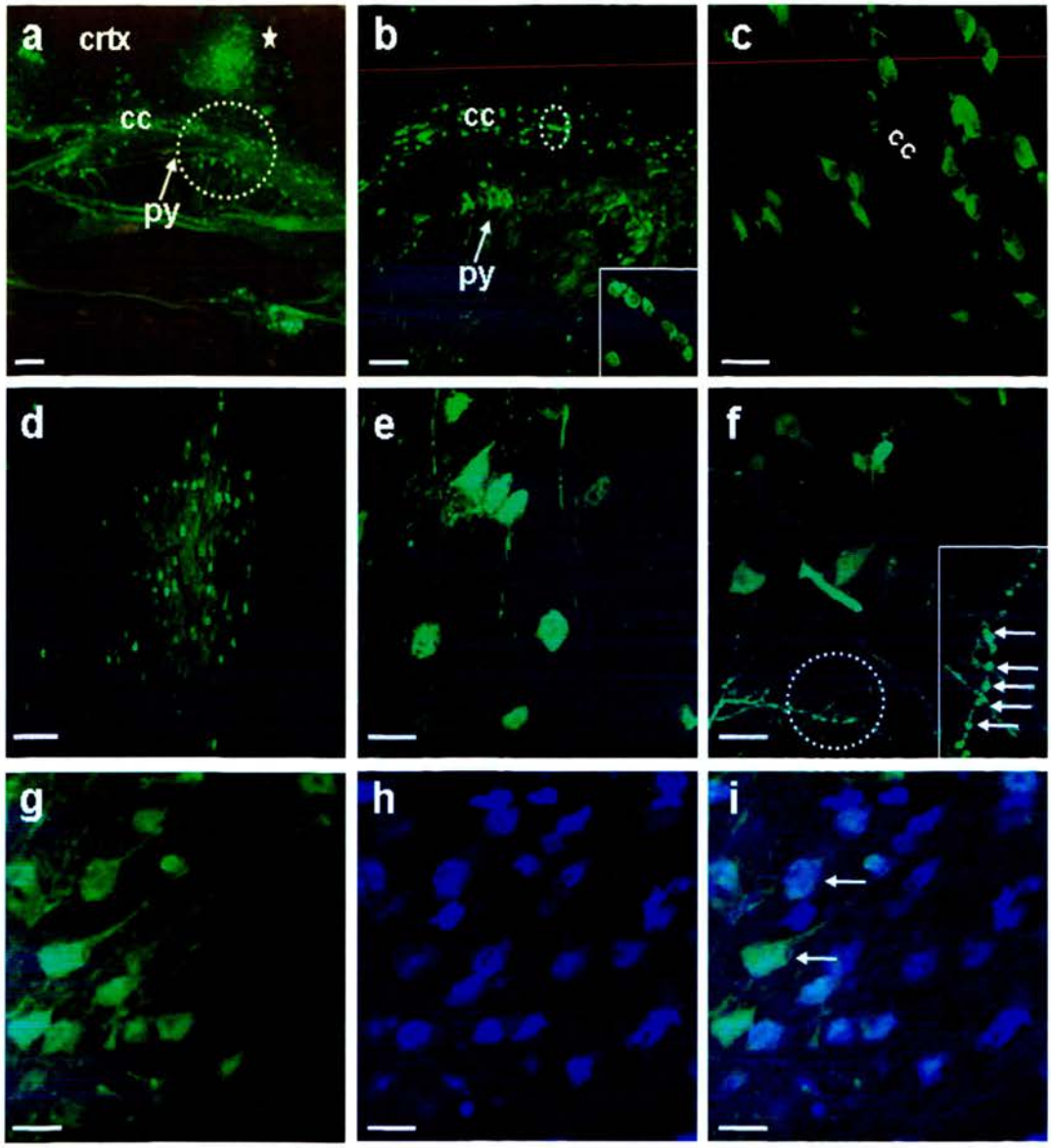

Figure 4.12. eGFP expression and distribution in the brain following i.c. inoculation of Balb/c mice with SFV4-steGFP. (a) Low magnification image showing infection of the corpus callosum (cc), the pyramidal neurons of the hippocampus (py) and the cerebral cortex (crtx); a large focus of infection in the cortex is marked with an asterisk. Bar represents 50 μm. The area in the dotted circle is shown in higher magnification in panel **(b)**. Infection of the cc and of the py was extensive. The area surrounded by the dotted circle is magnified in the inset; these cells have the characteristic morphology of oligodendrocytes and were in an area of the brain rich in oligodendrocytes. Bar represents 100 μm. **(c)** Oligodendrocytes (by morphology and anatomic position) infected with SFV4-steGFP. Note that most of the eGFP signal is in the cytoplasm of these cells. Bar represents 20 μm. **(d)** A focus of infection in the brain cortex, bar represents 100 μm. **(e)** Higher magnification image of infected cortical neurons. eGFP was present in the cell body and the axonal

processes. Levels of eGFP fluorescence varied; signal intensity probably corresponds to the stage of infection, the brighter cells being the ones infected first. Bar represents 20 μm. **(f)**. In this field eGFP expressing axons can be seen. The area inside the dotted circle is magnified in the inset. White arrows point to varicosities on a neurite if an infected neuron. Bar represents 20 μm. **(g)**, **(h)**, and **(i)** SFV4-steGFP infected cortical neurons. The section was treated with To-Pro3 nuclear marker (blue). Merged image of the two channels verified that eGFP was present in the nucleus of infected neurons. Typical cells are pointed by white arrows. Bars in these panels represent 20 μm. All sections are from SFV4-steGFP infected animals sampled on PID3. Images acquired using a Zeiss Axioskop confocal microscope.

eGFP expression vs nsP3 non-structural protein expression

Intracerebral inoculation of SFV4-steGFP resulted in a large number of infected cells expressing variable levels of fluorescence in the brain. During *in vitro* studies, it was observed that in SFV4-steGFP infected cultures, a small percentage of cells stained positive for nsP3 protein but were eGFP-negative. To investigate if the situation was the same *in vivo*, frozen sections from the brains of animals sampled on PID 3 were immunostained with anti-nsP3 antibody.

Microscopic examination of multiple brain sections (at least 6 slides with 3 sections each) immunostained with an antibody recognising the nsP3 non-structural protein showed that there was almost complete correspondence between nsP3 and eGFP staining. In Figure 4.13 three different sections of SFV4-steGFP infected brain tissue stained with anti-nsP3 antibody are shown. It can be observed, especially in panels a – c which show a large area of infection, that all eGFP-positive cells (green) are also nsP3-positive (red). Rarely, cells which were nsP3-positive but eGFP-negative were observed. These cells could either have been infected with a virus which had eliminated the eGFP insert or could have been just recently infected (eGFP had not accumulated enough to be clearly visible). An example of a putative recently infected cell is shown in panels g – i.(marked with an asterisk); this cell has strong positive nsP3 staining, which would be expected since levels of non-structural proteins are very high at the early stages of viral replication, but the eGFP signal is low.

The distribution of nsP3-specific staining was identical to that previously observed, cytoplasmic and punctate (insets in Figure 4.13f &4.13i). Each one of these spots probably corresponds to virus replication complexes on the surface of modified endosomes and lysosomes (Froshauer *et al.*, 1988). It is worth mentioning that the intensity of the nsP3-specific signal was linked to the intensity of the eGFP fluorescence. Dull green cells stained very strongly for nsP3 (cells marked with asterisk in 4.13d – f) whereas bright green cells had dull red signal (dotted circle in the same panels). The variety in the intensity of the eGFP/nsP3 signals may provide a way to distinguish between cells that have been infected for different lengths of time.

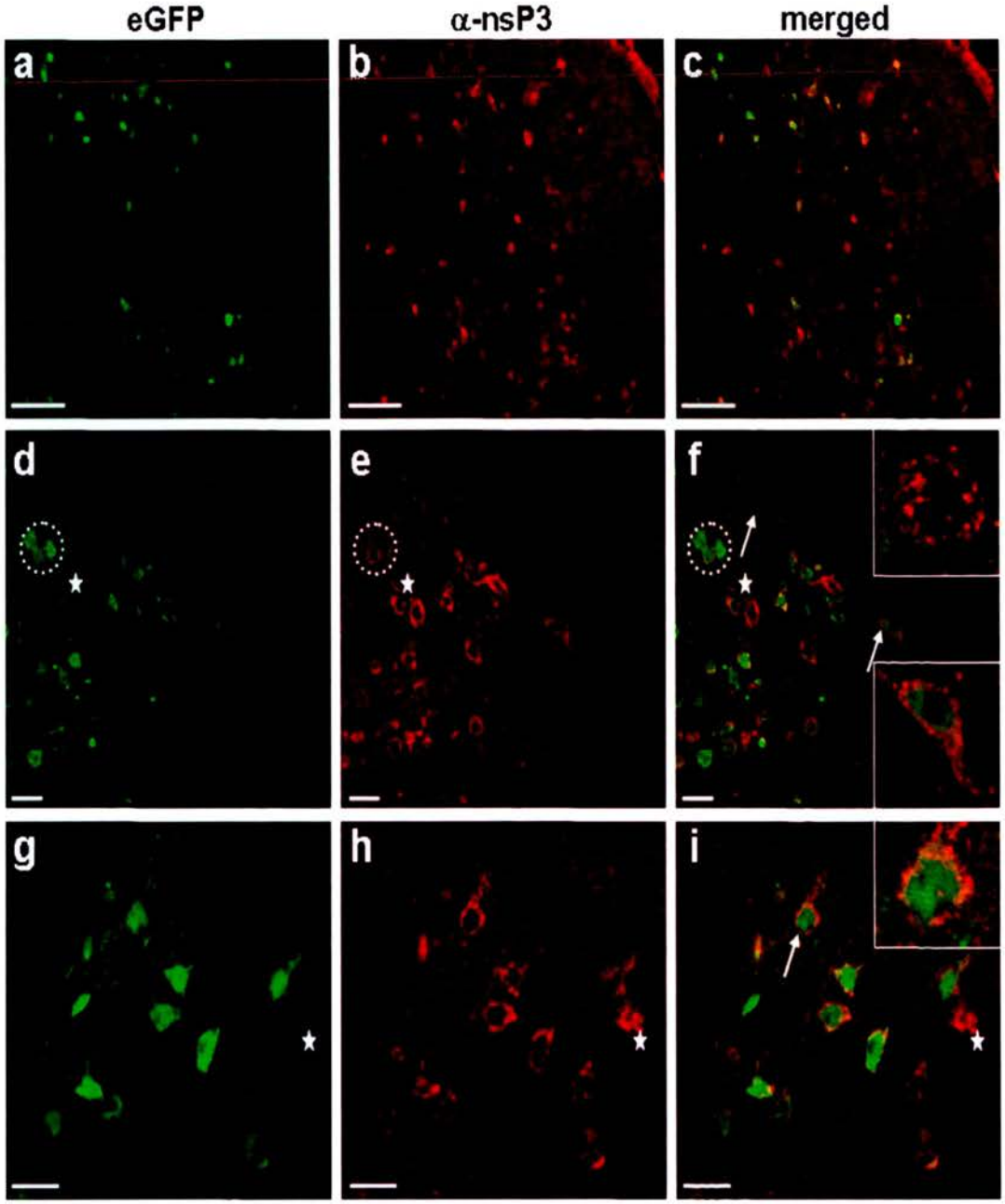

Figure 4.13. eGFP expression and nsP3 expression in the brains of SFV4-steGFP infected mice. (a) low magnification of eGFP expression. Variable levels of eGFP fluorescence can be seen. **(b)** low magnification of nsP3-specific staining on the same section. **(c)** merged image of **(a)** and **(b)**. Note that all eGFP-positive cells (green) are also nsP3-positive (red). Bar in panels **a – c** represents 100 μm. **(d)** eGFP expression in a focus of infection in the brain cortex. **(e)** nsP3-specific staining on the same section. **(f)** merged image of **(d)** and **(e)**. In the insets of this panel two cells with cytoplasmic, punctate nsP3-specific signal are shown; these cells are marked with arrows. The area surrounded by the dotted circle in all panels contains bright green cells with low intensity red signal for nsP3. An area exhibiting the opposite

pattern is marked with an asterisk. Bar in panels **d – f** represents 20 μm. **(g)** SFV4-steGFP infected cells in the midbrain. **(h)** nsP3-specific staining of the same area **(i)** merged image of **(g)** and **(h)**. The arrow points to a cell with characteristic nsP3 staining shown in large magnification in the inset. The asterisk in all panels marks a cell with dull green signal but very strong nsP3-specific signal. Bar 20 μm in all panels. All tissue sections shown here were cut from brains sampled on PID 3. Appropriate controls were included. Results of the controls were identical to those previously observed (Figure 3.13). All images were acquired with a Zeiss confocal microscope.

eGFP expression vs SFV structural proteins expression

When BHK-21 cells were infected with SFV4-steGFP at high multiplicity of infection (M.O.I) it was observed that although approximately 100% cells were infected (as shown by the presence of eGFP fluorescence) only a fraction (15 – 20%) of these stained positive for the viral structural proteins when a polyclonal antibody against SFV structural proteins was used (Figure 4.6). To study if the situation was similar *in vivo*, frozen sections of brain tissue from Balb/c mice infected with SFV4-steGFP were stained and examined using fluorescent microscopy.

Microscopic examination of multiple sections (at least 6 slides with 3 sections per slide) showed that almost every eGFP-positive cell stained positive for viral structural proteins (Figure 4.14a – 4.14c & .4.14d – 4.14f). eGFP was distributed evenly throughout the cell cytoplasm and nucleus whereas, SFV immunostaining was exclusively cytoplasmic. Rarely, there were eGFP-positive cells that were negative for viral structural proteins (Figure 4.14g – 4.14i). These eGFP-positive cells were most often found at the edges of foci of infection and were dull green. As mentioned earlier, SFV forms foci of infection around blood vessels in the brain (Fazakerley *et al.*, 1993). The cells in the middle of the focus of infection are therefore the first to be infected while those at the outer edges are the ones most recently infected. It is most likely therefore that the dull green cells negative for viral proteins are the most recently infected cells in which structural proteins have not yet accumulated to adequate levels to be detected by immunostaining. Furthermore, cells that had the highest expression levels of eGFP also had the strongest signal when stained for virus structural proteins. Similarly, cells with lower levels of eGFP fluorescence had less structural protein immunostaining. Taken together, these observations suggest that detection of eGFP was more sensitive than detection by immunostaining of the virus structural proteins but that eGFP and viral proteins were always expressed in a similar ratio, as would be expected since they are derived from the same ORF.

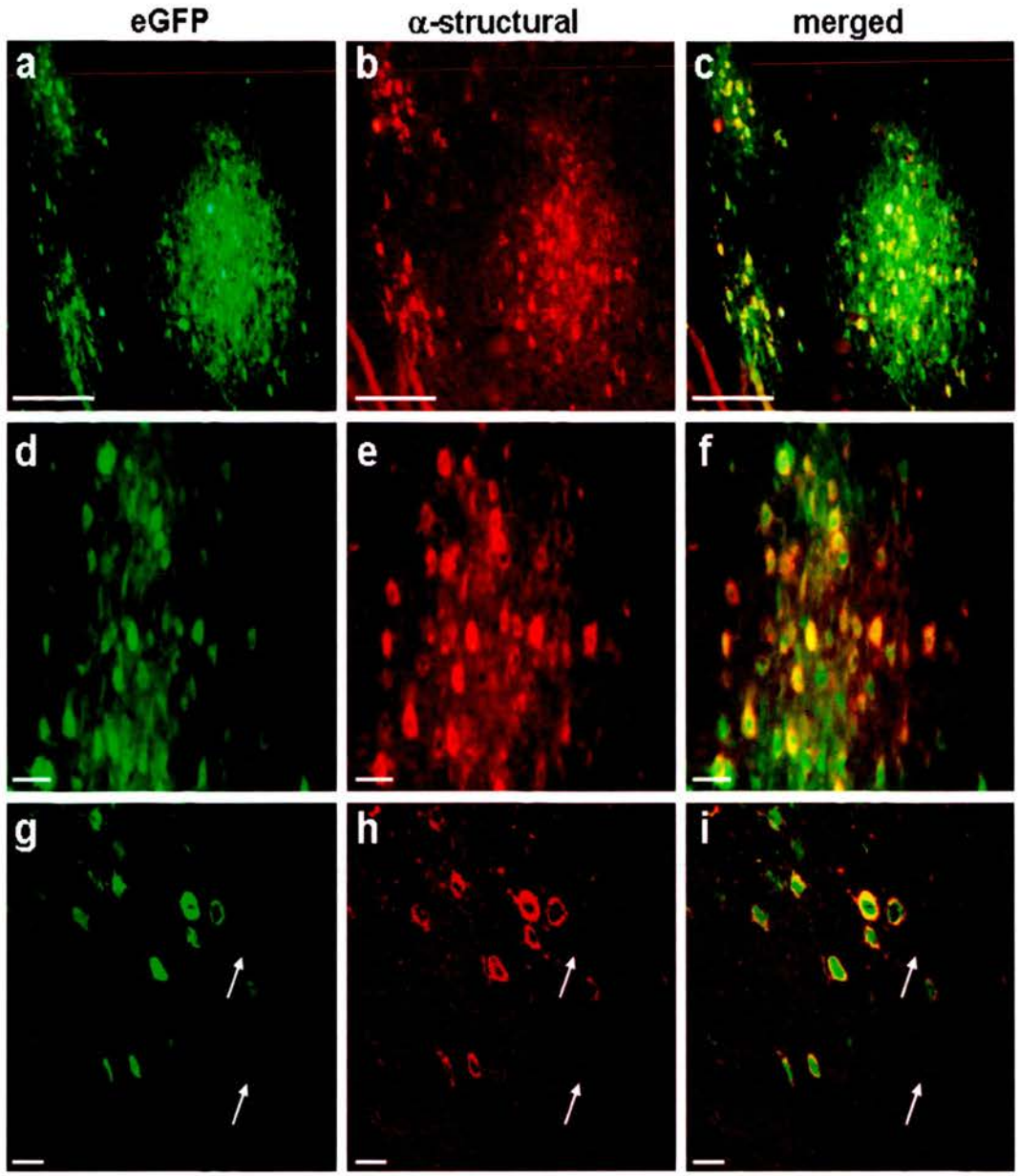

Figure 4.14. eGFP expression and viral structural protein expression in the brain of SFV4-steGFP infected mice. (a) Foci of infection in the cortex of the brain showing high levels of eGFP expression **(b)** anti-SFV staining on the same area. **(c)** merged image of **(a)** and **(b)**. Note that brightest cells are in the centre of the focus of infection and that the SFV immunostaining follows a very similar pattern. Bar in panels **a – c** represents 100 μm. **(d)** High magnification image of a focus of infection. eGFP levels were very variable with the brightest cells being in the centre of the area and the cells with less bright signal at the edges. **(e)** anti-SFVstaining of the same area. **(f)** merged image of **(d)** and **(e)**. Cells with very high levels of eGFP also have high levels of SFV-specific staining and vice versa. Bar in panels **d – f** represents 20 μm. **(g)** Another area with infected cells which have variable levels of eGFP expression. **(h)** SFV-specific immunostaining of that area. **(i)** merged image of **g – h**

eGFP was distributed evenly in the cytoplasm and the nucleus of most infected cells. In contrast SFV structural proteins were found exclusively in the cytoplasm. Arrows point to dull green cells which did not stain positive for SFV proteins. These are probably cells at the early stages of infection. Bar in panels **g – i** represents 20 μm. Appropriate controls were included and were identical to the ones shown in Figure 3.15. All tissue sections shown here were cut from brains sampled on PID 3. All images were acquired with a Zeiss microscope.

Cell tropism of SFV4-steGFP in the CNS

Amongst other potential applications, marker viruses, like SFV4-steGFP could be used for *in vivo* pathogenesis studies to investigate the tropism of the virus in various animal models (for example in mice with deficient type I interferon responses). SFV in particular has been used extensively in studies on viral encephalitis (Fazakerley, 2002) and on the tropism of neurotropic positive-strand RNA viruses in murine models (Balluz *et al.*, 1993). These studies can be greatly simplified by the use of a virus expressing a marker protein like eGFP. The ability of SFV4-steGFP to infect three different cell types in the mouse brain was investigated by immunostaining. The cell types chosen for this study were neurons, oligodendrocytes and astrocytes. The antibodies used were anti-NeuN, anti-CNPase and anti-GFAP.

Immunostaining for the neuronal marker NeuN showed that many of the SFV4-steGFP infected cells were neurons. It was previously assumed that a large percentage of the cells infected by this virus were neurons based on their morphology and their anatomic position in the brain; the immunostaining result verified this assumption. Infected neurons were found scattered throughout the brains of the infected animals. In Figure 4.15 examples from two different areas of the brain, the cerebral cortex (panels a – c) and the hippocampal region are shown (panels d – i). Most of the infected cells in the cortex were neurons as demonstrated by positive staining with the anti-NeuN antibody. In the inset of 4.15c some double-labelled cells can be seen in high magnification. Infection was widespread in the pyramidal layer of neurons in the hippocampus (py); cells expressing eGFP were visible in all the fields (CA1-3) of Ammon's horn. This structure, together with the granular dentate gyrus (GrDG) consists of neuronal cell bodies, which stained positive allowing their direct visualisation just by looking at the channel corresponding to the NeuN immunostaining (Figure 4.15e). That compensated for the absence of the standard histopathology stains (eosin and haematoxylin) which cannot be used in conjunction with fluorescence because the fluorescent signal is quenched. A high magnification of infected neurons in the hippocampus can be seen in panel g. All the infected cells in this section also stained positive for NeuN (panels h & i). Some cells with typical pyramidal neuron morphology are marked with an asterisk.

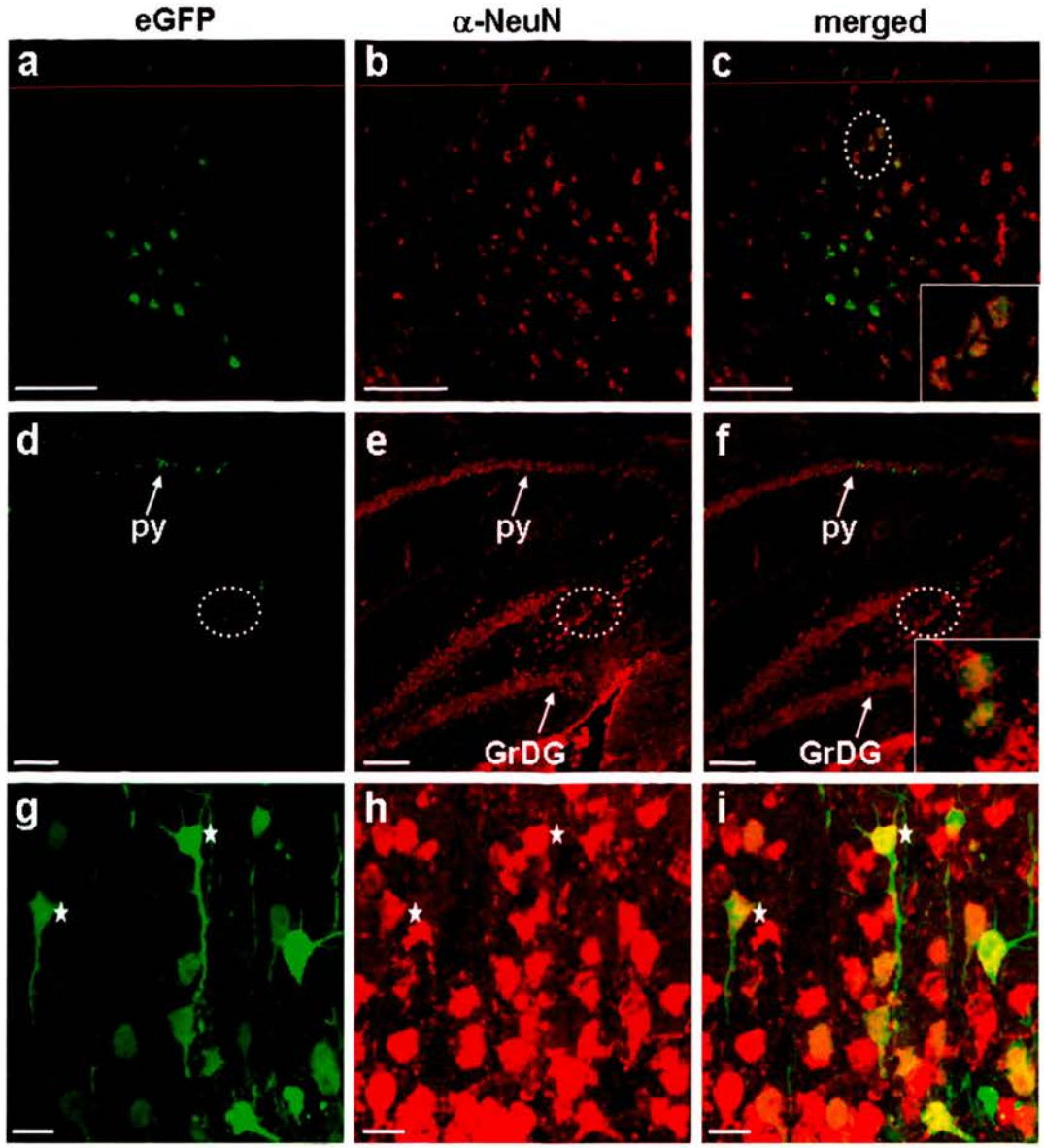

Figure 4.15. Immunostaining using NeuN neuronal marker on brain sections from Balb/c mice infected i.c. with SFV4-steGFP. (a) Focus of infection in the brain cortex. **(b).** Positive NeuN immunostaining of the same area. **(c)** merged image of **(a)** and **(b).** The orange colour is indicative of co-localisation of eGFP (virus) and NeuN signals indicating that the infected cells are neurons. Typical double-labelled cells (inside the dotted circle) are shown in high magnification in the inset of this panel. Bars represent 100 μm in all panels. **(d)** Low magnification image of eGFP expressing cells in the pyramidal layer of neurons in the hippocampus (py). Infection has spread in all fields (CA1-3) of Ammon's horn. **(e)** NeuN specific staining on the same area. The granular dentate gyrus (GrDG) is also visible. **(f)** merged image of **(d)** and **(e)**. At low power it is difficult to determine co-localisation of the two signals. However, double-labelled cells (dotted circle) are shown in high magnification in the inset. Bars represent 20 μm in all panels. **(g)** Z-stack of an infected region in py.

Cells with characteristic morphology of pyramidal neurons are marked with an asterisk. **(h)** NeuN-specific staining of the same region. **(i)** merged image of **(g)** and **(h)**. All eGFP-positive cells appear to be NeuN-positive. Bars represent 20 μm in all panels. Negative control (no secondary antibody on brain sections from a non-infected animal) was included and found to be identical to the one shown in Figure 3.17. All other tissue sections shown here were cut from brains sampled on PID 3. All images were acquired with a Zeiss confocal microscope.

Oligodendrocytes are a known target of various strains of SFV including SFV4 (the backbone virus of SFV4-steGFP) and the avirulent strain A7(74) (Balluz *et al.*, 1993; Fazakerley *et al.*, 2006). To examine if the insertion of eGFP in the structural ORF altered the ability of the virus to infect oligodendrocytes, brain tissue sections were immunostained with anti-CNPase antibody.

Infected CNPase-positive oligodendrocytes were found in both the cortex (Figure 4.16a – c) and in white matter tracts (Figure 4.16d – f) indicating that the recombinant virus was still able to infect these cells.

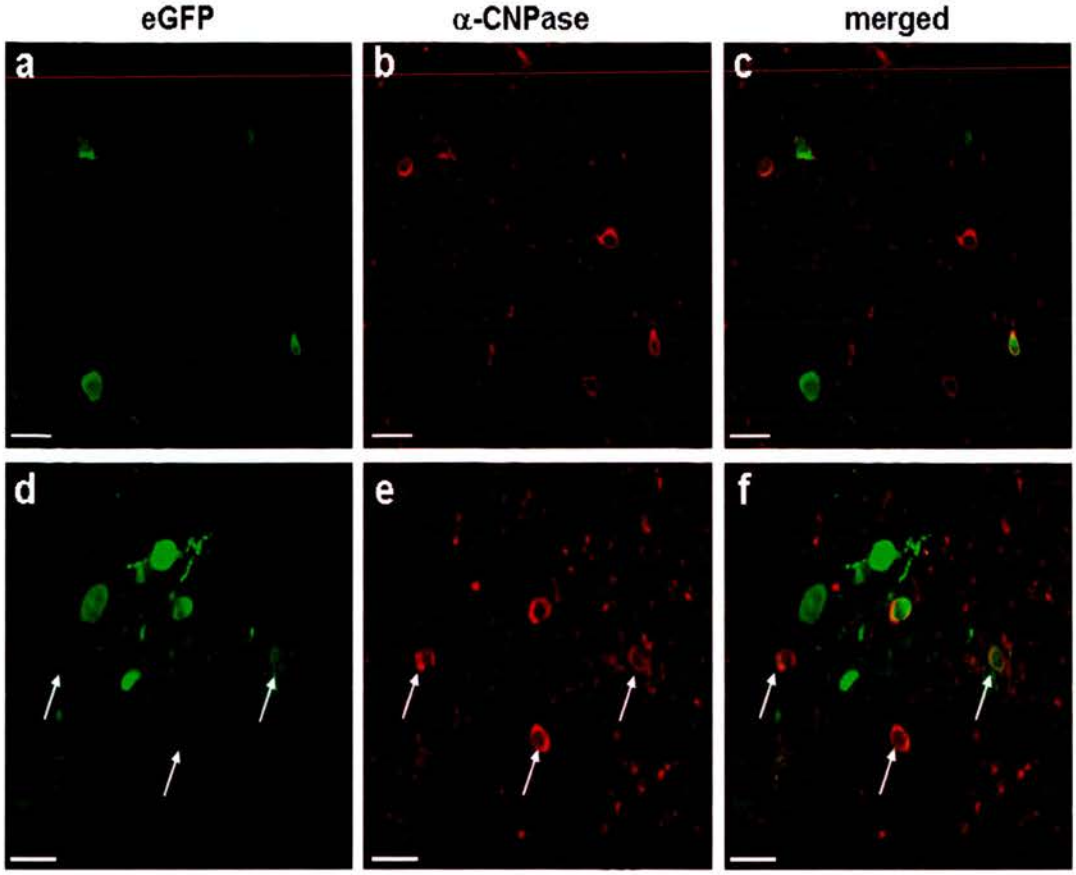

Figure 4.16. Immunostaining using CNPase as oligodendrocyte marker on brain sections from Balb/c mice infected i.c. with SFV4-steGFP. (a) Infected cells expressing eGFP in the brain cortex. **(b)** CNPase-specific staining in the same section. **(c)** merged image of **(a)** and **(b)**. Three different kinds of cells can be seen: cells that are non-infected but CNPase-positive (red), infected cells which are CNPase-negative (green) and double-labelled cells (green & red). Bars represent 20 μm in all panels. **(d)** Focus of infection in a white matter tract. **(e)** CNPase-specific staining of the same section. **(f)** merged image of **(d)** and **(e)**. White arrows point to infected cells which stained positive for CNPase. Bars represent 20 μm in all panels. Appropriate negative control was included. The secondary antibody was the same as the one used for anti-nsP3 and anti-structural immunostainings was used; therefore negative controls can be seen in Figure 3.13 or 3.15. All sections shown here were cut from brains sampled on PID 3. All images were acquired with a Zeiss confocal microscope.

Although astrocytes can be infected by SFV *in vitro* (McKimmie & Fazakerley, 2005) there are no reports supporting the ability of SFV to infect this cell type *in vivo*. The ability of SFV4-steGFP to infect astrocytes was investigated by immunostaining sections of infected brain with anti-GFAP antibody. In response to infection or trauma, astrocytes around the area of infection/trauma get activated. This was observed in SFV infected brains. Multiple tissue sections (at least 6 slides with 3 sections on each slide) were immunostained and thoroughly examined using fluorescent microscopy. No infected GFAP-positive cells were found in areas of white matter (cc) or in areas of gray matter (py) (Figure 4.17).

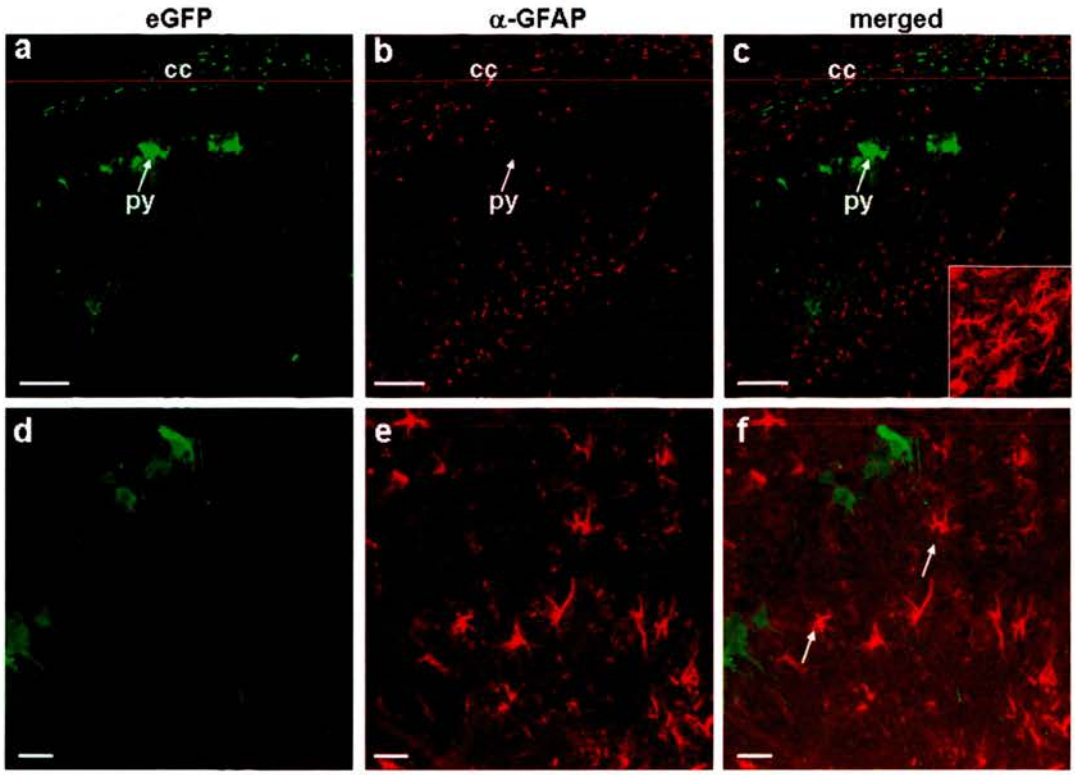

Figure 4.17. Immunostaining using GFAP as astrocyte marker on brain sections from Balb/c mice infected i.c. with SFV4-steGFP. (a) Widespread infection in the corpus callosum (cc) and the pyramidal layer of neurons in the hippocampus. **(b)** Cells with GFAP-specific staining in the same section **(c).** merged image of **(a)** and **(b)** GFAP-positive cells appear to be around the infected cells but it was not possible to determine at this magnification if any of the infected cells had positive immunostaining for GFAP. In the inset typical astrocytes with star-like shape are shown. Bars in all panels represent 100 μm. **(d)** Infected hippocampal neurons. **(e)** GFAP-specific staining of the same section. **(f)** merged image of **(d)** and **(e)** Astrocytes are found around the infected cells but no green cells stained positively for GFAP. Bars represent 20 μm in all panels. Appropriate negative control was included. Same secondary antibody as the one used for anti-nsP3 and anti-structural immunostainings was used; therefore negative controls can be seen in Figure 3.13 or 3.15. Sections were cut from brains sampled on PID 3. All images were acquired with a Zeiss confocal microscope.

In vivo phenotypic and genotypic stability of SFV4-steGFP in Balb/c mice

Experimental design

In vitro, almost all SFV4-steGFP plaque purified viruses eliminated the eGFP insert after the 4th passage. To determine genetic stability *in vivo*, SFV4-steGFP was passaged 5 times in the brain of Balb/c mice as previously described.

Phenotypic stability of SFV4-steGFP in vivo

Balb/c mice were infected with 1,000 PFU of SFV4-steGFP intracerebrally. On PID 3 the brain was removed and homogenised. Homogenate was used to infect a new mouse. This process was repeated 5 times. At the end of the procedure 96 viruses from each passage were plaque purified and used to infect monolayers of BHK-21 cells. Presence of eGFP was monitored using fluorescent microscopy. All (100%) of plaque purified viruses from passage 1 to passage 4 were able to express eGFP. Approximately 95% (94.8%) of the viruses purified after the 5th passage were still expressing eGFP (Figure 4.18a).

Genotypic stability of SFV4-steGFP in vivo

RT-PCR with primers flanking the eGFP insertion in the structural ORF was performed using total RNA extracted from the brain of infected mice. SFV4 plasmid DNA was used as a positive control for the amplification. The expected amplicon had a size of 826 bp if eGFP insert was absent and a size of ~1,650 bp if the eGFP insert was intact. The results obtained confirmed the phenotypic stability results. Between passage 1 and 4 no band corresponding to complete or partial deletion of the eGFP insert was detectable. All PCR products detected had a size of ~1,650 bp. After the 5th passage, the passage that eGFP-negative viruses were first observed during the phenotypic stability passage, few bands indicating partial deletion of the eGFP insert were detected. However, the amplification product corresponding to

eGFP-positive virus was present in greater abundance than these partial deletion products. The PCR results of passage 2 to passage 5 are shown in Figure 4.18b.

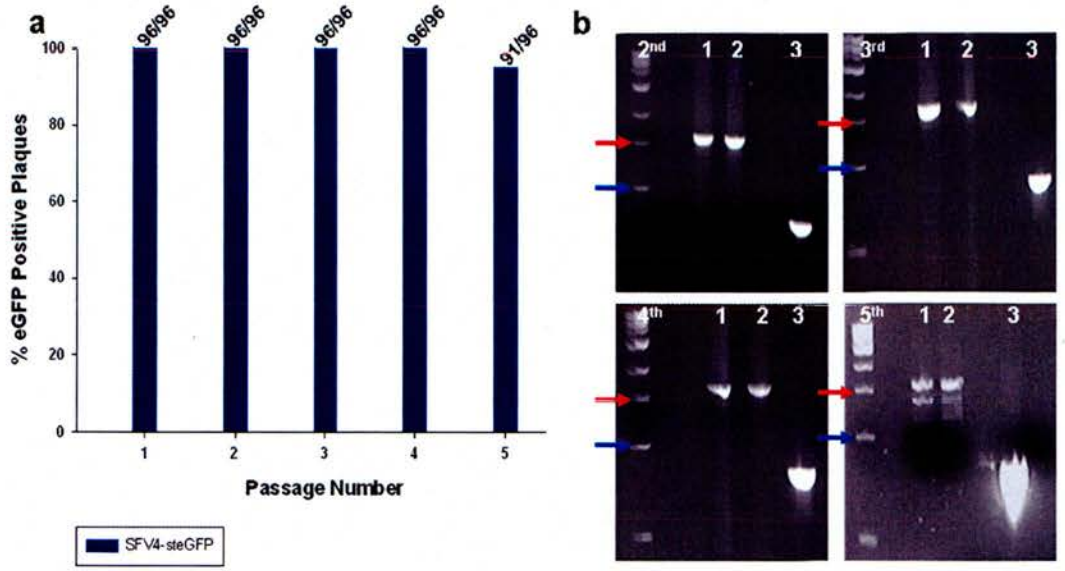

Figure 4.18. ***In vivo*** **phenotypic and genotypic stability of SFV4-steGFP. (a)** Percentage of eGFP-positive plaque purified viruses after 5 passages in the brain of Balb/c mice. **(b)** RT-PCR genotyping of SFV4-steGFP using capsid – E3 primers on RNA samples isolated from infected brain material at passages 2, 3, 4 and 5; The passage number is shown in top left of each panel. In all panels, lanes 1 and 2 are the duplicate passages of SFV4-steGFP and lane three is the SFV4-specific PCR product (positive control). The red arrow corresponds to the 1.5 kb band of the DNA ladder and the blue arrow corresponds to the 0.5 kb band of the DNA ladder.

Summary of Findings

Summary of in vitro analysis of SFV4-steGFP

- Insertion of eGFP into the structural ORF resulted in the production of viable virus able to replicate in BHK-21 cells to levels similar to parental SFV4. However, SFV4-steGFP replication was slower. The virus was able to express high levels of eGFP. Insertion of eGFP slightly attenuated the virus; in SFV4-steGFP infected BHK-21 cells, cytopathic effect (CPE) developed 16 – 20 hours later than in cells infected with SFV4.
- In BHK-21 cells all viral non-structural proteins, structural proteins and eGFP were processed to give free proteins. However, the presence of eGFP-2A-p62 fusion protein indicates that the "cleavage" efficiency of the 2A sequence was not 100%.
- In infected BHK-21 cells, eGFP was exclusively cytoplasmic. The majority of the fluorescent protein was concentrated around the nucleus. The distribution of nsP3-positive virus replication complexes and of viral structural proteins was as expected. Virtually, all eGFP-positive cells stained positive for nsP3 protein. In contrast, only 15-20% of the eGFP-positive cells stained positive for viral structural proteins.
- After 3 *in vitro* passages SFV4-steGFP lost its ability to express eGFP. RT-PCR showed that the eGFP insert was rapidly eliminated upon passage in BHK-21 cells.
- SFV4-steGFP infected C6/36 cells (*Aedes albopictus*) and rat hippocampal neurons and produced eGFP in both. Notably eGFP was present in both the cytoplasm and the nucleus of both cell types.

Summary of in vivo analysis of SFV4-steGFP

- Following intraperitoneal inoculation of SFV4-steGFP, 100% of Balb/c mice survived the infection without any clinical signs. Titration of whole blood showed that the virus did not readily establish a peripheral viraemia.
- A129 mice infected i.p. with SFV4 succumbed to infection more rapidly than mice infected with SFV4-steGFP indicating that insertion of eGFP in the structural ORF slightly attenuated the virus. Cells expressing eGFP were found in brain, heart valves, the myocardium, spleen (especially in the marginal zone), pancreas (acinar cells of the exocrine pancreas), kidneys, lungs and adipose tissue.
- Intracerebral inoculation of Balb/c mice with SFV4 or SFV4-steGFP resulted in fulminant encephalitis in all animals. Nevertheless, SFV4-steGFP infected mice survived longer than SFV4 infected mice and had slightly but significantly lower virus titres in their brains.
- Following intracerebral inoculation infection was widespread and eGFP expression reached very high levels. Virtually all eGFP-positive cells stained positive for nsP3 and virus structural proteins. Punctate cytoplasmic staining for nsP3 and cytoplasmic staining for viral structural proteins.
- The tropism of SFV4-steGFP was not altered by insertion of eGFP. The virus infected neurons and oligodendrocytes but not astrocytes.
- *In vivo* SFV4-steGFP was much more stable than *in vitro*. After 5 passages in the brain of Balb/c mice 94.8% of plaque purified viruses were able to express eGFP. RT-PCR verified the findings of the phenotypic stability; only partial deletions were observed after the 5^{th} passage.

Discussion

One of the important factors that should be considered when replication-competent alphavirus vectors are constructed is that insertion of foreign genes in the native transcriptional units can have an impact on virus viability and replication efficiency. It appears that the position of insertion, the size of the insert and its nature play a key role in the genetic stability of recombinant alphaviruses (Hahn *et al.*, 1992; Thomas *et al.*, 2003; Atasheva *et al.*, 2007).

SFV4-steGFP construction was based on a design described for SV which takes advantage of the properties of the 2A sequence of foot-and-mouth disease virus (FMDV), an apthovirus of the picornaviridae. As for most RNA viruses with a positive strand genome, FMDV encodes its proteins in the form of large polyproteins which after processing release the functional proteins (Donnelly *et al.*, 2001a; Donnelly *et al.*, 2001b). FMDV 2A appears to function in a novel, unique manner self-cleaving at its C-terminus. Unlike most viral polypeptides involved in polyprotein processing 2A does not act proteolytically. The mechanism of action is not completely elucidated but the predominant theory is that 2A cleavage occurs co-translationally and intraribosomally; the ribosome skips the formation of a glycyl-propyl peptide bond at the C-terminus of the 2A sequence (Donnelly *et al.*, 2001b; de Felipe *et al.*, 2003). The complete sequence of 2A is 18 amino acid residues long. However, previous studies have shown that the minimum length required for 2A to be functional is 13 residues. 2A is active in all eukaryotic organisms tested to date, these include insect, plant, mammalian, fungal and yeast cells (Ryan & Drew, 1994; de Felipe *et al.*, 1999; El Amrani *et al.*, 2004; de Felipe & Ryan, 2004). In applied virology, the 2A sequence has been used widely; some examples include multicistronic lentiviral and retroviral vectors, adeno-associated viruses and recombinant poliovirus vectors (Mattion *et al.*, 1996; Furler *et al.*, 2001; Chinnasamy *et al.*, 2006).

In the present study, the 2A sequence was added to the C-terminus of eGFP and this was placed between the capsid and the p62 protein of SFV4. During replication of this virus and following protein synthesis the eGFP protein should be released free by the activities of the flanking capsid protease and the 2A sequence. SFV4-steGFP

had a slight delay in its replication in BHK-21 cells compared to the parental SFV4. In a similar way to the viruses described in Chapter 3 virus replication caught up with the wild-type virus titres. The delay in replication is probably due to the increased size of the genome, which needs longer time to be replicated and transcribed and delayed production of properly processed viral structural proteins. Western blotting on cell lysates from SFV4-steGFP infected BHK-21 cells (Figure 4.3) showed that the 2A mediated cleavage was not 100% efficient and that an eGFP-2A-p62 fusion protein was present. Given the presence of this fusion protein, which most probably cannot be packaged into new infectious viral particles, SFV4-steGFP may produce correctly processed glycoproteins more slowly than SFV4; this could explain the delay in early replication as assessed by infectious virus production of SFV4-steGFP in the one-step growth curve. Another factor that could contribute to the delayed replication of SFV4-steGFP is reduced production of viral glycoproteins due to termination of translation after 2A. It has been shown in experiments using *in vitro* polyprotein expression systems that proteins at the N-terminus of 2A are found in greater abundance than proteins at its C-terminus (Donnelly *et al.*, 2001b). In FMDV the replicase proteins are downstream of the 2A sequence and the structural proteins upstream. The current hypothesis is that late in infection structural protein synthesis is favoured over replicase protein synthesis and that 2A regulates this process (personal communication with Dr Martin Ryan). This hypothesis is logical since late in infection virus does not need non-structural proteins but it does need large amounts of structural proteins to form new virions. If 2A carried over this property when placed between eGFP and p62 expression of the viral glycoproteins would be reduced and fewer infectious viral particles would be released from each cell giving rise to the observed slower replication rate. In contrast to SFV4-steGFP which caught up with the SFV4 titres, the very similar SV denoted GFP/2A had approximately 100-fold lower yields in BHK-21 cells compared to its parental virus SV TR339 (Thomas *et al.*, 2003). Although insertion of genes in the structural ORF of alphaviruses has an effect on their replication efficiency, studies suggest that this is milder compared to the effect observed in the replication of recombinant viruses with duplicated subgenomic promoter because in these constructs the two promoters compete for viral replication complexes (Raju & Huang, 1991).

Cytopathic effect (CPE) in BHK-21 cells infected with SFV4 is usually observed around 24 hours post-infection and cell lysis is complete at approximately 48 hours (Vaha-Koskela *et al.*, 2003). BHK-21 cultures infected with SFV4(3H)-eGFP or SFV4(3L)-eGFP developed CPE in an identical way. In contrast, CPE was delayed in BHK-21 cultures infected with SFV4-steGFP. The delay in the appearance of CPE could be linked to reduced production of viral glycoproteins by this recombinant virus. Studies with SV have shown that strains of SV that synthesise high levels of structural proteins cause CPE more rapidly than strains which synthesise lower levels of these proteins (Frolov & Schlesinger, 1994a). In C6/36 cells from *Aedes albopictus* no CPE was observed after infection with SFV4, SFV4(3H)-eGFP or SFV4-steGFP. This was expected since many alphaviruses including SFV and SV have previously been reported to persistently infect these cells (Davey & Dalgarno, 1974; Karpf *et al.*, 1997b). Rat hippocampal neurons infected with the same viruses developed CPE at the same time post-infection. This might suggest that high levels of eGFP expression were possibly toxic for these neuronal cultures; eGFP has been previously reported to trigger apoptosis in cultured mouse cortical neurons (Detrait *et al.*, 2002). Like SFV, SV is also able to infect neurons *in vitro* and cause CPE (Glasgow *et al.*, 1997; Vernon & Griffin, 2005). Recently many vectors with reduced cytotoxicity in neurons have been constructed (Ehrengruber *et al.*, 1999; Kim *et al.*, 2004). Thomas *et al.* (2003) report that SV GFP/2A induces CPE in BHK-21 cells but do not provide any further information.

In terms of eGFP expression, in all cell types tested (BHK, C6/36 & rat hippocampal neurons), SFV4-steGFP was superior to both the recombinant viruses expressing eGFP as a cleavable component of their replicase polyprotein. *In vitro*, expression was long lasting and the fluorescent signal was very strong. *In vivo*, eGFP expression was much more widespread with SFV4-steGFP compared to SFV4(3H)-eGFP and almost all infected cells (assessed by immunostaining for nsP3 and viral structural proteins) were eGFP-positive whereas for SFV4(3H)-eGFP the rapid degradation of eGFP resulted in expression only in recently infected cells. In neurons, the higher levels of expression from the SFV4-steGFP virus allowed visualisation of neuronal processes. Strong expression of eGFP was not surprising. Multiple *in vitro* and *in vivo* studies using alphaviruses or alphavirus-based vectors expressing eGFP under

the control of the subgenomic promoter have shown very high levels of prolonged expression of this particular marker protein both *in vitro* and *in vivo*. Examples include SFV, SV, VEE and chikungunya viruses (Thomas *et al.*, 2003; Vaha-Koskela *et al.*, 2003; Sato *et al.*, 2004; Kim *et al.*, 2004; Gehrke *et al.*, 2005; Vanlandingham *et al.*, 2005).

An interesting observation was that in BHK-21 cells infected with SFV4-steGFP, the eGFP signal was cytoplasmic and large amounts were perinuclear, possibly at the endoplasmic reticulum. This is in contrast to what was observed in BHK-21 cells infected with SFV and SV viruses expressing eGFP either as a part of the non-structural ORF or under the direct control of a duplicated subgenomic promoter (Lundstrom *et al.*, 2003; Frolova *et al.*, 2006; Tamberg *et al.*, 2007; Atasheva *et al.*, 2007). In these studies eGFP is distributed evenly throughout the cytoplasm and the nucleus of the infected cells. Possible explanations for this interesting observation are given below.

During the normal course of infection by an alphavirus, the capsid protein is self-cleaved (co-translationally at its C-terminus like the 2A sequence) from the following polyprotein which is subsequently translocated to the endoplasmic reticulum by the emerging signal sequence in p62 (Bonatti & Blobel, 1979; Melancon & Garoff, 1986; Garoff *et al.*, 1990; Strauss & Strauss, 1994). Many polyproteins of RNA viruses have internal signal sequences that facilitate their translocation to the ER and processing of the polyprotein (Melancon & Garoff, 1986; Fazakerley & Ross, 1989; Wu, 2001). As shown by western blotting, the 2A-mediated cleavage is not 100% efficient and an eGFP-2A-p62 fusion protein is also synthesised. If the signal sequence (ss) of p62 is active internally it would transfer and anchor the eGFP-2A-ss-p62 fusion polypeptide to the ER (eGFP being on the cytosolic side), signalise processing would release p62 but the eGFP-2A-ss would remain anchored in the ER membrane. This would explain the high concentration of the eGFP signal around the nucleus. Nuclear exclusion of eGFP could also be attributed to its increased size (by the addition of the 2A and p62 sequences at the C-terminus); eGFP does not have a nuclear localisation signal, it diffuses passively to the nuclei of cells in which it is expressed due to its small size (Miron *et al.*, 2004).

Functionality of the 2A sequence may be cell type specific because in C6/36 cells and in rat hippocampal neurons eGFP was present in both the cytoplasm and the nucleus of the infected cells. The difference between these cells and BHK-21 cells could be explained as follows. If protein synthesis of the structural polyprotein stops after the 2A sequence and not even the p62 signal sequence is synthesised, eGFP would be released from the ribosomes into the cytoplasm and it would be free to diffuse into the nucleus. Functionality of the 2A sequence may also depend on the presence or absence of host defence responses; BHK-21 cells do not have a type-I IFN system whereas neurons do, or even on differentiation states or cell cycle of individual cell types.

The data of the present study is consistent with that of Thomas *et al.* (2003). Cells infected with SV GFP/2A exhibited cytoplasmic fluorescence in BHK-21 cells. Also eGFP-positive cells were observed in the brains of CD-1 mice infected subcutaneously with this virus. However, no pictures showing eGFP expression in cells or tissues were shown in the Thomas study so the precise localisation of the eGFP signal is not clear.

The genetic stability of SFV4-steGFP was assessed both *in vitro* in BHK-21 cells and *in vivo* after serial passaging in the brain of adult Balb/c mice. *In vitro*, SFV4-steGFP showed low genetic stability. No eGFP-positive viruses were detected after five passages in BHK-21 cells whereas more than 90% of SFV4(3H)-eGFP viruses and 50% of SFV4(3L)-eGFP viruses were able to express eGFP after five passages in the same cell line. Possibly, insertion of a foreign gene in the structural ORF imposes greater stress on virus replication (deficient particle formation) and thus it is eliminated more quickly. Like SFV4(3H)-eGFP, SFV4-steGFP was very stable *in vivo* and therefore suitable for pathogenesis studies. The difference between the *in vitro* and *in vivo* genetic stability of SFV4-steGFP can probably be attributed to the amount of virus passaged, which in the case of the brain serial passaging is much lower than for BHK-21 cells. In addition, BHK-21 cells do not have an active interferon system and therefore more viruses are produced in each passage whereas the functional IFN system of the mouse suppresses the uncontrolled production of new viral particles and therefore delays the growth of eGFP-negative viruses, which upon their appearance quickly outnumber the eGFP carrying viruses due to their

replication advantage (smaller genome and thus faster replication). In the study of Thomas *et al.* (2003) eGFP expression was maintained for at least 10 passages in BHK-21 cells. However, the M.O.I used in that study was higher and the method employed to assess expression stability not as sensitive as the method used here. It seems that eGFP is better tolerated between capsid and p62 protein in the SV than in the SFV genome.

Alphavirus replication is cytoplasmic and occurs on the surface of membranous structures of endosomic and lysosomic origin called cytoplasmic vacuoles (CPVs) (Froshauer *et al.*, 1988). On the surface of CPVs invaginations called spherules are located. In these spherules the viral replication complexes are anchored and RNA synthesis takes place (Grimley *et al.*, 1968; Kujala *et al.*, 2001; Salonen *et al.*, 2003). As with SFV4(3H)-eGFP and SFV4(3L)-eGFP, when anti-nsP3 antibody was used to immunostain BHK-21 cells infected with SFV4-steGFP typical punctate staining corresponding to the position of the replication complexes was observed. Surprisingly, when SFV4-steGFP infected cells were immunostained with an antibody targeting the viral structural proteins only a fraction of the infected cells stained positive for these proteins although 100% of the cells in culture were eGFP-positive indicating that the structural ORF was translated at least as far as eGFP. In addition, the observation appears to be specific for BHK-21 cells because in infected brain sections stained with the same antibody virtually all eGFP-positive cells were also positive by immunostaining. The 2A sequence has previously been shown to be functional in BHK-21 cells (de Felipe *et al.*, 1999). Possibly the 2A sequence used in SFV4-steGFP has reduced efficiency in BHK-21 cells. That some SFV4-steGFP infected, eGFP-positive cells stained positive for virus structural proteins and some did not is intriguing and could also be attributed to differential functionality of the 2A sequence at different times of the cell cycle.

SFV4-steGFP was used to infect immunocompetent mice intraperitoneally. Previous studies (Chapter 3) have shown that SFV4 and SFV4-based recombinant viruses are poorly neuroinvasive and SFV4-steGFP was not different. The poor neuroinvasiveness of SFV4 was attributed to the low level plasma viraemia. In contrast to mice infected with SFV4 and SFV4(3H)-eGFP that had low but detectable titres of virus in their blood, mice infected with SFV4-steGFP had no

detectable virus in their blood. This finding suggests that insertion of eGFP-2A further attenuated SFV4. Perhaps problematic packaging delayed virus production sufficiently for host defences to then prevent a productive infection.

The protective effect of type-I interferon (IFN) against the spread of viral infection in the murine CNS has been shown for many viruses including Dugbe, Sindbis, and Venezuelan equine encephalitis virus (Grieder & Vogel, 1999; Ryman *et al.*, 2000; Boyd *et al.*, 2006). The importance of the type-I IFN system is further shown by the fact that avirulent strains of viruses establish widespread infections in mice lacking an intact IFN system (Mrkic *et al.*, 1998; Ryman *et al.*, 2000; Bray, 2001). When SFV4(3H)-eGFP was used to infect IFN α/β knockout mice, eGFP was visible only in the pancreas and the spleen of these mice. In contrast, when the same strain of mice was infected with SFV4-steGFP, fluorescent signal was visible in most peripheral tissues (heart, spleen, pancreas, kidney, adipose tissue and lung) and in the brain. This result could be explained by the 42S genomic promoter being less active in some cell types than in others. Further studies are however required to verify this hypothesis. Interestingly, SFV4-steGFP exhibited a selective cellular tropism. For example, cells of the exocrine but not the endocrine pancreas were heavily infected. Similarly, in the heart many cells of the heart valves were infected compared to few cells of the myocardium. SFV and SV are known to infect cells of the heart *in vitro* and *in vivo* (Dätwyler *et al.*, 1999; Loot *et al.*, 2004). Other viruses are also known to infect the heart and especially the valves, examples include enteroviruses in mice and patients with chronic rheumatic heart disease (Burch *et al.*, 1966; Li *et al.*, 2002). In the spleen most infected cells were found at the marginal zone between the red pulp and the white pulp (most likely macrophages). In a study by Ryman *et al.* (2000) IFN α/β knockout mice infected with SV showed similar distribution of virus in the spleen and these cells were shown to be cells of the macrophage/dendritic lineage. The magnitude of the effect that the IFN system exerts on viral replication was seen when immunocompetent mice infected with SFV4-steGFP were examined. No sign of eGFP expression was evident despite examination of many sections. The IFN system appears to be capable of powerfully suppressing alphavirus replication and in the absence of a functional IFN system the true tropism and the potential of SFV4-steGFP was revealed.

The attenuating effect that insertion of eGFP at this position of the genome has in the virus was further proven following i.p. inoculation of IFN α/β knockout mice. The virus reached approximately 100-fold (2 Log_{10} PFU/ml) lower titres in the blood of these mice compared to SFV4 and SFV4(3H)-eGFP. This result suggests that factors other than type-I IFN may contribute to the control of the peripheral replication of SFV.

As with SFV4 and recombinant viruses which express eGFP as part of their replicase ORF, SFV4-steGFP was virulent when administered directly into the brain of mice. However, these mice survived one day longer than mice inoculated i.c. with SFV4; suggesting that neurovirulence of SFV4-steGFP was affected by the insertion of eGFP. As mentioned before, determinants of neurovirulence for alphaviruses lie in both the non-structural and the structural ORFs as well as on the 5' and 3' NTR (Kuhn *et al.*, 1992; Tuittila *et al.*, 2000; Galbraith *et al.*, 2006). In the structural region of the genome determinants of neurovirulence are located in the E1 and E2 proteins (Lustig *et al.*, 1988; Glasgow *et al.*, 1991; Santagati *et al.*, 1995; Tucker *et al.*, 1997). It is reminded that eGFP-2A is inserted directly upstream the E2 protein (p62) and it appears that 2A cleavage is not 100% efficient as eGFP-2A-p62 fusion protein is detected by western blotting. Slower processing of the structural polyprotein probably delays the formation and budding of viral particles and therefore attenuates the neurovirulence of SFV4-steGFP.

Cell tropism of SFV4-steGFP was not altered compared to SFV4. Infection of neurons and oligodendrocytes but not of astrocytes was evident. The cell tropism observed has been previously reported for SFV4 and SFV A7(74) (Balluz *et al.*, 1993; Fazakerley *et al.*, 2006). When SFV4(3H)-eGFP was used to infect mice i.c. no double-labelled neurons were found (eGFP and NeuN neuronal marker). The situation was totally different when mice were inoculated with SFV4-steGFP and a large percentage of the infected cells was found to be neurons (were both eGFP and NeuN-positive). The hypothesis that the 42S genomic is switched off more rapidly in some cell types is reinforced by this result.

Although slightly attenuated, SFV4-steGFP is suitable for *in vivo* pathogenesis studies. Expression of eGFP is strong and long lasting and the virus infected all tissues and cell types previously known to be infected by SFV4. The use of SFV4-

steGFP will simplify pathogenesis studies since it abolishes the requirement for double immunostaining. Furthermore, the virus can be used together with SFV4(3H)-eGFP to examine events at early and late stages of infection. Possibly a virus expressing a different marker (DSRed for example) or a virus expressing two different fluorescent proteins, one from the replicase and one from the structural ORF, can be engineered to facilitate such studies.

Chapter 5: SFV vectors expressing Cre recombinase

Contents

Introduction

In order to avoid recognition and elimination by the immune system and establish a persistent infection, viruses have evolved numerous evasive mechanisms. Among the most successful strategies for immune evasion is the infection of areas with limited surveillance by the immune system, so-called immunoprivileged sites. One such site, which is the target for many viral infections, is the central nervous system (CNS) (Cserr & Knopf, 1992; McGavern *et al.*, 2002). The factors that contribute to make the CNS an immunoprivileged site are the low levels of MHC expression, and the presence of the blood brain barrier (BBB), which excludes serum antibodies, complement proteins and lymphocytes (Cserr & Knopf, 1992; Fabry *et al.*, 1994). However, upon infection activated B and T cells and large amounts of intrathecal antibody are present in the CNS (Morris *et al.*, 1997; Pachner *et al.*, 2007). The unique immune responses of the CNS allow the persistence of many RNA viruses including Borna, Theiler's murine encephalomyelitis, mouse hepatitis, lymphocytic choriomeningitis and measles viruses (Schneider-Schaulies *et al.*, 1993; Rodriguez *et al.*, 1996; Matthews *et al.*, 2001; de la Torre, 2002).

In rodents with deficiencies in immune responses, alphaviruses are able to establish persistent infections. Examples include Ross river virus (RRV), Venezuelan equine encephalitis virus (VEEV), Sindbis virus (SV) and Semliki Forest virus (SFV) (Levine *et al.*, 1991; Linn *et al.*, 1996; Fazakerley, 2002; Navarro *et al.*, 2005). Persistence of SFV and SV in the CNS has been studied extensively. In the brain of immunocompetent mice, infectious SFV and SV are cleared within 7 – 8 days post-inoculation (Johnson *et al.*, 1972; Amor *et al.*, 1996). In mice with severe combined immunodeficiency (SCID) both SFV and SV can persist for long periods of time in the CNS (Levine *et al.*, 1991; Ubol *et al.*, 1995; Fazakerley, 2002). Passive transfer of hyperimmune serum (HI) has been shown to clear infectivity but when administration of HI serum is withdrawn infectivity returns suggesting that antibody responses are important to control virus persistence (Levine *et al.*, 1991; Levine & Griffin, 1992; Dixon, 2007, PhD thesis). SFV infection of athymic *nu/nu* mice results in a lifelong persistent infection of the CNS (Fazakerley & Webb, 1987; Atkins *et al.*, 1999). SFV and SV are also known to persist *in vitro* in mammalian and insect cells

(Meinkoth & Kennedy, 1980; Dryga *et al.*, 1997; Karpf *et al.*, 1997a). In terms of RNA persistence, numerous studies have shown that the RNA of both SFV and SV can persist in the CNS of immunocompetent and immunocompromised mice for long periods of time (Levine & Griffin, 1992; Donnelly *et al.*, 1997).

Regulation of alphavirus persistence appears to be multi-factorial but the nature of this persistent infection is not clear. The virus may persist in the same cell for many months or virus infection in any individual cell could be cleared after time and other cells infected. Clearance of the virus could be cytotoxic or non-cytotoxic. Depending on the mechanism of clearance the fate of infected cells, especially of long-living cells like neurons would be determined.

In the present study, a system with the potential to clarify the fate of neurons following infection by an RNA virus was utilised; the Cre-*LoxP* system. Cre-*LoxP* is a widely used method of conditional mutagenesis (Nagy, 2000; Morozov *et al.*, 2003), which utilises the properties of Cre recombinase, a 38 kDa protein of the integrase family naturally found in bacteriophage P1. Cre recombinase has the ability to recognise a 34 bp long consensus sequence (*LoxP*) and facilitates the recombination between two *LoxP* sites. Depending on the orientation of the *LoxP* system the outcome of recombination is different; the possibilities are excision and inversion (Voziyanov *et al.*, 1999; Aranda *et al.*, 2001; Ghosh & Van Duyne, 2002; Lee & Sadowski, 2003). Early studies have shown that Cre recombinase is also functional in mammalian cells (Sauer & Henderson, 1988; Sauer & Henderson, 1989). The system has been extensively used for developmental studies in mice using conditional transgene activation or inactivation including studies on neuronal development in the brain (Hirasawa *et al.*, 2001; Adams *et al.*, 2003; Morozov *et al.*, 2003). In most studies, two mouse strains, one with the gene of interest flanked by two *LoxP* sites and another which expresses Cre recombinase only in the cells of interest under the control of a specific promoter (for example a brain region-selective promoter), are bred and the outcome of Cre-mediated recombination is visible in the offspring (Kilby *et al.*, 1993; Tsien *et al.*, 1996). An alternative approach for the delivery of Cre recombinase in the CNS is the use of viral vectors. To date Cre delivery vectors have been constructed based on adenovirus, adeno-associated virus, retroviruses, feline immunodeficiency virus (FIV) and herpes virus (Brooks *et al.*,

2000; Kaspar *et al.*, 2002; Ahmed *et al.*, 2004; Sinnayah *et al.*, 2004; Tashiro *et al.*, 2007).

The hypothesis to be tested was that infection of SFV carrying Cre recombinase in Cre-reporter mice would result upon infection in permanent marking of infected cells and that the nature of the CNS infection could be determined by observing whether all marked cells contained virus (proteins or RNA). Marked cells containing no trace of virus would indicate that cells, perhaps neurons which are relatively resistant to apoptosis can eliminate the infection and survive (Fazakerley & Allsopp, 2001). All marked cells containing virus would indicate that cells either cannot eliminate the infection on that they cannot do so without dying. It is a fundamental unanswered question in virology; can infected cells *in vivo* eliminate a virus infection and survive?

In the present study, novel SFV-based viruses and virus-like particles (VLPs) carrying Cre recombinase were constructed. The Cre gene was inserted, as a cleavable component, in two different positions in the SFV4 genome; the non-structural or the structural ORF. The viruses were characterised *in vitro* and *in vivo* and used to infect Cre-reporter mice.

Objectives

The objectives of this study were:

- To construct viruses expressing Cre as a cleavable component of the non-structural or the structural ORF of SFV and investigate if the insertion of euCre has an effect on the replication efficiency of the virus.
- To examine the effect of the Cre insertion on the *in vitro* and *in vivo* virulence of SFV4.
- To assess the phenotypic and genotypic stability of recombinant viruses *in vitro* and *in vivo*.
- To evaluate the suitability of the recombinant viruses for *in vivo* pathogenesis studies using Cre-reporter mice.
- To assess the status of the CNS infection by determining whether marked cells always contain viral material.

Construction of recombinant viruses and VLPs expressing Cre recombinase

Recombinant viruses used for this project were constructed by Professor Andres Merits at the Estonian Biocentre. The three novel replicating vectors expressing foreign proteins as a cleavable component of the non-structural (pSFV4(3L) and pSFV4(3H)) and the structural (pSFV4-st) ORF described in Chapter 3 and Chapter 4 of this thesis respectively were used to express Cre recombinase. A plasmid expressing Cre recombinase with a nuclear localisation signal and modified for optimal expression in eukaryotic cells (denoted euCre in this chapter) was kindly donated by Dr Andras Nagy (Mount Sinai Hospital, Toronto). The fragment of the plasmid corresponding to euCre was amplified using primers incorporating *Apa*I and *Bgl*II adapter sites (shown in the materials and methods chapter). The three vectors, pSFV4(3L), pSFV4(3H) and pSFV4-st were digested with *Apa*I and *Bam*HI whereas the euCre insert was digested with *Apa*I and *Bgl*II (producing compatible ends with *Bam*HI). The insert was then ligated into position using T4 DNA ligase. The resulting constructs were designated pSFV4(3H)-euCre, pSFV4(3L)-euCre and pSFV4-steuCre. Using the method described by Liljestrom *et al.* (1991) infectious viruses were produced from the icDNA clones. These newly made viruses were annotated SFV4(3H)-euCre, SFV4(3L)-euCre (Figure 5.1a) and SFV4-steuCre (Figure 5.1b). Another infectious virus expressing euCre as a cleavable component of the structural ORF was constructed. The only difference in this virus compared to SFV4-steuCre was a single amino acid change at the nuclear localisation signal of nsP2 which consists of three consecutive arginine residues (RRR). During infection 50% of nsP2 protein localises in the nucleus of infected cells. Mutation of the nuclear localisation signal of nsP2 from RRR to RDR leads to the production of an avirulent virus (Rikkonen *et al.*, 1992). This mutant virus expressing euCre was annotated SFV4-RDR-steuCre.

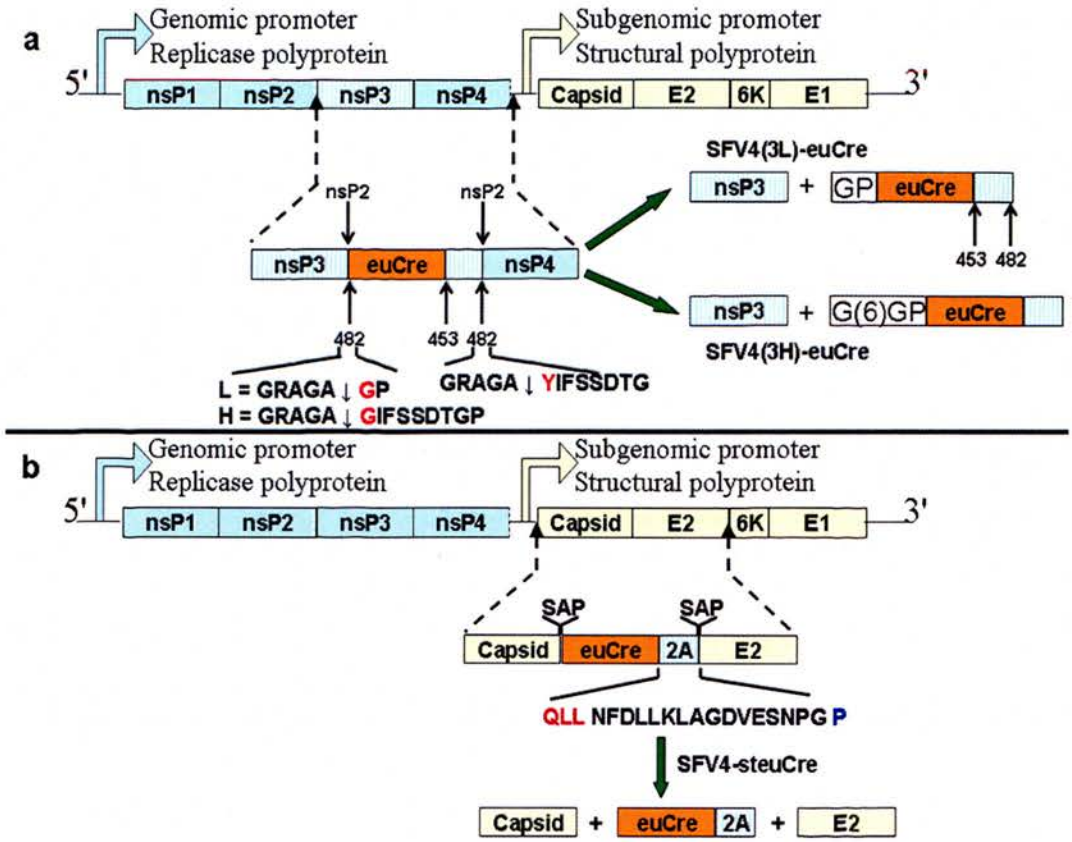

Figure 5.1. Schematic representation of euCre expressing replicating vectors. (a). SFV4(3L)-euCre and SFV4(3H)-euCre, construction and predicted processing of the non-structural polyprotein. The amino acid sequence, the position of both the artificial and the native nsP2 protease recognition sites and the 30 amino acids (453-482) from the C-terminus of nsP3 which were fused at the C-terminus of euCre are shown. Tyrosine residue in the native cleavage site and glycine residue in the artificial sites are shown in red. In the predicted processing of SFV4(3H)-euCre, (6) corresponds to the IFSSDT sequence. The proline (P) residue at the end of both L and H constructs is the result of the insertion of *Apa*I restriction site. **(b).** Construction and predicted processing of the structural polyprotein in SFV4-steuCre. The first three N-terminal amino acids of p62 protein (E2) were duplicated upstream of the euCre gene. A 16 amino acid long FMDV 2A protease flanked by three amino acids (red) from the C-terminus of FMDV 1D protein and the N-terminal proline, which is essential for efficient cleavage, (blue) from FMDV 2B protein, was fused to the C-terminus of euCre. Following expression of the structural ORF, all structural proteins and euCre with the 2A sequence fused to its C-terminus were expected to be released free.

To construct virus like particles (VLPs) expressing euCre, the coding sequence of euCre was amplified using primers incorporating a *Bgl*II restriction site at the 5' end of the gene and a *Sma*I restriction site at its 3' end. The amplified product was blunt-ended and inserted into a commercial vector in order to be sequenced. Sequencing showed that the product had no incorporated errors and that it was suitable for further experiments. The SFV replicon plasmid (pSFV1, Figure 5.2a) was digested with *Bam*HI and *Sma*I restriction endonucleases and the euCre insert was digested with *Bgl*II and *Sma*I. The two fragments were ligated using T4 DNA ligase and the resulting construct was annotated pSFV1-euCre (Figure5.2b). Correct insertion of the euCre gene was verified by restriction analysis. To generate VLPs, pSFV1-euCre and pHelper plasmid were linearised, *in vitro* transcribed and the two RNAs co-electroporated in BHK-21 cells. Expression of euCre was verified by western blotting (Figure 5.4).

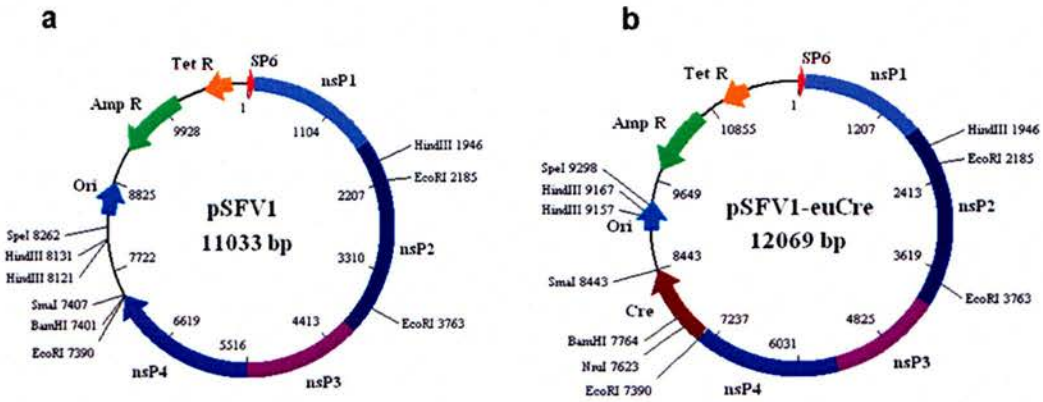

Figure 5.2. Schematic representation of pSFV1 and pSFV1-euCre. (a). plasmid map of pSFV1 vector. **(b).** plasmid map of pSFV1-euCre.

Virus viability and replication efficiency following insertion of Cre recombinase gene into the non-structural and the structural ORFs of SFV4.

Experimental design

To assess the effect of euCre insertion on virus viability and replication efficiency, BHK-21 cells were infected with SFV4, SFV4(3H)-euCre, SFV4-steuCre or SFV4-RDR-steuCre at a multiplicity of infection (M.O.I) of 10 in triplicate and virus replication was compared in a one-step growth curve. Parallel cultures of BHK-21 cells were infected to investigate the effect of euCre insertion on the *in vitro* virulence of SFV4 and the induction of cytopathic effect (CPE).

One-step growth curves

All viruses with euCre inserted in their genome were viable and able to replicate *in* vitro. However, one-step growth curves (Figure 5.3a) suggested that insertion of the euCre gene into either the non-structural or the structural ORF of SFV4 had a significant effect on replication efficiency. All viruses tested were able to infect BHK-21 cells but production of new infectious virus particles was significantly reduced compared to the parental virus ($P<0.05$). SFV4(3H)-euCre and SFV4-steuCre replicated in a very similar way and reached peak titres which were not significantly different ($P>0.05$). Both these viruses had significantly lower titres ($P<0.05$) compared to SFV4 throughout the 12 hours of the experiment.

Insertion of the coding sequence of euCre into the structural ORF of SFV4-RDR, which is a well characterised attenuated SFV strain, severely affected its growth efficiency. According to Rikkonen *et al.* (1992), SFV4-RDR replicates slower but reaches catches up with SFV4. SFV4-RDR-steuCre had significantly lower titres compared to SFV4 ($P<0.05$) throughout the experiment. In addition, its peak titres were also significantly lower compared to these of both SFV4(3H)-euCre and SFV4-steuCre ($P<0.05$). Titres at each time-point were compared using a paired t-test.

In vitro virulence and development of CPE in BHK-21 cells

Although all euCre expressing viruses had reduced growth rates compared to SFV4 no difference was observed in their *in vitro* virulence. Cultures of BHK-21 cells infected with SFV4, SFV4(3H)-euCre, SFV4-steuCre or SFV4-RDR-steuCre were dead by 48 hours post-infection (Figure 5.3c). At early time-points cells looked healthy and had the typical elongated morphology of BHK-21 cells with no signs of CPE (Figure 5.3b). Evidence of CPE was initially observed between 16-20 hours post-infection for SFV4 and SFV4(3H)-euCre. CPE induction was delayed when monolayers of BHK-21 cells were infected with SFV4-steuCre or SFV4-RDR-steuCre and it was first apparent approximately 36 hours post-infection for both viruses. To investigate if euCre was expressed, infected cells were fixed and immunostained using a specific anti-Cre antibody but all attempts at immunostaining were unsuccessful.

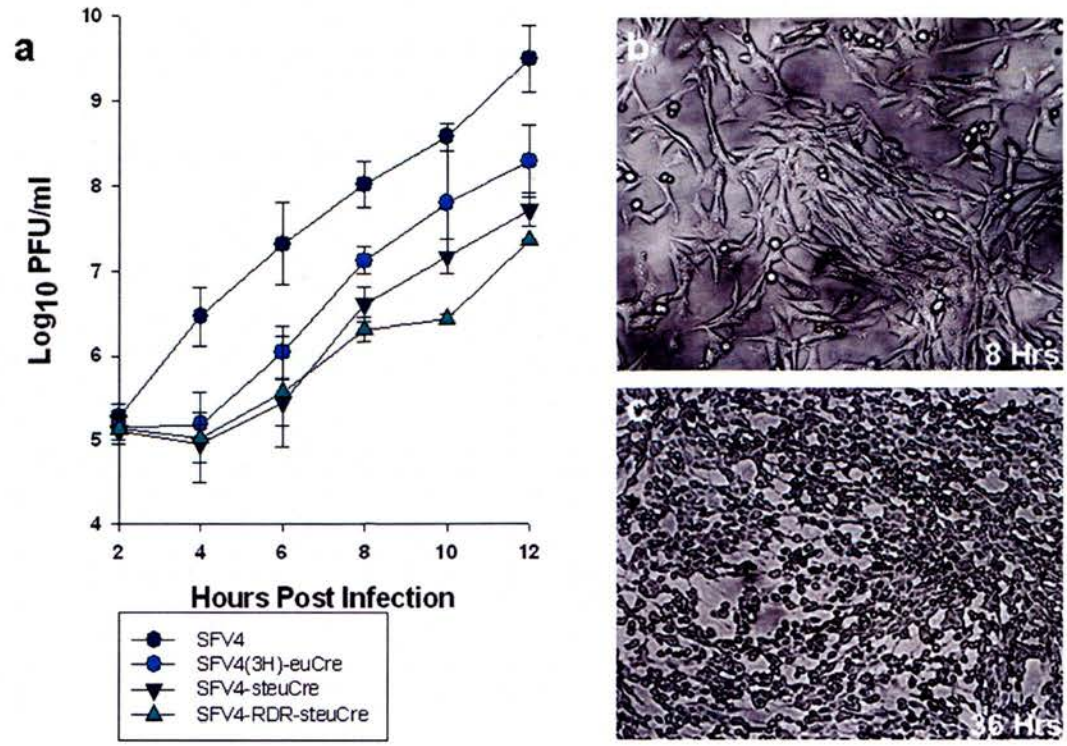

Figure 5.3. Growth curves and CPE following infection of BHK-21 cells with euCre expressing viruses. (a) Monolayers of BHK-21 cells were infected in triplicate with SFV4 (dark blue circles), SFV4(3H)-euCre (light blue circles), SFV4-steuCre (inverted dark blue triangles) or SFV4-RDR-steuCre (green triangle) at an M.O.I of 10. Supernatant samples were collected every 2 hours for 12 hours and titrated for infectious virus. Each point represents the mean of 3 samples. The bar represents the standard deviation (SD). All growth curves shown in this thesis were performed in parallel. The data for SFV4 presented in this figure is identical to that shown in Figures 3.2a and 4.2a allowing comparison of the growth of all recombinant viruses. **(b)** and **(c)** Images of BHK-21 cells infected with SFV4-steuCre virus at an M.O.I of 10 taken 8 and 36 hours post-infection, respectively. Early after infection **(b)** typical morphology of BHK-21 cells can be observed. All viruses used in this study caused cell death **(c)**. CPE was evident approximately 16-20 hours earlier for the viruses expressing euCre as part of their replicase ORF but in all cases most cells were dead by 48 hours post infection.

Expression of euCre protein from euCre expressing viruses and virus-like particles (VLPs)

Experimental design

To determine if recombinant viruses and virus-like particles (VLPs) were able to properly express euCre as a cleavable component of their replicase or structural ORFs, BHK-21 cells were infected with SFV4(3H)-euCre, SFV4(3L)-euCre, SFV-steuCre, SFV-RDR-steuCre or SFV1-euCre VLPs at an M.O.I of 20. PBSA was used as a negative control to mock-infect cells. After 6 hours, cells were lysed and samples corresponding to 100,000 cells were separated on an SDS-PAGE gel and proteins were transferred to a nitrocellulose membrane. An α-Cre antibody was used to detect Cre recombinase protein. Since SFV4(3H) and SFV4(3L) vectors were previously shown to express the viral non-structural proteins properly these western blottings were not repeated.

Expression of euCre in BHK-21 cells

All recombinant viruses and virus-like particles (VLPs) expressed euCre as can be seen in Figure 5.4. Processing of viruses expressing euCre as a cleavable component of the non-structural ORF appears to be very efficient and no bands corresponding to euCre-nsP4 fusion protein can be seen (Figure 5.4a). As expected expression under the control of the subgenomic promoter was very strong; the density of the bands corresponding to euCre is indicative of the amount of protein produced (Figure 5.4b & 5.4c). However, when cells were infected with SFV4-steuCre or SFV4-RDR-steuCre a strong band with higher molecular weight was observed. This band probably corresponds to an euCre-2A-p62 fusion protein suggesting that the efficiency of the 2A sequence is not optimal. This was also observed with SFV4-steGFP virus (Chapter 4; Figure 4.3).

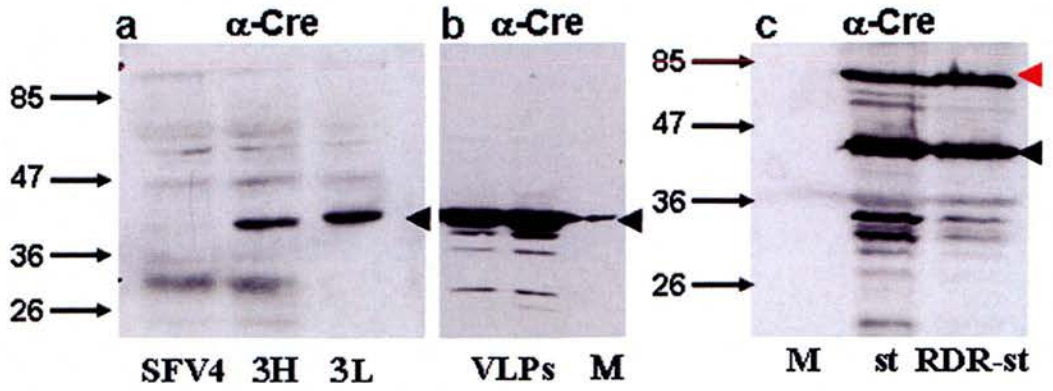

Figure 5.4. Expression of euCre by recombinant viruses and virus-like particles. **(a)** Western blotting of cell lysates of BHK-21 cells infected with SFV4, SFV4(3H)-euCre (**3H**) or SFV4(3L)-euCre (**3L**) (M.O.I 20). Specific bands of the appropriate molecular weight for euCre are shown with a black arrowhead. **(b)** Western blotting of cell lysates infected with euCre expressing VLPs or mock-infected with PBSA (**M**). Black arrowhead marks specific bands corresponding to euCre protein. **(c)** Western blotting of cell lysates of BHK-21 cells infected with SFV4-steuCre (**st**), SFV4-RDR-steuCre (**RDR-st**) or mock-infected with PBSA (**M**). euCre specific bands are shown with a black arrowhead. euCre-2A-p62 fusion protein is marked with a red arrowhead.

In vitro phenotypic and genotypic stability of SFV4(3H)-euCre, SFV4(3L)-euCre and SFV4-steuCre in BHK-21 cells

Experimental design

To examine whether the recombinant viruses maintained their ability to express euCre or if the inserted gene was eliminated after several passages *in vitro*, SFV4(3H)-euCre, SFV4(3L)-euCre or SFV4-steuCre were passaged 5 times in BHK-21 cells at an M.O.I of 0.01. Since euCre cannot be visualised a Cre reporter cell line was required to assess the phenotypic stability of the euCre expressing viruses. A mouse embryonic fimbroblast (MEF) cell line was made from ROSA26 Cre reporter mice. An additional Cre reporter cell line named K562-DSRed[eGFP] was kindly donated by Dr Peter Ponsaerts (Van den Plas *et al.*, 2003). This cell line constitutively expresses DSRed and upon Cre-mediated recombination expresses eGFP. More specifically, the coding sequence of DSRed is flanked by *LoxP* sites and is under the control of the CMV promoter. The stop codon at the end of DSRed gene prohibits expression of eGFP. Following Cre-mediated recombination, the DSRed coding sequence is removed and eGFP expression occurs. Both these cell lines were used to determine if euCre expressed by SFV recombinant viruses was functional. Genotypic stability of the euCre expressing viruses was performed using RT-PCR as previously described on the respective sections of Chapters 3 & 4 of this thesis.

Phenotypic stability of euCre expressing viruses

Initially, in order to establish if the Cre reporter ROSA26 MEFs and K562-DSRed[eGFP] cells were functional, cells were electroporated with a euCre expressing plasmid, in which the expression of euCre is driven by a cytomegalovirus (CMV) promoter. ROSA26 MEFs were expected to express eGFP following Cre-mediated recombination but no sign of eGFP expression was observed in two consecutive experiments. In contrast, K562-DSRed[eGFP] cells expressed eGFP following electroporation of the euCre plasmid. Expression was first evident four days post electroporation of euCre expressing plasmid (Figure 5.5). Other groups in

the department have also tried to use MEFs obtained from ROSA26 mice unsuccessfully. For that reason it was decided to use K562-DSRed[eGFP] to investigate the functionality of euCre following expression by recombinant SFV viruses. However, infected cells died before reporting Cre-mediated recombination and it was not possible to assess phenotypic stability of euCre viruses using this cell line. The designers of this cell line have shown that optimal Cre-mediated DSRed excision occurs 5 days after electroporation with Cre recombinase mRNA (Van den Plas *et al.*, 2003), cells infected with euCre expressing viruses or VLPs were dead by 48 hours post-infection.

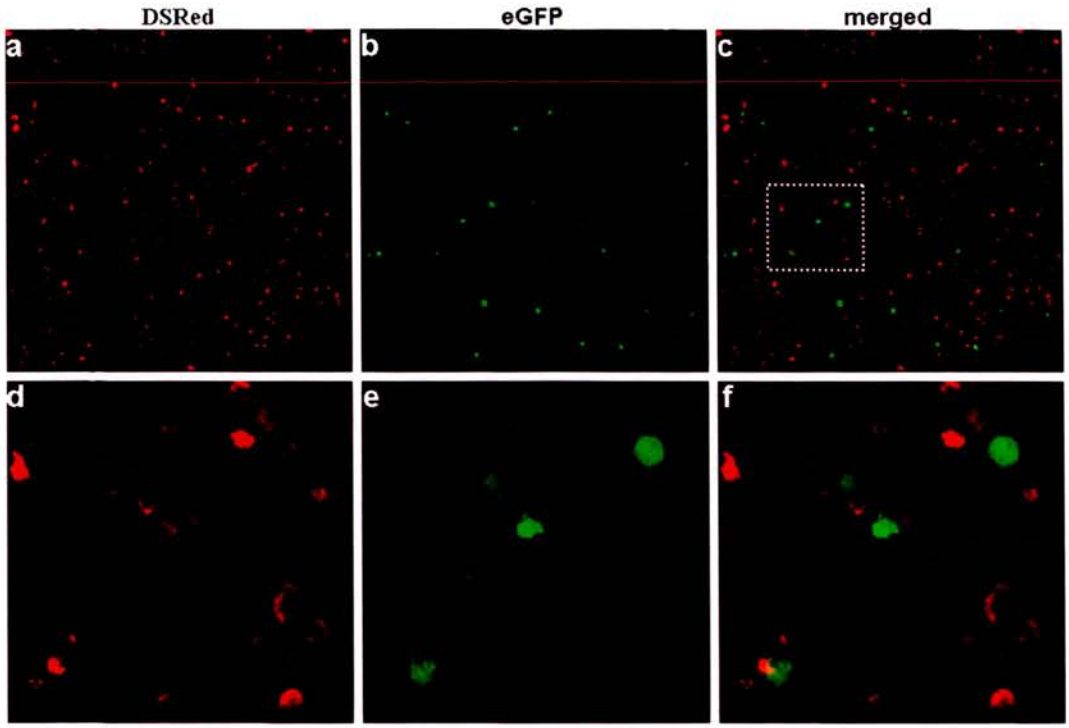

Figure 5.5. eGFP expression in K562-DSRed[eGFP] cells following Cre-mediated recombination. (a) K562-DSRed[eGFP] cells constitutively express DSRed, following Cre-mediated recombination DSRed gene is excised and eGFP is expressed **(b)** eGFP expressing K562-DSRed[eGFP] cells 4 days post electroporation with euCre expressing plasmid. **(c)** Merged image of **(a)** and **(b)** the area in the dotted square is shown in higher magnification in panels **d** – **f**. Note that eGFP expressing cells are not DSRed-positive. All images acquired using a Zeiss AxioSkop confocal microscope.

Genotypic stability of SFV4(3H)-euCre, SFV4(3L)-euCre and SFV4-steuCre

As previously described, RNA was extracted from virus infected BHK-21 cells and used for RT-PCR in order to determine how quickly the euCre expressing recombinant viruses were eliminating the euCre gene inserted in either the non-structural or the structural ORF of SFV. For the amplification, primers flanking the areas of the euCre insertion were used. The viruses expressing euCre as part of their replicase ORF would produce an amplicon with a size of approximately 1800 bp if the insert was intact. For the viruses expressing euCre as a cleavable component of the structural region the product corresponding to a virus with a complete euCre gene would have a size of approximately 1950 bp. If the insert was eliminated, the expected products would have sizes of approximately 670 bp and 826 bp, respectively.

When SFV4(3H)-euCre and SFV4(3L)-euCre were passaged in BHK-21 cells, the intensity of the band, and therefore the amount of PCR product corresponding to a virus with complete elimination of the euCre insert (~670 bp) increased gradually between the 2nd and the 5th passage. After the last passage, the amount of product corresponding to euCre-negative viruses exceeded that of euCre positive (~1800 bp). Although the density of the bands was not analysed it can be seen that elimination of the inserted sequence in both SFV4(3H)-euCre and SFV4(3L)-euCre progressed in a very similar way. In addition, it should be pointed out that after the 5th passage a percentage of the passaged viruses were still euCre positive and viruses with incomplete deletions had appeared (Figure 5.6a).

In contrast, elimination of euCre insert was more rapid when SFV4-steuCre was passaged in BHK-21 cells and euCre-positive viruses disappeared after the 4th passage. Bands corresponding to euCre-negative viruses were detected already after the 2nd passage. After the 3rd passage the amount of euCre-positive viruses (product of ~1950 bp) dramatically decreased and was much lower compared to the amount of euCre viruses. The multiple bands corresponding to viruses which have eliminated the euCre sequences suggest deletions of fragments with different sizes. All these deletions must have been in frame otherwise they would have been deleterious for the viruses. Notably, the elimination of euCre insert was not complete and some

small fragments of the inserted sequences remained intact even after the 5th passage (Figure 5.6b).

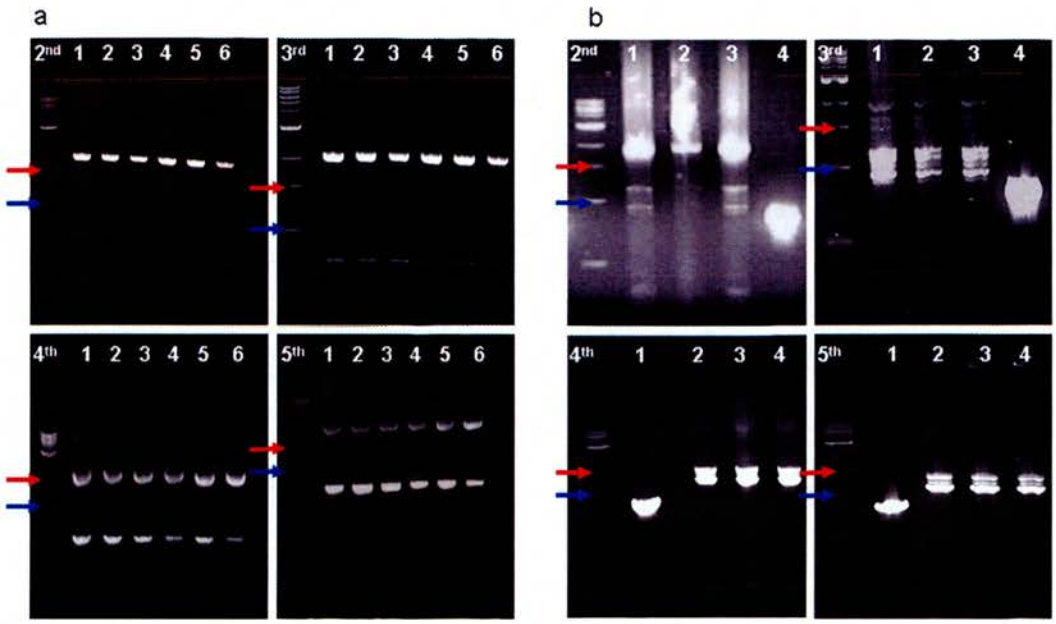

Figure 5.6. *In vitro* genotypic stability of euCre expressing viruses. (a) RT-PCR genotyping of virus RNA using nsP3 – nsP4 primers on RNA samples isolated from BHK-21 monolayers at passages 2, 3, 4 and 5; the passage number is indicated at the top left of each panel. In all panels, lanes 1 – 3 are the triplicate passages of SFV4(3H)-euCre and lanes 4 – 6 are the triplicate passages of SFV4(3L)-euCre. The red arrow corresponds to the 1.5 kb band of the DNA ladder and the blue arrow corresponds to the 1 kb band of the DNA ladder. **(b)** RT-PCR genotyping of SFV4-steuCre using capsid – E3 primers on RNA samples isolated fom BHK-21 monolayers at passages 2, 3, 4 and 5; the passage number is indicated at the top left of each panel. In the panels corresponding to 2nd and 3rd passage, lanes 1 – 3 are the triplicate passages of SFV4-steuCre and lane 4 is the SFV4-specific PCR product (positive control). In the panels corresponding to 4th and 5th passage, lanes 2 – 4 are the triplicate passages of SFV4-steuCre and lane 1 is the SFV4-specific PCR product (positive control). The red arrow corresponds to the 1.5 kb band of the DNA ladder and the blue arrow corresponds to the 1 kb band of the DNA ladder.

In vivo pathogenesis of euCre expressing viruses

To study the course of recombinant virus infection *in vivo* following intraperitoneal (i.p.) and intracerebral (i.c.) infection and compare it with that of wild type SFV4 infection two experiments were performed.

Experiment I-Assessment of in vivo virulence following i.p. and i.c. inoculation

Experimental design

To assess the virulence of euCre expressing viruses following i.p. inoculation, groups (n=10) of adult (4-5 week old female) Balb/c mice were inoculated i.p. with 5 x 10^3 PFU of SFV4, SFV4(3H)-euCre, SFV4(3L)-euCre, SFV4-steuCre, SFV L10 (virulent strain of SFV) or mock-infected with PBSA. Mice were kept for 10 days or until signs indicative of terminal disease were obvious.
To assess the virulence of euCre expressing viruses following i.c. inoculation, groups (n=10) of adult (4-5 week old female) Balb/c mice were inoculated i.c. with 1,000 PFU of SFV4, SFV4(3H)-euCre, SFV4-steuCre, SFV4-RDR-steuCre or mock-infected with PBSA. Mice were kept for 10 days or until signs indicative of terminal disease were obvious.

Results

Data on the survival of mice after inoculation via the i.p. or the i.c. route was used to plot survival curves (Figure 5.7). In Figure 5.7a the data obtained following i.p. inoculation is shown. All mice of the SFV L10 infected group were either dead or moribund on PID 3 and they were euthanised. None of the animals infected with SFV4, SFV4(3H)-euCre, SFV4(3L)-euCre or SFV4-steuCre exhibited signs of viral encephalitis and 100% of these animals survived throughout the 10 days of that experiment. Previous experiments described on Chapters 3 and 4 have shown similar results so this finding was expected. SFV4-RDR-steuCre was not included in this

study because it is known that the virus is avirulent following i.p. inoculation in adult mice (Rikkonen *et al.*, 1992).

In Figure 5.7b the data obtained following i.c. inoculation is plotted. Since SFV4(3H)-euCre and SFV4(3L)-euCre viruses appear to be very similar only the first one was used in this study. All animals infected with SFV4 or SFV4(3H)-euCre succumbed to infection on PID 2 having reached clinically defined terminal end-points indicative of substantial disease (limb paralysis and ataxia). Mice infected with SFV4-steuCre also died (100%) but one day later on PID 3. In contrast, all mice (10/10) infected with SFV4-RDR-steuCre survived the infection without any clinical symptoms. None of the PBSA mock-infected animals had any symptoms. At PID 10 this experiment was also terminated.

These results further illustrate the poor neuroinvasiveness of SFV4 and SFV4-based recombinant viruses and suggest that insertion of a foreign gene in the structural ORF has a more severe effect on the *in vivo* virulence of the virus than insertion of the same gene in the non-structural ORF.

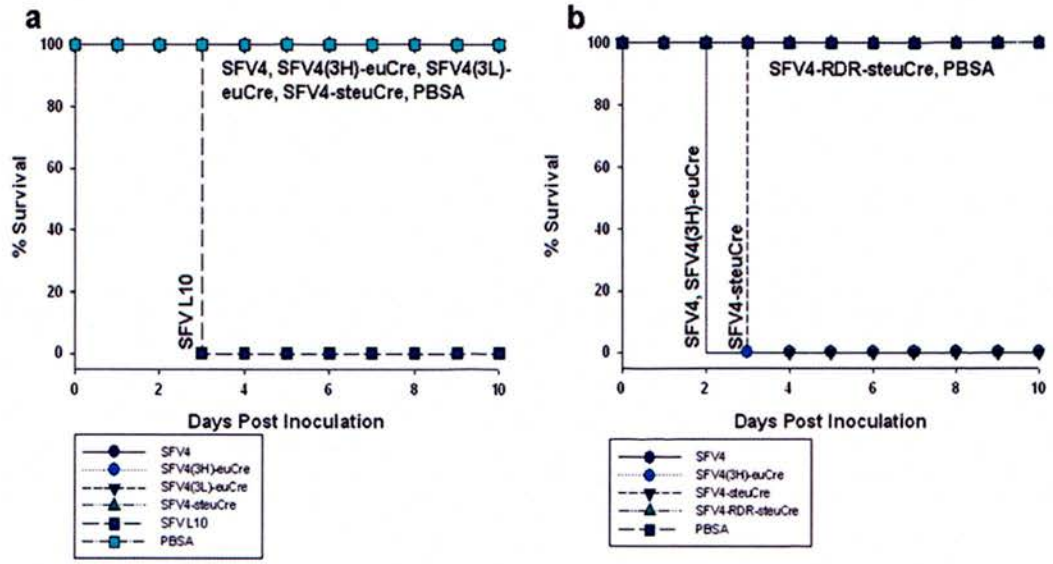

Figure 5.7. Survival rates of Balb/c mice following i.p. and i.c. inoculation with SFV. (a). Survival rates of mice (n=10) following i.p. inoculation. **(b).** Survival rates of mice (n=10) following i.c. inoculation.

Experiment II-Blood and brain virus titres following i.p. and i.c. inoculation

Experimental design

To examine if the recombinant viruses were able to establish a plasma viraemia, groups (n=6) of adult Balb/c mice (4-5 weeks old) were inoculated i.p. with 5 x 10^3 PFU of SFV4, SFV4(3H)-euCre, SFV4-steuCre, SFV A7(74), SFV L10 or mock-infected with PBSA. Twenty-four hours post-infection mice were euthanised and heparinised blood was collected and titrated for infectious virus.
Additionally, to compare the peak titres of the euCre expressing recombinant viruses in the brain of infected mice and to compare them with SFV4 groups (n=6) of adult Balb/c mice (4-5 weeks old) were inoculated i.c. with 1,000 PFU of SFV4, SFV4(3H)-euCre, SFV4-steuCre or mock-infected with PBSA. When the mice reached clinically defined terminal end-points indicative of substantial disease they were euthanised and their brains snap frozen for virus titration.

Results

Both SFV4 and SFV4(3H)-euCre were able to establish a low level plasma viraemia 24 hours post-inoculation. In both groups, 5 out of 6 mice (83.3%) had detectable levels of infectious virus. The average titre in SFV4 infected mice was 3.3 Log_{10} PFU/ml (SD: 1.4). The average titre for SFV4(3H)-euCre was 4.0 Log_{10} PFU/ml (SD: 1.0). In contrast, none of the animals infected with SFV4-steuCre had detectable levels of infectious virus at this time-point. When compared using paired t-test the titres of SFV4 and SFV4(3H)-euCre showed no significant statistical difference ($P>0.05$). Titration of blood samples from mice infected with avirulent SFV A7(74) or virulent SFV L10 showed that 100% of mice infected with these two viruses (6 in each group) had high levels of plasma viraemia. The average titres and the standard deviations were 7.2 Log_{10} PFU/ml (SD: 0.4) for SFV A7(74) infected mice and 6.6 Log_{10} PFU/ml (SD: 0.7) for SFV L10 infected mice. Statistical analysis using paired t-test showed no significant difference between the titres of SFV A7(74) and SFV L10 ($P>0.05$). Both these viruses had significantly higher titres to SFV4

and SFV4(3H)-euCre ($P<0.05$) (Figure 5.8a). The findings of this experiment suggest that insertion of euCre into the structural ORF had greater impact on the ability of the virus to replicate following extraneural infection than did insertion of euCre into the replicase ORF. This is probably due to delayed virus replication and problematic morphogenesis of virus infectious particles.

Following intracerebral inoculation of SFV4, SFV4(3H)-euCre and SFV4-steuCre all infected mice succumbed to infection exhibiting signs of viral encephalitis. However, SFV4-steuCre mice died a day later (PID 3) compared to the mice infected with SFV4 or SFV4(3H)-euCre. The infectious virus in the brains of the infected animals was titrated as close to the time of death of the animals to estimate the peak virus titres. SFV4 infected mice had an average infectious virus titre of 9.5 Log_{10} PFU/g of brain tissue (SD: 0.1). The average infectious virus titre in the brains of SFV4(3H)-euCre was 8.8 Log_{10} PFU/g of brain (SD: 0.4). Comparison by paired t-test showed that the peak titres of SFV4(3H)-euCre were significantly lower to the respective titres of SFV4 ($P<0.05$). SFV4-steuCre produced even lower peak titres compared to the other two viruses mentioned above. The average titre was 8.0 Log_{10} PFU/g; SD: 0.4. Paired t-tests showed that the peak titres of SFV4-steuCre infected brains were significantly lower compared to both SFV4 and SFV4(3H)-euCre ($P<0.05$), Figure 5.8b. These results indicate that insertion of euCre had a slight attenuating effect when inserted in the non-structural ORF. This effect was more severe when the gene was inserted into the structural region of the genome.

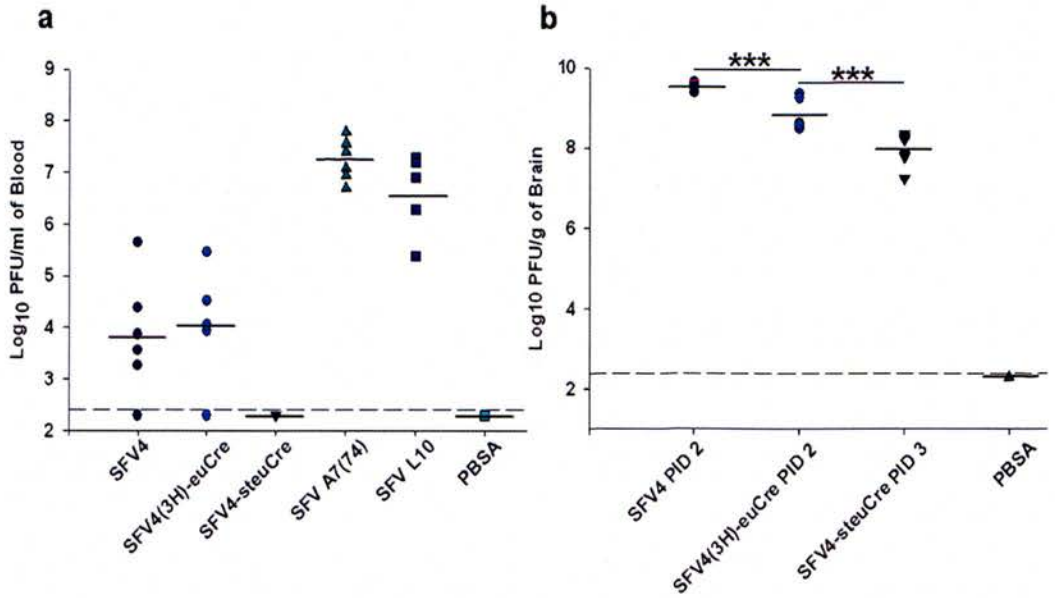

Figure 5.8. Comparison of plasma viraemia and brain virus titres caused by various SFV strains. (a) SFV4 (dark blue circle) and SFV4(3H)-euCre (light blue circle) had significantly lower titres than SFV A7(74) (green triangle) or SFV L10 (dark blue square) ($P<0.05$; paired t-test). SFV4 and SFV A7(74) were not significantly different to SFV4(3H)-euCre and SFV L10 respectively ($P>0.05$; paired t-test). All samples were collected at 24 hours after i.p. inoculation. **(b)** Following i.c. inoculation SFV4 (dark blue circle) had significantly higher peak-titres compared to both SFV4(3H)-euCre (light blue circle) and SFV4-steuCre (dark blue inverted triangle) ($P<0.05$; paired t-test). SFV4-steuCre titres were significantly lower compared to these of SFV4(3H)-euCre ($P<0.05$; paired t-test)

In vivo genotypic stability of Cre expressing viruses in Balb/c mice

Experimental design

To determine the genetic stability of SFV4(3H)-euCre and SFV4-steuCre after several passages *in vivo*. The viruses were passaged 5 times through the brain of Balb/c mice and examined for genotypic changes after each passage using RT-PCR. Phenotypic stability was not examined due to the absence of a valid system for that kind of experiment.

Genotypic stability of SFV4(3H)-euCre and SFV4-steuCre in vivo

Total RNA was extracted from the brains of the infected animals and used for RT-PCR to examine the genetic stability of SFV4(3H)-euCre and SFV4-steuCre after serial passaging. SFV4(3H)-euCre showed remarkable stability and only minor amounts of euCre-negative virus (indicated by a ~670 bp band) were present after the 5^{th} passage (Figure 5.9a). In contrast, SFV4-steuCre exhibited high instability. After the 3rd passage no recombinant virus with a euCre insert was detectable by RT-PCR. The detectable product had a slightly larger molecular mass compared to the product obtained by amplification of the same region of the SFV4 genome (~826 bp band) suggesting incomplete removal of inserted sequence.

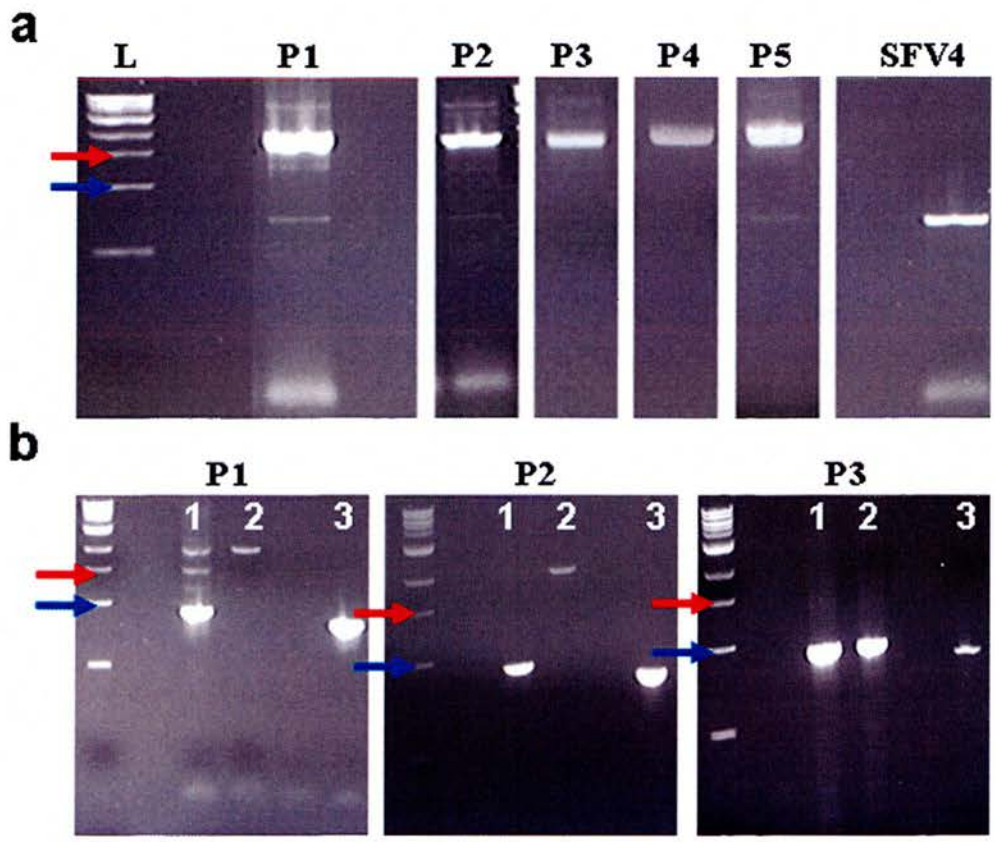

Figure 5.9. *In vivo* genotypic stability of SFV4(3H)-euCre and SFV4-steuCre. (a) RT-PCR genotyping of SFV4(3H)-euCre using nsP3 – nsP4 primers on RNA samples isolated from infected brain material after passages 1, 2, 3, 4 and 5. The passage number is indicated at the top of each strip. The strip labelled SFV4 is the SFV4-specific PCR product (positive control). **(b)** RT-PCR genotyping of SFV4-steuCre. Passage number is indicated at the top of each panel. In all panels, lanes 1 and 2 are the duplicate passages of SFV4-steuCre and lane 3 is the SFV4-specific PCR product (positive control). The red arrow corresponds to the 1.5 kb band of the DNA ladder and the blue arrow corresponds to the 0.5 kb band of the DNA ladder.

In vivo Cre-mediated recombination following infection with euCre expressing viruses

To investigate if euCre expressing viruses were able to induce Cre-mediated recombination *in vivo*, four different Cre-reporter mouse strains were used. ROSA26 (Mao *et al.*, 2001), ROSA26-EYFP (Srinivas *et al.*, 2001), sGFP7 (Gilchrist *et al.*, 2003) and sGFP97, kindly donated by the Medvinsky Group, Kings Buildings, Edinburgh. Initially, groups of mice (n=3) were inoculated intracerebrally with 1,000 PFU of SFV4(3H)-euCre or SFV4-steuCre. When the mice exhibited symptoms of viral encephalitis, generally between 2 and 3 days, they were euthanised and various tissues including brain, heart, lung, liver, spleen, pancreas and kidney were collected and processed for frozen sections.

Multiple sections from various tissues (at least 6 slides with 3 sections per slide) from the infected Cre-reporter mice were examined for the presence of fluorescence. No positive cells/tissues were observed.

Viruses expressing euCre were constructed to study the nature of the SFV CNS infection. This required survival of the infected animals for long enough to express their Cre recombination marker. Previous studies using viral vectors for the delivery of Cre recombinase in the brain have shown that the first evidence of Cre-mediated recombination appears between 3 and 7 days (Ahmed *et al.*, 2004; Sinnayah *et al.*, 2004). Given that the mice were generally sampled at 2 – 3 days post-infection, insufficient time may have resulted in the negative result.

In a second experiment, avirulent SFV4-RDR-steuCre and euCre expressing VLPs were used in groups of sGFP7 mice (n=3; 1,000 PFU of virus per animal). Also groups of sGFP7 mice (n=3) inoculated with SFV4(3H)-euCre or SFV4-steuCre (1,000 PFU per animal) were rescued using hyper-immune (HI) serum against SFV on PID 2, 5, 8 and 11 (raised by Dr C. Dixon). All animals except the mice inoculated with VLPs, which surprisingly succumbed to infection on PID 3, were sampled on PID 14 and same tissues as mentioned above were collected. In the second experiment only sGFP7 mice were used because experiments by other groups in the department had shown these mice to successfully report Cre-mediated recombination, at least in the spleen. The mice survived for 14 days. Examination of

many tissue sections again resulted in no cells expressing marker of recombination. This result will be discussed later in this chapter.

Brain sections from both experiments were immunostained for Cre-recombinase but multiple attempts were unsuccessful. A new Cre antibody is currently in production but it was not available in time for this project. Also tissue sections were stained for SFV structural proteins but none was detected. This was expected since the virus is cleared from the CNS 7 – 8 days after infection (Amor *et al.*, 1996). An additional problem was that the supply of mice was not constant and only small numbers of animals was used for each experiment. For that reason it was impossible to repeat the experiment in the timeframe of this project.

Summary of Findings

Summary of in vitro analysis of euCre expressing viruses

- Insertion of euCre in the non-structural or the structural ORF of SFV4 resulted in the production of viable viruses which were able to replicate in BHK-21 cells. All recombinant viruses were considerably slower in their replication and their peak titres were significantly lowered compared to SFV4. In cells infected with viruses with euCre insertion in the non-structural ORF cytopathic effect developed at the same time as in cells infected with SFV4. Development of CPE was delayed when viruses with euCre insertion in the structural ORF were used.
- All viruses and VLPs were able to express the euCre recombinase protein as shown by western blotting. Only a percentage of SFV4(3H)-euCre and SFV4(3L)-euCre maintained the euCre insert after the 5th passage in BHK-21 cells. SFV4-steuCre had almost completely eliminated the insert after the 4th *in vitro* passage.

Summary of in vivo analysis of euCre expressing viruses

- As with SFV4, none of the euCre expressing viruses was able to cause fatal disease in any animal infected intraperitoneally. SFV4(3H)-euCre was able to establish a low level plasma viraemia which was not different compared to the levels of viraemia established by SFV4. SFV4-steuCre however, was not detectable by plaque assay at the same time. This result is indicative of the more severe effect that insertion of euCre in the structural ORF has on the *in vivo* ability of the virus to replicate efficiently.
- Intracerebral inoculation of Balb/c mice with SFV4(3H)-euCre and SFV4-steuCre resulted in death in 100% of the inoculated mice. Mice inoculated with SFV4(3H)-euCre succumbed to infection 48 hours post-inoculation concurrently with SFV4 infected animals. Development of symptoms and death was delayed in mice inoculated with SFV4-steuCre. These animals died

24 hours later (PID 3). As expected SFV4-RDR-steuCre was avirulent. Surprisingly VLPs which are supposed to be avirulent because they can only undergo a single round of replication killed the animals for unknown reasons. SFV4(3H)-euCre and SFV4-steuCre had significantly lower peak titres compared to SFV4. Insertion of euCre in the structural ORF appears to affect *in vivo* pathogenesis of SFV4 more drastically that the same insertion in the replicase ORF. No Cre-mediated recombination was observed when Cre-reporter mice were inoculated with Cre expressing viruses and VLPs.

- *In vivo*, SFV4(3H)-euCre was very stable. RT-PCR analysis of material passaged 5 times in Balb/c mice brain showed minor amounts of recombinant viruses with complete elimination of the euCre insert. In contrast, SFV4-steuCre was genetically unstable. After the 3rd passage no recombinant virus carrying the inserted sequences was detectable using the same method.

Discussion

Insertion of eGFP in the non-structural and the structural ORFs of SFV4 resulted in the production of viable, replicating recombinant viruses with properties suitable for *in vivo* pathogenesis studies. Alphavirus replicating and non-replicating vectors based on SV and SFV have been used extensively in neurobiology. Levels and length of gene expression and gene transfer efficiency in neurons have been shown to be superior in alphavirus vector systems compared to other widely used viral vectors (Levine *et al.*, 1996; Gwag *et al.*, 1998; Ehrengruber *et al.*, 2001; Ehrengruber, 2002; Vaha-Koskela *et al.*, 2003; Sato *et al.*, 2004). To address fundamental questions on the nature of SFV infection of the CNS, the gene encoding Cre recombinase was inserted into the SFV4 genome.

It was previously mentioned that the size and the nature of the inserted sequence as well as its position in the viral genome is critical for the virus viability, replication efficiency and genetic stability. Insertion of euCre in either the replicase or the structural ORF of SFV4 affected the virus more severely than did eGFP insertion at exactly the same positions. All euCre expressing viruses replicated slower than SFV4 and eGFP expressing viruses and in contrast to the eGFP recombinants they did not reach similar titres to the parental virus. This can perhaps be attributed to the increased size of the genome (euCre is ~300 bp larger than the eGFP insert). Insertion of the larger euCre gene in the non-structural ORF may have further delayed the formation of viral replication complexes and slowed down the production of virus progeny. It can also be hypothesised that insertion of a foreign gene at the C-terminus of nsP3 might have an effect on minus-strand RNA synthesis and thus delay replication. The same insertion in the structural ORF, may affect the packaging of the genome and formation of new virus particles perhaps due to the larger genome size and to the non-efficient processing of the structural polyprotein. The western blotting for SFV4-steuCre and SFV4-RDR-steuCre showed high levels of euCre-2A-p62 fusion protein. This suggests that the 2A sequence was not as efficient in the context of these viruses; this could have affected the processing of the structural polyprotein as discussed in Chapter 4 resulting in reduced numbers of budding viruses. The size of the genome appears to be very important. Thomas *et al.*

(2003) showed that viruses expressing longer transgenes as a cleavable component of their structural ORF replicate less efficiently compared to viruses with shorter foreign sequences. In their studies a virus expressing eGFP replicated more efficiently compared to the same virus expressing VP7, a structural protein of bluetongue virus involved in virus attachment and penetration which has approximately twice the size of eGFP (Xu *et al.*, 1997). The impact of euCre insertion on virus growth could have been more severe if insertion had been under the control of a duplicated subgenomic promoter because as well as the longer size of genome the virus would have to overcome the competition between the two 26S promoters for replication complexes (Raju & Huang, 1991). Notably, both viruses expressing euCre as part of the replicase or the structural ORF replicated in a very similar way. In contrast, replication of SFV4-RDR-steuCre was less efficient. This was expected since this virus, as well as the euCre insert, has a point mutation in the nuclear localisation signal of nsP2 and alphaviruses with mutations in that protein are known to have slower replication and lower virulence (Rikkonen *et al.*, 1992; Dryga *et al.*, 1997).

In vitro, SFV4(3H)-euCre and SFV4(3L)-euCre have similar genotypic stability with the respective viruses expressing eGFP as part of the replicase ORF. SFV4-steuCre was less stable following five serial passages in BHK-21 cells compared to SFV4-steGFP and truncated genomes indicating deletions of the euCre gene were observed more rapidly. This difference can be attributed to the longer genome size of SFV4-steuCre. Similar instabilities were observed in the very similar recombinant SV described by Thomas *et al.* (2003). More specifically, expression of VP7 protein from that virus declined after the 6^{th} passage in BHK-21 cells whereas eGFP expression was unchanged for at least 10 passages. It is hypothesised that the secondary structure that might be introduced in the genome of an RNA virus by two different transgenes has a possible impact on genome stability. Secondary structure of RNA has been previously shown to be important for genome stability of viruses like HCV (Smith *et al.*, 2002; Thomas *et al.*, 2003).

In vivo, SFV4(3H)-euCre had high genotypic stability and after 5 passages minor amounts of euCre-negative viruses were detected by RT-PCR. Insertion in that position of the genome appears to be well tolerated in both SFV and SV constructs

(Frolova *et al.*, 2006; Tamberg *et al.*, 2007). In contrast, no euCre-positive genomes were detected after 3 passages of SFV4-steuCre in Balb/c mice. Elimination of the euCre insert was very fast. This is not surprising because insertion of a foreign gene does not offer any selective advantage to the virus. In addition, viruses with shorter genomes replicate more efficiently and therefore swiftly outnumber the ones replicating slower (Caley *et al.*, 1999; Thomas *et al.*, 2003; Tamberg *et al.*, 2007).

A major problem during this project was the absence of a suitable cell line to assess the functionality of euCre following serial passaging of viruses *in vitro* and *in vivo*. Cre-mediated recombination is a slow process; SFV infection killed the reporter cells by 48 hours most probably before recombination took place (Van den Plas *et al.*, 2003). This problem could be possibly solved by using a cell line resistant to SFV induced cell death such as a mosquito cell line. Cell lines derived from mosquitoes do not die, they become persistently infected by SFV and SV (Davey & Dalgarno, 1974; Karpf *et al.*, 1997b). However a mosquito Cre reporter cell line was not available. Possibly in the future the construct used in K562-DSRed[eGFP] cells could be used to produce a stable mosquito cell line. The advantage of a cell line like that will be double; it will help assess the functionality of euCre expressed by the viruses described in this chapter and additionally has potential uses for *in vitro* virus persistence studies.

The *in vivo* virulence of SFV4 does not appear to be impaired following insertion of euCre in the non-structural ORF. All mice inoculated i.c. succumbed to infection at the same time post-inoculation. As previously discussed, SFV4 and viruses based on that backbone are poorly neuroinvasive; consequently mice inoculated i.p. showed no signs of viral encephalitis. Poor neuroinvasiveness is attributed to deficient peripheral replication of these viruses. However, SFV4(3H)-euCre reached very similar levels of plasma viraemia compared to SFV4. Insertion of euCre in the structural ORF has a more substantial effect on SFV4. Although direct inoculation of SFV4-steuCre in the CNS resulted in fulminant encephalitis and death, the course of infection was delayed for 24 hours. In addition, the peak-titres that SFV4-steuCre reached in the brain were significantly lower compared to SFV4 and SFV4-steGFP. These differences possibly arise from the delayed replication of SFV4-steuCre.

The main objective of this project was to study alphavirus persistence in the CNS using the conditional marker gene activation offered by the Cre-*LoxP* system. This objective was not accomplished. The possible reasons for this one discussed below.

Cre-mediated recombination has been used extensively to study development and functions of different areas and genes of the brain, in murine models. Examples include studies on the function of dopamine and serotonin neurons and on the function of genes specifically found on the cardiovascular circuits of the mouse brain (Hirasawa *et al.*, 2001; Thevenot *et al.*, 2003; Zhuang *et al.*, 2005; Sinnayah *et al.*, 2006). Cre recombinase is delivered to the area of interest either by breeding of a mouse expressing Cre recombinase under the control of a cell/tissue specific promoter (for example murine neurofilament-H promoter) with a Cre-reporter mouse or by inoculation of viral vectors expressing the Cre gene.

Various viruses have been used for that purpose. Among the most common viral vectors used for Cre recombinase delivery are adenoviral, lentiviral, retroviral, and adeno-associated vectors (Pfeifer *et al.*, 2001; Kaspar *et al.*, 2002; Thevenot *et al.*, 2003; Ahmed *et al.*, 2004). Usually, Cre-mediated recombination in the brain is assessed 7 – 9 days after inoculation suggesting that it is a fairly slow procedure. This has also been shown *in vitro* in the K562-DSRed[eGFP] cell line (Kaspar *et al.*, 2002; Thevenot *et al.*, 2003; Van den Plas *et al.*, 2003).

In the present study, an alphavirus expressing Cre recombinase was described for the first time. However, no Cre-mediated recombination was observed *in vitro* or *in vivo* using euCre expressing SFV viruses and VLPs. The most obvious reason for that would be expression of non-functional Cre recombinase. However, this seems highly unlikely because SFV replicating and non replicating vectors have been used successfully for the expression of many different genes and the plasmid from which the euCre gene was extracted has been previously used for various studies (Hardouin & Nagy, 2000; Liang *et al.*, 2004). Assuming that the euCre protein produced by the recombinant viruses was functional, the absence of Cre-mediated recombination can be explained fairly easily *in vitro*; reporter cell lines did not survive long enough for recombination to occur. To circumvent the problem of cell death a cell line surviving for longer should be used. No such cell line was available during this project.

Possible solutions include the use of mosquito cell lines for the construction of Cre-reporter cell lines or cultures of neurons from Cre-reporter mice.

In vivo, the explanation is more complicated; lack of Cre-mediated recombination could be due to either the Cre-reporter mice or the recombinant viruses expressing euCre. Since all mouse strains used in this project have shown extensive recombination following viral delivery of Cre recombinase it can be hypothesised that recombination did not occur for reasons entirely attributed to the viruses used.

A possibility is that the virus did not express Cre recombinase long enough for recombination to occur. This is a likely explanation for SFV4(3H)-euCre. Any foreign gene inserted in the pSFV4(3H) vector has the last 30 amino acid residues of nsP3 fused to its C-terminus and it is believed that this sequence contains a degron signal. If euCre was degraded as quickly as eGFP (Figure 3.3), and taking into account that Cre-mediated recombination is a slow procedure, it is not surprising that recombination did not take place. However, this should not be the case for SFV4-steuCre, SFV4-RDR-steuCre and Cre-expressing VLPs. An alternative explanation is that the fusion of 2A to the C-terminus of euCre affected the euCre functionality, to investigate this possibility; a construct expressing euCre-2A fusion protein under the control of a eukaryotic promoter (CMV for example) could be used.

It has been previously shown that SFV recombinant viruses and vectors expressing foreign genes under the control of the 26S subgenomic promoter offer long-term strong expression (Vaha-Koskela *et al.*, 2003). Two experiments were performed using SFV4-steuCre. In the first one infection was allowed to progress and mice died on PID 3 before being able to report Cre-mediated recombination. In the second experiment mice were rescued by passive transfer or HI serum. The first dose of HI serum was given on PID 2; probably administration of HI serum cleared the virus from the brain too early and did not give enough time for recombination to occur. SFV4-RDR-steuCre was avirulent following i.c. inoculation and mice survived for the 14 days of this study but examination of multiple brain and peripheral tissue sections did not show any evidence of recombination. Most probably the virus was cleared by the immune response quickly and thus it was not possible to induce recombination. The absence of a working immunostaining for Cre recombinase did not allow us to assess for how long after inoculation Cre was expressed. A possible

solution to these problems would be to use the replicating SFV A7(74) vector described by Vaha-Koskela *et al.* (2003) for expression of Cre recombinase. This virus is able to persist in the brain of infected animals for at least 7 days therefore it would give enough time for the recombination to occur (Amor *et al.*, 1996). However, such a system would be limited due to the reduced efficiency of SFV A7(74) to replicate in neurons of adult mice (Fazakerley *et al.*, 1993). Another explanation for the absence of cells that recombination had happened is that all the infected cells died. Neurovirulence of virulent strains of SFV is due to its ability to replicate in neurons and kill them before the intervention of the immune response (Gates *et al.*, 1985; Smyth *et al.*, 1990).

Studies on the cytotoxicity of SFV-based vectors showed that following stereotaxic inoculation vectors persist at the site of inoculation and express the foreign gene for up to 21 days in neuronal cell bodies this time should have been enough for recombination to take place (Graham *et al.*, 2006). Surprisingly, mice inoculated with Cre recombinase expressing VLPs were found dead on PID 3. A possible explanation is that the high levels of Cre recombinase expressed by the VLPs were cytotoxic and caused the death of the animals. Studies have shown that high levels of Cre recombinase are toxic *in vitro* and *in vivo* (Loonstra *et al.*, 2001; Forni *et al.*, 2006). This problem has been addressed by the use of vectors in which the Cre gene is flanked by *LoxP* sites and therefore it is self-excised (Pfeifer *et al.*, 2001; Silver & Livingston, 2001). This approach is not applicable in SFV-based systems because the Cre-*LoxP* system is only active on DNA genomes.

In conclusion, the Cre-*LoxP* system is a powerful system which has potential applications in studies of virus persistence. However, during the time available in this project it was not possible to establish the system.

Concluding remarks

During this project, replication competent vectors expressing eGFP and euCre recombinase as a cleavable component of the non-structural or of the structural ORF of SFV4 were constructed.

Viruses expressing eGFP as a cleavable component of the non-structural ORF were viable, genetically stable and able to replicate to high titres similar to the parental SFV4. Although rapid degradation of eGFP was an unexpected finding, this feature might prove advantageous for *in vivo* pathogenesis studies because it offers a means to distinguish cells recently infected from cells infected for some time. Furthermore, these viruses allow us to identify cells and tissues in which the genomic promoter is switched off. Atasheva *et al.* (2007) showed that the genome of SV can tolerate insertions of multiple reporter genes (eGFP and cherry red) in the replicase ORF. A recombinant SFV expressing two different reporters from the genomic and subgenomic promoter respectively might provide the ability to distinguish cells in which the genomic or the subgenomic promoter is active indicating the stage of infection of individual cells without any requirement for immunostaining. The putative degron signal at the C-terminus of nsP3 discovered during these studies might be very useful in biotechnological applications in which rapid degradation of proteins is required.

The virus incorporating eGFP as a cleavable component of the structural ORF gave prolonged, high level expression and its usefulness for *in vivo* pathogenesis studies was exhibited in both immunocompetent and immunodeficient animals. This virus, although slightly attenuated, highlighted in a very obvious way the major impact of type-I interferon response on virus replication following extraneural inoculation. The FMDV 2A sequence used to facilitate release of eGFP from the rest of the structural polyprotein was not 100% efficient and may be responsible for the different distributions of eGFP in certain cell types; in which case efficiency of the 2A-mediated cleavage is dependent on the cell type. Sub-optimal efficiency of the 2A sequence has been previously demonstrated in a recombinant equine arteritis virus (van den Born *et al.*, 2007).

Concluding remarks

Insertion of the euCre recombinase gene into the replicase or the structural ORF of SFV4 produced viable viruses capable of expressing the gene. However, the replication of these viruses and their genetic stability was reduced compared to the eGFP expressing viruses. These results point out the impact that the size and the nature of the inserted sequence might have on virus fitness. In the three years of this PhD project, unfortunately was not possible to get the Cre/*LoxP* system working but this technology has the potential to answer a fundamental virological question and further studies using various strains of virus or replicons with insertions of euCre recombinase in different positions of the genome may be required to determine if Cre-mediated recombination can occur following expression by SFV.

Overall, the work undertaken during this project has shown that SFV can tolerate and express multiple genes as part of its natural transcription units. In addition, the application of these novel reporter viruses was established. Following on from the studies of this thesis, additional marker genes including DSRed and *Renilla* luciferase have been inserted in the same positions into the genome of SFV4 extending our capabilities for future studies.

References

Adams, L. D., Choi, L., Xian, H. Q., Yang, A., Sauer, B., Wei, L. & Gottlieb, D. I. (2003). Double lox targeting for neural cell transgenesis. *Molecular Brain Research* **110**, 220-233.

Aguilar, P. V., Paessler, S., Carrara, A. S., Baron, S., Poast, J., Wang, E., Moncayo, A. C., Anishchenko, M., Watts, D., Tesh, R. B. & Weaver, S. C. (2005). Variation in Interferon Sensitivity and Induction among Strains of Eastern Equine Encephalitis Virus. *J Virol* **79**, 11300-11310.

Ahmed, B., Chakravarthy, S., Eggers, R., Hermens, W., Zhang, J., Niclou, S., Levelt, C., Sablitzky, F., Anderson, P., Lieberman, A. R. & Verhaagen, J. (2004). Efficient delivery of Cre-recombinase to neurons in vivo and stable transduction of neurons using adeno-associated and lentiviral vectors. *BMC Neuroscience* **5**, 4.

Ahola, T. & Kaariainen, L. (1995). Reaction in Alphavirus mRNA Capping: Formation of a Covalent Complex of Nonstructural Protein nsP1 with 7-Methyl-GMP. *PNAS, USA* **92**, 507-511.

Ahola, T., Laakkonen, P., Vihinen, H. & Kaariainen, L. (1997). Critical residues of Semliki Forest virus RNA capping enzyme involved in methyltransferase and guanylyltransferase-like activities. *J Virol* **71**, 392-397.

Ahola, T., Kujala, P., Tuittila, M., Blom, T., Laakkonen, P., Hinkkanen, A. & Auvinen, P. (2000). Effects of Palmitoylation of Replicase Protein nsP1 on Alphavirus Infection. *J Virol* **74**, 6725-6733.

Allsopp, T. E. & Fazakerley, J. K. (2000). Altruistic cell suicide and the specialized case of the virus-infected nervous system. *Trends Neurosci* **23**, 284-290.

Allsopp, T. E., Scallan, M. F., Williams, A. & Fazakerley, J. K. (1998). Virus infection induces neuronal apoptosis: A comparison with trophic factor withdrawal. *Cell Death Differ* **5**, 50-59.

Amor, S., Scallan, M. F., Morris, M. M., Dyson, H. & Fazakerley, J. K. (1996). Role of immune responses in protection and pathogenesis during Semliki Forest virus encephalitis. *J Gen Virol* **77**, 281-291.

Anishchenko, M., Paessler, S., Greene, I. P., Aguilar, P. V., Carrara, A. S. & Weaver, S. C. (2004). Generation and Characterization of Closely Related Epizootic and Enzootic Infectious cDNA Clones for Studying Interferon Sensitivity and Emergence Mechanisms of Venezuelan Equine Encephalitis Virus. *J Virol* **78**, 1-8.

References

Aranda, M., Kanellopoulou, C., Christ, N., Peitz, M., Rajewsky, K. & Droge, P. (2001). Altered directionality in the Cre-LoxP site-specific recombination pathway. *J Mol Biol* **311**, 453-459.

Atasheva, S., Gorchakov, R., English, R., Frolov, I. & Frolova, E. (2007). Development of Sindbis Viruses Encoding nsP2/GFP Chimeric Proteins and Their Application for Studying nsP2 Functioning. *J Virol* **81**, 5046-5057.

Atkins, G. J., Carter, J. & Sheahan, B. J. (1982). Effect of alphavirus infection on mouse embryos. *Infect Immun* **38**, 1285-1290.

Atkins, G. J. & Sheahan, B. J. (1982). Semliki forest virus neurovirulence mutants have altered cytopathogenicity for central nervous system cells. *Infect Immun* **36**, 333-341.

Atkins, G. J., Sheahan, B. J. & Liljestrom, P. (1999). The molecular pathogenesis of Semliki Forest virus: a model virus made useful? *J Gen Virol* **80**, 2287-2297.

Atkins, G. J., Sheahan, B. J. & Mooney, D. A. (1990). Pathogenicity of Semliki Forest virus for the rat central nervous system and primary rat neural cell cultures: possible implications for the pathogenesis of multiple sclerosis. *Neuropathol Appl Neurobiol* **16**, 57-68.

Balluz, I. M., Glasgow, G. M., Killen, H. M., Mabruk, M. J., Sheahan, B. J. & Atkins, G. J. (1993). Virulent and avirulent strains of Semliki Forest virus show similar cell tropism for the murine central nervous system but differ in the severity and rate of induction of cytolytic damage. *Neuropathol Appl Neurobiol* **19**, 233-239.

Berglund, P., Sjoberg, M., Garoff, H., Atkins, G. J., Sheahan, B. J. & Liljestrom, P. (1993). Semliki Forest virus expression system: production of conditionally infectious recombinant particles. *Biotechnology (N Y)* **11**, 916-920.

Berglund, P., Smerdou, C., Fleeton, M. N., Tubulekas, I. & Liljestrom, P. (1998). Enhancing immune responses using suicidal DNA vaccines. *Nat Biotechnol* **16**, 562-565.

Bick, M. J., Carroll, J. W., Gao, G., Goff, S. P., Rice, C. M. & MacDonald, M. R. (2003). Expression of the Zinc-Finger Antiviral Protein Inhibits Alphavirus Replication. *J Virol* **77**, 11555-11562.

Bonatti, S. & Blobel, G. (1979). Absence of a cleavable signal sequence in Sindbis virus glycoprotein PE2. *J Biol Chem* **254**, 12261-12264.

Boorsma, M., Nieba, L., Koller, D., Bachmann, M. F., Bailey, J. E. & Renner, W. A. (2000).A temperature-regulated replicon-based DNA expression system. *Nat Biotechnol* **18**, 429-432.

Boyd, A., Fazakerley, J. K. & Bridgen, A. (2006). Pathogenesis of Dugbe virus infection in wild-type and interferon-deficient mice. *J Gen Virol* **87**, 2005-2009.

Bradish, C. J., Allner, K. & Fitzgeorge, R. (1975). Immunomodification and the expression of virulence in mice by defined strains of Semliki Forest virus: the effects of cyclophosphamide. *J Gen Virol* **28**, 225-237.

Bradish, C. J., Allner, K. & Maber, H. B. (1971). The virulence of original and derived strains of Semliki forest virus for mice, guinea-pigs and rabbits. *J Gen Virol* **12**, 141-160.

Bradish, C. J. & Titmuss, D. (1981). The effects of interferon and double-stranded RNA upon the virus-host interaction: studies with togavirus strains in mice. *J Gen Virol* **53**, 21-30.

Bray, M. (2001). The role of the Type I interferon response in the resistance of mice to filovirus infection. *J Gen Virol* **82**, 1365-1373.

Breakwell, L., (2006). The role of interferon in Semliki Forest virus encephalitis. PhD Thesis, The University of Edinburgh.

Breakwell, L., Dosenovic, P., Karlsson Hedestam, G. B., D'Amato, M., Liljestrom, P., Fazakerley, J. & McInerney, G. M. (2007). Semliki Forest virus nonstructural protein 2 is involved in suppression of the type I interferon response. *J Virol* **81**, 8677-8684.

Brodie, C., Weizman, N., Katzoff, A., Lustig, S. & Kobiler, D. (1997). Astrocyte activation by Sindbis virus: expression of GFAP, cytokines, and adhesion molecules. *Glia* **19**, 275-285.

Brooks, A. I., Cory-Slechta, D. A. & Federoff, H. J. (2000). Gene-experience interaction alters the cholinergic septohippocampal pathway of mice. *PNAS USA* **97**, 13378-13383.

Burch, G. E., DePasquale, N. P., Sun, S. C., Mogabgab, W. J. & Hale, A. R. (1966). Endocarditis in mice infected with Coxsackie virus B4. *Science* **151**, 447-448.

Burdeinick-Kerr, R., Wind, J. & Griffin, D. E. (2007). Synergistic roles of antibody and interferon in noncytolytic clearance of Sindbis virus from different regions of the central nervous system. *J Virol* **81**, 5628-5636.

Byrnes, A. P., Durbin, J. E. & Griffin, D. E. (2000). Control of Sindbis virus infection by antibody in interferon-deficient mice. *J Virol* **74**, 3905-3908.

Caley, I. J., Betts, M. R., Davis, N. L., Swanstrom, R., Frelinger, J. A. & Johnston, R. E. (1999). Venezuelan equine encephalitis virus vectors expressing HIV-1 proteins: vector design strategies for improved vaccine efficacy. *Vaccine* **17**, 3124-3135.

Camara, A., Diaz, G., Vega, V., Basualdo, M. & Contigiani, M. (2003). Seroprevalence of antibodies to Venezuelan equine encephalitis complex (subtypes IAB and VI) in humans from General Belgrano island, Formosa, Argentina. *Rev Inst Med Trop Sao Paulo* **45**, 201-204.

Charles, P. C., Walters, E., Margolis, F. & Johnston, R. E. (1995). Mechanism of Neuroinvasion of Venezuelan Equine Encephalitis Virus in the Mouse. *Virology* **208**, 662-671.

Chen, J. P., Miller, D., Katow, S. & Frey, T. K. (1995). Expression of the rubella virus structural proteins by an infectious Sindbis virus vector. *Arch Virol* **140**, 2075-2084.

Cheng, R. H., Kuhn, R. J., Olson, N. H., Rossmann, M. G., Choi, H. K., Smith, T. J. & Baker, T. S. (1995). Nucleocapsid and glycoprotein organization in an enveloped virus. *Cell* **80**, 621-630.

Chinnasamy, D., Milsom, M. D., Shaffer, J., Neuenfeldt, J., Shaaban, A. F., Margison, G. P., Fairbairn, L. J. & Chinnasamy, N. (2006). Multicistronic lentiviral vectors containing the FMDV 2A cleavage factor demonstrate robust expression of encoded genes at limiting MOI. *Virol J* **3**, 14.

Collins, W. E. (1963). Studies on the transmission of Semliki Forest virus by anopheline mosquitoes. *Am J Hyg* **77**, 109-113.

Cook, S. H. & Griffin, D. E. (2003). Luciferase imaging of a neurotropic viral infection in intact animals. *J Virol* **77**, 5333-5338.

Cristea, I. M., Carroll, J. W., Rout, M. P., Rice, C. M., Chait, B. T. & MacDonald, M. R. (2006). Tracking and elucidating alphavirus-host protein interactions. *J Biol Chem*, M603980200.

Cserr, H. F. & Knopf, P. M. (1992). Cervical lymphatics, the blood-brain barrier and the immunoreactivity of the brain: a new view. *Immunol Today* **13**, 507-512.

D'Apuzzo, M., Mandolesi, G., Reis, G. & Schuman, E. M. (2001). Abundant GFP Expression and LTP in Hippocampal Acute Slices by In Vivo Injection of Sindbis Virus. *J Neurophysiol* **86**, 1037-1042.

Dalrymple, J. M., Young, O. P., Eldridge, B. F. & Russell, P. K. (1972). Ecology of arboviruses in a Maryland freshwater swamp. 3. Vertebrate hosts. *Am J Epidemiol* **96**, 129-140.

Dätwyler, D. A., Magyar, J., Bailey, J., Koller, D. & Eppenberger, H. (1999). Efficient gene delivery into adult cardiomyocytes by recombinant Sindbis virus. 77 edn, pp. 859-864.

Davey, M. W. & Dalgarno, L. (1974). Semliki Forest virus replication in cultured Aedes albopictus cells: studies on the establishment of persistence. *J Gen Virol* **24**, 453-463.

Davis, N. L., Willis, L. V., Smith, J. F. & Johnston, R. E. (1989). In vitro synthesis of infectious venezuelan equine encephalitis virus RNA from a cDNA clone: analysis of a viable deletion mutant. *Virology* **171**, 189-204.

Davison, I. G. & Katz, L. C. (2007). Sparse and Selective Odor Coding by Mitral/Tufted Neurons in the Main Olfactory Bulb. *J Neurosci* **27**, 2091-2101.

de Felipe, P., Martin, V., Cortes, M. L., Ryan, M. & Izquierdo, M. (1999). Use of the 2A sequence from foot-and-mouth disease virus in the generation of retroviral vectors for gene therapy. *Gene Ther* **6**, 198-208.

de Felipe, P. & Ryan, M. D. (2004). Targeting of proteins derived from self-processing polyproteins containing multiple signal sequences. *Traffic* **5**, 616-626.

de Felipe, P., Hughes, L. E., Ryan, M. D. & Brown, J. D. (2003). Co-translational, Intraribosomal Cleavage of Polypeptides by the Foot-and-mouth Disease Virus 2A Peptide. *J Biol Chem* **278**, 11441-11448.

de Groot, R. J., Hardy, W. R., Shirako, Y. & Strauss, J. H. (1990). Cleavage-site preferences of Sindbis virus polyproteins containing the non-structural proteinase. Evidence for temporal regulation of polyprotein processing in vivo. *EMBO J* **9**, 2631-2638.

de Groot, R. J., Rumenapf, T., Kuhn, R. J., Strauss, E. G. & Strauss, J. H. (1991). Sindbis Virus RNA Polymerase is Degraded by the N-End Rule Pathway. *PNAS* **88**, 8967-8971.

de Haan, C. A. M., Haijema, B. J., Boss, D., Heuts, F. W. H. & Rottier, P. J. M. (2005). Coronaviruses as Vectors: Stability of Foreign Gene Expression. *J Virol* **79**, 12742-12751.

de la Torre, J. C. (2002). Bornavirus and the brain. *J Infect Dis* **186 Suppl 2**, S241-S247.

Del Piero, F., Wilkins, P. A., Dubovi, E. J., Biolatti, B. & Cantile, C. (2001). Clinical, Pathologic, Immunohistochemical, and Virologic Findings of Eastern Equine Encephalomyelitis in Two Horses. *Vet Pathol* **38**, 451-456.

Detrait, E. R., Bowers, W. J., Halterman, M. W., Giuliano, R. E., Bennice, L., Federoff, H. J. & Richfield, E. K. (2002). Reporter gene transfer induces apoptosis in primary cortical neurons. *Mol Ther* **5**, 723-730.

DeTulleo, L. & Kirchhausen, T. (1998). The clathrin endocytic pathway in viral infection. *EMBO J* **17**, 4585-4593.

Deuber, S. A. & Pavlovic, J. (2007). Virulence of a mouse-adapted Semliki Forest virus strain is associated with reduced susceptibility to interferon. *J Gen Virol* **88**, 1952-1959.

DiCiommo, D. P. & Bremner, R. (1998). Rapid, High Level Protein Production Using DNA-based Semliki Forest Virus Vectors. *J Biol Chem* **273**, 18060-18066.

Dietrich, C. & Maiss, E. (2003). Fluorescent labelling reveals spatial separation of potyvirus populations in mixed infected Nicotiana benthamiana plants. *J Gen Virol* **84**, 2871-2876.

Ding, M. X. & Schlesinger, M. J. (1989). Evidence that Sindbis virus NSP2 is an autoprotease which processes the virus nonstructural polyprotein. *Virology* **171**, 280-284.

Dixon, C. M. (2007). Role of immune responses in Semliki Forest virus encephalitis. PhD Thesis, The University of Edinburgh.

Doherty, F. J., Dawson, S. & Mayer, R. J. (2002). The ubiquitin-proteasome pathway of intracellular proteolysis. *Essays Biochem* **38**, 51-63.

Dolja, V. V., Herndon, K. L., Pirone, T. P. & Carrington, J. C. (1993). Spontaneous mutagenesis of a plant potyvirus genome after insertion of a foreign gene. *J Virol* **67**, 5968-5975.

Donnelly, M. L. L., Hughes, L. E., Luke, G., Mendoza, H., ten Dam, E., Gani, D. & Ryan, M. D. (2001a). The 'cleavage' activities of foot-and-mouth disease virus 2A site-directed mutants and naturally occurring '2A-like' sequences. *J Gen Virol* **82**, 1027-1041.

Donnelly, M. L. L., Luke, G., Mehrotra, A., Li, X., Hughes, L. E., Gani, D. & Ryan, M. D. (2001b). Analysis of the aphthovirus 2A/2B polyprotein 'cleavage' mechanism indicates not a proteolytic reaction, but a novel translational effect: a putative ribosomal 'skip'. *J Gen Virol* **82**, 1013-1025.

Donnelly, S. M., Sheahan, B. J. & Atkins, G. J. (1997). Long-term effects of Semliki Forest virus infection in the mouse central nervous system. *Neuropathol Appl Neurobiol* **23**, 235-241.

Dryga, S. A., Dryga, O. A. & Schlesinger, S. (1997). Identification of mutations in a Sindbis virus variant able to establish persistent infection in BHK cells: the importance of a mutation in the nsP2 gene. *Virology* **228**, 74-83.

Dubensky, T. W., Jr., Driver, D. A., Polo, J. M., Belli, B. A., Latham, E. M., Ibanez, C. E., Chada, S., Brumm, D., Banks, T. A., Mento, S. J., Jolly, D. J. & Chang, S. M. (1996). Sindbis virus DNA-based expression vectors: utility for in vitro and in vivo gene transfer. *J Virol* **70**, 508-519.

References

Duprex, W. P., Collins, F. M. & Rima, B. K. (2002). Modulating the Function of the Measles Virus RNA-Dependent RNA Polymerase by Insertion of Green Fluorescent Protein into the Open Reading Frame. *J Virol* **76**, 7322-7328.

Duprex, W. P., Mcquaid, S., Hangartner, L., Billeter, M. A. & Rima, B. K. (1999). Observation of Measles Virus Cell-to-Cell Spread in Astrocytoma Cells by Using a Green Fluorescent Protein-Expressing Recombinant Virus. *J Virol* **73**, 9568-9575.

Duprex, W. P., Mcquaid, S., Roscic-Mrkic, B., Cattaneo, R., Mccallister, C. & Rima, B. K. (2000). In Vitro and In Vivo Infection of Neural Cells by a Recombinant Measles Virus Expressing Enhanced Green Fluorescent Protein. *J Virol* **74**, 7972-7979.

Ehrengruber, M. U., Lundstrom, K., Schweitzer, C., Heuss, C., Schlesinger, S. & Gahwiler, B. H. (1999). Recombinant Semliki Forest virus and Sindbis virus efficiently infect neurons in hippocampal slice cultures. *PNAS, USA* **96**, 7041-7046.

Ehrengruber, M. U. (2002). Alphaviral gene transfer in neurobiology. *Brain Research Bulletin* **59**, 13-22.

Ehrengruber, M. U., Hennou, S., Bueler, H., Naim, H. Y., Deglon, N. & Lundstrom, K. (2001). Gene Transfer into Neurons from Hippocampal Slices: Comparison of Recombinant Semliki Forest Virus, Adenovirus, Adeno-Associated Virus, Lentivirus, and Measles Virus. *Molecular and Cellular Neuroscience* **17**, 855-871.

El Amrani, A., Barakate, A., Askari, B. M., Li, X., Roberts, A. G., Ryan, M. D. & Halpin, C. (2004). Coordinate Expression and Independent Subcellular Targeting of Multiple Proteins from a Single Transgene. *Plant Physiol* **135**, 16-24.

Fabry, Z., Raine, C. S. & Hart, M. N. (1994). Nervous tissue as an immune compartment: the dialect of the immune response in the CNS. *Immunol Today* **15**, 218-224.

Fauconnier, B. (1971).[Effect of an anti-interferon serum on experimental viral pathogenicity in vivo]. *Pathol Biol (Paris)* **19**, 575-578.

Fayzulin, R., Gorchakov, R., Petrakova, O., Volkova, E. & Frolov, I. (2005). Sindbis Virus with a Tricomponent Genome. *J Virol* **79**, 637-643.

Fazakerley, J. K. (2001). Neurovirology and developmental neurobiology. *Adv Virus Res* **56**, 73-124.

Fazakerley, J. K. (2002). Pathogenesis of Semliki Forest virus encephalitis. *J Neurovirol* **8 Suppl 2**, 66-74.

Fazakerley, J. K. (2004). Semliki forest virus infection of laboratory mice: a model to study the pathogenesis of viral encephalitis. *Arch Virol Suppl*, 179-190.

Fazakerley, J. K. & Allsopp, T. E. (2001). Programmed cell death in virus infections of the nervous system. *Curr Top Microbiol Immunol* **253**, 95-119.

Fazakerley, J. K., Boyd, A., Mikkola, M. L. & Kaariainen, L. (2002).A single amino acid change in the nuclear localization sequence of the nsP2 protein affects the neurovirulence of Semliki Forest virus. *J Virol* **76**, 392-396.

Fazakerley, J. K., Cotterill, C. L., Lee, G. & Graham, A. (2006). Virus tropism, distribution, persistence and pathology in the corpus callosum of the Semliki Forest virus-infected mouse brain: a novel system to study virus-oligodendrocyte interactions. *Neuropathol Appl Neurobiol* **32**, 397-409.

Fazakerley, J. K., Pathak, S., Scallan, M., Amor, S. & Dyson, H. (1993). Replication of the A7(74) strain of Semliki Forest virus is restricted in neurons. *Virology* **195**, 627-637.

Fazakerley, J. K. & Ross, A. M. (1989). Computer analysis suggests a role for signal sequences in processing polyproteins of enveloped RNA viruses and as a mechanism of viral fusion. *Virus Genes* **2**, 223-239.

Fazakerley, J. K. & Webb, H. E. (1987). Semliki Forest virus-induced, immune-mediated demyelination: adoptive transfer studies and viral persistence in nude mice. *J Gen Virol* **68**, 377-385.

Finke, S., Brzozka, K. & Conzelmann, K. K. (2004). Tracking Fluorescence-Labeled Rabies Virus: Enhanced Green Fluorescent Protein-Tagged Phosphoprotein P Supports Virus Gene Expression and Formation of Infectious Particles. *J Virol* **78**, 12333-12343.

Finter, N. B. (1966). Interferon as an antiviral agent in vivo: quantitative and temporal aspects of the protection of mice against Semliki Forest virus. *Br J Exp Pathol* **47**, 361-371.

Forni, P. E., Scuoppo, C., Imayoshi, I., Taulli, R., Dastru, W., Sala, V., Betz, U. A. K., Muzzi, P., Martinuzzi, D., Vercelli, A. E., Kageyama, R. & Ponzetto, C. (2006). High Levels of Cre Expression in Neuronal Progenitors Cause Defects in Brain Development Leading to Microencephaly and Hydrocephaly. *J Neurosci* **26**, 9593-9602.

Foster, T. P., Rybachuk, G. V. & Kousoulas, K. G. (1998). Expression of the enhanced green fluorescent protein by herpes simplex virus type 1 (HSV-1) as an in vitro or in vivo marker for virus entry and replication. *Journal of Virological Methods* **75**, 151-160.

Fragkoudis, R., Breakwell L., McKimmie, C. S., Boyd, A., Barry G., Kohl, A., Merits, A. & Fazakerley, J. K. (2007). The type-I interferon system protects mice from Semliki Forest virus by preventing widespread virus dissemination

in extraneural tissues but does not mediate the restricted replication of avirulent virus in CNS neurons. *J Gen Virol* **88,** In Press.

Frolov, I. & Schlesinger, S. (1994a). Comparison of the effects of Sindbis virus and Sindbis virus replicons on host cell protein synthesis and cytopathogenicity in BHK cells. *J Virol* **68**, 1721-1727.

Frolov, I. & Schlesinger, S. (1994b). Translation of Sindbis virus mRNA: effects of sequences downstream of the initiating codon. *J Virol* **68**, 8111-8117.

Frolov, I., Hoffman, T. A., Pragai, B. M., Dryga, S. A., Huang, H. V., Schlesinger, S. & Rice, C. M. (1996). Alphavirus-based expression vectors: Strategies and applications. *PNAS* **93**, 11371-11377.

Frolova, E., Frolov, I. & Schlesinger, S. (1997). Packaging signals in alphaviruses. *J Virol* **71**, 248-258.

Frolova, E. I., Fayzulin, R. Z., Cook, S. H., Griffin, D. E., Rice, C. M. & Frolov, I. (2002). Roles of nonstructural protein nsP2 and Alpha/Beta interferons in determining the outcome of Sindbis virus infection. *J Virol* **76**, 11254-11264.

Frolova, E., Gorchakov, R., Garmashova, N., Atasheva, S., Vergara, L. A. & Frolov, I. (2006). Formation of nsP3-Specific Protein Complexes during Sindbis Virus Replication. *J Virol* **80**, 4122-4134.

Froshauer, S., Kartenbeck, J. & Helenius, A. (1988). Alphavirus RNA replicase is located on the cytoplasmic surface of endosomes and lysosomes. *J Cell Biol* **107**, 2075-2086.

Furler, S., Paterna, J. C., Weibel, M. & Bueler, H. (2001). Recombinant AAV vectors containing the foot and mouth disease virus 2A sequence confer efficient bicistronic gene expression in cultured cells and rat substantia nigra neurons. *Gene Ther* **8**, 864-873.

Galbraith, S. E., Sheahan, B. J. & Atkins, G. J. (2006). Deletions in the hypervariable domain of the nsP3 gene attenuate Semliki Forest virus virulence. *J Gen Virol* **87**, 937-947.

Garoff, H., Huylebroeck, D., Robinson, A., Tillman, U. & Liljestrom, P. (1990). The signal sequence of the p62 protein of Semliki Forest virus is involved in initiation but not in completing chain translocation. *J Cell Biol* **111**, 867-876.

Gates, M. C., Sheahan, B. J. & Atkins, G. J. (1984). The pathogenicity of the M9 mutant of Semliki Forest virus in immune-compromised mice. *J Gen Virol* **65**, 73-80.

Gates, M. C., Sheahan, B. J., O'Sullivan, M. A. & Atkins, G. J. (1985). The pathogenicity of the A7, M9 and L10 strains of Semliki Forest virus for

weanling mice and primary mouse brain cell cultures. *J Gen Virol* **66**, 2365-2373.

Gehrke, R., Heinz, F. X., Davis, N. L. & Mandl, C. W. (2005). Heterologous gene expression by infectious and replicon vectors derived from tick-borne encephalitis virus and direct comparison of this flavivirus system with an alphavirus replicon. *J Gen Virol* **86**, 1045-1053.

Ghosh, K. & Van Duyne, G. D. (2002). Cre-loxP biochemistry. *Methods* **28**, 374-383.

Gilchrist, D. S., Ure, J., Hook, L. & Medvinsky, A. (2003). Labeling of hematopoietic stem and progenitor cells in novel activatable EGFP reporter mice. *Genesis* **36**, 168-176.

Glasgow, G. M., McGee, M. M., Sheahan, B. J. & Atkins, G. J. (1997). Death mechanisms in cultured cells infected by Semliki Forest virus. *J Gen Virol* **78**, 1559-1563.

Glasgow, G. M., McGee, M. M., Tarbatt, C. J., Mooney, D. A., Sheahan, B. J. & Atkins, G. J. (1998). The Semliki Forest virus vector induces p53-independent apoptosis. *J Gen Virol* **79**, 2405-2410.

Glasgow, G. M., Sheahan, B. J., Atkins, G. J., Wahlberg, J. M., Salminen, A. & Liljestrom, P. (1991). Two mutations in the envelope glycoprotein E2 of Semliki Forest virus affecting the maturation and entry patterns of the virus alter pathogenicity for mice. *Virology* **185**, 741-748.

Glomb-Reinmund, S. & Kielian, M. (1998). The role of low pH and disulfide shuffling in the entry and fusion of Semliki Forest virus and Sindbis virus. *Virology* **248**, 372-381.

Gomez, d. C., Ehsani, N., Mikkola, M. L., Garcia, J. A. & Kaariainen, L. (1999).RNA helicase activity of Semliki Forest virus replicase protein NSP2. *FEBS Lett* **448**, 19-22.

Graham, A., Walker, R., Baird, P., Hahn, C. N. & Fazakerley, J. K. (2006).CNS gene therapy applications of the Semliki Forest virus 1 vector are limited by neurotoxicity. *Mol Ther* **13**, 631-635.

Grieder, F. B. & Vogel, S. N. (1999). Role of Interferon and Interferon Regulatory Factors in Early Protection against Venezuelan Equine Encephalitis Virus Infection. *Virology* **257**, 106-118.

Griffin, D. E. (1995). Arboviruses and the central nervous system. *Springer Semin Immunopathol* **17**, 121-132.

Griffin, D. E. (2007). Alphaviruses. Field's Virology, Knipe, M. D., Howley, M. H., 5th edn, pp. 1023-1067: Lippincott Williams & Wilkins.

Grimley, P. M., Berezesky, I. K. & Friedman, R. M. (1968). Cytoplasmic structures associated with an arbovirus infection: loci of viral ribonucleic acid synthesis. *J Virol* **2**, 1326-1338.

Grimley, P. M. & Friedman, R. M. (1970). Arboviral infection of voluntary striated muscles. *J Infect Dis* **122**, 45-52.

Gross, P. M., Sposito, N. M., Pettersen, S. E., Panton, D. G. & Fenstermacher, J. D. (1987). Topography of capillary density, glucose metabolism, and microvascular function within the rat inferior colliculus. *J Cereb Blood Flow Metab* **7**, 154-160.

Gwag, B. J., Kim, E. Y., Ryu, B. R., Won, S. J., Ko, H. W., Oh, Y. J., Cho, Y. G., Ha, S. J. & Sung, Y. C. (1998).A neuron-specific gene transfer by a recombinant defective Sindbis virus. *Brain Res Mol Brain Res* **63**, 53-61.

Hahn, C. S., Hahn, Y. S., Braciale, T. J. & Rice, C. M. (1992). Infectious Sindbis Virus Transient Expression Vectors for Studying Antigen Processing and Presentation. *PNAS* **89**, 2679-2683.

Hahn, Y. S., Strauss, E. G. & Strauss, J. H. (1989). Mapping of RNA- temperature-sensitive mutants of Sindbis virus: assignment of complementation groups A, B, and G to nonstructural proteins. *J Virol* **63**, 3142-3150.

Hardouin, N. & Nagy, A. (2000). Gene-trap-based target site for cre-mediated transgenic insertion. *Genesis* **26**, 245-252.

Hardy, W. R. & Strauss, J. H. (1989). Processing the nonstructural polyproteins of sindbis virus: nonstructural proteinase is in the C-terminal half of nsP2 and functions both in cis and in trans. *J Virol* **63**, 4653-4664.

Helenius, A., Morein, B., Fries, E., Simons, K., Robinson, P., Schirrmacher, V., Terhorst, C. & Strominger, J. L. (1978). Human (HLA-A and HLA-B) and murine (H-2K and H-2D) histocompatibility antigens are cell surface receptors for Semliki Forest virus. *PNAS, USA* **75**, 3846-3850.

Higgs, S., Oray, C. T., Myles, K., Olson, K. E. & Beaty, B. J. (1999). Infecting larval arthropods with a chimeric, double subgenomic Sindbis virus vector to express genes of interest. *Biotechniques* **27**, 908-911.

Hill, K. R., Hajjou, M., Hu, J. Y. & Raju, R. (1997).RNA-RNA recombination in Sindbis virus: roles of the 3' conserved motif, poly(A) tail, and nonviral sequences of template RNAs in polymerase recognition and template switching. *J Virol* **71**, 2693-2704.

Hirasawa, M., Cho, A., Sreenath, T., Sauer, B., Julien, J. P. & Kulkarni, A. B. (2001). Neuron-specific expression of Cre recombinase during the late phase of brain development. *Neuroscience Research* **40**, 125-132.

Hwang Kim, K., Rumenapf, T., Strauss, E. G. & Strauss, J. H. (2004). Regulation of Semliki Forest virus RNA replication: a model for the control of alphavirus pathogenesis in invertebrate hosts. *Virology* **323**, 153-163.

Isaacs, A. & Lindenmann, J. (1957). Virus interference. I. The interferon. *Proc R Soc Lond B Biol Sci* **147**, 258-267.

Jeromin, A., Yuan, L. L., Frick, A., Pfaffinger, P. & Johnston, D. (2003).A Modified Sindbis Vector for Prolonged Gene Expression in Neurons. *J Neurophysiol* **90**, 2741-2745.

Johnson, B. W., Olson, K. E., Allen-Miura, T., Rayms-Keller, A., Carlson, J. O., Coates, C. J., Jasinskiene, N., James, A. A., Beaty, B. J. & Higgs, S. (1999). Inhibition of luciferase expression in transgenic Aedes aegypti mosquitoes by Sindbis virus expression of antisense luciferase RNA. *PNAS USA* **96**, 13399-13403.

Johnson, R. T., McFarland, H. F. & Levy, S. E. (1972). Age-dependent resistance to viral encephalitis: studies of infections due to Sindbis virus in mice. *J Infect Dis* **125**, 257-262.

Kaariainen, L. & Soderlund, H. (1978). Structure and replication of alpha-viruses. *Curr Top Microbiol Immunol* **82**, 15-69.

Kang, S. M., Cho, M. S., Seo, H., Yoon, C. J., Oh, S. K., Choi, Y. M. & Kim, D. W. (2007). Efficient Induction of Oligodendrocytes from Human Embryonic Stem Cells. *Stem Cells* **25**, 419-424.

Kao, C. C., Singh, P. & Ecker, D. J. (2001). De novo initiation of viral RNA-dependent RNA synthesis. *Virology* **287**, 251-260.

Karlsson, G. B. & Liljestrom, P. (2003). Live viral vectors: Semliki Forest virus. *Methods Mol Med* **87**, 69-82.

Karpf, A. R., Lenches, E., Strauss, E. G., Strauss, J. H. & Brown, D. T. (1997a). Superinfection exclusion of alphaviruses in three mosquito cell lines persistently infected with Sindbis virus. *J Virol* **71**, 7119-7123.

Karpf, A. R., Blake, J. M. & Brown, D. T. (1997b). Characterization of the infection of Aedes albopictus cell clones by Sindbis virus. *Virus Research* **50**, 1-13.

Kaspar, B. K., Vissel, B., Bengoechea, T., Crone, S., Randolph-Moore, L., Muller, R., Brandon, E. P., Schaffer, D., Verma, I. M., Lee, K. F., Heinemann, S. F. & Gage, F. H. (2002). Adeno-associated virus effectively mediates conditional gene modification in the brain. *PNAS, USA* **99**, 2320-2325.

Kilby, N. J., Snaith, M. R. & Murray, J. A. (1993). Site-specific recombinases: tools for genome engineering. *Trends Genet* **9**, 413-421.

Kim, J., Dittgen, T., Nimmerjahn, A., Waters, J., Pawlak, V., Helmchen, F., Schlesinger, S., Seeburg, P. H. & Osten, P. (2004). Sindbis vector SINrep(nsP2S726): a tool for rapid heterologous expression with attenuated cytotoxicity in neurons. *Journal of Neuroscience Methods* **133**, 81-90.

Klimstra, W. B., Ryman, K. D., Bernard, K. A., Nguyen, K. B., Biron, C. A. & Johnston, R. E. (1999). Infection of Neonatal Mice with Sindbis Virus Results in a Systemic Inflammatory Response Syndrome. *J Virol* **73**, 10387-10398.

Klimstra, W. B., Ryman, K. D. & Johnston, R. E. (1998). Adaptation of Sindbis virus to BHK cells selects for use of heparan sulfate as an attachment receptor. *J Virol* **72**, 7357-7366.

Klimstra, W. B., Nangle, E. M., Smith, M. S., Yurochko, A. D. & Ryman, K. D. (2003).DC-SIGN and L-SIGN Can Act as Attachment Receptors for Alphaviruses and Distinguish between Mosquito Cell- and Mammalian Cell-Derived Viruses. *J Virol* **77**, 12022-12032.

Kuhn, R. J. (2007).*Togaviridae*: The Viruses and Their Replication. Field's Virology, Knipe, M. D., Howley, M. H., 5th edn, pp. 1001-1022: Lippincott Williams & Wilkins.

Kuhn, R. J., Griffin, D. E., Zhang, H., Niesters, H. G. & Strauss, J. H. (1992). Attenuation of Sindbis virus neurovirulence by using defined mutations in nontranslated regions of the genome RNA. *J Virol* **66**, 7121-7127.

Kujala, P., Ikaheimonen, A., Ehsani, N., Vihinen, H., Auvinen, P. & Kaariainen, L. (2001). Biogenesis of the Semliki Forest Virus RNA Replication Complex. *J Virol* **75**, 3873-3884.

Laakkonen, P., Ahola, T. & Kaariainen, L. (1996). The effects of palmitoylation on membrane association of Semliki forest virus RNA capping enzyme. *J Biol Chem* **271**, 28567-28571.

Laakkonen, P., Hyvonen, M., Peranen, J. & Kaariainen, L. (1994). Expression of Semliki Forest virus nsP1-specific methyltransferase in insect cells and in Escherichia coli. *J Virol* **68**, 7418-7425.

LaStarza, M. W., Lemm, J. A. & Rice, C. M. (1994). Genetic analysis of the nsP3 region of Sindbis virus: evidence for roles in minus-strand and subgenomic RNA synthesis. *J Virol* **68**, 5781-5791.

Lastarza, M. W., Grakoui, A. & Rice, C. M. (1994). Deletion and Duplication Mutations in the C-Terminal Nonconserved Region of Sindbis Virus nsP3: Effects on Phosphorylation and on Virus Replication in Vertebrate and Invertebrate Cells. *Virology* **202**, 224-232.

Lee, L. & Sadowski, P. D. (2003). Sequence of the loxP Site Determines the Order of Strand Exchange by the Cre Recombinase. *Journal of Molecular Biology* **326**, 397-412.

Lemm, J. A. & Rice, C. M. (1993a). Assembly of functional Sindbis virus RNA replication complexes: requirement for coexpression of P123 and P34. *J Virol* **67**, 1905-1915.

Lemm, J. A. & Rice, C. M. (1993b). Roles of nonstructural polyproteins and cleavage products in regulating Sindbis virus RNA replication and transcription. *J Virol* **67**, 1916-1926.

Lemm, J. A., Rumenapf, T., Strauss, E. G., Strauss, J. H. & Rice, C. M. (1994). Polypeptide requirements for assembly of functional Sindbis virus replication complexes: a model for the temporal regulation of minus- and plus-strand RNA synthesis. *EMBO J* **13**, 2925-2934.

Levine, B., Goldman, J. E., Jiang, H. H., Griffin, D. E. & Hardwick, J. M. (1996). Bc1-2 protects mice against fatal alphavirus encephalitis. *PNAS USA* **93**, 4810-4815.

Levine, B. & Griffin, D. E. (1992). Persistence of viral RNA in mouse brains after recovery from acute alphavirus encephalitis. *J Virol* **66**, 6429-6435.

Levine, B., Hardwick, J. M., Trapp, B. D., Crawford, T. O., Bollinger, R. C. & Griffin, D. E. (1991). Antibody-mediated clearance of alphavirus infection from neurons. *Science* **254**, 856-860.

Li, Y., Pan, Z., Ji, Y., Peng, T., Archard, L. C. & Zhang, H. (2002). Enterovirus replication in valvular tissue from patients with chronic rheumatic heart disease. *Eur Heart J* **23**, 567-573.

Liang, L., Tanaka, M., Kawaguchi, Y. & Baines, J. D. (2004). Cell lines that support replication of a novel herpes simplex virus 1 UL31 deletion mutant can properly target UL34 protein to the nuclear rim in the absence of UL31. *Virology* **329**, 68-76.

Liljestrom, P. & Garoff, H. (1991).A new generation of animal cell expression vectors based on the Semliki Forest virus replicon. *Biotechnology (N Y)* **9**, 1356-1361.

Lindsay, M., Oliveira, N., Jasinska, E., Johansen, C., Harrington, S., Wright, A. E. & Smith, D. (1996). An outbreak of Ross River virus disease in Southwestern Australia. *Emerg Infect Dis* **2**, 117-120.

Linn, M. L., Aaskov, J. G. & Suhrbier, A. (1996). Antibody-dependent enhancement and persistence in macrophages of an arbovirus associated with arthritis. *J Gen Virol* 77, 407-411.

Loewy, A., Smyth, J., von Bonsdorff, C. H., Liljestrom, P. & Schlesinger, M. J. (1995). The 6-kilodalton membrane protein of Semliki Forest virus is involved in the budding process. *J Virol* **69**, 469-475.

Loonstra, A., Vooijs, M., Beverloo, H. B., Allak, B. A., van Drunen, E., Kanaar, R., Berns, A. & Jonkers, J. (2001). Growth inhibition and DNA damage induced by Cre recombinase in mammalian cells. *PNAS* **98**, 9209-9214.

Loot, A. E., Henning, R. H., Deelman, L. E., Tio, R. A., Schoen, P., Wilschut, J. C., van Gilst, W. H. & Roks, A. J. (2004). Semliki Forest virus is an efficient and selective vector for gene delivery in infarcted rat heart. *J Mol Cell Cardiol* **37**, 137-142.

Lu, Y. E., Cassese, T. & Kielian, M. (1999). The cholesterol requirement for sindbis virus entry and exit and characterization of a spike protein region involved in cholesterol dependence. *J Virol* **73**, 4272-4278.

Lulla, A., Lulla, V., Tints, K., Ahola, T. & Merits, A. (2006). Molecular determinants of substrate specificity for Semliki Forest virus nonstructural protease. *J Virol* **80**, 5413-5422.

Lundstrom, K. (1997). Alphaviruses as expression vectors. *Curr Opin Biotechnol* **8**, 578-582.

Lundstrom, K., Abenavoli, A., Malgaroli, A. & Ehrengruber, M. U. (2003). Novel semliki forest virus vectors with reduced cytotoxicity and temperature sensitivity for long-term enhancement of transgene expression. *Molecular Therapy* **7**, 202-209.

Lundstrom, K., Schweitzer, C., Rotmann, D., Hermann, D., Schneider, E. M. & Ehrengruber, M. U. (2001). Semliki Forest virus vectors: efficient vehicles for in vitro and in vivo gene delivery. *FEBS Letters* **504**, 99-103.

Lustig, S., Jackson, A. C., Hahn, C. S., Griffin, D. E., Strauss, E. G. & Strauss, J. H. (1988). Molecular basis of Sindbis virus neurovirulence in mice. *J Virol* **62**, 2329-2336.

Mabruk, M. J., Glasglow, G. M., Flack, A. M., Folan, J. C., Bannigan, J. G., Smyth, J. M., O'Sullivan, M. A., Sheahan, B. J. & Atkins, G. J. (1989). Effect of infection with the ts22 mutant of Semliki Forest virus on development of the central nervous system in the fetal mouse. *J Virol* **63**, 4027-4033.

Mao, X., Fujiwara, Y., Chapdelaine, A., Yang, H. & Orkin, S. H. (2001). Activation of EGFP expression by Cre-mediated excision in a new ROSA26 reporter mouse strain. *Blood* **97**, 324-326.

Mathiot, C. C., Grimaud, G., Garry, P., Bouquety, J. C., Mada, A., Daguisy, A. M. & Georges, A. J. (1990). An outbreak of human Semliki Forest virus infections in Central African Republic. *Am J Trop Med Hyg* **42**, 386-393.

Matthews, A. E., Weiss, S. R., Shlomchik, M. J., Hannum, L. G., Gombold, J. L. & Paterson, Y. (2001). Antibody is required for clearance of infectious murine hepatitis virus A59 from the central nervous system, but not the liver. *J Immunol* **167**, 5254-5263.

Mattion, N. M., Harnish, E. C., Crowley, J. C. & Reilly, P. A. (1996). Foot-and-mouth disease virus 2A protease mediates cleavage in attenuated Sabin 3 poliovirus vectors engineered for delivery of foreign antigens. *J Virol* **70**, 8124-8127.

McGavern, D. B., Homann, D. & Oldstone, M. B. (2002).T cells in the central nervous system: the delicate balance between viral clearance and disease. *J Infect Dis* **186 Suppl 2**, S145-S151.

McInerney, G. M., Smit, J. M., Liljestrom, P. & Wilschut, J. (2004). Semliki Forest virus produced in the absence of the 6K protein has an altered spike structure as revealed by decreased membrane fusion capacity. *Virology* **325**, 200-206.

McKimmie, C. S. & Fazakerley, J. K. (2005). In response to pathogens, glial cells dynamically and differentially regulate Toll-like receptor gene expression. *Journal of Neuroimmunology* **169**, 116-125.

Mehta, S., Pathak, S. & Webb, H. E. (1990). Induction of membrane proliferation in mouse CNS by gold sodium thiomalate with reference to increased virulence of the avirulent Semliki Forest virus. *Biosci Rep* **10**, 271-279.

Meinkoth, J. & Kennedy, S. I. (1980). Semliki forest virus persistence in mouse L929 cells. *Virology* **100**, 141-155.

Melancon, P. & Garoff, H. (1986). Reinitiation of translocation in the Semliki Forest virus structural polyprotein: identification of the signal for the E1 glycoprotein. *EMBO J* **5**, 1551-1560.

Mellink, J. J. (1982). Estimation of the amount of Venezuelan equine encephalomyelitis virus transmitted by a single infected Aedes aegypti (Diptera: Culicidae). *J Med Entomol* **19**, 275-280.

Merits, A., Vasiljeva, L., Ahola, T., Kaariainen, L. & Auvinen, P. (2001). Proteolytic processing of Semliki Forest virus-specific non-structural polyprotein by nsP2 protease. *J Gen Virol* **82**, 765-773.

Mi, S. & Stollar, V. (1991). Expression of Sindbis virus nsP1 and methyltransferase activity in Escherichia coli. *Virology* **184**, 423-427.

Miron, M. J., Gallouzi, I. E., Lavoie, J. N. & Branton, P. E. (2004). Nuclear localization of the adenovirus E4orf4 protein is mediated through an arginine-rich motif and correlates with cell death. *Oncogene* **23**, 7458-7468.

Mitchell, C. J., Niebylski, M. L., Smith, G. C., Karabatsos, N., Martin, D., Mutebi, J. P., Craig, G. B., Jr. & Mahler, M. J. (1992). Isolation of eastern equine encephalitis virus from Aedes albopictus in Florida. *Science* **257**, 526-527.

Mokhtarian, F., Huan, C. M., Roman, C. & Raine, C. S. (2003). Semliki Forest virus-induced demyelination and remyelination--involvement of B cells and anti-myelin antibodies. *J Neuroimmunol* **137**, 19-31.

Mokhtarian, F., Shi, Y., Zhu, P. F. & Grob, D. (1994). Immune responses, and autoimmune outcome, during virus infection of the central nervous system. *Cell Immunol* **157**, 195-210.

Moradpour, D., Evans, M. J., Gosert, R., Yuan, Z., Blum, H. E., Goff, S. P., Lindenbach, B. D. & Rice, C. M. (2004). Insertion of Green Fluorescent Protein into Nonstructural Protein 5A Allows Direct Visualization of Functional Hepatitis C Virus Replication Complexes. *J Virol* **78**, 7400-7409.

Morozov, A., Kellendonk, C., Simpson, E. & Tronche, F. (2003). Using conditional mutagenesis to study the brain. *Biological Psychiatry* **54**, 1125-1133.

Morris, M. M., Dyson, H., Baker, D., Harbige, L. S., Fazakerley, J. K. & Amor, S. (1997). Characterization of the cellular and cytokine response in the central nervous system following Semliki Forest virus infection. *J Neuroimmunol* **74**, 185-197.

Morris-Downes, M. M., Phenix, K. V., Smyth, J., Sheahan, B. J., Lileqvist, S., Mooney, D. A., Liljestrom, P., Todd, D. & Atkins, G. J. (2001). Semliki Forest virus-based vaccines: persistence, distribution and pathological analysis in two animal systems. *Vaccine* **19**, 1978-1988.

Mrkic, B., Pavlovic, J., Rulicke, T., Volpe, P., Buchholz, C. J., Hourcade, D., Atkinson, J. P., Aguzzi, A. & Cattaneo, R. (1998). Measles virus spread and pathogenesis in genetically modified mice. *J Virol* **72**, 7420-7427.

Mueller, S. & Wimmer, E. (1998). Expression of Foreign Proteins by Poliovirus Polyprotein Fusion: Analysis of Genetic Stability Reveals Rapid Deletions and Formation of Cardioviruslike Open Reading Frames. *J Virol* **72**, 20-31.

Muller, U., Steinhoff, U., Reis, L. F., Hemmi, S., Pavlovic, J., Zinkernagel, R. M. & Aguet, M. (1994). Functional role of type I and type II interferons in antiviral defense. *Science* **264**, 1918-1921.

Nagy, A. (2000). Cre recombinase: the universal reagent for genome tailoring. *Genesis* **26**, 99-109.

Navarro, J. C., Medina, G., Vasquez, C., Coffey, L. L., Wang, E., Suarez, A., Biord, H., Salas, M. & Weaver, S. C. (2005). Postepizootic persistence of

Venezuelan equine encephalitis virus, Venezuela. *Emerg Infect Dis* **11**, 1907-1915.

Nordstrom, E. K. L., Forsell, M. N. E., Barnfield, C., Bonin, E., Hanke, T., Sundstrom, M., Karlsson, G. B. & Liljestrom, P. (2005). Enhanced immunogenicity using an alphavirus replicon DNA vaccine against human immunodeficiency virus type 1. *J Gen Virol* **86**, 349-354.

Oliver, K. R. & Fazakerley, J. K. (1997). Transneuronal spread of Semliki Forest virus in the developing mouse olfactory system is determined by neuronal maturity. *Neuroscience* **82**, 867-877.

Oliver, K. R., Scallan, M. F., Dyson, H. & Fazakerley, J. K. (1997). Susceptibility to a neurotropic virus and its changing distribution in the developing brain is a function of CNS maturity. *J Neurovirol* **3**, 38-48.

Pachner, A. R., Li, L. & Narayan, K. (2007). Intrathecal antibody production in an animal model of multiple sclerosis. *Journal of Neuroimmunology* **185**, 57-63.

Paredes, A. M., Brown, D. T., Rothnagel, R., Chiu, W., Schoepp, R. J., Johnston, R. E. & Prasad, B. V. (1993). Three-dimensional structure of a membrane-containing virus. *PNAS, USA* **90**, 9095-9099.

Pathak, S. & Webb, H. E. (1978). An electron-microscopic study of avirulent and virulent Semliki forest virus in the brains of different ages of mice. *J Neurol Sci* **39**, 199-211.

Peranen, J. & Kaariainen, L. (1991). Biogenesis of type I cytopathic vacuoles in Semliki Forest virus-infected BHK cells. *J Virol* **65**, 1623-1627.

Peranen, J., Rikkonen, M., Liljestrom, P. & Kaariainen, L. (1990). Nuclear localization of Semliki Forest virus-specific nonstructural protein nsP2. *J Virol* **64**, 1888-1896.

Perri, S., Driver, D. A., Gardner, J. P., Sherrill, S., Belli, B. A., Dubensky, T. W., Jr. & Polo, J. M. (2000). Replicon Vectors Derived from Sindbis Virus and Semliki Forest Virus That Establish Persistent Replication in Host Cells. *J Virol* **74**, 9802-9807.

Petrakova, O., Volkova, E., Gorchakov, R., Paessler, S., Kinney, R. M. & Frolov, I. (2005). Noncytopathic Replication of Venezuelan Equine Encephalitis Virus and Eastern Equine Encephalitis Virus Replicons in Mammalian Cells. *J Virol* **79**, 7597-7608.

Pfeifer, A., Brandon, E. P., Kootstra, N., Gage, F. H. & Verma, I. M. (2001). Delivery of the Cre recombinase by a self-deleting lentiviral vector: Efficient gene targeting in vivo. *PNAS* **98**, 11450-11455.

Phalen, T. & Kielian, M. (1991). Cholesterol is required for infection by Semliki Forest virus. *J Cell Biol* **112**, 615-623.

Pierro, D. J., Myles, K. M., Foy, B. D., Beaty, B. J. & Olson, K. E. (2003). Development of an orally infectious Sindbis virus transducing system that efficiently disseminates and expresses green fluorescent protein in Aedes aegypti. *Insect Molecular Biology* **12**, 107-116.

Polo, J. M., Belli, B. A., Driver, D. A., Frolov, I., Sherrill, S., Hariharan, M. J., Townsend, K., Perri, S., Mento, S. J., Jolly, D. J., Chang, S. M., Schlesinger, S. & Dubensky, T. W., Jr. (1999). Stable alphavirus packaging cell lines for Sindbis virus and Semliki Forest virus-derived vectors. *PNAS* **96**, 4598-4603.

Powers, A. M., Brault, A. C., Shirako, Y., Strauss, E. G., Kang, W., Strauss, J. H. & Weaver, S. C. (2001). Evolutionary Relationships and Systematics of the Alphaviruses. *J Virol* **75**, 10118-10131.

Pugachev, K. V., Mason, P. W., Shope, R. E. & Frey, T. K. (1995). Double-Subgenomic Sindbis Virus Recombinants Expressing Immunogenic Proteins of Japanese Encephalitis Virus Induce Significant Protection in Mice against Lethal JEV Infection. *Virology* **212**, 587-594.

Pugachev, K. V., Tzeng, W. P. & Frey, T. K. (2000). Development of a Rubella Virus Vaccine Expression Vector: Use of a Picornavirus Internal Ribosome Entry Site Increases Stability of Expression. *J Virol* **74**, 10811-10815.

Pushko, P., Parker, M., Ludwig, G. V., Davis, N. L., Johnston, R. E. & Smith, J. F. (1997). Replicon-helper systems from attenuated Venezuelan equine encephalitis virus: expression of heterologous genes in vitro and immunization against heterologous pathogens in vivo. *Virology* **239**, 389-401.

Pusztai, R., Gould, E. A. & Smith, H. (1971). Infection patterns in mice of an avirulent and virulent strain of Semliki Forest virus. *Br J Exp Pathol* **52**, 669-677.

Raju, R. & Huang, H. V. (1991). Analysis of Sindbis virus promoter recognition in vivo, using novel vectors with two subgenomic mRNA promoters. *J Virol* **65**, 2501-2510.

Rice, C. M., Levis, R., Strauss, J. H. & Huang, H. V. (1987). Production of infectious RNA transcripts from Sindbis virus cDNA clones: mapping of lethal mutations, rescue of a temperature-sensitive marker, and in vitro mutagenesis to generate defined mutants. *J Virol* **61**, 3809-3819.

Rikkonen, M. (1996). Functional Significance of the Nuclear-Targeting and NTP-Binding Motifs of Semliki Forest Virus Nonstructural Protein nsP2. *Virology* **218**, 352-361.

Rikkonen, M., Peranen, J. & Kaariainen, L. (1992). Nuclear and nucleolar targeting signals of Semliki Forest virus nonstructural protein nsP2. *Virology* **189**, 462-473.

Rikkonen, M., Peranen, J. & Kaariainen, L. (1994a).ATPase and GTPase activities associated with Semliki Forest virus nonstructural protein nsP2. *J Virol* **68**, 5804-5810.

Rikkonen, M., Peranen, J. & Kaariainen, L. (1994b). Nuclear targeting of Semliki Forest virus nsP2. *Arch Virol Suppl* **9**, 369-377.

Rivas, F., Diaz, L. A., Cardenas, V. M., Daza, E., Bruzon, L., Alcala, A., De la, H. O., Caceres, F. M., Aristizabal, G., Martinez, J. W., Revelo, D., De la, H. F., Boshell, J., Camacho, T., Calderon, L., Olano, V. A., Villarreal, L. I., Roselli, D., Alvarez, G., Ludwig, G. & Tsai, T. (1997). Epidemic Venezuelan equine encephalitis in La Guajira, Colombia, 1995. *J Infect Dis* **175**, 828-832.

Rodriguez, M., Pavelko, K. D., Njenga, M. K., Logan, W. C. & Wettstein, P. J. (1996). The balance between persistent virus infection and immune cells determines demyelination. *J Immunol* **157**, 5699-5709.

Rubio, N., Rodriguez, R. & Arevalo, M. A. (2004). In vitro myelination by oligodendrocyte precursor cells transfected with the neurotrophin-3 gene. *Glia* **47**, 78-87.

Ryan, M. D. & Drew, J. (1994). Foot-and-mouth disease virus 2A oligopeptide mediated cleavage of an artificial polyprotein. *EMBO J* **13**, 928-933.

Ryan, M. D., King, A. M. & Thomas, G. P. (1991). Cleavage of foot-and-mouth disease virus polyprotein is mediated by residues located within a 19 amino acid sequence. *J Gen Virol* **72**, 2727-2732.

Ryman, K. D., Klimstra, W. B., Nguyen, K. B., Biron, C. A. & Johnston, R. E. (2000). Alpha/beta interferon protects adult mice from fatal Sindbis virus infection and is an important determinant of cell and tissue tropism. *J Virol* **74**, 3366-3378.

Ryman, K. D., Meier, K. C., Nangle, E. M., Ragsdale, S. L., Korneeva, N. L., Rhoads, R. E., MacDonald, M. R. & Klimstra, W. B. (2005). Sindbis Virus Translation Is Inhibited by a PKR/RNase L-Independent Effector Induced by Alpha/Beta Interferon Priming of Dendritic Cells. *J Virol* **79**, 1487-1499.

Salonen, A., Ahola, T. & Kaariainen, L. (2005). Viral RNA replication in association with cellular membranes. *Curr Top Microbiol Immunol* **285**, 139-173.

Salonen, A., Vasiljeva, L., Merits, A., Magden, J., Jokitalo, E. & Kaariainen, L. (2003). Properly Folded Nonstructural Polyprotein Directs the Semliki Forest Virus Replication Complex to the Endosomal Compartment. *J Virol* **77**, 1691-1702.

Sammin, D. J., Butler, D., Atkins, G. J. & Sheahan, B. J. (1999). Cell death mechanisms in the olfactory bulb of rats infected intranasally with Semliki forest virus. *Neuropathol Appl Neurobiol* **25**, 236-243.

Santagati, M. G., Maatta, J. A., Itaranta, P. V., Salmi, A. A. & Hinkkanen, A. E. (1995). The Semliki Forest virus E2 gene as a virulence determinant. *J Gen Virol* **76**, 47-52.

Sato, Y., Shiraishi, Y. & Furuichi, T. (2004). Cell specificity and efficiency of the Semliki forest virus vector- and adenovirus vector-mediated gene expression in mouse cerebellum. *Journal of Neuroscience Methods* **137**, 111-121.

Sauer, B. & Henderson, N. (1988). Site-specific DNA recombination in mammalian cells by the Cre recombinase of bacteriophage P1. *PNAS, USA* **85**, 5166-5170.

Sauer, B. & Henderson, N. (1989). Cre-stimulated recombination at loxP-containing DNA sequences placed into the mammalian genome. *Nucleic Acids Res* **17**, 147-161.

Sawicki, D. L., Perri, S., Polo, J. M. & Sawicki, S. G. (2006). Role for nsP2 Proteins in the Cessation of Alphavirus Minus-Strand Synthesis by Host Cells. *J Virol* **80**, 360-371.

Scallan, M. F., Allsopp, T. E. & Fazakerley, J. K. (1997).bcl-2 acts early to restrict Semliki Forest virus replication and delays virus-induced programmed cell death. *J Virol* **71**, 1583-1590.

Scallan, M. F. & Fazakerley, J. K. (1999). Aurothiolates enhance the replication of Semliki Forest virus in the CNS and the exocrine pancreas. *J Neurovirol* **5**, 392-400.

Schneider-Schaulies, S., Schneider-Schaulies, J., Bayer, M., Loffler, S. & Ter, M., V (1993). Spontaneous and differentiation-dependent regulation of measles virus gene expression in human glial cells. *J Virol* **67**, 3375-3383.

Schoneboom, B. A., Fultz, M. J., Miller, T. H., McKinney, L. C. & Grieder, F. B. (1999). Astrocytes as targets for Venezuelan equine encephalitis virus infection. *J Neurovirol* **5**, 342-354.

Schubert, S., Moller-Ehrlich, K., Singethan, K., Wiese, S., Duprex, W. P., Rima, B. K., Niewiesk, S. & Schneider-Schaulies, J. (2006).A mouse model of persistent brain infection with recombinant Measles virus. *J Gen Virol* **87**, 2011-2019.

Schuffenecker, I., Iteman, I., Michault, A., Murri, S., Frangeul, L., Vaney, M. C., Lavenir, R., Pardigon, N., Reynes, J. M., Pettinelli, F., Biscornet, L., Diancourt, L., Michel, S., Duquerroy, S., Guigon, G., Frenkiel, M. P., Brehin, A. C., Cubito, N., Despres, P., Kunst, F., Rey, F. A., Zeller, H. & Brisse, S. (2006). Genome microevolution of chikungunya viruses causing the Indian Ocean outbreak. *PLoS Med* **3**, e263.

Scott, T. W. & Weaver, S. C. (1989). Eastern equine encephalomyelitis virus: epidemiology and evolution of mosquito transmission. *Adv Virus Res* **37**, 277-328.

Seamer, J., Randles, W. J. & Fitzgeorge, R. (1967). The course of Semliki Forest virus infection in mice. *Br J Exp Pathol* **48**, 395-402.

Shafee, N. & AbuBakar, S. (2003). Dengue virus type 2 NS3 protease and NS2B-NS3 protease precursor induce apoptosis. *J Gen Virol* **84**, 2191-2195.

Sherman, L. A. & Griffin, D. E. (1990). Pathogenesis of encephalitis induced in newborn mice by virulent and avirulent strains of Sindbis virus. *J Virol* **64**, 2041-2046.

Shirako, Y. & Strauss, J. H. (1994). Regulation of Sindbis virus RNA replication: uncleaved P123 and nsP4 function in minus-strand RNA synthesis, whereas cleaved products from P123 are required for efficient plus-strand RNA synthesis. *J Virol* **68**, 1874-1885.

Silver, D. P. & Livingston, D. M. (2001). Self-Excising Retroviral Vectors Encoding the Cre Recombinase Overcome Cre-Mediated Cellular Toxicity. *Molecular Cell* **8**, 233-243.

Sims, A. C., Baric, R. S., Yount, B., Burkett, S. E., Collins, P. L. & Pickles, R. J. (2005). Severe Acute Respiratory Syndrome Coronavirus Infection of Human Ciliated Airway Epithelia: Role of Ciliated Cells in Viral Spread in the Conducting Airways of the Lungs. *J Virol* **79**, 15511-15524.

Singh, I. & Helenius, A. (1992). Role of ribosomes in Semliki Forest virus nucleocapsid uncoating. *J Virol* **66**, 7049-7058.

Sinnayah, P., Lazartigues, E., Sakai, K., Sharma, R. V., Sigmund, C. D. & Davisson, R. L. (2006). Genetic Ablation of Angiotensinogen in the Subfornical Organ of the Brain Prevents the Central Angiotensinergic Pressor Response. *Circ Res* **99**, 1125-1131.

Sinnayah, P., Lindley, T. E., Staber, P. D., Davidson, B. L., Cassell, M. D. & Davisson, R. L. (2004). Targeted viral delivery of Cre recombinase induces conditional gene deletion in cardiovascular circuits of the mouse brain. *Physiol Genomics* **18**, 25-32.

Sjoberg, E. M., Suomalainen, M. & Garoff, H. (1994).A significantly improved Semliki Forest virus expression system based on translation enhancer segments from the viral capsid gene. *Biotechnology (N Y)* **12**, 1127-1131.

Smerdou, C. & Liljestrom, P. (1999). Two-Helper RNA System for Production of Recombinant Semliki Forest Virus Particles. *J Virol* **73**, 1092-1098.

Smillie, J., Pusztai, R. & Smith, H. (1973). Studies of the influence of host deference mechanisms on infection of mice with an avirulent or virulent strain of Semliki Forest virus. *Br J Exp Pathol* **54**, 260-266.

Smith, R. M., Walton, C. M., Wu, C. H. & Wu, G. Y. (2002). Secondary Structure and Hybridization Accessibility of Hepatitis C Virus 3'-Terminal Sequences. *J Virol* **76**, 9563-9574.

Smith, T. J., Cheng, R. H., Olson, N. H., Peterson, P., Chase, E., Kuhn, R. J. & Baker, T. S. (1995). Putative receptor binding sites on alphaviruses as visualized by cryoelectron microscopy. *PNAS, USA* **92**, 10648-10652.

Smithburn, K. C. & Haddow, W. J. (1944). Semliki Forest virus. I. Isolation and pathogenic properties. *J Immunol* **49**, 141-145.

Smyth, J. M. B., Sheahan, B. J. & Atkins, G. J. (1990). Multiplication of virulent and demyelinating Semliki Forest virus in the mouse central nervous system: consequences in BALB/c and SJL mice. *J Gen Virol* **71**, 2575-2583.

Soilu-Hanninen, M., Eralinna, J. P., Hukkanen, V., Roytta, M., Salmi, A. A. & Salonen, R. (1994). Semliki Forest virus infects mouse brain endothelial cells and causes blood-brain barrier damage. *J Virol* **68**, 6291-6298.

Srinivas, S., Watanabe, T., Lin, C. S., William, C., Tanabe, Y., Jessell, T. & Costantini, F. (2001). Cre reporter strains produced by targeted insertion of EYFP and ECFP into the ROSA26 locus. *BMC Developmental Biology* **1**, 4.

Strauss, E. G., Rice, C. M. & Strauss, J. H. (1983). Sequence coding for the alphavirus nonstructural proteins is interrupted by an opal termination codon. *PNAS, USA* **80**, 5271-5275.

Strauss, J. H. & Strauss, E. G. (1994). The alphaviruses: gene expression, replication, and evolution. *Microbiol Rev* **58**, 491-562.

Subak-Sharpe, I., Dyson, H. & Fazakerley, J. (1993). In vivo depletion of CD8+ T cells prevents lesions of demyelination in Semliki Forest virus infection. *J Virol* **67**, 7629-7633.

Suckling, A. J., Jagelman, S. & Webb, H. E. (1982). Immunoglobulin synthesis in nude (nu/nu), nu/+ and reconstituted nu/nu mice infected with a demyelinating strain of Semliki Forest virus. *Clin Exp Immunol* **47**, 283-288.

Suopanki, J., Sawicki, D. L., Sawicki, S. G. & Kaariainen, L. (1998). Regulation of alphavirus 26S mRNA transcription by replicase component nsP2. *J Gen Virol* **79**, 309-319.

Takkinen, K. (1986). Complete nucleotide sequence of the nonstructural protein genes of Semliki Forest virus. *Nucleic Acids Res* **14**, 5667-5682.

Tamberg, N., Lulla, V., Fragkoudis, R., Lulla, A., Fazakerley, J. K. & Merits, A. (2007). Insertion of EGFP into the replicase gene of Semliki Forest virus results in a novel, genetically stable marker virus. *J Gen Virol* **88**, 1225-1230.

Tarbatt, C. J., Glasgow, G. M., Mooney, D. A., Sheahan, B. J. & Atkins, G. J. (1997). Sequence analysis of the avirulent, demyelinating A7 strain of Semliki Forest virus. *J Gen Virol* **78**, 1551-1557.

Tashiro, A., Zhao, C. & Gage, F. H. (2007). Retrovirus-mediated single-cell gene knockout technique in adult newborn neurons in vivo. *Nat Protocols* **1**, 3049-3055.

ten Dam, E., Flint, M. & Ryan, M. D. (1999). Virus-encoded proteinases of the Togaviridae. *J Gen Virol* **80**, 1879-1888.

Thevenot, E., Cote, F., Colin, P., He, Y., Leblois, H., Perricaudet, M., Mallet, J. & Vodjdani, G. (2003). Targeting conditional gene modification into the serotonin neurons of the dorsal raphe nucleus by viral delivery of the Cre recombinase. *Molecular and Cellular Neuroscience* **24**, 139-147.

Thomas, J. M., Klimstra, W. B., Ryman, K. D. & Heidner, H. W. (2003). Sindbis Virus Vectors Designed To Express a Foreign Protein as a Cleavable Component of the Viral Structural Polyprotein. *J Virol* **77**, 5598-5606.

Trgovcich, J., Aronson, J. F., Eldridge, J. C. & Johnston, R. E. (1999).TNFalpha, interferon, and stress response induction as a function of age-related susceptibility to fatal Sindbis virus infection of mice. *Virology* **263**, 339-348.

Tsien, J. Z., Chen, D. F., Gerber, D., Tom, C., Mercer, E. H., Anderson, D. J., Mayford, M., Kandel, E. R. & Tonegawa, S. (1996). Subregion- and cell type-restricted gene knockout in mouse brain. *Cell* **87**, 1317-1326.

Tsuji, M., Bergmann, C. C., Takita-Sonoda, Y., Murata, K., Rodrigues, E. G., Nussenzweig, R. S. & Zavala, F. (1998). Recombinant Sindbis viruses expressing a cytotoxic T-lymphocyte epitope of a malaria parasite or of influenza virus elicit protection against the corresponding pathogen in mice. *J Virol* **72**, 6907-6910.

Tubulekas, I., Berglund, P., Fleeton, M. & Liljestrom, P. (1997). Alphavirus expression vectors and their use as recombinant vaccines: a minireview. *Gene* **190**, 191-195.

Tucker, P. C., Lee, S. H., Bui, N., Martinie, D. & Griffin, D. E. (1997). Amino acid changes in the Sindbis virus E2 glycoprotein that increase neurovirulence improve entry into neuroblastoma cells. *J Virol* **71**, 6106-6112.

Tuittila, M. T., Santagati, M. G., Roytta, M., Maatta, J. A. & Hinkkanen, A. E. (2000). Replicase Complex Genes of Semliki Forest Virus Confer Lethal Neurovirulence. *J Virol* **74**, 4579-4589.

Ubol, S., Levine, B., Lee, S. H., Greenspan, N. S. & Griffin, D. E. (1995). Roles of immunoglobulin valency and the heavy-chain constant domain in antibody-mediated downregulation of Sindbis virus replication in persistently infected neurons. *J Virol* **69**, 1990-1993.

Vaha-Koskela, M. J., Tuittila, M. T., Nygardas, P. T., Nyman, J. K., Ehrengruber, M. U., Renggli, M. & Hinkkanen, A. E. (2003).A novel neurotropic expression vector based on the avirulent A7(74) strain of Semliki Forest virus. *J Neurovirol* **9**, 1-15.

Vaha-Koskela, M. J. V., Kallio, J. P., Jansson, L. C., Heikkila, J. E., Zakhartchenko, V. A., Kallajoki, M. A., Kahari, V. M. & Hinkkanen, A. E. (2006). Oncolytic Capacity of Attenuated Replicative Semliki Forest Virus in Human Melanoma Xenografts in Severe Combined Immunodeficient Mice. *Cancer Res* **66**, 7185-7194.

van den Born, E., Posthuma, C. C., Knoops, K. & Snijder, E. J. (2007). An infectious recombinant equine arteritis virus expressing green fluorescent protein from its replicase gene. *J Gen Virol* **88**, 1196-1205.

van den Born, E., Stein, D. A., Iversen, P. L. & Snijder, E. J. (2005). Antiviral activity of morpholino oligomers designed to block various aspects of Equine arteritis virus amplification in cell culture. *J Gen Virol* **86**, 3081-3090.

Van den Plas, D., Ponsaerts, P., Van Tendeloo, V., Van Bockstaele, D. R., Berneman, Z. N. & Merregaert, J. (2003). Efficient removal of LoxP-flanked genes by electroporation of Cre-recombinase mRNA. *Biochemical and Biophysical Research Communications* **305**, 10-15.

van der Meer, Y., van Tol, H., Krijnse Locker, J. & Snijder, E. J. (1998).ORF1a-Encoded Replicase Subunits Are Involved in the Membrane Association of the Arterivirus Replication Complex. *J Virol* **72**, 6689-6698.

Vanlandingham, D. L., Tsetsarkin, K., Hong, C., Klingler, K., McElroy, K. L., Lehane, M. J. & Higgs, S. (2005). Development and characterization of a double subgenomic chikungunya virus infectious clone to express heterologous genes in Aedes aegypti mosqutioes. *Insect Biochemistry and Molecular Biology* **35**, 1162-1170.

Varshavsky, A. (1996). The N-end rule: functions, mysteries, uses. *PNAS, USA* **93**, 12142-12149.

Vasiljeva, L., Merits, A., Auvinen, P. & Kaariainen, L. (2000). Identification of a Novel Function of the Alphavirus Capping Apparatus. RNA 5'-Triphosphatase Activity Of Nsp2. *J Biol Chem* **275**, 17281-17287.

Vasiljeva, L., Merits, A., Golubtsov, A., Sizemskaja, V., Kaariainen, L. & Ahola, T. (2003). Regulation of the Sequential Processing of Semliki Forest Virus Replicase Polyprotein. *J Biol Chem* **278**, 41636-41645.

Vasiljeva, L., Valmu, L., Kaariainen, L. & Merits, A. (2001). Site-specific Protease Activity of the Carboxyl-terminal Domain of Semliki Forest Virus Replicase Protein nsP2. *J Biol Chem* **276**, 30786-30793.

Ventoso, I., Sanz, M. A., Molina, S., Berlanga, J. J., Carrasco, L. & Esteban, M. (2006). Translational resistance of late alphavirus mRNA to eIF2{alpha} phosphorylation: a strategy to overcome the antiviral effect of protein kinase PKR. *Genes Dev* **20**, 87-100.

Vernon, P. S. & Griffin, D. E. (2005). Characterization of an In Vitro Model of Alphavirus Infection of Immature and Mature Neurons. *J Virol* **79**, 3438-3447.

Vihinen, H., Ahola, T., Tuittila, M., Merits, A. & Kaariainen, L. (2001). Elimination of Phosphorylation Sites of Semliki Forest Virus Replicase Protein nsP3. *J Biol Chem* **276**, 5745-5752.

Vodkin, M. H., McLaughlin, G. L., Day, J. F., Shope, R. E. & Novak, R. J. (1993).A Rapid Diagnostic Assay for Eastern Equine Encephalomyelitis Viral RNA. *Am J Trop Med Hyg* **49**, 772-776.

Voziyanov, Y., Pathania, S. & Jayaram, M. (1999).A general model for site-specific recombination by the integrase family recombinases. *Nucleic Acids Res* **27**, 930-941.

Wahlberg, J. M., Bron, R., Wilschut, J. & Garoff, H. (1992). Membrane fusion of Semliki Forest virus involves homotrimers of the fusion protein. *J Virol* **66**, 7309-7318.

Wahlberg, J. M. & Garoff, H. (1992). Membrane fusion process of Semliki Forest virus. I: Low pH-induced rearrangement in spike protein quaternary structure precedes virus penetration into cells. *J Cell Biol* **116**, 339-348.

Wang, K. S., Kuhn, R. J., Strauss, E. G., Ou, S. & Strauss, J. H. (1992). High-affinity laminin receptor is a receptor for Sindbis virus in mammalian cells. *J Virol* **66**, 4992-5001.

Wang, Y. F., Sawicki, S. G. & Sawicki, D. L. (1994). Alphavirus nsP3 functions to form replication complexes transcribing negative-strand RNA. *J Virol* **68**, 6466-6475.

Weaver, S. C., (2006). Evolutionary Influences in Arboviral Disease. *Curr Top Microbiol Immunol* **299**, 285-314.

Wengler, G., Gros, C. & Wengler, G. (1996). Analyses of the role of structural changes in the regulation of uncoating and assembly of alphavirus cores. *Virology* **222**, 123-132.

White, J. & Helenius, A. (1980).pH-dependent fusion between the Semliki Forest virus membrane and liposomes. *PNAS, USA* **77**, 3273-3277.

Willems, W. R., Kaluza, G., Boschek, C. B., Bauer, H., Hager, H., Schutz, H. J. & Feistner, H. (1979). Semliki forest virus: cause of a fatal case of human encephalitis. *Science* **203**, 1127-1129.

Wu, J. Z. (2001). Internally located signal peptides direct hepatitis C virus polyprotein processing in the ER membrane. *IUBMB Life* **51**, 19-23.

Xiong, C., Levis, R., Shen, P., Schlesinger, S., Rice, C. M. & Huang, H. V. (1989). Sindbis virus: an efficient, broad host range vector for gene expression in animal cells. *Science* **243**, 1188-1191.

Xu, G., Wilson, W., Mecham, J., Murphy, K., Zhou, E. M. & Tabachnick, W. (1997).VP7: an attachment protein of bluetongue virus for cellular receptors in Culicoides variipennis. *J Gen Virol* **78**, 1617-1623.

Yamaga, A. K. & Ou, J. h. (2002). Membrane Topology of the Hepatitis C Virus NS2 Protein. *J Biol Chem* **277**, 33228-33234.

Zhimin Liang and Guangpu Li (2005). Recombinant Sindbis virus expressing functional GFP in the nonstructural protein nsP3. 9 edn, pp. 317-323.

Zhuang, X., Masson, J., Gingrich, J. A., Rayport, S. & Hen, R. (2005). Targeted gene expression in dopamine and serotonin neurons of the mouse brain. *Journal of Neuroscience Methods* **143**, 27-32.

Zusinaite, E., Tints, K., Kiiver, K., Spuul, P., Karo-Astover, L., Merits, A. & Sarand, I. (2007). Mutations at the palmitoylation site of non-structural protein nsP1 of Semliki Forest virus attenuate virus replication and cause accumulation of compensatory mutations. *J Gen Virol* **88**, 1977-1985.

Appendix I: Common Solutions and Reagents

Common solutions and reagents used in this thesis are appended here:

Virus-Like Particles and Viruses

TNE buffer:

To make 10X TNE buffer for long-term storage of viruses and virus-like particles the following recipe was followed:

In 800 ml of dH_2O 12.1 g of Trizma Base (Sigma, UK), 3.7 g of disodium EDTA (Sigma, UK) and 116.8 g NaCl (Sigma, UK) were added. The pH was adjusted to 7.4 and the solution was made up to a final volume of 1 L. Following autoclaving 10X TNE buffer was diluted with nuclease-free water (Sigma, UK) to give 1X TNE and used.

Centrifuges and Centrifuge Rotors

For clarification of supernatants a Beckman J2-21 centrifuge and the JA-20 rotor was used. For ultracentrifugation of VLP and virus stocks through sucrose cushions a Beckman L8-70M ultracentrifuge and the SW-28 swing-out rotor was used.

***In vitro* transcription**

Reagents used in the *in vitro* transcription reaction were

10X SP6 buffer. This was custom made and it contained the following:

400 mM HEPES potassium salt (Sigma, UK) pH adjusted to 7.4.
60 mM magnesium acetate tetrahydrate (Sigma, UK).
20 mM Spermidine trihydrochoride (Sigma, UK).
The buffer was filter sterilised using a 0.22 µm filter (Sartorius, bought through SLS, UK).
M^7GpppG (cap analog) was purchased from Amersham Biosciences, UK.
DTT was purchased from Sigma, UK.
rNTPs used were purchased from Amersham Biosciences, UK in the form of stock solutions (40 mM) ATP, CTP, UTP and GTP.
H_2O (DNase, RNase-free water) was purchased from Sigma, UK.
RNAsin inhibitor was purchased from Promega, UK.
SP6 RNA polymerase was purchased from Amersham Biosciences, UK.

Animal work

PBSA was made by adding 3.75 g of Bovine Serum Albumin (Sigma, UK) in 500 ml of dH_2O. The solution was filter sterilised through a 0.22 μm Sartorius filter (SLS, UK).
RNA*later* for the storage of animal tissues for RNA extraction was purchased either from Sigma, UK or Ambion, UK.
OCT medium was purchased from the European branch of Sakura, Japan.

Immunostaining

Triton X-100 was purchased from BDH, UK.
Proteinase K was purchased from Sigma, UK.
To-Pro nuclear marker was a Molecular Probes product (Invitrogen, UK).
Propidium iodide containing mounting medium was purchased from VectorLabs, USA.
PBS was purchased in the form of tablets from VWR international (UK branch).
CAS block is a Zymed, US product. The company is now part of Invitrogen, UK.

Cell Lines

All media used in this thesis were purchased from Gibco, UK. The company is now part of Invitrogen, UK.

Western Blotting

0.5 M Tris-base pH 6.8
30 g Tris-base
500 ml dH_2O
pH to 6.8
Tris-base was purchased from Sigma, UK.

1.5M Tris-base pH8.8
98.6 g Tris-base
500 ml dH_2O
pH to 8.8

10% APS (ammonium persulphate)

1 g APS (Sigma, UK)

10 ml dH_2O
Preferably, use fresh, alternatively store at -20^0C in 100 μl aliquots

Resolving Gel (12% Acrylamide)

30 ml 40% Acrylamide (Sigma, UK)
43 ml dH_2O
25 ml 1.5M Tris-base pH8.8

1 ml 10% SDS
Store at 4^0C in dark, max 1 month

Stacking Gel (4% Acrylamide)

10 ml 40% Acrylamide (Sigma, UK)
64 ml dH_2O
25 ml 0.5M Tris-base pH6.8
1 ml 10% SDS
Store at 4^0C in dark, max 1 month

Running Buffer

BioRad 10x Tris/Glycine/SDS Buffer
(BioRad, UK)
Dilute to 1x with dH_2O

Transfer Buffer

3.03 g Tris-base
14.4 g Glycine (Sigma, UK)
200 ml Methanol (Sigma, UK)
800 ml dH_2O

PBST

999 ml 1x PBS (VWR International, UK Branch)
1 ml Triton X-100 (BDH, UK)

Blocking Solution

10 g Dried Milk
200 ml PBST (Tween-20 was purchased from BDH, UK).
Spin ~1500 rpm, 5min to remove any lumps

Laemmli Sample Buffer, 2x

(Sigma, UK. Store at -20^0C)
Mix 1:1 with sample

ECL Kit was purchased from Amersham Biosciences, UK.

Hybond ECL Nitrocellulose was purchased from Amersham, Biosciences, UK.

RNA extraction

RNeasy Lipid tissue kit is a product of Qiagen, UK.

Reverse transcription and Polymerase Chain Reaction (PCR)

For RT-PCR the SuperScript II RNase H^+ reverse transcriptase enzyme kit (Invitrogen, UK) was used. OligodT primer, dNTPs and RNasin inhibitor were purchased from Promega, UK. Nuclease-free water was purchased from Sigma, UK. For PCR, *Pfx* DNA polymerase was purchased from Invitrogen, UK. *Taq* polymerase was purchased from Promega.

Agarose Gel Electrophoresis

Agarose gels were made using 0.5M TBE buffer and agarose powder purchased from Promega, UK. The synthesis of the TBE buffer was:

1 litre 5X TBE buffer stock
54 g Tris Base
27.5 g boric acid
20 ml 0.5M EDTA (pH 8)

All reagents were from Sigma, UK.

DNA ladders used for size comparisons were purchased from New England Biolabs, UK.

Molecular Cloning

Two different commercially available cloning kits were used for the purposes of this project; Zero-Blunt TOPO obtained from Invitrogen, UK. And pGEM-T Easy kit obtained from Promega, UK.
For dephosphorylation of linearised vectors calf intestinal alkaline phosphatase (CIAP) was used. This was purchased from Roche, UK.
To purify digested plasmids the Jetquick PCR purification kit (Genomed, Germany) was used.

Bacterial Techniques

Two different strains of recombinant *E. coli* bacteria were used during this project. DH5α (Invitrogen, UK) and XL-10 gold (Stratagene, UK). To grow liquid cultures LB (Luria-Bertani) medium was used. The composition of LB medium was 10 grams tryptone, 5 grams of yeast extract, 10 grams of NaCl. This was purchased as premixed powder from Fischer, UK and 15 grams of the powder mix were added to 500 ml of dH_2O. The medium was then autoclaved and used.
Following transformation a rich medium was used to help recovery of bacteria. The medium of choice was SOC (Invitrogen, UK). The composition of SOC medium is as that of LB with the addition of KCl, $MgCl_2$, $MgSO_4$ and glucose

Sequencing

For sequence analysis the BioEdit software of Ibis Biosciences (USA) was used.

Appendix II: Sequencing

Sequencing of recombination products of SFV4(3H)-eGFP.

The beginning of PCR primers is marked with red for the forward primer (in nsP3) and brown for the reverse primer in nsP4.
30 aa from end of nsP3 are highlighted with yellow.
nsP2 protease recognition sites are highlighted with blue.
The start codon of eGFP is highlighted with red.
When a nucleotide is missing (deletion) this is marked with a —.

>del843

```
                ....|....| ....|....| ....|....| ....|....| ....|....| ....|....|
                     5         15         25         35         45         55
(3H)-eGFP       ATACCATGTA GATGGGGTGC AGAAGGTAAA GTGCGAGAAG GTTCTCCTGT TCGACCCGAC
del843          ATACCATGTA GATGGGGTGC AGAAGGTAAA GTGCGAGAAG GTTCTCCTGT TCGACCCGAC

                ....|....| ....|....| ....|....| ....|....| ....|....| ....|....|
                    65         75         85         95        105        115
(3H)-eGFP       GGTACCTTCA GTGGTTAGTC CGCGGAAGTA TGCCGCATCT ACGACGGACC ACTCAGATCG
del843          GGTACCTTCA GTGGTTAGTC CGCGGAAGTA TGCCGCATCT ACGACGGACC ACTCAGATCG

                ....|....| ....|....| ....|....| ....|....| ....|....| ....|....|
                   125        135        145        155        165        175
(3H)-eGFP       GTCGTTACGA GGGTTTGACT TGGACTGGAC CACCGACTCG TCTTCCACTG CCAGCGATAC
del843          GTCGTTACGA GGGTTTGACT TGGACTGGAC CACCGACTCG TCTTCCACTG CCAGCGATAC

                ....|....| ....|....| ....|....| ....|....| ....|....| ....|....|
                   185        195        205        215        225        235
(3H)-eGFP       CATGTCGCTA CCCAGTTTGC AGTCGTGTGA CATCGACTCG ATCTACGAGC CAATGGCTCC
del843          CATGTCGCTA CCCAGTTTGC AGTCGTGTGA CATCGACTCG ATCTACGAGC CAATGGCTCC

                ....|....| ....|....| ....|....| ....|....| ....|....| ....|....|
                   245        255        265        275        285        295
(3H)-eGFP       CATAGTAGTG ACGGCTGACG TACACCCTGA ACCCGCAGGC ATCGCGGACC TGGCGGCAGA
del843          CATAGTAGTG ACGGCTGACG TACACCCTGA ACCCGCAGGC ATCGCGGACC TGGCGGCAGA

                ....|....| ....|....| ....|....| ....|....| ....|....| ....|....|
                   305        315        325        335        345        355
(3H)-eGFP       TGTGCACCCT GAACCCGCAG ACCATGTGGA CCTCGAGAAC CCGATTCCTC CACCGCGCCC
del843          TGTGCACCCT GAACCCGCAG ACCATGTGGA CCTCGAGAAC CCGATTCCTC CACCGCGCCC

                ....|....| ....|....| ....|....| ....|....| ....|....| ....|....|
                   365        375        385        395        405        415
(3H)-eGFP       GAAGAGAGCT GCATACCTTG CCTCCCGCGC GGCGGAGCGA CCGGTGCCGG CGCCGAGAAA
del843          GAAGAGAGCT GCATACCTTG CCTCCCGCGC GGCGGAGCGA CCGGTGCCGG CGCCGAGAAA

                ....|....| ....|....| ....|....| ....|....| ....|....| ....|....|
                   425        435        445        455        465        475
(3H)-eGFP       GCCGACGCCT GCCCCAAGGA CTGCGTTTAG GAACAAGCTG CCTTTGACGT TCGGCGACTT
del843          GCCGACGCCT GCCCCAAGGA CTGCGTTTAG GAACAAGCTG CCTTTGACGT TCGGCGACTT

                ....|....| ....|....| ....|....| ....|....| ....|....| ....|....|
                   485        495        505        515        525        535
(3H)-eGFP       TGACGAGCAC GAGGTCGATG CGTTGGCCTC CGGGATTACT TTCGGAGACT TCGACGACGT
del843          TGACGAGCAC GAGGTCGATG CGTTGGCCTC CGGGATTACT TTCGGAGACT TCGACGACGT

                ....|....| ....|....| ....|....| ....|....| ....|....| ....|....|
                   545        555        565        575        585        595
(3H)-eGFP       CCTGCGACTA GGCCGCGCGG GTGCAGGGAT TTTCTCCTCG GACACTGGGC CCGGGATGGT
del843          CCTGCGACTA GGCCGCGCGG GTGCAGGGAT TTTCTCCTCG GACACTG--- ----------

                ....|....| ....|....| ....|....| ....|....| ....|....| ....|....|
                   605        615        625        635        645        655
(3H)-eGFP       GAGCAAGGGC GAGGAGCTGT TCACCGGGGT GGTGCCCATC CTGGTCGAGC TGGACGGCGA
del843          ---------- ---------- ---------- ---------- ---------- ----------
```

```
                ....|....| ....|....| ....|....| ....|....| ....|....| ....|....|
                   665        675        685        695        705        715
(3H)-eGFP       CGTAAACGGC CACAAGTTCA GCGTGTCCGG CGAGGGCGAG GGCGATGCCA CCTACGGCAA
del843          ---------- ---------- ---------- ---------- ---------- ----------

                ....|....| ....|....| ....|....| ....|....| ....|....| ....|....|
                   725        735        745        755        765        775
(3H)-eGFP       GCTGACCCTG AAGTTCATCT GCACCACCGG CAAGCTGCCC GTGCCCTGGC CCACCCTCGT
del843          ---------- ---------- ---------- ---------- ---------- ----------

                ....|....| ....|....| ....|....| ....|....| ....|....| ....|....|
                   785        795        805        815        825        835
(3H)-eGFP       GACCACCCTG ACCTACGGCG TGCAGTGCTT CAGCCGCTAC CCCGACCACA TGAAGCAGCA
del843          ---------- ---------- ---------- ---------- ---------- ----------

                ....|....| ....|....| ....|....| ....|....| ....|....| ....|....|
                   845        855        865        875        885        895
(3H)-eGFP       CGACTTCTTC AAGTCCGCCA TGCCCGAAGG CTACGTCCAG GAGCGCACCA TCTTCTTCAA
del843          ---------- ---------- ---------- ---------- ---------- ----------

                ....|....| ....|....| ....|....| ....|....| ....|....| ....|....|
                   905        915        925        935        945        955
(3H)-eGFP       GGACGACGGC AACTACAAGA CCCGCGCCGA GGTGAAGTTC GAGGGCGACA CCCTGGTGAA
del843          ---------- ---------- ---------- ---------- ---------- ----------

                ....|....| ....|....| ....|....| ....|....| ....|....| ....|....|
                   965        975        985        995       1005       1015
(3H)-eGFP       CCGCATCGAG CTGAAGGGCA TCGACTTCAA GGAGGACGGC AACATCCTGG GGCACAAGCT
del843          ---------- ---------- ---------- ---------- ---------- ----------

                ....|....| ....|....| ....|....| ....|....| ....|....| ....|....|
                  1025       1035       1045       1055       1065       1075
(3H)-eGFP       GGAGTACAAC TACAACAGCC ACAACGTCTA TATCATGGCC GACAAGCAGA AGAACGGCAT
del843          ---------- ---------- ---------- ---------- ---------- ----------

                ....|....| ....|....| ....|....| ....|....| ....|....| ....|....|
                  1085       1095       1105       1115       1125       1135
(3H)-eGFP       CAAGGTGAAC TTCAAGATCC GCCACAACAT CGAGGACGGC AGCGTGCAGC TCGCCGACCA
del843          ---------- ---------- ---------- ---------- ---------- ----------

                ....|....| ....|....| ....|....| ....|....| ....|....| ....|....|
                  1145       1155       1165       1175       1185       1195
(3H)-eGFP       CTACCAGCAG AACACCCCCA TCGGCGACGG CCCCGTGCTG CTGCCCGACA ACCACTACCT
del843          ---------- ---------- ---------- ---------- ---------- ----------

                ....|....| ....|....| ....|....| ....|....| ....|....| ....|....|
                  1205       1215       1225       1235       1245       1255
(3H)-eGFP       GAGCACCCAG TCCGCCCTGA GCAAAGACCC CAACGAGAAG CGCGATCACA TGGTCCTGCT
del843          ---------- ---------- ---------- ---------- ---------- ----------

                ....|....| ....|....| ....|....| ....|....| ....|....| ....|....|
                  1265       1275       1285       1295       1305       1315
(3H)-eGFP       GGAGTTCGTG ACCGCCGCCG GGATCACTCT CGGCATGGAC GAGCTGTACA AGGGATCCGA
del843          ---------- ---------- ---------- ---------- ---------- ----------

                ....|....| ....|....| ....|....| ....|....| ....|....| ....|....|
                  1325       1335       1345       1355       1365       1375
(3H)-eGFP       CTTTGACGAG CACGAGGTCG ATGCGTTGGC CTCCGGGATT ACTTTCGGAG ACTTCGACGA
del843          ---------- ---------- ---------- ---------- ---------- ----------
```

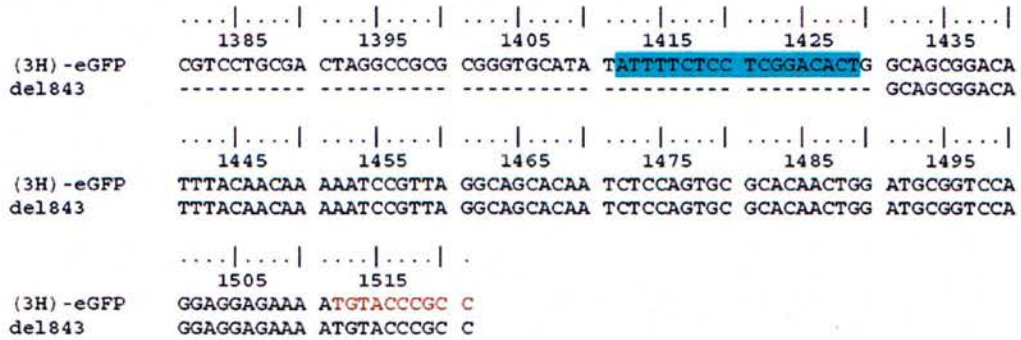
....|....| ....|....| ....|....| ....|....| ....|....| ....|....|
1385 1395 1405 1415 1425 1435
(3H)-eGFP CGTCCTGCGA CTAGGCCGCG CGGGTGCATA TATTTTCTCC TCGGACACTG GCAGCGGACA
del843 ---------- ---------- ---------- ---------- ---------- GCAGCGGACA
....|....| ....|....| ....|....| ....|....| ....|....| ....|....|
1445 1455 1465 1475 1485 1495
(3H)-eGFP TTTACAACAA AAATCCGTTA GGCAGCACAA TCTCCAGTGC GCACAACTGG ATGCGGTCCA
del843 TTTACAACAA AAATCCGTTA GGCAGCACAA TCTCCAGTGC GCACAACTGG ATGCGGTCCA
....|....| ....|....| .
1505 1515
(3H)-eGFP GGAGGAGAAA ATGTACCCGC C
del843 GGAGGAGAAA ATGTACCCGC C

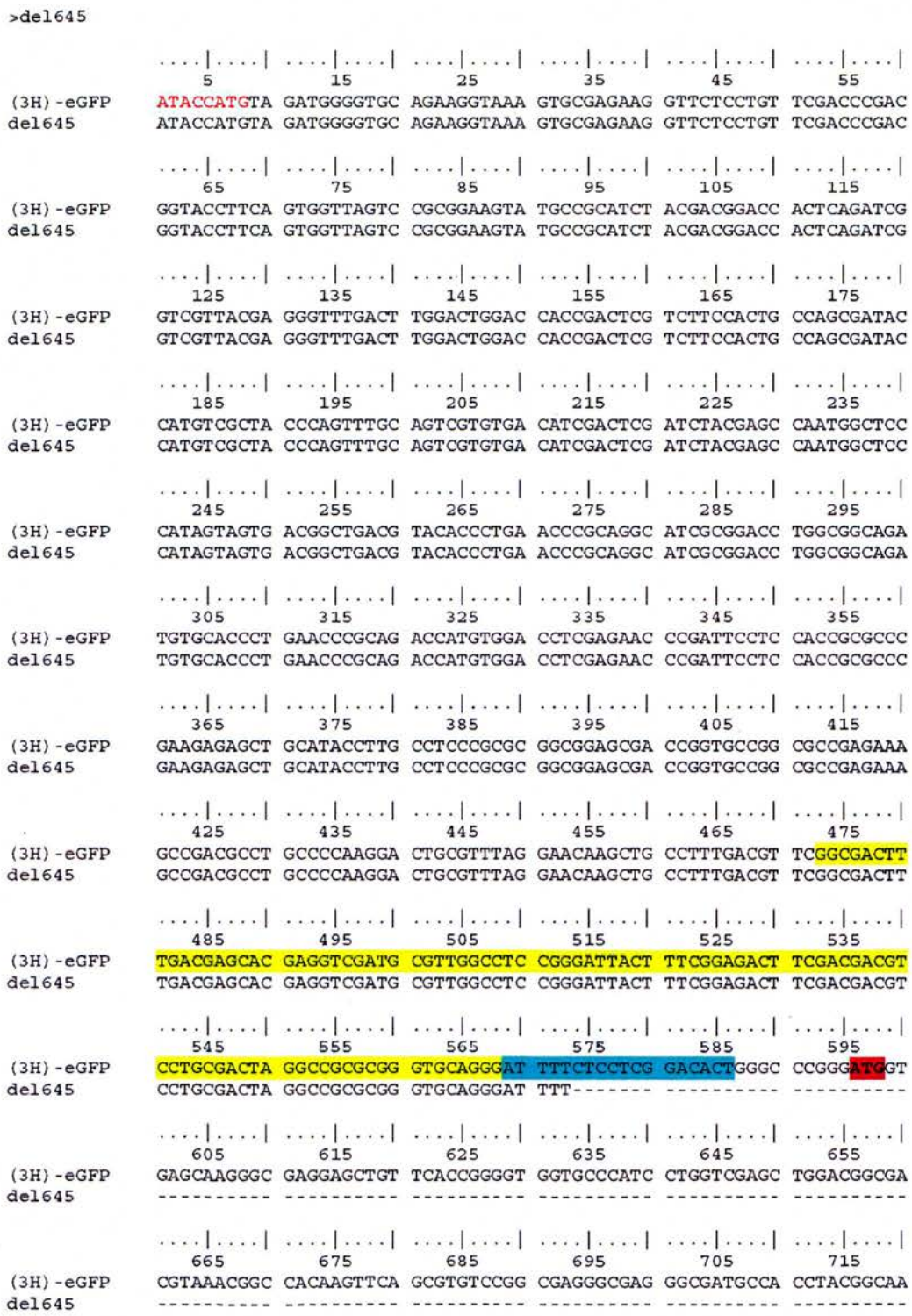
>del645
5 15 25 35 45 55
(3H)-eGFP ATACCATGTA GATGGGGTGC AGAAGGTAAA GTGCGAGAAG GTTCTCCTGT TCGACCCGAC
del645 ATACCATGTA GATGGGGTGC AGAAGGTAAA GTGCGAGAAG GTTCTCCTGT TCGACCCGAC
65 75 85 95 105 115
(3H)-eGFP GGTACCTTCA GTGGTTAGTC CGCGGAAGTA TGCCGCATCT ACGACGGACC ACTCAGATCG
del645 GGTACCTTCA GTGGTTAGTC CGCGGAAGTA TGCCGCATCT ACGACGGACC ACTCAGATCG
125 135 145 155 165 175
(3H)-eGFP GTCGTTACGA GGGTTTGACT TGGACTGGAC CACCGACTCG TCTTCCACTG CCAGCGATAC
del645 GTCGTTACGA GGGTTTGACT TGGACTGGAC CACCGACTCG TCTTCCACTG CCAGCGATAC
185 195 205 215 225 235
(3H)-eGFP CATGTCGCTA CCCAGTTTGC AGTCGTGTGA CATCGACTCG ATCTACGAGC CAATGGCTCC
del645 CATGTCGCTA CCCAGTTTGC AGTCGTGTGA CATCGACTCG ATCTACGAGC CAATGGCTCC
245 255 265 275 285 295
(3H)-eGFP CATAGTAGTG ACGGCTGACG TACACCCTGA ACCCGCAGGC ATCGCGGACC TGGCGGCAGA
del645 CATAGTAGTG ACGGCTGACG TACACCCTGA ACCCGCAGGC ATCGCGGACC TGGCGGCAGA
305 315 325 335 345 355
(3H)-eGFP TGTGCACCCT GAACCCGCAG ACCATGTGGA CCTCGAGAAC CCGATTCCTC CACCGCGCCC
del645 TGTGCACCCT GAACCCGCAG ACCATGTGGA CCTCGAGAAC CCGATTCCTC CACCGCGCCC
365 375 385 395 405 415
(3H)-eGFP GAAGAGAGCT GCATACCTTG CCTCCCGCGC GGCGGAGCGA CCGGTGCCGG CGCCGAGAAA
del645 GAAGAGAGCT GCATACCTTG CCTCCCGCGC GGCGGAGCGA CCGGTGCCGG CGCCGAGAAA
425 435 445 455 465 475
(3H)-eGFP GCCGACGCCT GCCCCAAGGA CTGCGTTTAG GAACAAGCTG CCTTTGACGT TCGGCGACTT
del645 GCCGACGCCT GCCCCAAGGA CTGCGTTTAG GAACAAGCTG CCTTTGACGT TCGGCGACTT
485 495 505 515 525 535
(3H)-eGFP TGACGAGCAC GAGGTCGATG CGTTGGCCTC CGGGATTACT TTCGGAGACT TCGACGACGT
del645 TGACGAGCAC GAGGTCGATG CGTTGGCCTC CGGGATTACT TTCGGAGACT TCGACGACGT
545 555 565 575 585 595
(3H)-eGFP CCTGCGACTA GGCCGCGCGG GTGCAGGGAT TTTCTCCTCG GACACTGGGC CCGGGATGGT
del645 CCTGCGACTA GGCCGCGCGG GTGCAGGGAT TTT------- ---------- ----------
605 615 625 635 645 655
(3H)-eGFP GAGCAAGGGC GAGGAGCTGT TCACCGGGGT GGTGCCCATC CTGGTCGAGC TGGACGGCGA
del645 ---------- ---------- ---------- ---------- ---------- ----------
665 675 685 695 705 715
(3H)-eGFP CGTAAACGGC CACAAGTTCA GCGTGTCCGG CGAGGGCGAG GGCGATGCCA CCTACGGCAA
del645 ---------- ---------- ---------- ---------- ---------- ----------

```
                ....|....| ....|....| ....|....| ....|....| ....|....| ....|....|
                   725        735        745        755        765        775
(3H)-eGFP       GCTGACCCTG AAGTTCATCT GCACCACCGG CAAGCTGCCC GTGCCCTGGC CCACCCTCGT
del645          ---------- ---------- ---------- ---------- ---------- ----------

                ....|....| ....|....| ....|....| ....|....| ....|....| ....|....|
                   785        795        805        815        825        835
(3H)-eGFP       GACCACCCTG ACCTACGGCG TGCAGTGCTT CAGCCGCTAC CCCGACCACA TGAAGCAGCA
del645          ---------- ---------- ---------- ---------- ---------- ----------

                ....|....| ....|....| ....|....| ....|....| ....|....| ....|....|
                   845        855        865        875        885        895
(3H)-eGFP       CGACTTCTTC AAGTCCGCCA TGCCCGAAGG CTACGTCCAG GAGCGCACCA TCTTCTTCAA
del645          ---------- ---------- ---------- ---------- ---------- ----------

                ....|....| ....|....| ....|....| ....|....| ....|....| ....|....|
                   905        915        925        935        945        955
(3H)-eGFP       GGACGACGGC AACTACAAGA CCCGCGCCGA GGTGAAGTTC GAGGGCGACA CCCTGGTGAA
del645          ---------- ---------- ---------- ---------- ---------- ----------

                ....|....| ....|....| ....|....| ....|....| ....|....| ....|....|
                   965        975        985        995       1005       1015
(3H)-eGFP       CCGCATCGAG CTGAAGGGCA TCGACTTCAA GGAGGACGGC AACATCCTGG GGCACAAGCT
del645          ---------- ---------- ---------- ---------- ---------- ----------

                ....|....| ....|....| ....|....| ....|....| ....|....| ....|....|
                  1025       1035       1045       1055       1065       1075
(3H)-eGFP       GGAGTACAAC TACAACAGCC ACAACGTCTA TATCATGGCC GACAAGCAGA AGAACGGCAT
del645          ---------- ---------- ---------- ---------- ---------- ----------

                ....|....| ....|....| ....|....| ....|....| ....|....| ....|....|
                  1085       1095       1105       1115       1125       1135
(3H)-eGFP       CAAGGTGAAC TTCAAGATCC GCCACAACAT CGAGGACGGC AGCGTGCAGC TCGCCGACCA
del645          ---------- ---------- ---------- ---------- ---------- ----------

                ....|....| ....|....| ....|....| ....|....| ....|....| ....|....|
                  1145       1155       1165       1175       1185       1195
(3H)-eGFP       CTACCAGCAG AACACCCCCA TCGGCGACGG CCCCGTGCTG CTGCCCGACA ACCACTACCT
del645          ---------- ---------- ---------- ---------- ---------- ----------

                ....|....| ....|....| ....|....| ....|....| ....|....| ....|....|
                  1205       1215       1225       1235       1245       1255
(3H)-eGFP       GAGCACCCAG TCCGCCCTGA GCAAAGACCC CAACGAGAAG CGCGATCACA TGGTCCTGCT
del645          ---------- ---------A GCAAAGACCC CAACGAGAAG CGCGATCACA TGGTCCTGCT

                ....|....| ....|....| ....|....| ....|....| ....|....| ....|....|
                  1265       1275       1285       1295       1305       1315
(3H)-eGFP       GGAGTTCGTG ACCGCCGCCG GGATCACTCT CGGCATGGAC GAGCTGTACA AGGGATCCGA
del645          GGAGTTCGTG ACCGCCGCCG GGATCACTCT CGGCATGGAC GAGCTGTACA AGGGATCCGA

                ....|....| ....|....| ....|....| ....|....| ....|....| ....|....|
                  1325       1335       1345       1355       1365       1375
(3H)-eGFP       CTTTGACGAG CACGAGGTCG ATGCGTTGGC CTCCGGGATT ACTTTCGGAG ACTTCGACGA
del645          CTTTGACGAG CACGAGGTCG ATGCGTTGGC CTCCGGGATT ACTTTCGGAG ACTTCGACGA

                ....|....| ....|....| ....|....| ....|....| ....|....| ....|....|
                  1385       1395       1405       1415       1425       1435
(3H)-eGFP       CGTCCTGCGA CTAGGCCGCG CGGGTGCATA TATTTTCTCC TCGGACACTG GCAGCGGACA
del645          CGTCCTGCGA CTAGGCCGCG CGGGTGCATA TATTTTCTCC TCGGACACTG GCAGCGGACA
```

```
                ....|....| ....|....| ....|....| ....|....| ....|....| ....|....|
                   1445       1455       1465       1475       1485       1495
(3H)-eGFP       TTTACAACAA AAATCCGTTA GGCAGCACAA TCTCCAGTGC GCACAACTGG ATGCGGTCCA
del645          TTTACAACAA AAATCCGTTA GGCAGCACAA TCTCCAGTGC GCACAACTGG ATGCGGTCCA

                ....|....| ....|....| .
                   1505       1515
(3H)-eGFP       GGAGGAGAAA ATGTACCCGC C
del645          GGAGGAGAAA ATGTACCCGC C
```

>del603

```
                 ....|....| ....|....| ....|....| ....|....| ....|....| ....|....|
                      5         15         25         35         45         55
(3H)-eGFP        ATACCATGTA GATGGGGTGC AGAAGGTAAA GTGCGAGAAG GTTCTCCTGT TCGACCCGAC
del603           ATACCATGTA GATGGGGTGC AGAAGGTAAA GTGCGAGAAG GTTCTCCTGT TCGACCCGAC

                 ....|....| ....|....| ....|....| ....|....| ....|....| ....|....|
                      65         75         85         95        105        115
(3H)-eGFP        GGTACCTTCA GTGGTTAGTC CGCGGAAGTA TGCCGCATCT ACGACGGACC ACTCAGATCG
del603           GGTACCTTCA GTGGTTAGTC CGCGGAAGTA TGCCGCATCT ACGACGGACC ACTCAGATCG

                 ....|....| ....|....| ....|....| ....|....| ....|....| ....|....|
                     125        135        145        155        165        175
(3H)-eGFP        GTCGTTACGA GGGTTTGACT TGGACTGGAC CACCGACTCG TCTTCCACTG CCAGCGATAC
del603           GTCGTTACGA GGGTTTGACT TGGACTGGAC CACCGACTCG TCTTCCACTG CCAGCGATAC

                 ....|....| ....|....| ....|....| ....|....| ....|....| ....|....|
                     185        195        205        215        225        235
(3H)-eGFP        CATGTCGCTA CCCAGTTTGC AGTCGTGTGA CATCGACTCG ATCTACGAGC CAATGGCTCC
del603           CATGTCGCTA CCCAGTTTGC AGTCGTGTGA CATCGACTCG ATCTACGAGC CAATGGCTCC

                 ....|....| ....|....| ....|....| ....|....| ....|....| ....|....|
                     245        255        265        275        285        295
(3H)-eGFP        CATAGTAGTG ACGGCTGACG TACACCCTGA ACCCGCAGGC ATCGCGGACC TGGCGGCAGA
del603           CATAGTAGTG ACGGCTGACG TACACCCTGA ACCCGCAGGC ATCGCGGACC TGGCGGCAGA

                 ....|....| ....|....| ....|....| ....|....| ....|....| ....|....|
                     305        315        325        335        345        355
(3H)-eGFP        TGTGCACCCT GAACCCGCAG ACCATGTGGA CCTCGAGAAC CCGATTCCTC CACCGCGCCC
del603           TGTGCACCCT GAACCCGCAG ACCATGTGGA CCTCGAGAAC CCGATTCCTC CACCGCGCCC

                 ....|....| ....|....| ....|....| ....|....| ....|....| ....|....|
                     365        375        385        395        405        415
(3H)-eGFP        GAAGAGAGCT GCATACCTTG CCTCCCGCGC GGCGGAGCGA CCGGTGCCGG CGCCGAGAAA
del603           GAAGAGAGCT GCATACCTTG CCTCCCGCGC GGCGGAGCGA CCGGTGCCGG CGCCGAGAAA

                 ....|....| ....|....| ....|....| ....|....| ....|....| ....|....|
                     425        435        445        455        465        475
(3H)-eGFP        GCCGACGCCT GCCCCAAGGA CTGCGTTTAG GAACAAGCTG CCTTTGACGT TCGGCGACTT
del603           GCCGACGCCT GCCCCAAGGA CTGCGTTTAG GAACAAGCTG CCTTTGACGT TCGGCGACTT

                 ....|....| ....|....| ....|....| ....|....| ....|....| ....|....|
                     485        495        505        515        525        535
(3H)-eGFP        TGACGAGCAC GAGGTCGATG CGTTGGCCTC CGGGATTACT TTCGGAGACT TCGACGACGT
del603           TGACGAGCAC GAGGTCGATG CGTTGGCCTC CGGGATTACT TTCGGAGACT TCGACGACGT

                 ....|....| ....|....| ....|....| ....|....| ....|....| ....|....|
                     545        555        565        575        585        595
(3H)-eGFP        CCTGCGACTA GGCCGCGCGG GTGCAGGGAT TTTCTCCTCG GACACTGGGC CCGGGATGGT
del603           CCTGCGACTA GGCCGCGCGG GTGCAGGGAT TTTCTCCTCG GACACT---- ----------

                 ....|....| ....|....| ....|....| ....|....| ....|....| ....|....|
                     605        615        625        635        645        655
(3H)-eGFP        GAGCAAGGGC GAGGAGCTGT TCACCGGGGT GGTGCCCATC CTGGTCGAGC TGGACGGCGA
del603           ---------- ---------- ---------- ---------- ---------- ----------

                 ....|....| ....|....| ....|....| ....|....| ....|....| ....|....|
                     665        675        685        695        705        715
(3H)-eGFP        CGTAAACGGC CACAAGTTCA GCGTGTCCGG CGAGGGCGAG GGCGATGCCA CCTACGGCAA
del603           ---------- ---------- ---------- ---------- ---------- ----------
```

```
                ....|....| ....|....| ....|....| ....|....| ....|....| ....|....|
                   725        735        745        755        765        775
(3H)-eGFP       GCTGACCCTG AAGTTCATCT GCACCACCGG CAAGCTGCCC GTGCCCTGGC CCACCCTCGT
del603          ---------- ---------- ---------- ---------- ---------- ----------

                ....|....| ....|....| ....|....| ....|....| ....|....| ....|....|
                   785        795        805        815        825        835
(3H)-eGFP       GACCACCCTG ACCTACGGCG TGCAGTGCTT CAGCCGCTAC CCCGACCACA TGAAGCAGCA
del603          ---------- ---------- ---------- ---------- ---------- ----------

                ....|....| ....|....| ....|....| ....|....| ....|....| ....|....|
                   845        855        865        875        885        895
(3H)-eGFP       CGACTTCTTC AAGTCCGCCA TGCCCGAAGG CTACGTCCAG GAGCGCACCA TCTTCTTCAA
del603          ---------- ---------- ---------- ---------- ---------- ----------

                ....|....| ....|....| ....|....| ....|....| ....|....| ....|....|
                   905        915        925        935        945        955
(3H)-eGFP       GGACGACGGC AACTACAAGA CCCGCGCCGA GGTGAAGTTC GAGGGCGACA CCCTGGTGAA
del603          ---------- ---------- ---------- ---------- ---------- ----------

                ....|....| ....|....| ....|....| ....|....| ....|....| ....|....|
                   965        975        985        995       1005       1015
(3H)-eGFP       CCGCATCGAG CTGAAGGGCA TCGACTTCAA GGAGGACGGC AACATCCTGG GGCACAAGCT
del603          ---------- ---------- ---------- ---------- ---------- ----------

                ....|....| ....|....| ....|....| ....|....| ....|....| ....|....|
                  1025       1035       1045       1055       1065       1075
(3H)-eGFP       GGAGTACAAC TACAACAGCC ACAACGTCTA TATCATGGCC GACAAGCAGA AGAACGGCAT
del603          ---------- ---------- ---------- ---------- ---------- ----------

                ....|....| ....|....| ....|....| ....|....| ....|....| ....|....|
                  1085       1095       1105       1115       1125       1135
(3H)-eGFP       CAAGGTGAAC TTCAAGATCC GCCACAACAT CGAGGACGGC AGCGTGCAGC TCGCCGACCA
del603          ---------- ---------- ---------- ---------- ---------- ----------

                ....|....| ....|....| ....|....| ....|....| ....|....| ....|....|
                  1145       1155       1165       1175       1185       1195
(3H)-eGFP       CTACCAGCAG AACACCCCCA TCGGCGACGG CCCCGTGCTG CTGCCCGACA ACCACTACCT
del603          ---------- ---------- ---------- ---------- ---------A ACCACTACCT

                ....|....| ....|....| ....|....| ....|....| ....|....| ....|....|
                  1205       1215       1225       1235       1245       1255
(3H)-eGFP       GAGCACCCAG TCCGCCCTGA GCAAAGACCC CAACGAGAAG CGCGATCACA TGGTCCTGCT
del603          GAGCACCCAG TCCGCCCTGA GCAAAGACCC CAACGAGAAG CGCGATCACA TGGTCCTGCT

                ....|....| ....|....| ....|....| ....|....| ....|....| ....|....|
                  1265       1275       1285       1295       1305       1315
(3H)-eGFP       GGAGTTCGTG ACCGCCGCCG GGATCACTCT CGGCATGGAC GAGCTGTACA AGGGATCCGA
del603          GGAGTTCGTG ACCGCCGCCG GGATCACTCT CGGCATGGAC GAGCTGTACA AGGGATCCGA

                ....|....| ....|....| ....|....| ....|....| ....|....| ....|....|
                  1325       1335       1345       1355       1365       1375
(3H)-eGFP       CTTTGACGAG CACGAGGTCG ATGCGTTGGC CTCCGGGATT ACTTTCGGAG ACTTCGACGA
del603          CTTTGACGAG CACGAGGTCG ATGCGTTGGC CTCCGGGATT ACTTTCGGAG ACTTCGACGA

                ....|....| ....|....| ....|....| ....|....| ....|....| ....|....|
                  1385       1395       1405       1415       1425       1435
(3H)-eGFP       CGTCCTGCGA CTAGGCCGCG CGGGTGCATA TATTTTCTCC TCGGACACTG GCAGCGGACA
del603          CGTCCTGCGA CTAGGCCGCG CGGGTGCATA TATTTTCTCC TCGGACACTG GCAGCGGACA
```

```
                ....|....| ....|....| ....|....| ....|....| ....|....| ....|....|
                   1445       1455       1465       1475       1485       1495
(3H)-eGFP       TTTACAACAA AAATCCGTTA GGCAGCACAA TCTCCAGTGC GCACAACTGG ATGCGGTCCA
del603          TTTACAACAA AAATCCGTTA GGCAGCACAA TCTCCAGTGC GCACAACTGG ATGCGGTCCA

                ....|....| ....|....| .
                   1505       1515
(3H)-eGFP       GGAGGAGAAA ATGTACCCGC C
del603          GGAGGAGAAA ATGTACCCGC C
```

>del537del75

```
                ....|....|  ....|....|  ....|....|  ....|....|  ....|....|  ....|....|
                     5          15          25          35          45          55
(3H)-eGFP       ATACCATGTA GATGGGGTGC AGAAGGTAAA GTGCGAGAAG GTTCTCCTGT TCGACCCGAC
del537del75     ATACCATGTA GATGGGGTGC AGAAGGTAAA GTGCGAGAAG GTTCTCCTGT TCGACCCGAC

                ....|....|  ....|....|  ....|....|  ....|....|  ....|....|  ....|....|
                     65          75          85          95          105         115
(3H)-eGFP       GGTACCTTCA GTGGTTAGTC CGCGGAAGTA TGCCGCATCT ACGACGGACC ACTCAGATCG
del537del75     GGTACCTTCA GTGGTTAGTC CGCGGAAGTA TGCCGCATCT ACGACGGACC ACTCAGATCG

                ....|....|  ....|....|  ....|....|  ....|....|  ....|....|  ....|....|
                    125         135         145         155         165         175
(3H)-eGFP       GTCGTTACGA GGGTTTGACT TGGACTGGAC CACCGACTCG TCTTCCACTG CCAGCGATAC
del537del75     GTCGTTACGA GGGTTTGACT TGGACTGGAC CACCGACTCG TCTTCCACTG CCAGCGATAC

                ....|....|  ....|....|  ....|....|  ....|....|  ....|....|  ....|....|
                    185         195         205         215         225         235
(3H)-eGFP       CATGTCGCTA CCCAGTTTGC AGTCGTGTGA CATCGACTCG ATCTACGAGC CAATGGCTCC
del537del75     CATGTCGCTA CCCAGTTTGC AGTCGTGTGA CATCGACTCG ATCTACGAGC CAATGGCTCC

                ....|....|  ....|....|  ....|....|  ....|....|  ....|....|  ....|....|
                    245         255         265         275         285         295
(3H)-eGFP       CATAGTAGTG ACGGCTGACG TACACCCTGA ACCCGCAGGC ATCGCGGACC TGGCGGCAGA
del537del75     CATAGTAGTG ACGGCTGACG TACACCCTGA ACCCGCAGGC ATCGCGGACC TGGCGGCAGA

                ....|....|  ....|....|  ....|....|  ....|....|  ....|....|  ....|....|
                    305         315         325         335         345         355
(3H)-eGFP       TGTGCACCCT GAACCCGCAG ACCATGTGGA CCTCGAGAAC CCGATTCCTC CACCGCGCCC
del537del75     TGTGCACCCT GAACCCGCAG ACCATGTGGA CCTCGAGAAC CCGATTCCTC CACCGCGCCC

                ....|....|  ....|....|  ....|....|  ....|....|  ....|....|  ....|....|
                    365         375         385         395         405         415
(3H)-eGFP       GAAGAGAGCT GCATACCTTG CCTCCCGCGC GGCGGAGCGA CCGGTGCCGG CGCCGAGAAA
del537del75     GAAGAGAGCT GCATACCTTG CCTCCCGCGC GGCGGAGCGA CCGGTGCCGG CGCCGAGAAA

                ....|....|  ....|....|  ....|....|  ....|....|  ....|....|  ....|....|
                    425         435         445         455         465         475
(3H)-eGFP       GCCGACGCCT GCCCCAAGGA CTGCGTTTAG GAACAAGCTG CCTTTGACGT TCGGCGACTT
del537del75     GCCGACGCCT GCCCCAAGGA CTGCGTTTAG GAACAAGCTG CCTTTGACGT TCGGCGACTT

                ....|....|  ....|....|  ....|....|  ....|....|  ....|....|  ....|....|
                    485         495         505         515         525         535
(3H)-eGFP       TGACGAGCAC GAGGTCGATG CGTTGGCCTC CGGGATTACT TTCGGAGACT TCGACGACGT
del537del75     TGACGAGCAC GAGGTCGATG CGTTGGCCTC CGGGAT---- ---------- ----------

                ....|....|  ....|....|  ....|....|  ....|....|  ....|....|  ....|....|
                    545         555         565         575         585         595
(3H)-eGFP       CCTGCGACTA GGCCGCGCGG GTGCAGGGAT TTTCTCCTCG GACACTGGGC CCGGGATGGT
del537del75     ---------- ---------- ---------- ---------- ---------- ----------

                ....|....|  ....|....|  ....|....|  ....|....|  ....|....|  ....|....|
                    605         615         625         635         645         655
(3H)-eGFP       GAGCAAGGGC GAGGAGCTGT TCACCGGGGT GGTGCCCATC CTGGTCGAGC TGGACGGCGA
del537del75     ---------- ---------- ---------- ---------- ---------- ----------
```

```
                ....|....| ....|....| ....|....| ....|....| ....|....| ....|....|
                   665        675        685        695        705        715
(3H)-eGFP5      CGTAAACGGC CACAAGTTCA GCGTGTCCGG CGAGGGCGAG GGCGATGCCA CCTACGGCAA
del537del75     ---------- ---------- ---------- ---------- ---------- ----------

                ....|....| ....|....| ....|....| ....|....| ....|....| ....|....|
                   725        735        745        755        765        775
(3H)-eGFP       GCTGACCCTG AAGTTCATCT GCACCACCGG CAAGCTGCCC GTGCCCTGGC CCACCCTCGT
del537del75     ---------- ---------- ---------- ---------- ---------- ----------

                ....|....| ....|....| ....|....| ....|....| ....|....| ....|....|
                   785        795        805        815        825        835
(3H)-eGFP       GACCACCCTG ACCTACGGCG TGCAGTGCTT CAGCCGCTAC CCCGACCACA TGAAGCAGCA
del537del75     ---------- ---------- ---------- ---------- ---------- ----------

                ....|....| ....|....| ....|....| ....|....| ....|....| ....|....|
                   845        855        865        875        885        895
(3H)-eGFP       CGACTTCTTC AAGTCCGCCA TGCCCGAAGG CTACGTCCAG GAGCGCACCA TCTTCTTCAA
del537del75     ---------- ---------- ---------- ---------- ---------- ----------

                ....|....| ....|....| ....|....| ....|....| ....|....| ....|....|
                   905        915        925        935        945        955
(3H)-eGFP       GGACGACGGC AACTACAAGA CCCGCGCCGA GGTGAAGTTC GAGGGCGACA CCCTGGTGAA
del537del75     ---------- ---------- ---------- ---------- ---------- ----------

                ....|....| ....|....| ....|....| ....|....| ....|....| ....|....|
                   965        975        985        995       1005       1015
(3H)-eGFP       CCGCATCGAG CTGAAGGGCA TCGACTTCAA GGAGGACGGC AACATCCTGG GGCACAAGCT
del537del75     ---------- ---------- ---------- ---------- ---------- ----------

                ....|....| ....|....| ....|....| ....|....| ....|....| ....|....|
                  1025       1035       1045       1055       1065       1075
(3H)-eGFP       GGAGTACAAC TACAACAGCC ACAACGTCTA TATCATGGCC GACAAGCAGA AGAACGGCAT
del537del75     ---------- ---------- ---------- ---CATGGCC GACAAGCAGA AGAACGGCAT

                ....|....| ....|....| ....|....| ....|....| ....|....| ....|....|
                  1085       1095       1105       1115       1125       1135
(3H)-eGFP       CAAGGTGAAC TTCAAGATCC GCCACAACAT CGAGGACGGC AGCGTGCAGC TCGCCGACCA
del537del75     CAAGGTGAAC TTCAAGATCC GCCACAACAT CGAGGACGGC AGCGTGCAGC TCGCCGACC-

                ....|....| ....|....| ....|....| ....|....| ....|....| ....|....|
                  1145       1155       1165       1175       1185       1195
(3H)-eGFP       CTACCAGCAG AACACCCCCA TCGGCGACGG CCCCGTGCTG CTGCCCGACA ACCACTACCT
del537del75     ---------- ---------- ---------- ---------- ---------- ----------

                ....|....| ....|....| ....|....| ....|....| ....|....| ....|....|
                  1205       1215       1225       1235       1245       1255
(3H)-eGFP       GAGCACCCAG TCCGCCCTGA GCAAAGACCC CAACGAGAAG CGCGATCACA TGGTCCTGCT
del537del75     ---------- ----CCCTGA GCAAAGACCC CAACGAGAAG CGCGATCACA TGGTCCTGCT

                ....|....| ....|....| ....|....| ....|....| ....|....| ....|....|
                  1265       1275       1285       1295       1305       1315
(3H)-eGFP       GGAGTTCGTG ACCGCCGCCG GGATCACTCT CGGCATGGAC GAGCTGTACA AGGGATCCGA
del537del75     GGAGTTCGTG ACCGCCGCCG GGATCACTCT CGGCATGGAC GAGCTGTACA AGGGATCCGA

                ....|....| ....|....| ....|....| ....|....| ....|....| ....|....|
                  1325       1335       1345       1355       1365       1375
(3H)-eGFP       CTTTGACGAG CACGAGGTCG ATGCGTTGGC CTCCGGGATT ACTTTCGGAG ACTTCGACGA
del537del75     CTTTGACGAG CACGAGGTCG ATGCGTTGGC CTCCGGGATT ACTTTCGGAG ACTTCGACGA
```

```
                ....|....| ....|....| ....|....| ....|....| ....|....| ....|....|
                   1385       1395       1405       1415       1425       1435
(3H)-eGFP       CGTCCTGCGA CTAGGCCGCG CGGGTGCATA TATTTTCTCC TCGGACACTG GCAGCGGACA
del537del75     CGTCCTGCGA CTAGGCCGCG CGGGTGCATA TATTTTCTCC TCGGACACTG GCAGCGGACA

                ....|....| ....|....| ....|....| ....|....| ....|....| ....|....|
                   1445       1455       1465       1475       1485       1495
(3H)-eGFP       TTTACAACAA AAATCCGTTA GGCAGCACAA TCTCCAGTGC GCACAACTGG ATGCGGTCCA
del537del75     TTTACAACAA AAATCCGTTA GGCAGCACAA TCTCCAGTGC GCACAACTGG ATGCGGTCCA

                ....|....| ....|....| .
                   1505       1515
(3H)-eGFP       GGAGGAGAAA ATGTACCCGC C
del537del75     GGAGGAGAAA ATGTACCCGC C
```

Journal of General Virology (2007), **88**, 1225–1230 DOI 10.1099/vir.0.82436-0

Short Communication

Insertion of EGFP into the replicase gene of *Semliki Forest virus* results in a novel, genetically stable marker virus

Nele Tamberg,[1]† Valeria Lulla,[1]† Rennos Fragkoudis,[2] Aleksei Lulla,[3] John K. Fazakerley[2] and Andres Merits[1,3]

Correspondence
Andres Merits
andres.merits@ut.ee

[1]Estonian Biocentre, Tartu, Estonia

[2]Centre for Infectious Diseases, College of Medicine and Veterinary Medicine, University of Edinburgh, Edinburgh, UK

[3]Institute of Molecular and Cell Biology, University of Tartu, Tartu, Estonia

Received 31 July 2006
Accepted 10 December 2006

Alphavirus-based vector and replicon systems have been extensively used experimentally and are likely to be used in human and animal medicine. Whilst marker genes can be inserted easily under the control of a duplicated subgenomic promoter, these constructs are often genetically unstable. Here, a novel alphavirus construct is described in which an enhanced green fluorescent protein (EGFP) marker gene is inserted into the virus replicase open reading frame between nsP3 and nsP4, flanked by nsP2 protease-recognition sites. This construct has correct processing of the replicase polyprotein, produces viable virus and expresses detectable EGFP fluorescence upon infection of cultured cells and cells of the mouse brain. In comparison to parental virus, the marker virus has an approximately 1 h delay in virus RNA and infectious virus production. Passage of the marker virus *in vitro* and *in vivo* demonstrates good genetic stability. Insertion of different markers into this novel construct has potential for various applications.

Infectious cDNA (icDNA) clones and corresponding expression vectors have been developed for several alphaviruses (Liljestrom & Garoff, 1991; Strauss & Strauss, 1994; Simpson *et al.*, 1996). In most alphavirus-based expression vectors, the viral structural genes are replaced by foreign genes. These vectors are capable of only one round of infection and are thus non-mobilizable, a property that has severely hampered their use in studies that require a spreading, propagating infectious process. Marker and other recombinant alphaviruses have been produced by expressing the foreign gene from an internal ribosomal entry site element or from a duplicated 26S promoter (Raju & Huang, 1991; Hahn *et al.*, 1992; Pugachev *et al.*, 2000; Vaha-Koskela *et al.*, 2003). Double-subgenomic vectors containing marker genes allow direct observation of infection and have been used successfully in animal experiments (Levine *et al.*, 1996; Cook & Griffin, 2003). Unfortunately, these vectors tend to suffer from genome instability, probably because the inserted genes are introduced as separate transcription units and have no selective value (Pugachev *et al.*, 1995, 2000).

An alternative strategy is to insert genes into natural gene expression units. A marker gene has been inserted successfully into the Sindbis virus (SIN) structural gene (Thomas *et al.*, 2003). SIN genomes with markers inserted into the non-structural replicase to produce nsP3-fusion proteins have also been produced (Bick *et al.*, 2003; Frolova *et al.*, 2006). Production of non-structural–marker fusion proteins has also been successful in other viruses, including *Poliovirus*, *Hepatitis C virus*, *Equine arteritis virus* and several filamentous plant viruses (Mueller & Wimmer, 1998; Moradpour *et al.*, 2004; Rajamaki *et al.*, 2005; van den Born *et al.*, 2005). Here, we report that Semliki Forest virus (SFV) nsP3–enhanced green fluorescent protein (EGFP) fusion protein marker virus is viable, but genetically unstable; however, by the novel strategy of placing the EGFP insert between nsP3 and nsP4 flanked by duplications of the nsP3/4 nsP2 protease-recognition site, we have generated a viable, genetically stable virus with only minor changes in phenotype.

An SFV nsP3–EGFP fusion protein virus was engineered by subcloning and PCR-based mutagenesis. The C residue at position 5447 of pSFV4 (Liljestrom *et al.*, 1991) was changed to G and a 12 bp long sequence, GGGCCCAT-AGGATCC, was inserted after the modified codon. The resulting construct was designated pSFV(3F)4. The sequence encoding EGFP was PCR-amplified, cloned into pSFV(3F)4 and the resulting icDNA clone was designated pSFV(3F)4-EGFP (Fig. 1a). Infectious virus, SFV(3F)4-EGFP, was obtained by electroporation of capped *in vitro*

†These authors contributed equally to this work.

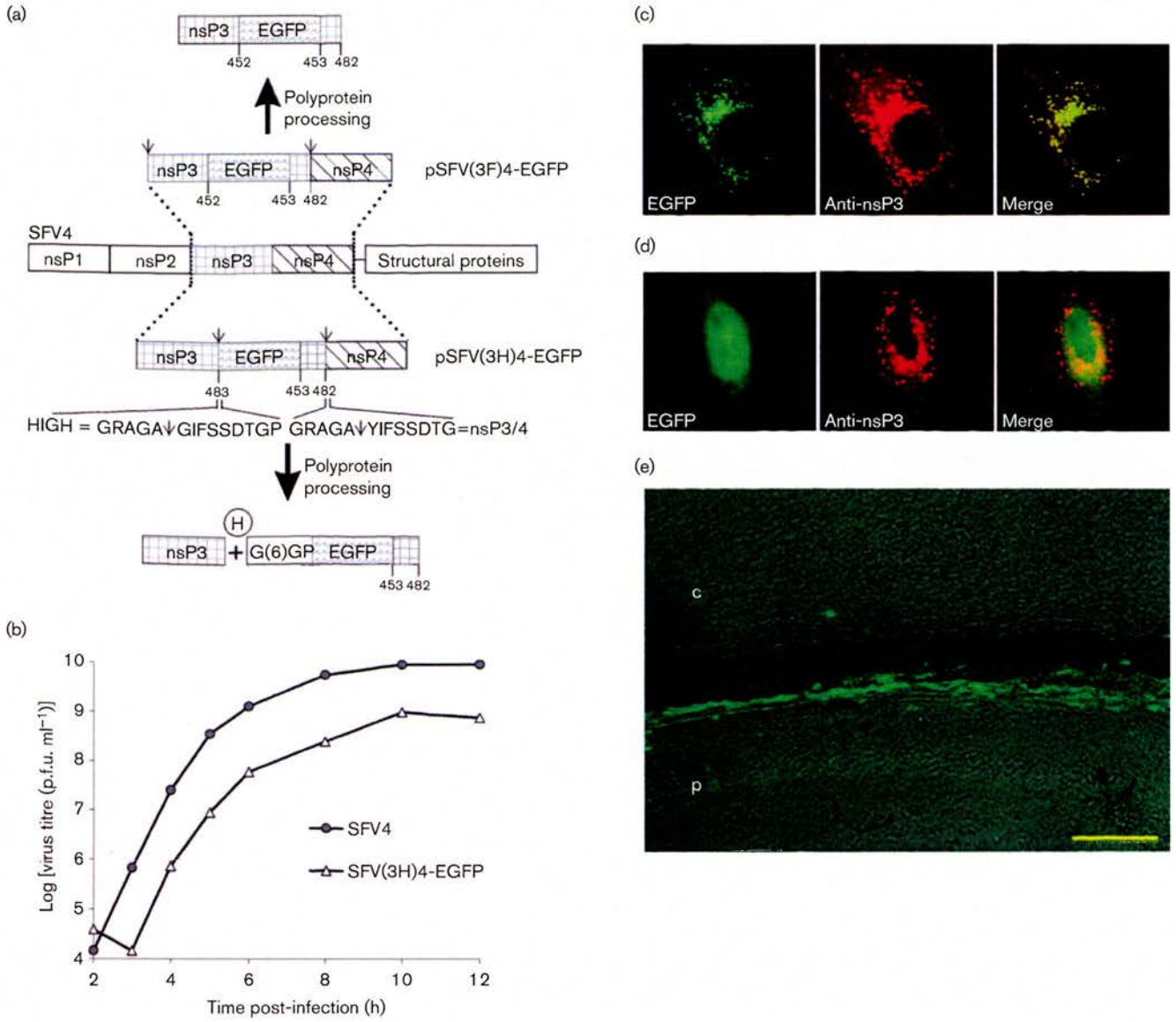

Fig. 1. (a) Schematic representation of recombinant SFV genomes. The sequences of the inserted High (H) site and the native nsP3/4 nsP2 cleavage sites are shown. The 30 aa sequence from the C terminus of the nsP3 (aa 453–482), which was fused to the C terminus of EGFP, is indicated. The nsP2 protease-cleavage sites are indicated by ↓. Numbers indicate positions of amino acid residues in nsP3; (6) indicates the sequence IFSSDT (from nsP4). (b) Growth of SFV4 and SFV(3H)4-EGFP in BHK-21 cells infected with P2 viruses. (c) Localization of EGFP and nsP3 in BHK-21 cells infected with SFV(3F)4-EGFP. (d) Localization of EGFP and nsP3 in BHK-21 cells infected with SFV(3H)4-EGFP. In both (c) and (d), cells infected at an m.o.i. of 1 were fixed at 5 h post-infection. EGFP was detected by its fluorescence, and nsP3 with a polyclonal antibody and a secondary antibody conjugated to Texas red. (e) Virus-infected EGFP-positive cells (green) in mouse brain 2 days post-inoculation, detected by confocal microscopy; p denotes the hippocampal pyramidal cell layer and c the cortex. Bar, 100 μm.

transcripts as described by Liljestrom *et al.* (1991). The primary virus stocks (P1) were collected after 24 h, titrated and used to infect fresh BHK-21 cells (m.o.i., 0.1). The second-passage stocks (P2) were also harvested at 24 h. SFV(3F)4-EGFP virus was viable and expressed the expected nsP3–EGFP fusion protein (Fig. 2a). However, plaque purification followed by analysis of the fluorescence produced by individual plaques and Western blotting demonstrated that this virus was genetically unstable; a truncated form of the nsP3–EGFP fusion protein was present even in cells transfected directly with *in vitro*-synthesized RNA. The genetic instability of this virus is most probably due to defect(s) in the formation or functioning of replication complexes. As with SIN nsP3-fusion

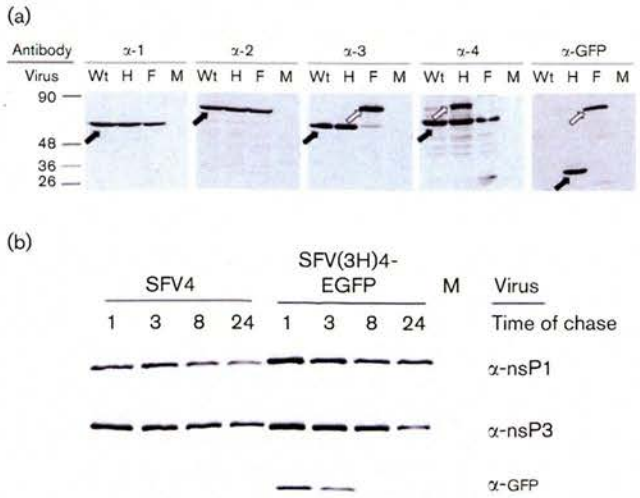

Fig. 2. (a) Expression of EGFP and viral ns proteins by recombinant viruses. BHK-21 cells were infected (m.o.i., 20) with SFV4 (wt), P2 stock of SFV(3H)4-EGFP (H) or P1 stock of SFV(3F)4-EGFP (F), or were mock-infected (M), and cell lysates were analysed by Western blotting. The antibody used for detection is indicated at the top of each panel. Specific signals for nsP1, nsP2, nsP3, nsP4 or EGFP are indicated with a solid arrow; bands corresponding to nsP3–EGFP and EGFP–nsP4 fusion proteins are marked with an open arrow. (b) Proteins synthesized in infected cells were labelled metabolically at 3 h post-infection and chased for 1, 3, 8 or 24 h. Cell lysates were immunoprecipitated with anti-nsP1, anti-nsP3 or anti-EGFP antibodies and analysed by SDS-PAGE.

constructs (Ryman *et al.*, 2005; Frolova *et al.*, 2006; Ventoso *et al.*, 2006), SFV(3F)4-EGFP and its analogues may have uses to study replicase gene expression, replicase protein localization and interactions, but its instability precludes application in *in vivo* pathogenesis studies.

In a novel strategy, a second virus was engineered in which EGFP was placed between nsP3 and nsP4 flanked by nsP2 cleavage sites. Starting with pSFV(3F)4-EGFP, the C terminus of nsP3 was restored and an nsP2 protease-recognition site was added between nsP3 and EGFP (Fig. 1a). The inserted protease-recognition sequence was based on the nsP3/4 junctional sequence, which is cleaved with high efficiency (Merits *et al.*, 2001; Vasiljeva *et al.*, 2001). The first amino acid residue after the inserted cleavage point was also changed from Tyr to Gly; nsP2 prefers Gly in the P1′ position and Gly represents a stabilizing amino acid (Lulla *et al.*, 2006; Varshavsky, 1996). The P1′ Gly was followed by aa 2–7 from the N terminus of nsP4 (Fig. 1a). The region encoding the C terminus of nsP3 with indicated downstream sequence was created by PCR amplification and cloned into pSFV(3F)4-EGFP. The resulting clone and virus were designated pSFV(3H)4-EGFP and SFV(3H)4-EGFP, respectively (Fig. 1a).

Infectious-centre assays (Gorchakov *et al.*, 2004) demonstrated that 3.1×10^5 to 4.4×10^5 plaques (μg transfected RNA)$^{-1}$ were obtained for both pSFV(3H)4-EGFP and pSFV4 transcripts, with no statistically significant difference between them. In one-step growth studies (m.o.i., 20), relative to SFV4, production of infectious SFV(3H)4-EGFP was delayed by approximately 1 h (Fig. 1b). However, as SFV(3H)4-EGFP was able to replicate to 10^9 p.f.u. ml^{-1} within 10 h, it can be concluded that insertion of EGFP between nsP3 and nsP4 did not affect virus replication substantially.

To determine whether the EGFP insertion in SFV(3H)4-EGFP was inherited stably, 96 virus plaques were purified from each of five *in vitro* passages (P1–P5) in BHK-21 cells (m.o.i., 0.1) and each of five *in vivo* passages (M1–M5) in mouse brains. After each passage, the percentage of viruses expressing EGFP was assessed by random selection of 96 plaques followed by determination of EGFP expression. All plaques from the P2 stock of SFV(3H)4-EGFP were EGFP-positive and >90 % were EGFP-positive after the fifth passage. Even greater stability was observed for *in vivo*-propagated stocks: after the fifth passage, only one plaque (1/96) was EGFP-negative. As an EGFP-negative phenotype could result from EGFP inactivation by point mutation or by deletion, we RT-PCR-amplified and sequenced the corresponding regions for several of the EGFP-negative (*in vitro*-passaged) plaque-purified viruses. In all cases, these genomes contained large in-frame deletions, indicating that deletions in the marker gene do occur upon passage of SFV(3H)4-EGFP. Whilst the frequency of this process may be low, given their growth advantage, deleted genomes are likely to increase in the viral population following multiple passages.

In SFV-infected cells, nsP3 is known to associate with modified endosomes and lysosomes (Froshauer *et al.*, 1988). In contrast, free EGFP is typically localized diffusely in the cytoplasm and more abundantly in the nucleus. In SFV(3F)4-EGFP-infected BHK-21 cells, EGFP co-localized with nsP3 to punctate cytoplasmic structures, presumably virus replicase complexes (Fig. 1c). In contrast, SFV(3H)4-EGFP-infected cells showed granular cytoplasmic staining for nsP3 and diffuse, predominantly nuclear staining for EGFP (Fig. 1d). The independent localization of nsP3 and EGFP in the SFV(3H)4-EGFP-infected cells indicates that EGFP was released from the replication complexes.

To determine the phenotype of SFV(3H)4-EGFP *in vivo*, groups of six 5–6-week-old female BALB/c mice were inoculated (20 μl) intracerebrally with SFV4(3H)-EGFP or SFV4. All animal experiments were carried out under the authority of a UK Home Office licence and were approved by the University of Edinburgh ethical-review process. Mice in both groups had clinical signs of encephalitis at day 2 and were sampled. Half brains were fixed in 4 % neutral-buffered formalin for 16 h, processed through graded sucrose solutions, frozen in OCT and cut into sections (12 μm). EGFP-positive cells were observed readily in all (n=6) brains infected with SFV(3H)4-EGFP (Fig. 1e).

Titration of the other half brain, as described previously (Fazakerley *et al.*, 1993), demonstrated titres of infectious virus ranging from 1×10^9 to 3×10^9 p.f.u. g^{-1}, with no difference between mice infected with SFV(3H)4-EGFP and those infected with parental SFV4. We conclude that, as with SFV4, SFV(3H)4-EGFP is neurovirulent and can replicate and spread efficiently in the mouse brain and that SFV(3H)4-EGFP-infected brain cells express sufficient EGFP to be observed readily by fluorescence microscopy.

Expression of the ns proteins in SFV(3H)4-EGFP- and SFV(3F)4-EGFP-infected BHK-21 cells was examined by Western blotting (Fig. 2a). At 6 h post-infection, cells were lysed in Laemmli buffer and samples corresponding to 100 000 cells were separated by SDS-PAGE. Monospecific rabbit polyclonal antibodies were used to detect nsP1, nsP3 and nsP4, and a mouse monoclonal antibody was used to detect nsP2 (Peränen *et al.*, 1988; Laakkonen *et al.*, 1994; Rikkonen *et al.*, 1994; Kujala *et al.*, 1997). Individual nsP1, nsP2, nsP3, nsP4 and EGFP were observed readily in SFV(3H)4-EGFP-infected cells. No nsP3–EGFP fusion protein was detected, but a small amount of unprocessed EGFP–nsP4 was detected by antibodies to both nsP4 and EGFP. In SFV(3F)4-EGFP-infected cells, nsP3 was, as expected, present predominantly as an nsP3–EGFP fusion protein. A small amount of free nsP3 was also present; this may have resulted from the rapid generation of EGFP-negative genomes.

To study the dynamics of cleavage of the SFV(3H)4-EGFP polyprotein, infected cells (m.o.i., 100) were pulse labelled metabolically for 15 min with 50 μCi (1.85 MBq) [^{35}S]methionine and [^{35}S]cysteine, and nsP3 and its precursors were immunoprecipitated with antiserum against nsP3 and Protein A–Sepharose. Immunocomplexes were separated by SDS-PAGE and radiolabelled proteins were visualized by autoradiography. In pulse-labelled cells, the P123–EGFP, P3–EGFP–4 and P3–EGFP processing intermediates were all detected, whereas in chased samples, processing intermediates were not detected or were present in lower quantities, and the amount of fully processed nsP3 was increased (data not shown). Thus, all expected processing products, except the very rapidly processed P123–EGFP–4, were detected and no apparent disturbance of processing was observed.

In BHK-21 cells, EGFP is generally quite stable, with an estimated half-life of 24 h. However, in BHK-21 cells infected with SFV(3H)4-EGFP, the EGFP signal detected late in infection by fluorescence microscopy had decreased considerably, suggesting low EGFP stability. To assess the stability of the EGFP and ns proteins, BHK-21 cells infected with SFV(3H)4-EGFP or SFV4 were labelled metabolically, chased and EGFP, nsP1 and nsP3 were immunoprecipitated. For both viruses, only a small decrease in nsP1 and nsP3 was detected over 24 h (Fig. 2b). In contrast, by 24 h, the amount of EGFP was below the detection limit of this analysis (Fig. 2b). Thus, the low amounts of EGFP observed by microscopy indeed represent rapid degradation of EGFP. The processed EGFP has a Gly residue at its N terminus that, according the N-end rule, is stabilizing. Most likely, EGFP instability results from the duplicated C-terminal sequence of nsP3 (Fig. 1a), which, as a result of the construction strategy, remains attached to the C terminus of EGFP. If this is the case, then the effect of this same sequence in its native location (C terminus of nsP3) is either different or is suppressed by interaction(s) with other components of the replicase complex.

Virus RNA synthesis by SFV4 and SFV(3H)4-EGFP was compared by [^{3}H]uridine labelling. Relative to SFV4-infected

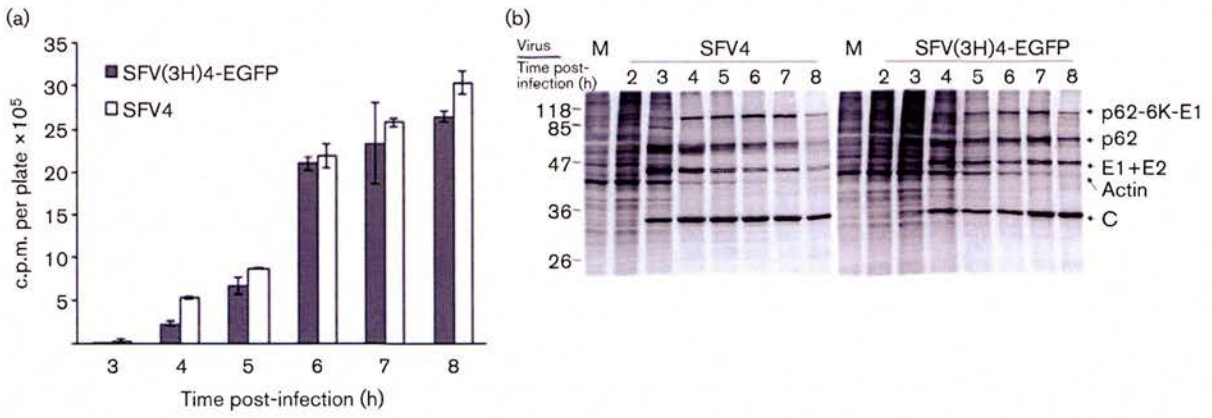

Fig. 3. (a) Synthesis of virus RNA. BHK-21 cells were infected with SFV4 or SFV(3H)4-EGFP; at 1 h post-infection, actinomycin D (2 μg ml^{-1}) and, at 2 h, 25 μCi (0.925 MBq) [^{3}H]uridine, were added. Cells were collected at 3, 4, 5, 6, 7 and 8 h post-infection. Total RNA was precipitated by trichloroacetic acid. Incorporated radioactivity was measured by liquid scintillation. Each bar represents the mean of six replicates; error bars indicate SD. (b) Shutdown of cellular translation in BHK-21 cells infected with SFV4 or SFV(3H)4-EGFP. Proteins synthesized in infected cells were labelled metabolically at 1 h intervals and cell lysates were analysed by SDS-PAGE. M, Mock-infected cells.

cells, SFV(3H)4-EGFP-infected cells had a delay in virus RNA synthesis (Fig. 3a); this was most obvious at 3–5 h post-infection and less so at later time points. To analyse whether insertion of the marker gene altered the temporal expression of SFV structural proteins or the shutdown of host-cell translation, protein synthesis in infected BHK-21 cells was studied by metabolic labelling. As observed with virus growth (Fig. 1b) and RNA synthesis (Fig. 3a), production of viral proteins C, E1 and p62 in SFV(3H)4-EGFP-infected cells started approximately 1 h later than in SFV4-infected cells. A longer, approximately 2 h, delay was observed for host-cell translational shutdown (Fig. 3b).

In all measurements of virus replication and growth, SFV(3H)4-EGFP was slightly slower than SFV4. The possible reasons for this include effects resulting from larger ns polyprotein sizes and delays or defects in replicase-complex formation. However, these changes are unlikely to preclude use of this virus, as it replicates to high titres and remains neurovirulent. Despite the small duplication of viral sequence necessitated by the addition of the nsP2 processing site upstream of EGFP, SFV(3H)4-EGFP demonstrated remarkably improved genetic stability relative to SFV(3F)4-EGFP. However, it should be noted that, at late passages *in vitro*, some genomes with a deletion in the marker gene were present. Attempts to reduce this by removing the duplicated 6 aa from the N terminus of EGFP, or by decreasing the length of the nsP3 C-terminal fragment fused to the C terminus of EGFP, resulted in viable viruses, but did not increase their genetic stability (data not shown). Importantly, following replication and spread of SFV(3H)4-EGFP in the mouse brain, no deletion variants were observed until passage M5, demonstrating the utility of this virus for *in vivo* pathogenesis studies.

Acknowledgements

We are grateful to the research group of Leevi Kääriäinen for their help at the start of this project and to Eva Žusinaite and Kaja Kiiver for their experimental help. This research was supported by grants from the European Union SFvectors programme, grant 067575 from the Wellcome Trust and grants 5055 and 6609 from the Estonian Science Foundation.

References

Bick, M. J., Carroll, J. W., Gao, G., Goff, S. P., Rice, C. M. & MacDonald, M. R. (2003). Expression of the zinc-finger antiviral protein inhibits alphavirus replication. *J Virol* **77**, 11555–11562.

Cook, S. H. & Griffin, D. E. (2003). Luciferase imaging of a neurotropic viral infection in intact animals. *J Virol* **77**, 5333–5338.

Fazakerley, J. K., Pathak, S., Scallan, M., Amor, S. & Dyson, H. (1993). Replication of the A7(74) strain of Semliki Forest virus is restricted in neurons. *Virology* **195**, 627–637.

Frolova, E., Gorchakov, R., Garmashova, N., Atasheva, S., Vergara, L. A. & Frolov, I. (2006). Formation of nsP3-specific protein complexes during Sindbis virus replication. *J Virol* **80**, 4122–4134.

Froshauer, S., Kartenbeck, J. & Helenius, A. (1988). Alphavirus RNA replicase is located on the cytoplasmic surface of endosomes and lysosomes. *J Cell Biol* **107**, 2075–2086.

Gorchakov, R., Frolova, E., Williams, B. R., Rice, C. M. & Frolov, I. (2004). PKR-dependent and -independent mechanisms are involved in translational shutoff during Sindbis virus infection. *J Virol* **78**, 8455–8467.

Hahn, C. S., Hahn, Y. S., Braciale, T. J. & Rice, C. M. (1992). Infectious Sindbis virus transient expression vectors for studying antigen processing and presentation. *Proc Natl Acad Sci U S A* **89**, 2679–2683.

Kujala, P., Rikkonen, M., Ahola, T., Kelve, M., Saarma, M. & Kääriäinen, L. (1997). Monoclonal antibodies specific for Semliki Forest virus replicase protein nsP2. *J Gen Virol* **78**, 343–351.

Laakkonen, P., Hyvönen, M., Peränen, J. & Kääriäinen, L. (1994). Expression of Semliki Forest virus nsP1-specific methyltransferase in insect cells and in *Escherichia coli*. *J Virol* **68**, 7418–7425.

Levine, B., Goldman, J. E., Jiang, H. H., Griffin, D. E. & Hardwick, J. M. (1996). Bcl-2 protects mice against fatal alphavirus encephalitis. *Proc Natl Acad Sci U S A* **93**, 4810–4815.

Liljestrom, P. & Garoff, H. (1991). A new generation of animal cell expression vectors based on the Semliki Forest virus replicon. *Biotechnology (N Y)* **9**, 1356–1361.

Liljestrom, P., Lusa, S., Huylebroeck, D. & Garoff, H. (1991). In vitro mutagenesis of a full-length cDNA clone of Semliki Forest virus: the small 6,000-molecular-weight membrane protein modulates virus release. *J Virol* **65**, 4107–4113.

Lulla, A., Lulla, V., Tints, K., Ahola, T. & Merits, A. (2006). Molecular determinants of substrate specificity for Semliki Forest virus nonstructural protease. *J Virol* **80**, 5413–5422.

Merits, A., Vasiljeva, L., Ahola, T., Kääriäinen, L. & Auvinen, P. (2001). Proteolytic processing of Semliki Forest virus-specific non-structural polyprotein by nsP2 protease. *J Gen Virol* **82**, 765–773.

Moradpour, D., Evans, M. J., Gosert, R., Yuan, Z., Blum, H. E., Goff, S. P., Lindenbach, B. D. & Rice, C. M. (2004). Insertion of green fluorescent protein into nonstructural protein 5A allows direct visualization of functional hepatitis C virus replication complexes. *J Virol* **78**, 7400–7409.

Mueller, S. & Wimmer, E. (1998). Expression of foreign proteins by poliovirus polyprotein fusion: analysis of genetic stability reveals rapid deletions and formation of cardioviruslike open reading frames. *J Virol* **72**, 20–31.

Peränen, J., Takkinen, K., Kalkkinen, N. & Kääriäinen, L. (1988). Semliki Forest virus-specific non-structural protein nsP3 is a phosphoprotein. *J Gen Virol* **69**, 2165–2178.

Pugachev, K. V., Mason, P. W., Shope, R. E. & Frey, T. K. (1995). Double-subgenomic Sindbis virus recombinants expressing immunogenic proteins of Japanese encephalitis virus induce significant protection in mice against lethal JEV infection. *Virology* **212**, 587–594.

Pugachev, K. V., Tzeng, W. P. & Frey, T. K. (2000). Development of a rubella virus vaccine expression vector: use of a picornavirus internal ribosome entry site increases stability of expression. *J Virol* **74**, 10811–10815.

Rajamaki, M. L., Kelloniemi, J., Alminaite, A., Kekarainen, T., Rabenstein, F. & Valkonen, J. P. (2005). A novel insertion site inside the potyvirus P1 cistron allows expression of heterologous proteins and suggests some P1 functions. *Virology* **342**, 88–101.

Raju, R. & Huang, H. V. (1991). Analysis of Sindbis virus promoter recognition in vivo, using novel vectors with two subgenomic mRNA promoters. *J Virol* **65**, 2501–2510.

Rikkonen, M., Peränen, J. & Kääriäinen, L. (1994). ATPase and GTPase activities associated with Semliki Forest virus nonstructural protein nsP2. *J Virol* **68**, 5804–5810.

Ryman, K. D., Meier, K. C., Nangle, E. M., Ragsdale, S. L., Korneeva, N. L., Rhoads, R. E., MacDonald, M. R. & Klimstra, W. B. (2005).

Sindbis virus translation is inhibited by a PKR/RNase L-independent effector induced by alpha/beta interferon priming of dendritic cells. *J Virol* **79**, 1487–1499.

Simpson, D. A., Davis, N. L., Lin, S. C., Russell, D. & Johnston, R. E. (1996). Complete nucleotide sequence and full-length cDNA clone of S.A.AR86 a South African alphavirus related to Sindbis. *Virology* **222**, 464–469.

Strauss, J. H. & Strauss, E. G. (1994). The alphaviruses: gene expression, replication, and evolution. *Microbiol Rev* **58**, 491–562.

Thomas, J. M., Klimstra, W. B., Ryman, K. D. & Heidner, H. W. (2003). Sindbis virus vectors designed to express a foreign protein as a cleavable component of the viral structural polyprotein. *J Virol* **77**, 5598–5606.

Vaha-Koskela, M. J., Tuittila, M. T., Nygardas, P. T., Nyman, J. K., Ehrengruber, M. U., Renggli, M. & Hinkkanen, A. E. (2003). A novel neurotropic expression vector based on the avirulent A7(74) strain of Semliki Forest virus. *J Neurovirol* **9**, 1–15.

van den Born, E., Stein, D. A., Iversen, P. L. & Snijder, E. J. (2005). Antiviral activity of morpholino oligomers designed to block various aspects of *Equine arteritis virus* amplification in cell culture. *J Gen Virol* **86**, 3081–3090.

Varshavsky, A. (1996). The N-end rule: functions, mysteries, uses. *Proc Natl Acad Sci U S A* **93**, 12142–12149.

Vasiljeva, L., Valmu, L., Kaariainen, L. & Merits, A. (2001). Site-specific protease activity of the carboxyl-terminal domain of Semliki Forest virus replicase protein nsP2. *J Biol Chem* **276**, 30786–30793.

Ventoso, I., Sanz, M. A., Molina, S., Berlanga, J. J., Carrasco, L. & Esteban, M. (2006). Translational resistance of late alphavirus mRNA to eIF2alpha phosphorylation: a strategy to overcome the antiviral effect of protein kinase PKR. *Genes Dev* **20**, 87–100.

JOURNAL OF VIROLOGY, May 2007, p. 4991–4999 Vol. 81, No. 10
0022-538X/07/$08.00+0 doi:10.1128/JVI.01933-06

La Crosse Bunyavirus Nonstructural Protein NSs Serves To Suppress the Type I Interferon System of Mammalian Hosts▽

Gjon Blakqori,[1]† Sophie Delhaye,[2] Matthias Habjan,[1] Carol D. Blair,[3] Irma Sánchez-Vargas,[3] Ken E. Olson,[3] Ghassem Attarzadeh-Yazdi,[4] Rennos Fragkoudis,[4] Alain Kohl,[4] Ulrich Kalinke,[5] Siegfried Weiss,[6] Thomas Michiels,[2] Peter Staeheli,[1] and Friedemann Weber[1]*

Department of Virology, University of Freiburg, D-79008 Freiburg, Germany[1]; Université Catholique de Louvain, Christian de Duve Institute of Cellular Pathology, Brussels, Belgium[2]; Colorado State University, Fort Collins, Colorado 80523[3]; Centre for Infectious Diseases, College of Medicine and Veterinary Medicine, University of Edinburgh, Edinburgh EH9 1QH, United Kingdom[4]; Paul Ehrlich Institut, Langen, Germany[5]; and Helmholtz Zentrum für Infektionsforschung, Braunschweig, Germany[6]

Received 5 September 2006/Accepted 12 February 2007

La Crosse virus (LACV) is a mosquito-transmitted member of the *Bunyaviridae* family that causes severe encephalitis in children. For the LACV nonstructural protein NSs, previous overexpression studies with mammalian cells had suggested two different functions, namely induction of apoptosis and inhibition of RNA interference (RNAi). Here, we demonstrate that mosquito cells persistently infected with LACV do not undergo apoptosis and mount a specific RNAi response. Recombinant viruses that either express (rLACV) or lack (rLACVdelNSs) the NSs gene similarly persisted and were prone to the RNAi-mediated resistance to superinfection. Furthermore, in mosquito cells overexpressed LACV NSs was unable to inhibit RNAi against Semliki Forest virus. In mammalian cells, however, the rLACVdelNSs mutant virus strongly activated the antiviral type I interferon (IFN) system, whereas rLACV as well as overexpressed NSs suppressed IFN induction. Consequently, rLACVdelNSs was attenuated in IFN-competent mouse embryo fibroblasts and animals but not in systems lacking the type I IFN receptor. In situ analyses of mouse brains demonstrated that wild-type and mutant LACV mainly infect neuronal cells and that NSs is able to suppress IFN induction in the central nervous system. Thus, our data suggest little relevance of the NSs-induced apoptosis or RNAi inhibition for growth or pathogenesis of LACV in the mammalian host and indicate that NSs has no function in the insect vector. Since deletion of the viral NSs gene can be fully complemented by inactivation of the host's IFN system, we propose that the major biological function of NSs is suppression of the mammalian innate immune response.

La Crosse virus (LACV) is an important mosquito-borne pathogen in North America, causing severe encephalitis and aseptic meningitis in children and young adults (37, 42, 57). Around 75 to 100 cases of La Crosse encephalitis requiring hospitalization are reported annually (12), and up to 57% percent of these patients need to be admitted to the intensive care unit (37). More than 10% of the hospitalized patients will have long-lasting neurological deficits (37, 38), with severe economic and social consequences (52). As less than 1.5% of LACV infections are clinically apparent, it is estimated that more than 300,000 infections occur annually in the Midwestern United States alone (11, 38).

Like other arboviruses, LACV cycles between vertebrate and invertebrate hosts, able to replicate both in mammals and in insects. Depending on the host, however, the outcome of infection is different (7). In mammalian cells, infection is lytic and causes host cell shutoff and cell death. In insect cells, infection is noncytolytic and leads to long-term viral persistence.

LACV belongs to the California serogroup of the genus *Orthobunyavirus*, family *Bunyaviridae* (7). Bunyaviruses are a large group of mainly arthropod-transmitted viruses. They are classified into five genera: *Orthobunyavirus*, *Phlebovirus*, *Hantavirus*, *Nairovirus*, and *Tospovirus*. Some members are human pathogens and can cause encephalitis, febrile illness, or hemorrhagic fever; among them are LACV, Oropouche virus, Hantaan virus, Rift Valley fever virus (RVFV), and Crimean-Congo hemorrhagic fever virus (19, 56). Bunyaviruses are enveloped and have a trisegmented single-stranded RNA genome of negative or ambisense polarity, replicate in the cytoplasm, and bud into the Golgi apparatus. They encode four common structural proteins: the viral polymerase (L) on the large (L) segment, two glycoproteins (Gn and Gc) on the medium (M) segment, and the viral nucleocapsid protein (N) on the smallest (S) segment.

Some bunyaviruses encode on their S segment a nonstructural protein which is termed NSs. For LACV, two different functions for viral pathogenicity have been assigned to this accessory protein. Firstly, NSs has similarity to the *Drosophila* protein reaper and is an efficient inducer of apoptosis if overexpressed in mammalian cells (14). Our own studies using recombinant LACV expressing or lacking NSs supported this

* Corresponding author. Mailing address: Department of Virology, University of Freiburg, Hermann Herder Str. 11, Freiburg D-79008, Germany. Phone: 49 761 203 6614. Fax: 49 761 203 6634. E-mail: friedemann.weber@uniklinik-freiburg.de.

† Present address: Centre for Biomolecular Sciences, School of Biology, University of St. Andrews, North Haugh, St. Andrews KY16 9ST, Scotland, United Kingdom.

▽ Published ahead of print on 7 March 2007.

notion (6). Secondly, overexpressed NSs was shown to efficiently suppress RNA interference (RNAi) in mammalian cells (49), suggesting that LACV NSs is important for evasion of this antiviral system. By contrast, in vivo studies with the orthobunyavirus Bunyamwera virus (BUNV) or the phlebovirus RVFV provided evidence that their NSs proteins are efficient inhibitors of type I interferon (IFN-α/β) synthesis and that this activity is relevant for infection of mammalian hosts (8, 25, 55).

IFNs are cytokines which establish a first line of defense against viral pathogens by stimulating the synthesis of antiviral proteins and activating the adaptive immune system (43). In most cell types, virus infection activates a signaling pathway that results in the immediate synthesis of IFN-β and IFN-α4, which is followed by a second burst of IFN which comprises a large number (at least 14 in mice) of different α subtypes (36, 53). In plasmacytoid dendritic cells, which are the professional IFN producers of the immune system, IFN-α is directly synthesized after stimulation (13).

The biological function of LACV NSs in the mammalian host has to date not been clarified, and the role of NSs in infection of the insect vector has not been resolved for any of the bunyaviruses. Here, we used our recently generated recombinant LACV mutant lacking NSs (rLACVdelNSs) (6) to investigate these issues. Our results strongly suggest that LACV NSs evolved mainly to counteract the antiviral IFN system of the mammalian host.

MATERIALS AND METHODS

Chemicals, cells, and viruses. Poly(I · C) (Sigma) was dissolved and used as indicated by the manufacturer. Mouse embryo fibroblasts (MEFs) were prepared by trypsin digestion of 14-day-old embryos. The cultures were used between passages 3 to 8. MEFs and human 293 cells were cultivated in Dulbecco's modified Eagle's medium (DMEM) supplemented with 10% fetal calf serum (FCS). BSR-T7/5 cells (10), which constitutively express the bacteriophage T7 RNA polymerase, were additionally provided with 1 mg/ml geneticin (G418). *Aedes albopictus* C6/36 and U4.4 cells (a kind gift of D. T. Brown, North Carolina State University, Raleigh, NC) and *Aedes triseriatus* MAT cells were grown at 30°C (C6/36 and MAT cells) or 28°C (U4.4 cells) without CO_2 in Leibowitz L-15 medium (Gibco-BRL) supplemented with 10% FCS, antibiotics, and 4% tryptose phosphate broth (Difco). The recombinant virus strains rLACV and rLACVdelNSs were grown and maintained as described previously (6).

RNAi detection. Insect cells were infected with LACV at a multiplicity of infection of 10, and maintained in Leibovitz L-15 maintenance medium (1% fetal bovine serum). At predetermined times postinfection, the cells were harvested, RNA was extracted, and small RNAs were enriched by precipitation of high-molecular-weight species with 5% polyethylene glycol 8000–0.5 M NaCl (26). Low-molecular-weight RNAs were fractionated by 16% polyacrylamide–7 M urea gel electrophoresis, transferred to nylon filters, and hybridized at 42°C with a ^{32}P-labeled viral RNA sense probe. The S segment mRNA from the same extracts was separated by 1.2% agarose gel electrophoresis, blotted, and hybridized with the same probe.

Plaque assay. Vero cells grown on six-well plates to 90% confluence were inoculated with 10-fold serial dilutions of supernatants from infected cells, diluted in DMEM with 2% FCS. After a 1-h incubation at 37°C, the inoculum was removed, and the cells were overlaid with 3 ml of DMEM with 2% FCS, 0.02% DEAE dextran, and 0.3% agar noble (Difco); cells were incubated for another 72 h at 37°C. Cells were fixed and stained with 1% crystal violet, 3.6% formaldehyde, 1% methanol, and 20% ethanol, and titers were calculated from the plaque numbers according to the dilution.

Plasmid constructs and PCR. DNA plasmids were constructed and propagated using standard techniques. PCR was carried out with AccuPrime *Pfx* DNA polymerase (for cloning purposes; Invitrogen) or *Taq* DNA polymerase (for diagnostic purposes and addition of single adenosines for TA cloning; Eppendorf). TA cloning was done using a pcDNA3.1/V5-His TOPO TA Expression kit (Invitrogen) according to the manufacturer's instructions. A recombinant Semliki Forest virus (SFV) replicon encoding LACV NSs (SFV-LACV NSs) equipped with an N-terminal FLAG epitope was generated by PCR amplification and cloning into pSFV-1 (35) using the BamHI restriction site. SFV replicons SFV-Luc (expressing firefly luciferase), SFV-TSWV NSs (expressing the NSs of tomato spotted wilt virus), and SFV-NS1 (expressing the influenza A virus NS1 protein) were kindly provided by Michèle Bouloy (Institute Pasteur, Paris, France) and Marcel Prins (Wageningen University, Wageningen, The Netherlands) (22). The minireplicon plasmid pT7ribo-LACV-cM-GFP encoding the enhanced green fluorescent protein (EGFP) gene flanked by the antigenomic LACV M segment promoter sequences under control of the bacteriophage T7 promoter was constructed by inserting the EGFP coding sequence into the LACV M provector pT7ribo-LACV-cMPro (6), using engineered BpiI restriction enzyme sites. The eukaryotic expression plasmid pI.18-HA-LACV-NSs was constructed by ligating a PCR fragment encompassing the LACV NSs sequence with a 5′terminal hemagglutinin (HA) tag into the cloning vector pI.18 (kindly provided by Jim Robertson, National Institute for Biological Standards and Control, Hertfordshire, United Kingdom). The T7 promoter-driven expression constructs pTM-LACV-L and pTM-LACV-N were described previously (5). The firefly luciferase (FF-Luc) reporter plasmid for monitoring IFN-β promoter activation (p-125Luc) was kindly provided by Takashi Fujita, Institute for Virus Research, Kyoto University, Japan (58). The control plasmid pRL-SV40 (Promega) contains the *Renilla* luciferase (REN-Luc) gene under control of the constitutive simian virus 40 (SV40) promoter.

RNAi reporter assay. RNAi against an SFV replicon expressing FF-Luc in insect cells was established as described by Garcia et al. (22). pSFV-1-derived plasmids were linearized with SpeI (SFV-Luc and SFV-NS1) or SapI (SFV-TSWV NSs and SFV-LACV NSs) and in vitro transcribed and capped using SP6 RNA polymerase. Replicon RNA was purified using an RNeasy Mini Kit and resuspended in nuclease-free H_2O. For cotransfection experiments with replicon RNA, 2×10^5 U4.4 cells grown in 24-well dishes were transfected using 125 ng of each RNA (as indicated) and 0.75 μl of Lipofectamine 2000 (Invitrogen). Transfection mixes were not removed from the supernatant over the course of the experiment, and no cytopathic effect or difference in cell numbers was observed. At 3 days posttransfection, cells were lysed in 50 μl of passive lysis buffer per well, and luciferase activities were determined as described by the manufacturer (Promega).

In vivo reconstitution and passaging of LACV nucleocapsids. Subconfluent monolayers of BSR-T7/5 cells in six-well dishes were transfected with 0.5 μg each of plasmid pT7ribo-LAC-cM-GFP, pTM-LACV-L, and pTM-LACV-N using the Fugene 6 transfection reagent (Roche) in 200 μl of serum free-medium (OptiMEM; Gibco-BRL). At 24 h posttransfection, cells were infected with viruses at a multiplicity of infection of 5, incubated for 1 h, and washed two times with phosphate-buffered saline (PBS). After an incubation period of 24 h, cells and supernatants containing newly generated viruses were harvested by three freeze-thaw cycles, and centrifuged for 1 min at 14,000 × *g* to pellet residual cell debris, and 500 μl was used to infect C6/36 mosquito cells for 1 h. These C6/36 cells had been mock infected or persistently infected with recombinant viruses, as indicated in the text. The superinfected C6/36 cells were washed with medium and then incubated for 24 h. Expression of EGFP and LACV N was assayed by immunofluorescence microscopy as described previously (6).

RT-PCR analyses. Total RNA was extracted from infected cells using the TriFast reagent (Peqlab). For reverse transcription (RT), 1 μg of total RNA was incubated with 200 U of Superscript II reverse transcriptase (Gibco-BRL) and 100 ng of random hexanucleotides in 20 μl of 1× RT buffer (Gibco-BRL) supplied with a 1 mM concentration of each deoxynucleotide triphosphate, 20 U of RNasin, and 10 mM dithiothreitol. The resulting cDNA was amplified by 30 cycles of PCR, with each cycle consisting of 30 s at 94°C, 1 min at 58°C, and 1 min at 72°C, with a final 10-min step at 72°C. Primer sequences for amplifying mouse β-actin were from Shaw-Jackson and Michiels (46), those for IFN-β were from Marie et al. (36), and those for the LACV N gene were as published previously (6).

Transient transfections and reporter gene assays. Subconfluent cell monolayers grown in six-well dishes were transfected with 0.5 μg of p125-luc reporter plasmid (FF-Luc gene under control of the IFN-β promoter), 0.05 μg of control plasmid pRL-SV40 (REN-Luc gene under control of the SV40 promoter), and 1 μg of expression plasmid in 400 μl of OptiMEM (Gibco-BRL) containing 5 μl of DAC-30 (Eurogentec). At 8 h posttransfection, cells were transfected with 10 μg of poly(I · C) as described previously (55). After overnight incubation, cells were harvested and lysed in 200 μl of reporter lysis buffer (Promega). An aliquot of 20 μl of lysate was used to measure FF-Luc and REN-Luc activity as described by the manufacturer of the dual luciferase assay kit (Promega).

Virus growth in tissue culture. MEF cells were grown in six-well dishes to 80% confluence and infected with 0.0001 PFU per cell, washed twice with PBS, and

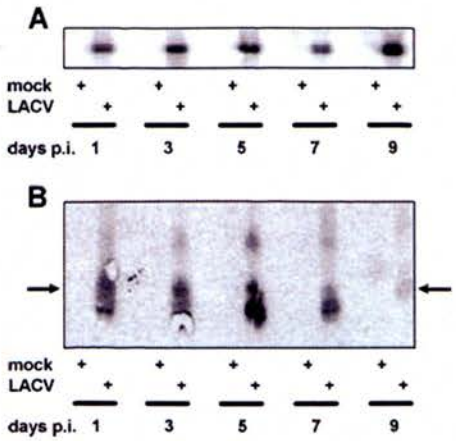

FIG. 1. Formation of LACV-specific small RNAs during persistent infection of C6/36 mosquito cells. Cells were infected with 10 PFU per cell of LACV and passaged twice weekly, and total RNAs were extracted at given time points. (A) To monitor infection, RNAs were separated by 1.2% agarose gel electrophoresis and hybridized to a negative sense S segment RNA probe. (B) Small RNAs were detected after precipitation of the RNA samples with 5% polyethylene glycol, separation on 16% polyacrylamide gels, and hybridization using the same RNA probe as used in panel A. Arrows show the positions of 20-nucleotide markers which were run on the same gel. p.i., postinfection.

supplied with DMEM containing 10% FCS. Supernatants were taken at various times postinfection and assayed in plaque assays on Vero cells.

Pathogenicity studies. Wild-type (wt) C57BL/6 mice and congenic mutant mice with targeted disruptions of the α-subunit of the IFN-α/β receptor (40) or the IFN-β gene (20) were bred locally. Groups of 6 mice at an age of 16 to 18 days were inoculated intraperitoneally with 10,000 PFU of virus in 0.1 ml of PBS. The animals were monitored twice daily over a 9-day period. Mice that were moribund or severely paralyzed were killed.

ISH studies. For in situ detection of IFN mRNAs, RNA probes described in Delhaye et al. (17) were used. The probe used for IFN-α detection was complementary to IFN-α5 (the predominant IFN subtype in the central nervous system) but can recognize other IFN-α subtypes as well. Brain preparation and in situ hybridizations (ISH) were performed as described previously (17). Sections were cut at 8 or 12 μm. Control hybridizations performed with positive-sense probes instead of antisense probes failed to yield any signal.

For ISH in combination with immunohistochemistry of neurons, sections were treated for immunohistochemistry immediately after the last washes of the hybridization. Sections were blocked in TNB (0.1 M Tris-HCl [pH 7.50] 0.15 M NaCl, 0.5% blocking reagent; Perkin-Elmer) and then incubated with the rabbit anti-LACV N antibody for 2 to 12 h at room temperature. The Dako CSA system (K1500) or Envision kit (K4006/K4010) were used for detection and diaminobenzidine staining.

Immunohistofluorescence analysis. Freshly collected brains were immersed in Tissue-Tek optimal cutting temperature compound (Sakura) and frozen at −80°C. Tissue sections 7 μm thick were cut in a cryostat, placed on SuperFrost Plus slides, and dried at 37°C overnight. Sections were fixed with ice-cold acetone for 10 min and washed before processing for immunohistofluorescence. Antibodies used for double labeling were a polyclonal antibody directed against the N protein of LACV and monoclonal antibodies directed against either the neuron-specific nuclear protein ([NeuN] MAB377; Chemicon), the astrocyte-specific glial fibrillary acidic protein ([GFAP] 13-0300; Zymed), the oligodendrocyte-specific myelin basic protein (MAB386; Chemicon), or the microglia/macrophage-specific markers CD11b (553308; Pharmingen) and F4/80 (MCA497R; Serotec). Secondary antibodies were either labeled with Alexa 488 or with Alexa 594 (Molecular probes).

RESULTS

Formation of short LACV-specific RNAs in persistently infected insect cells. Insects do not mount antibody-mediated immune responses (31). For the defense of viral pathogens, they deploy instead mechanisms like the ubiquitous RNAi system, which is based on the sequence-specific recognition and destruction of viral RNA (44, 54). We wondered whether insect cells are capable of mounting an RNAi response against LACV. To investigate this, we established persistent infection of *A. albopictus* C6/36 cells with LACV and monitored the formation of virus-specific small RNAs, the hallmark of RNAi. Conventional Northern blot analysis of RNAs which were extracted from mock-infected or LACV-infected C6/36 cells at predetermined time points postinfection confirmed that infection with LACV was stable and persistent (Fig. 1A; see also Fig. 2). Fractionation and detection of low-molecular-weight RNAs derived from LACV demonstrated that C6/36 cells indeed produce small RNAs in response to infection (Fig. 1B). We have cloned and sequenced the small RNAs from LACV-infected C6/36 cells and confirmed them to be derived from the LACV S segment (data not shown). Similar observations were obtained in *A. triseriatus* MAT cells (data not shown), indicating a general phenomenon. Of note, microscopic examinations of infected cell cultures did not reveal any signs of cell death (data not shown), as observed previously (7).

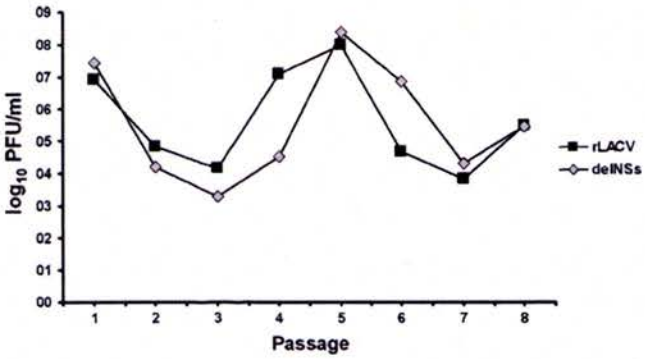

FIG. 2. Time course of persistent LACV infection of mosquito cells. C6/36 cells were infected with 10 PFU per cell of either rLACV or rLACVdelNSs and passaged twice weekly. Viral titers in the supernatants were determined by plaque assay.

NSs does not influence virus growth in insect cells. LACV NSs expressed from a transfected cDNA plasmid was previously shown to inhibit the RNAi pathway in mammalian cells (49). Our newly generated recombinant viruses expressing (rLACV) or lacking (rLACVdelNSs) NSs offer the possibility to evaluate the influence of NSs in the viral context. To determine if the anti-RNAi activity of NSs is important to establish or maintain infection in arthropods, we compared the persistence of rLACV and rLACVdelNSs in insect cells. C6/36 cells were infected with recombinant viruses, cells were passaged over several weeks, and titers in the supernatants were determined at every passage. As shown in Fig. 2, both viruses exhibited the wave-like titer pattern which is typical for growth of bunyaviruses in insect cells (45). No difference was observed between rLACV and rLACVdelNSs, indicating that NSs is not required for infection and persistence of LACV in insect cells.

Protection from superinfection. Insects infected with LACV are resistant to superinfection with California serogroup orthobunyaviruses but remain permissive for Bunyamwera serogroup orthobunyaviruses (1). This pathogen-derived resistance

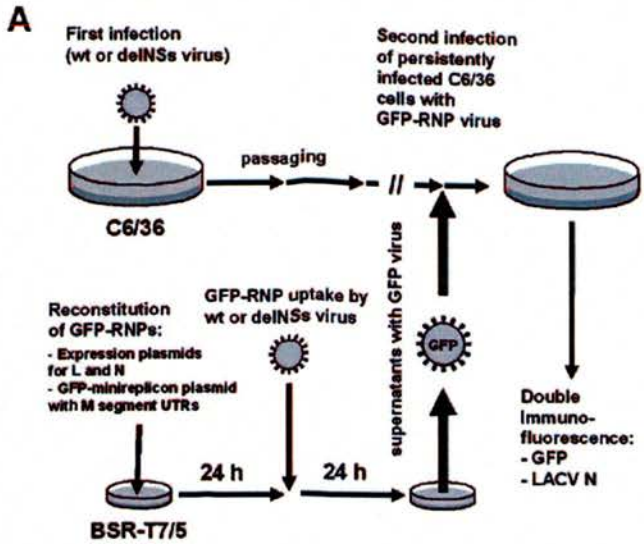

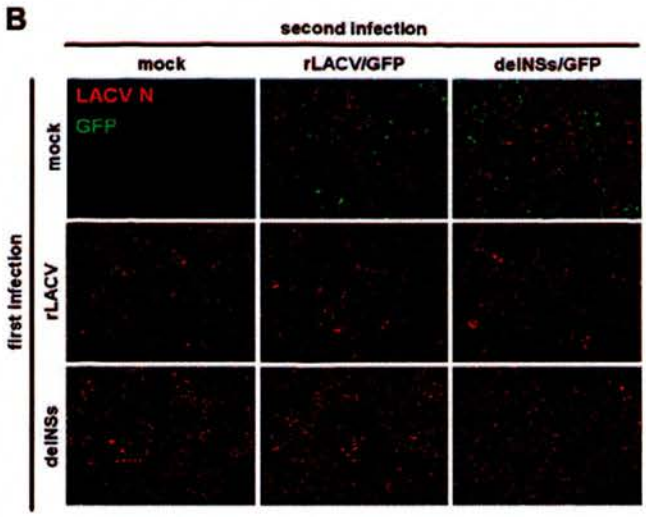

FIG. 3. Protection of C6/36 mosquito cells from superinfection. (A) Experimental outline. C6/36 mosquito cells were infected with LACV and maintained for several passages to establish persistent infection (first infection). The persistently infected cells were then superinfected with GFP-expressing reporter viruses (second infection). The reporter viruses were generated by incorporating GFP-RNPs (reconstituted by transfecting BSR-T7/5 cells with expression constructs for N, L, and a GFP minireplicon) into LACV particles as a fourth segment. Both first and second infections involved either wt viruses or delNSs mutants. (B) Results. C6/36 mosquito cells persistently infected with either rLACV or rLACVdelNSs or left uninfected (mock) were superinfected with GFP reporter viruses. At 24 h postinfection, cells were fixed and stained with antibodies against GFP and LACV N protein.

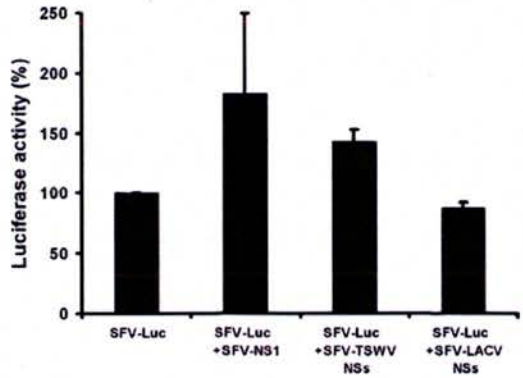

FIG. 4. Effect of LACV NSs on RNAi in insect cells. U4.4 cells were transfected with SFV-Luc SFV-NS1, SFV-TSWV NSs, or SFV-LACV NSs as indicated. At 3 days posttransfection, cells were lysed, and luciferase activities were determined. Mean values and standard deviations from three independent experiments are shown.

(PDR) is most likely based on RNAi (4, 21, 44), since expression of the LACV S sequences by recombinant Sindbis virus is sufficient to protect insect cells from infection with LACV (41). Given that LACV provokes an RNAi response in mosquito cells and that transfection of LACV NSs blocks RNAi in mammalian cells, we wondered about the influence of NSs on the PDR phenomenon in insect cells. To investigate this, we superinfected persistently infected insect cells with recombinant viruses expressing a reporter gene. The role of NSs was addressed by using viruses expressing or lacking NSs in the first, persistent infection, as well as in the second, the superinfection. The outline of the experiment is depicted in Fig. 3A. Insect cells infected with recombinant viruses and passaged to establish persistency were superinfected with GFP-expressing reporter viruses. For the generation of the reporter viruses, we took advantage of an improved version of our LACV RNP reconstitution system which allows efficient incorporation of GFP-expressing reporter gene segments into LACV particles (5). Detection of GFP in superinfected insect cells indicates that the second virus infection was successful, whereas absence of GFP indicates that PDR took place. As expected, mock-infected insect cells were readily infected with GFP-expressing rLACV or rLACVdelNSs (Fig. 3B). However, in persistently infected cells, no GFP expression was observed, indicating establishment of PDR. Importantly, all combinations of rLACV and rLACVdelNSs used for the first infection and/or the superinfection led to the same resistance to superinfection, strongly suggesting that neither the ability of the first viruses to establish PDR nor the inability of the second viruses to overcome it was dependent on NSs.

NSs does not inhibit RNAi in insect cells. We employed an SFV-based reporter assay (22) to test whether NSs would be capable of suppressing RNAi in insect cells. *A. albopictus* U4.4 cells were chosen because C6/36 cells show cytopathic effects after infection with SFV (15). Garcia et al. have demonstrated that FF-Luc expression by an SFV replicon (SFV-Luc) in insect cells is reduced due to RNAi over time but that expression can be rescued by coexpressed RNAi inhibitors (22). U4.4 cells were transfected with SFV-Luc and cultivated for 3 days to establish an RNAi response. Figure 4 shows that cotransfection with SFV-NS1 enhanced luciferase expression by SFV-Luc, as expected (22), since the double-stranded RNA (dsRNA)-binding NS1 can neutralize interference by small RNAs (34). Similarly, the NSs protein of TSWV, a known RNAi inhibitor (9), rescued SFV expression to some extent. By contrast, SFV-LACV NSs had no such enhancing effect, indicating the absence of anti-RNAi activity. Identical results were obtained

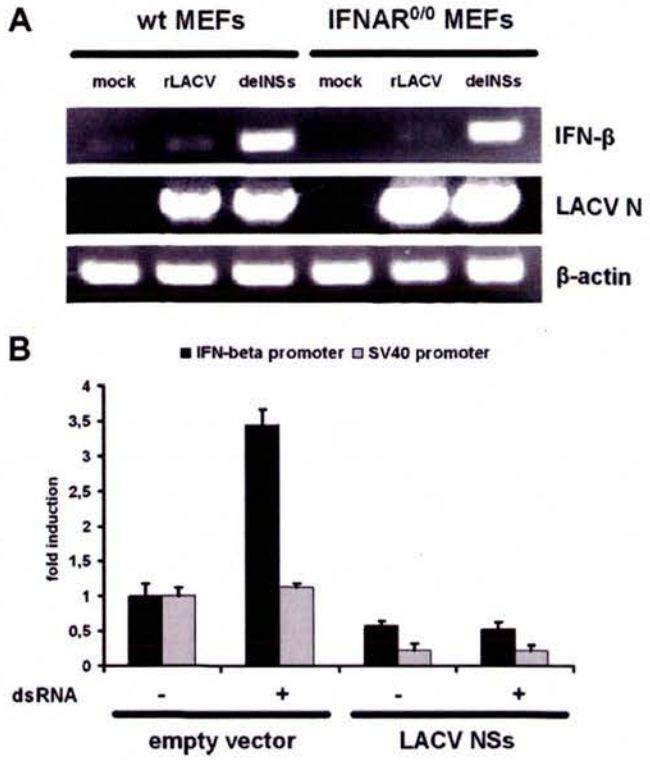

FIG. 5. Effect of LACV NSs on IFN induction. (A) Detection of IFN-β mRNA in infected mammalian cells. MEFs isolated from wt or IFNAR$^{0/0}$ mice were either mock infected or infected with rLACV or rLACVdelNSs. At 18 h postinfection, RNA was extracted and investigated by RT-PCR for the presence of mRNAs for IFN-β, LACV N protein, or β-actin. (B) Suppression of the IFN-β promoter by NSs. Human 293 cells were transfected with luciferase-expressing plasmids under control of either the IFN-β promoter (FF-Luc) or the constitutively active SV40 promoter (REN-Luc), along with the NSs expression plasmid pI.18-HA-LACV-NSs or the empty vector. At 8 h posttransfection, cells were either mock treated or transfected with dsRNA and lysed 18 h later to measure luciferase activity. Mean values and standard deviations from four independent experiments are shown.

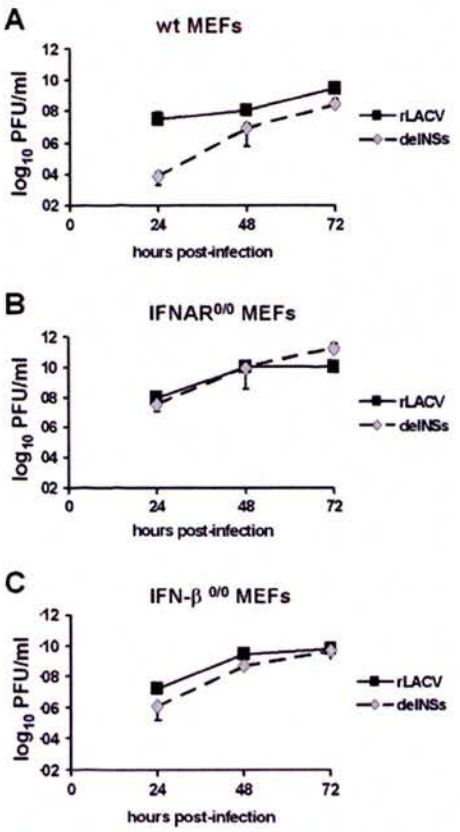

FIG. 6. Growth of viruses in IFN-competent and IFN-deficient cells. Primary MEFs derived from wt mice (A), IFNAR$^{0/0}$ mice (B), or IFN-β$^{0/0}$ mice (C) were infected with rLACV or rLACVdelNSs at 0.0001 PFU per cell, and virus titers in the supernatants were determined at 24, 48, and 72 h postinfection. Mean values and standard deviations from three independent experiments are shown.

with recombinant SFV suicide particles infecting *Aedes pseudoscutillaris* Ap61 cells (data not shown).

Together, our results shown so far imply that the LACV-specific RNAi response mounted in insect cells (Fig. 1) is not countered by NSs, since NSs neither confers a growth advantage (Fig. 2) nor influences PDR (Fig. 3) nor inhibits RNAi against a heterologous virus (Fig. 4). It therefore appears that the anti-RNAi activity of NSs observed in mammalian cells plays no decisive role for LACV in the mosquito vector.

Inhibition of IFN induction in fibroblasts. Previous work demonstrated that NSs proteins of BUNV as well as RVFV efficiently block the antiviral type I IFN response of mammalian hosts (3, 8, 55). To measure this activity for LACV, we infected IFN-competent wt MEFs with recombinant viruses and measured IFN induction by RT-PCR. Figure 5A shows that rLACVdelNSs strongly activated transcription of the IFN-β gene. NSs-expressing rLACV, by contrast, did not induce significant amounts of IFN. Similarly, MEFs derived from mice lacking the type I IFN receptor (IFNAR$^{0/0}$ MEFs) produced IFN-β after infection with rLACVdelNSs, indicating that IFN induction occurred in a direct manner and was independent of secreted IFN. Control RT-PCRs for the LACV N gene showed that viruses replicated to comparable levels, and RT-PCRs for the cellular β-actin mRNA demonstrated that all preparations contained similar amounts of RNA. Of note, RT-PCR analysis for some RNA polymerase II-dependent, constitutively expressed cellular genes shows a strong reduction in wt-infected cells (6), supporting the view that LACV NSs may influence cellular transcription in a manner similar to BUNV NSs and RVFV (32, 33, 51).

To confirm that the block in IFN induction is solely mediated by NSs, we measured its effect on IFN-β promoter activity independent of the viral context. Human 293 cells were transfected with an NSs-expressing plasmid and an IFN-β promoter reporter plasmid, and promoter activity was measured after stimulation of cells with synthetic dsRNA. As shown in Fig. 5B, expression of LACV NSs efficiently inhibits induction of the IFN-β promoter by dsRNA, confirming that NSs is sufficient to suppress IFN production.

Effect of NSs on viral growth in IFN-competent and -deficient systems. Given the strong effects of LACV NSs in mammalian cells on apoptosis (6, 14), RNAi (49), and IFN induction (Fig. 5), it was of interest for us to clarify which one of these activities is relevant to the virus multiplication in the

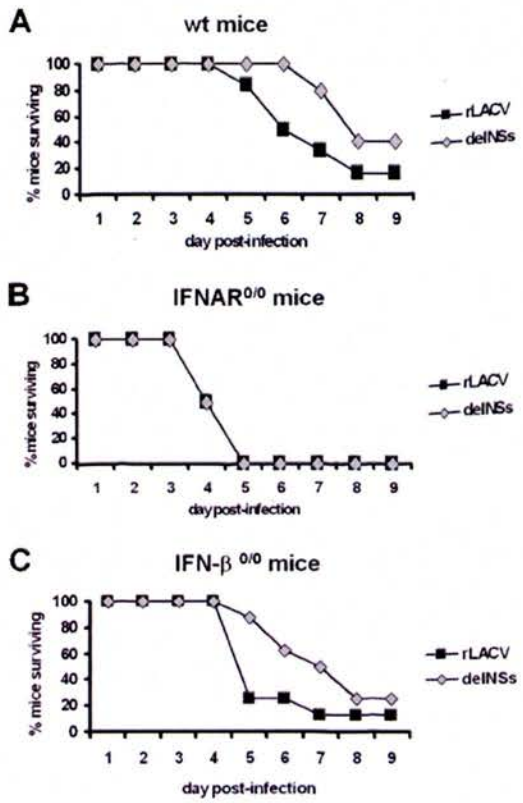

FIG. 7. IFN-dependent virulence of viruses in vivo. Survival of wt (A), IFNAR$^{0/0}$ (B), or IFN-β$^{0/0}$ mice (C) infected with 10,000 PFU of rLACV or rLACVdelNSs was monitored. Mice that were moribund or severely paralyzed were killed and scored dead on that day.

mammalian host. Cells lacking an IFN system are still able to undergo apoptosis induced by NSs (6), and in mammalian cells the antiviral IFN system dominates the RNAi system (18, 47). We therefore expected that an IFN-independent influence of NSs on virus replication would show up in IFN-deficient cells or animals. First, we compared the multistep growth of rLACV and rLACVdelNSs in primary MEFs derived from wt and IFNAR$^{0/0}$ mice. Since the delNSs mutant strongly activates IFN-β transcription (Fig. 5A), we also investigated the role of IFN-β by using cells from mice with a deleted IFN-β gene (IFN-β$^{0/0}$ MEFs). Figure 6A shows that in IFN-competent wt MEFs, the NSs-expressing rLACV had a clear growth advantage over the delNSs mutant. A difference of 4 log steps was observed at 24 h postinfection. Although this gap was reduced to a difference of about 1 log step at 72 h postinfection, rLACV was always superior to rLACVdelNSs. By contrast, in IFNAR$^{0/0}$ MEFs which are unable to respond to IFN, no apparent difference was observed at 24 h postinfection, and at 72 h postinfection the titers of rLACVdelNSs were even higher than those of rLACV (Fig. 6B). In IFN-β$^{0/0}$ MEFs, the delNSs mutant multiplied at a slightly lower rate than rLACV, but the difference between the two viruses was much less pronounced than in wt MEFs. This indicates that IFN-β contributes to the growth restriction of rLACVdelNSs in cell culture.

We also investigated the interaction of LACV NSs and the IFN system in vivo. wt and mutant mice were inoculated with

TABLE 1. Virus growth in brains of diseased IFNAR$^{0/0}$ mice

Virus	Animal no.	PFU/brain[a]
rLACV	1	8×10^7
	2	4×10^7
	3	6×10^7
rLACVdelNSs	1	6×10^7
	2	6×10^7
	3	4×10^7

[a] Brain weight was 0.4 g on average.

the recombinant viruses by the intraperitoneal route to mimic natural infection by mosquitoes (48). The NSs-expressing rLACV killed IFN-competent wt mice more rapidly and more efficiently than the delNSs mutant (Fig. 7A). IFNAR$^{0/0}$ mice, by contrast, were killed by both viruses with the same efficiency (Fig. 7B), and both viruses reached comparable titers in the brains of diseased animals (Table 1). IFN-β$^{0/0}$ mice displayed

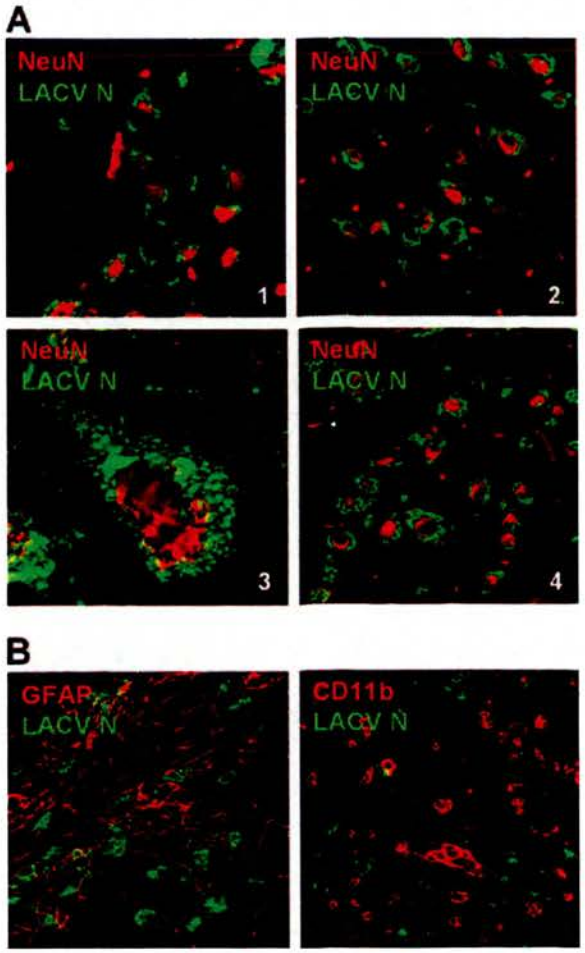

FIG. 8. Infection of neurons in vivo. (A) Brain sections of wt mice infected with rLACV (frame 1) or rLACVdelNSs (frames 2 to 4) were stained for viral antigen (green) and the neuron marker NeuN (red). Frames 1 to 3 show sections of the cortex, and frame 3 is a magnification of the section shown in frame 2. Frame 4 shows a section of the thalamus. (B) Brain sections from mice infected with rLACVdelNSs were double stained for viral antigen and markers for astrocytes (GFAP) or macrophages (CD11b).

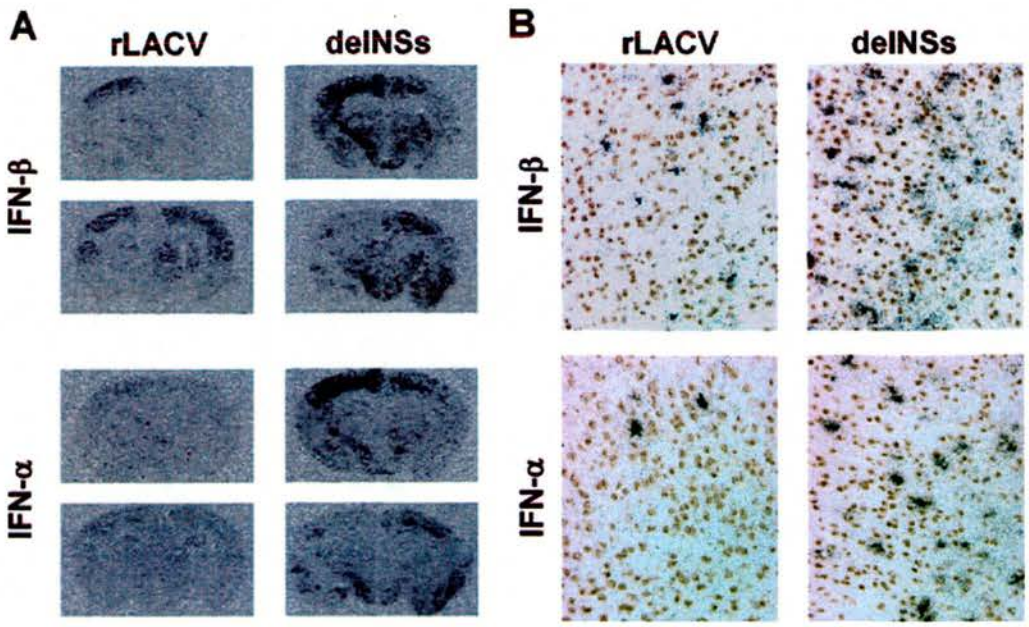

FIG. 9. Induction of IFN in the mouse brain. ISH with IFN-β or IFN-α probes (see Materials and Methods) was performed on brain sections of mice infected with rLACV or rLACVdelNSs. Macroscopic analysis (A) and microscopic analysis (B) using a combination of ISH to detect IFN-β or IFN-α mRNA (black silver grains) and immunohistochemical analysis for LACV N (brown stain).

an intermediate type of survival kinetics (Fig. 7C), as these animals succumbed more rapidly to infection than their wt counterparts but more slowly than the IFNAR$^{0/0}$ mice. This suggests that IFN-β plays a minor, but not a decisive, role in the protection from LACV infection in vivo.

Infection of neuronal cells. In the mammalian host, including humans, LACV is known to disseminate into the central nervous system and infect neuronal cells (28), causing severe aseptic encephalitis (23). To investigate whether rLACVdelNSs preferentially infects neuronal cells in a manner similar to rLACV, we analyzed the brains of wt mice with severe disease. In situ double immunofluorescence was performed using a rabbit polyclonal antibody directed against the LACV N protein together with various mouse monoclonal antibodies for markers of major brain cell types. NeuN-positive cells were heavily infected by both rLACV and rLACVdelNSs (Fig. 8A, frames 1 to 3), indicating that both viruses preferentially infected neurons. In some areas of the thalamus, almost 100% of the neurons were infected (Fig. 8A, frame 4). By contrast, in cells positive for the astrocyte marker GFAP, the oligodendrocyte marker myelin basic protein, or the macrophage markers CD11b and F4/80, no viral antigen was clearly detected (Fig. 8B and data not shown). Thus, rLACVdelNSs has the ability to disseminate in the brain and to preferentially infect neurons.

Induction of IFN by neurons. Given the similar ability of LACV possessing or lacking NSs to infect neurons, we wondered whether LACV would also block IFN induction in the central nervous system. To address this question, we compared IFN synthesis in brains from mice infected with either rLACV or rLACVdelNSs. ISH analysis of whole-brain slices demonstrated that rLACVdelNSs induced significantly higher IFN-β and IFN-α transcript levels than rLACV (Fig. 9A). To correlate in vivo IFN mRNA synthesis with virus infection, we combined the analysis of IFN mRNA with immunostaining against the LACV N protein. Examination of highly infected brain areas showed that brain cells infected with the delNSs mutant were more frequently positive for IFN mRNAs than those infected with rLACV (Fig. 9B). We therefore concluded that the IFN antagonist NSs of LACV is also functional in neurons.

DISCUSSION

In this study, we provided in vivo evidence that the IFN antagonism of LACV NSs constitutes its major biological function. In cells as well as in animals infected with wt rLACV, synthesis of antiviral type I IFN mRNAs was strongly impaired, demonstrating that LACV NSs abrogates IFN induction. Consequently, wt rLACV had a growth advantage over the delNSs mutant in IFN-competent cells and mice. By contrast, in all IFN-deficient systems including insect cells, no apparent difference was observed between the two viruses. Thus, NSs is only important in IFN-competent mammalian hosts and the deletion of the viral NSs gene can be fully complemented by inactivation of the host's IFN system. This strongly implies that bunyaviruses, which as arboviruses need to rapidly establish viremia in order to be transferred to new insect vectors, evolved the accessory NSs gene to overcome the fast-responding innate immune defense of the mammalian host.

Despite the strong effects of NSs on apoptosis (6, 14), no detectable differences in growth and virulence of our virus pair exist in IFN-deficient mammalian host systems (Fig. 6 and 7). This suggests that the proapoptotic function of LACV NSs has no apparent consequences for virus growth or virulence in vivo. The ability to promote (as well as to prevent) apoptosis was demonstrated for many different viruses (2), and it is thought

that the correct timing of cell death is important to optimize virus yields. However, reports have been contradictory with respect to the biological significance of virus-induced apoptosis. For influenza A virus, which strongly promotes apoptosis (27), reverse genetics experiments revealed no correlation between the levels of apoptosis in infected cells and the extent of virus replication (39). In line with this notion, it was found that BUNV NSs has the opposite activity of LACV NSs. It inhibits rather than promotes apoptosis (29), which raises a question about the role of programmed cell death in the bunyavirus infection cycle. The proapoptotic function of LACV NSs was shown in mammalian cells, and its importance for virus replication was inferred from its similarity with a C-terminal part of the proapoptotic *Drosophila* protein reaper (14). However, given the fact that reaper is an insect protein, it is curious that NSs-expressing LACV as well as other bunyaviruses do not induce cell death in insect cells (7). Thus, despite the sequence similarity to the proapoptotic *Drosophila* reaper, NSs has no apparent proapoptotic activity in insects, suggesting that NSs is not simply a reaper protein that was snatched by the bunyaviruses to promote cell death of infected cells. Rather, we favor the assumption that the proapoptotic function of LACV NSs is a side effect of its molecular mechanism to block IFN induction.

Expression of NSs from a cDNA construct was shown to counteract the RNAi effect of transfected RNA oligonucleotides (49). RNAi is regarded as an antiviral mechanism of insects (44), and we show that LACV infection provokes a strong RNAi response in insect cells (Fig. 1). In mammalian cells RNAi effects can be observed if the IFN system is deleted (47) or circumvented by using short dsRNAs to induce RNAi (18). Using recombinant viruses, we addressed the supposed role of NSs in RNAi inhibition both in the mosquito system and the mammalian host. Surprisingly, we could not detect any advantage conferred by NSs expression in insect cells (Fig. 2) or in IFN-deficient mammalian cells and animals (Fig. 6 and 7). Also, in insect cells the NSs-expressing rLACV virus established PDR to the same extent as the NSs-deleted mutant did, and both viruses were equally subject to PDR (Fig. 3). Furthermore, LACV NSs was unable to counteract RNAi in insect cells (Fig. 4), just as was shown for RVFV NSs (22). Similarly, the NSs of BUNV has no effect on viral transcription in insect cells (A., Kohl and R. M. Elliott, presented at the 12th International Conference on Negative-Strand Viruses, Pisa, Italy, 14 to 19 June 2003). These data do not support the view that bunyavirus NSs plays a role as an anti-RNAi factor in the context of infection. A similar negative conclusion was recently drawn for other viral proteins with a proposed anti-RNAi function (16, 30).

Our in vivo analyses not only established NSs as the IFN antagonist of LACV but also demonstrated that both IFN-β and IFN-α contribute to protection from LACV infection (Fig. 6 to 9). Nevertheless, a high percentage of wt mice eventually succumbed to infection with LACV, even when the strong IFN-inducer rLACVdelNSs was used (Fig. 7). It should be noted that the most effective IFN-induced protein with antiviral activity against LACV is the human MxA protein (24) and that the gene for the murine homologue Mx2 is defective in most inbred mouse strains including the C57BL/6 mice used in our experiments (50). We therefore assumed that our mice could not launch a pronounced antiviral response against rLACVdelNSs because they lack an Mx protein with antibunyaviral activity. To follow this up, we compared the antiviral effect of type I IFN against wt and delNSs virus in the MxA-expressing human Huh7 cells and the Mx-negative mouse 3T3 cells. IFN inhibited both viruses much more strongly (2 log steps) in the human cell line than in the mouse cell line (data not shown). Thus, the weak attenuation of the delNSs virus in wt mice is, indeed, most probably due to the lack of the suitable IFN effector protein.

In summary, we present evidence that the major biological function of LACV NSs is to inhibit the antiviral type I IFN system in the mammalian host. Further investigations of the molecular mechanism of NSs action might reveal an interesting link between apoptosis induction, the RNAi system, and the IFN system.

ACKNOWLEDGMENTS

We are indebted to Michèle Bouloy, Agnès Billecocq, and Marcel Prins for rapidly helping out with the SFV RNAi system and Karl-Klaus Conzelmann, Richard M. Elliott, Jim Robertson, and Takashi Fujita for providing reagents that were essential for this work. D. T. Brown (North Carolina State University, Raleigh, NC) is acknowledged for kindly providing the U4.4 mosquito cell line. We thank Otto Haller for support and helpful comments and Georg Kochs for critically reading the manuscript.

Work in our laboratories is supported by grants WE 2616/2-1 and WE 2616/2-2 from the Deutsche Forschungsgemeinschaft (F.W.), by the Belgian FRSM and ARC (T.M.), by the Wellcome Trust (A.K.), and by NIH grants AI32543 and AI34014 (C.D.B., I.S.-V., and K.E.O.).

REFERENCES

1. **Beaty, B. J., D. H. Bishop, M. Gay, and F. Fuller.** 1983. Interference between bunyaviruses in Aedes triseriatus mosquitoes. Virology **127:**83–90.
2. **Benedict, C. A., P. S. Norris, and C. F. Ware.** 2002. To kill or be killed: viral evasion of apoptosis. Nat. Immunol. **3:**1013–1018.
3. **Billecocq, A., M. Spiegel, P. Vialat, A. Kohl, F. Weber, M. Bouloy, and O. Haller.** 2004. NSs protein of Rift Valley fever virus blocks interferon production by inhibiting host gene transcription. J. Virol. **78:**9798–9806.
4. **Blair, C. D., Z. N. Adelman, and K. E. Olson.** 2000. Molecular strategies for interrupting arthropod-borne virus transmission by mosquitoes. Clin. Microbiol. Rev. **13:**651–661.
5. **Blakqori, G., G. Kochs, O. Haller, and F. Weber.** 2003. Functional L polymerase of La Crosse virus allows in vivo reconstitution of recombinant nucleocapsids. J. Gen. Virol. **84:**1207–1214.
6. **Blakqori, G., and F. Weber.** 2005. Efficient cDNA-based rescue of La Crosse bunyaviruses expressing or lacking the nonstructural protein NSs. J. Virol. **79:**10420–10428.
7. **Borucki, M. K., B. J. Kempf, B. J. Blitvich, C. D. Blair, and B. J. Beaty.** 2002. La Crosse virus: replication in vertebrate and invertebrate hosts. Microbes Infect. **4:**341–350.
8. **Bouloy, M., C. Janzen, P. Vialat, H. Khun, J. Pavlovic, M. Huerre, and O. Haller.** 2001. Genetic evidence for an interferon-antagonistic function of rift valley fever virus nonstructural protein NSs. J. Virol. **75:**1371–1377.
9. **Bucher, E., T. Sijen, P. De Haan, R. Goldbach, and M. Prins.** 2003. Negative-strand tospoviruses and tenuiviruses carry a gene for a suppressor of gene silencing at analogous genomic positions. J. Virol. **77:**1329–1336.
10. **Buchholz, U. J., S. Finke, and K. K. Conzelmann.** 1999. Generation of bovine respiratory syncytial virus (BRSV) from cDNA: BRSV NS2 is not essential for virus replication in tissue culture, and the human RSV leader region acts as a functional BRSV genome promoter. J. Virol. **73:**251–259.
11. **Calisher, C. H.** 1994. Medically important arboviruses of the United States and Canada. Clin. Microbiol. Rev. **7:**89–116.
12. **Centers for Disease Control and Prevention.** 2005. Confirmed and Probable California Serogroup Viral (mainly La Crosse) Encephalitis Cases, Human, United States, 1964–2005. Centers for Disease Control and Prevention, Atlanta, GA. http://www.cdc.gov/ncidod/dvbid/arbor/pdf/LACDOC07132006.pdf.
13. **Colonna, M., A. Krug, and M. Cella.** 2002. Interferon-producing cells: on the front line in immune responses against pathogens. Curr. Opin. Immunol. **14:**373–379.
14. **Colon-Ramos, D. A., P. M. Irusta, E. C. Gan, M. R. Olson, J. Song, R. I.**

Morimoto, R. M. Elliott, M. Lombard, R. Hollingsworth, J. M. Hardwick, G. K. Smith, and S. Kornbluth. 2003. Inhibition of translation and induction of apoptosis by bunyaviral nonstructural proteins bearing sequence similarity to reaper. Mol. Biol. Cell **14:**4162–4172.

15. **Condreay, L. D., and D. T. Brown.** 1988. Suppression of RNA synthesis by a specific antiviral activity in Sindbis virus-infected *Aedes albopictus* cells. J. Virol. **62:**346–348.
16. **Cullen, B. R.** 2006. Is RNA interference involved in intrinsic antiviral immunity in mammals? Nat. Immunol. **7:**563–567.
17. **Delhaye, S., S. Paul, G. Blakqori, M. Minet, F. Weber, P. Staeheli, and T. Michiels.** 2006. Neurons produce type I interferon during viral encephalitis. Proc. Natl. Acad. Sci. USA **103:**7835–7840.
18. **Elbashir, S. M., J. Harborth, W. Lendeckel, A. Yalcin, K. Weber, and T. Tuschl.** 2001. Duplexes of 21-nucleotide RNAs mediate RNA interference in cultured mammalian cells. Nature **411:**494–498.
19. **Elliott, R. M.** 1997. Emerging viruses: the *Bunyaviridae*. Mol. Med. **3:**572–577.
20. **Erlandsson, L., R. Blumenthal, M. L. Eloranta, H. Engel, G. Alm, S. Weiss, and T. Leanderson.** 1998. Interferon-beta is required for interferon-alpha production in mouse fibroblasts. Curr. Biol. **8:**223–226.
21. **Garcia, S., A. Billecocq, J. M. Crance, U. Munderloh, D. Garin, and M. Bouloy.** 2005. Nairovirus RNA sequences expressed by a Semliki Forest virus replicon induce RNA interference in tick cells. J. Virol. **79:**8942–8947.
22. **Garcia, S., A. Billecocq, J. M. Crance, M. Prins, D. Garin, and M. Bouloy.** 2006. Viral suppressors of RNA interference impair RNA silencing induced by a Semliki Forest virus replicon in tick cells. J Gen. Virol. **87:**1985–1989.
23. **Griot, C., F. Gonzalez-Scarano, and N. Nathanson.** 1993. Molecular determinants of the virulence and infectivity of California serogroup bunyaviruses. Annu. Rev. Microbiol. **47:**117–138.
24. **Haller, O., and G. Kochs.** 2002. Interferon-induced Mx proteins: dynamin-like GTPases with antiviral activity. Traffic **3:**710–717.
25. **Haller, O., G. Kochs, and F. Weber.** 2006. The interferon response circuit: induction and suppression by pathogenic viruses. Virology **344:**119–130.
26. **Hamilton, A. J., and D. C. Baulcombe.** 1999. A species of small antisense RNA in posttranscriptional gene silencing in plants. Science **286:**950–952.
27. **Hinshaw, V. S., C. W. Olsen, N. Dybdahl-Sissoko, and D. Evans.** 1994. Apoptosis: a mechanism of cell killing by influenza A and B viruses. J. Virol. **68:**3667–3673.
28. **Janssen, R., F. Gonzalez-Scarano, and N. Nathanson.** 1984. Mechanisms of bunyavirus virulence. Comparative pathogenesis of a virulent strain of La Crosse and an avirulent strain of Tahyna virus. Lab. Investig. **50:**447–455.
29. **Kohl, A., R. F. Clayton, F. Weber, A. Bridgen, R. E. Randall, and R. M. Elliott.** 2003. Bunyamwera virus nonstructural protein NSs counteracts interferon regulatory factor 3-mediated induction of early cell death. J. Virol. **77:**7999–8008.
30. **Kok, K. H., and D. Y. Jin.** 2006. Influenza A virus NS1 protein does not suppress RNA interference in mammalian cells. J. Gen. Virol. **87:**2639–2644.
31. **Kuno, G., and G. J. Chang.** 2005. Biological transmission of arboviruses: reexamination of and new insights into components, mechanisms, and unique traits as well as their evolutionary trends. Clin. Microbiol. Rev. **18:**608–637.
32. **Le May, N., S. Dubaele, L. P. De Santis, A. Billecocq, M. Bouloy, and J. M. Egly.** 2004. TFIIH transcription factor, a target for the Rift Valley hemorrhagic fever virus. Cell **116:**541–550.
33. **Leonard, V. H., A. Kohl, T. J. Hart, and R. M. Elliott.** 2006. Interaction of Bunyamwera *Orthobunyavirus* NSs protein with mediator protein MED8: a mechanism for inhibiting the interferon response. J. Virol. **80:**9667–9675.
34. **Li, W. X., H. Li, R. Lu, F. Li, M. Dus, P. Atkinson, E. W. Brydon, K. L. Johnson, A. Garcia-Sastre, L. A. Ball, P. Palese, and S. W. Ding.** 2004. Interferon antagonist proteins of influenza and vaccinia viruses are suppressors of RNA silencing. Proc. Natl. Acad. Sci. USA **101:**1350–1355.
35. **Liljestrom, P., and H. Garoff.** 1991. A new generation of animal cell expression vectors based on the Semliki Forest virus replicon. Biotechnology **9:**1356–1361.
36. **Marie, I., J. E. Durbin, and D. E. Levy.** 1998. Differential viral induction of distinct interferon-alpha genes by positive feedback through interferon regulatory factor-7. EMBO J. **17:**6660–6669.
37. **McJunkin, J. E., E. C. de los Reyes, J. E. Irazuzta, M. J. Caceres, R. R. Khan, L. L. Minnich, K. D. Fu, G. D. Lovett, T. Tsai, and A. Thompson.** 2001. La Crosse encephalitis in children. N. Engl. J. Med. **344:**801–807.
38. **McJunkin, J. E., R. R. Khan, and T. F. Tsai.** 1998. California-La Crosse encephalitis. Infect. Dis. Clin. N. Am. **12:**83–93.
39. **Morris, S. J., K. Nightingale, H. Smith, and C. Sweet.** 2005. Influenza A virus-induced apoptosis is a multifactorial process: exploiting reverse genetics to elucidate the role of influenza A virus proteins in virus-induced apoptosis. Virology **335:**198–211.
40. **Muller, U., U. Steinhoff, L. F. Reis, S. Hemmi, J. Pavlovic, R. M. Zinkernagel, and M. Aguet.** 1994. Functional role of type I and type II interferons in antiviral defense. Science **264:**1918–1921.
41. **Powers, A. M., K. E. Olson, S. Higgs, J. O. Carlson, and B. J. Beaty.** 1994. Intracellular immunization of mosquito cells to La Crosse virus using a recombinant Sindbis virus vector. Virus Res. **32:**57–67.
42. **Rust, R. S., W. H. Thompson, C. G. Matthews, B. J. Beaty, and R. W. Chun.** 1999. La Crosse and other forms of California encephalitis. J. Child Neurol. **14:**1–14.
43. **Samuel, C. E.** 2001. Antiviral actions of interferons. Clin. Microbiol. Rev. **14:**778–809.
44. **Sanchez-Vargas, I., E. A. Travanty, K. M. Keene, A. W. Franz, B. J. Beaty, C. D. Blair, and K. E. Olson.** 2004. RNA interference, arthropod-borne viruses, and mosquitoes. Virus Res. **102:**65–74.
45. **Scallan, M. F., and R. M. Elliott.** 1992. Defective RNAs in mosquito cells persistently infected with Bunyamwera virus. J Gen. Virol. **73:**53–60.
46. **Shaw-Jackson, C., and T. Michiels.** 1999. Absence of internal ribosome entry site-mediated tissue specificity in the translation of a bicistronic transgene. J. Virol. **73:**2729–2738.
47. **Sledz, C. A., M. Holko, M. J. de Veer, R. H. Silverman, and B. R. Williams.** 2003. Activation of the interferon system by short-interfering RNAs. Nat. Cell Biol. **5:**834–839.
48. **Soldan, S. S., and F. Gonzalez-Scarano.** 2005. Emerging infectious diseases: the *Bunyaviridae*. J. Neurovirol. **11:**412–423.
49. **Soldan, S. S., M. L. Plassmeyer, M. K. Matukonis, and F. Gonzalez-Scarano.** 2005. La Crosse virus nonstructural protein NSs counteracts the effects of short interfering RNA. J. Virol. **79:**234–244.
50. **Staeheli, P., and J. G. Sutcliffe.** 1988. Identification of a second interferon-regulated murine Mx gene. Mol. Cell. Biol. **8:**4524–4528.
51. **Thomas, D., G. Blakqori, V. Wagner, M. Banholzer, N. Kessler, R. M. Elliott, O. Haller, and F. Weber.** 2004. Inhibition of RNA polymerase II phosphorylation by a viral interferon antagonist. J. Biol. Chem. **279:**31471–31477.
52. **Utz, J. T., C. S. Apperson, J. N. MacCormack, M. Salyers, E. J. Dietz, and J. T. McPherson.** 2003. Economic and social impacts of La Crosse encephalitis in western North Carolina. Am. J. Trop. Med. Hyg. **69:**509–518.
53. **van Pesch, V., H. Lanaya, J. C. Renauld, and T. Michiels.** 2004. Characterization of the murine alpha interferon gene family. J. Virol. **78:**8219–8228.
54. **Wang, X. H., R. Aliyari, W. X. Li, H. W. Li, K. Kim, R. Carthew, P. Atkinson, and S. W. Ding.** 2006. RNA interference directs innate immunity against viruses in adult *Drosophila*. Science **312:**452–454.
55. **Weber, F., A. Bridgen, J. K. Fazakerley, H. Streitenfeld, R. E. Randall, and R. M. Elliott.** 2002. Bunyamwera bunyavirus nonstructural protein NSs counteracts the induction of alpha/beta interferon. J. Virol. **76:**7949–7955.
56. **Weber, F., and R. M. Elliott.** 2002. Antigenic drift, antigenic shift and interferon antagonists: how bunyaviruses counteract the immune system. Virus Res. **88:**129–136.
57. **Whitley, R. J., and J. W. Gnann.** 2002. Viral encephalitis: familiar infections and emerging pathogens. Lancet **359:**507–513.
58. **Yoneyama, M., W. Suhara, Y. Fukuhara, M. Fukuda, E. Nishida, and T. Fujita.** 1998. Direct triggering of the type I interferon system by virus infection: activation of a transcription factor complex containing IRF-3 and CBP/p300. EMBO J. **17:**1087–1095.

Journal of General Virology (2007), **88**, 000–000 DOI 10.1099/vir.0.83191-0

The type I interferon system protects mice from Semliki Forest virus by preventing widespread virus dissemination in extraneural tissues, but does not mediate the restricted replication of avirulent virus in central nervous system neurons

Rennos Fragkoudis,[1]† Lucy Breakwell,[1]† Clive McKimmie,[1] Amanda Boyd,[1] Gerald Barry,[1] Alain Kohl,[1] Andres Merits[2] and John K. Fazakerley[1]

Correspondence
John K. Fazakerley
John.Fazakerley@ed.ac.uk

[1]Virology, Centre for Infectious Diseases, College of Medicine and Veterinary Medicine, University of Edinburgh, UK

[2]Institute of Technology, University of Tartu, Estonia

Semliki Forest virus (SFV) infection of the mouse provides a powerful model to study the pathogenesis of virus encephalitis. SFV and other alphavirus-based vector systems are increasingly used in biotechnology and medicine. This study analysed the strong susceptibility of this virus to type I interferon (IFN) responses. Following intraperitoneal infection of adult mice, SFV strain A7(74) was efficiently (100 %) neuroinvasive. In contrast, SFV4 was poorly (21 %) neuroinvasive. Upon entry into the brain, both viruses activated type I IFN responses. As determined by quantitative RT-PCR, activation of the IFN-α gene was proportional to virus RNA load. An intact type I IFN system was required for protection against both strains of SFV. IFN strongly curtailed virus spread in many cell types and in many tissues. In mice with an intact type I IFN system, infected cells were rarely observed and tissue tropism was difficult to determine. In the absence of a functional type I IFN system, the tropism and the potential for rapid and widespread infection of this virus was revealed. Virus infection was readily observed in the myocardium, endocardium, exocrine pancreas, adipose tissue, smooth muscle cells and in the brain in meningeal cells, ependymal cells and oligodendrocytes. In the brains of mice with and without type I IFN responses, virus infection of neurons remained rare and focal, indicating that the previously described restricted replication of SFV A7(74) in neurons is not mediated by type I IFN responses.

Received 29 May 2007
Accepted 28 July 2007

INTRODUCTION

Semliki Forest virus (SFV) is a mosquito-borne virus that naturally circulates in sub-Saharan Africa. The virus is an alphavirus of the family *Togaviridae*. Natural human and equine infections have been described (Mathiot *et al.*, 1990). The virus is closely related to Chikungunya virus, responsible recently for an outbreak of severe arthralgia in the islands of the Indian Ocean (Schuffenecker *et al.*, 2006). Other alphaviruses include Sindbis virus in North Africa and Europe; Eastern, Western and Venezuelan equine encephalitis viruses in the Americas and Ross River virus in Australia. SFV infection of laboratory mice provides a tractable model system for the study of virus pathogenesis and in particular virus encephalitis (Fazakerley, 2004). Virulence in mice has been characterized for several natural isolates and their laboratory-passaged strains (Bradish *et al.*, 1971). The most commonly studied strains include A7 and A7(74), which are avirulent in adult mice, and L10 and the prototype, which are virulent in adult mice. All strains of SFV are virulent in neonatal or young suckling mice (Bradish *et al.*, 1971; Pusztai *et al.*, 1971; Seamer *et al.*, 1967).

The most characterized avirulent strain of SFV, A7(74), is virulent in mice infected at the age of 11 days or less, but is avirulent in older mice; virus dissemination in the central nervous system (CNS) is increasingly restricted with age (Oliver *et al.*, 1997). In 4–5-week-old mice, intraperitoneal inoculation of SFV A7(74) results in a high-titre plasma viraemia from which virus is seeded into perivascular foci in the brain and spinal cord; there is little spread of virus from cell to cell, foci do not enlarge with time and the infection is restricted in mature neurons (Fazakerley *et al.*,

†These authors contributed equally to this work.

1993). SFV A7(74) remains avirulent following direct intracerebral inoculation, but inoculation by this route results in a widespread infection of oligodendrocytes in the major white matter tracts (Fazakerley *et al.*, 2006). The underlying events resulting in restriction of this strain of the virus in mature neurons remain undetermined. Intraperitoneal infection with the virulent L10 strain also results in a high-titre plasma viraemia, but in this case neuronal infection is not restricted and perivascular foci of CNS infection rapidly enlarge to give rise to a fatal panencephalitis (Fazakerley *et al.*, 1993).

The prototype (SFV4) and A7(74) strains are available as molecular cDNA clones (Liljeström & Garoff, 1991; Vaha-Koskela *et al.*, 2003). Infectious RNA can be derived by *in vitro* transcription and infectious virus by electroporation of this RNA into eukaryotic cells. In mice, SFV4 virus is virulent by intranasal or intracerebral inoculation (Fazakerley *et al.*, 2002; Glasgow *et al.*, 1991). There are numerous genetic changes between the cDNA clones of SFV4 and SFV A7(74), but changes in non-structural protein 3 and the 5′-untranslated sequences appear to be the most important in determining the ability of the virus to replicate in the adult mouse brain (Tuittila *et al.*, 2000). Molecular engineering of the SFV cDNA has led to the generation of a series of replicon vectors that are increasingly used for protein expression, transient gene transfer and increasingly importantly vaccination (Karlsson & Liljeström, 2004). The vector replicon can be packaged into virus-like particles (VLPs), which have the ability to infect cells in the same way as virus (Smerdou & Liljeström, 1999). Following infection with virus or VLPs, or following transfection of replicon RNA, cells in continuous culture rapidly undergo apoptosis (Allsopp & Fazakerley, 2000; Glasgow *et al.*, 1997; Scallan *et al.*, 1997).

Not long after the discovery of the interferon (IFN) system, it was shown that a crude preparation of IFN derived from West Nile virus-infected mice could protect mice against the virulent MB strain of SFV (Finter, 1966). In this and subsequent studies, the extent of protection was clearly dependent on virus strain, dose and time of administration (Bradish & Titmuss, 1981; Smillie *et al.*, 1973). Conversely, administration of anti-IFN antibodies exacerbated SFV infection (Fauconnier, 1971). The kinetics of the type I IFN response in SFV A7(74)-infected mice parallels the plasma viraemia (Bradish *et al.*, 1975). In the original studies on mice with disruption of the type I IFN receptor α-chain (IFNAR-1$^{-/-}$), it was demonstrated that both adult and neonatal mice without a functional type I IFN system succumbed to infection with SFV much more rapidly than did wild-type (wt) mice (Hwang *et al.*, 1995; Muller *et al.*, 1994). The type I IFN system has also been demonstrated to be crucial for the protection of mice from nominally avirulent strains of the related alphaviruses Venezuelan equine encephalitis virus and Sindbis virus (Grieder & Vogel, 1999; Ryman *et al.*, 2000). Strains of SFV and eastern equine encephalitis virus vary in their sensitivity to IFN (Aguilar *et al.*, 2005; Deuber & Pavlovic, 2007). What remains to be determined for SFV is the role of the type I IFN system following infection with the most commonly used A7(74) and SFV4 strains. Furthermore, not only for alphaviruses but for many neurotropic viruses, the course and role of IFN responses in the brain during virus encephalitis remain to be fully characterized. In the case of SFV encephalitis, it remains to be determined whether the type I IFN system is involved in the restricted replication of A7(74) in neurons and in the age-related virulence (Fazakerley *et al.*, 1993). Here, we have shown that: (i) both A7(74) and SFV4 activate CNS type I IFN gene expression in the mature mouse brain; (ii) IFN gene expression is proportional to virus load; (iii) the type I IFN response is crucial for protection against SFV A7(74); and (iv) this protection works by strongly curtailing virus spread in many cell types in many tissues including some CNS cell types but is not responsible for the restricted dissemination of SFV A7(74) in mature CNS neurones.

METHODS

Viruses. The A7(74) strain of SFV was derived from the AR2066 strain by seven passages through neonatal mouse brain and colony selection on chick embryo fibroblasts; AR2066 was isolated from *Aedes argenteopunctatus* mosquitoes in Namancurra, Mozambique (McIntosh *et al.*, 1961). The L10 strain was derived from the original isolate of SFV (Smithburn & Haddow, 1944) by eight intracerebral passages through adult and two through baby mouse brains (Bradish *et al.*, 1971). Infectious SFV4 virus was generated from a cDNA plasmid derived from the prototype strain of SFV (Liljeström & Garoff, 1991). The full-length pSP6-SFV4 cDNA was a kind gift from Professor Peter Liljeström, (Karolinska Institute, Stockholm, Sweden).

SFV4 marker virus containing the gene for enhanced green fluorescent protein (eGFP) was constructed by inserting the coding sequence for eGFP followed by the foot-and-mouth disease virus 2A cleavage sequence between that for the capsid protein and p62 in the virus structural protein open reading frame. This strategy has been used previously to construct an eGFP-labelled Sindbis virus (Thomas *et al.*, 2003). The resulting SFV4 marker virus, designated SFV4-steGFP, replicated well *in vitro* and *in vivo* and infected cells showed strong green fluorescence (R. Fragkoudis and others, unpublished). SFV4 and SFV4-steGFP were generated from infectious cDNAs as described previously (Liljeström & Garoff, 1991). Briefly, the plasmid was linearized with *Spe*I and capped transcripts were produced by *in vitro* transcription with SP6 polymerase in the presence of m^{7}GpppG cap analogue (Amersham). RNA was electroporated into BHK-21 cells using two consecutive 140 V square-wave pulses with a pulse length of 25 ms on a Bio-Rad Gene Pulser X cell electroporator. Virus stocks were collected after 24 h at 37 °C, titrated on monolayers of BHK-21 cells and used to infect mice.

Virus infectivity assay. Virus titres were determined by plaque assay on BHK-21 cells as described previously (Fazakerley *et al.*, 1993). Briefly, BHK cells (4×10^5) were seeded into six-well plates in 2 ml Glasgow minimum essential medium with 10 % fetal calf serum and incubated at 5 % CO_2 and 37 °C until 80 % confluent. The growth medium was then removed, cells washed with PBS and 10-fold dilutions of test samples were titrated in duplicate. Infected cells were incubated for 1 h at room temperature in a humid atmosphere. After the addition of agar, the plates were incubated for a further 48 h and fixed with 10 % neutral buffered formaldehyde for 3 h before staining

with 0.1 % toluidine blue for at least 1 h. Plaques were counted after washing.

Mouse strains. Strain 129/Sv(ev) and 129/Sv(ev) mice with a disruption of the α-chain of the IFN-α/β receptor (IFNAR-1$^{-/-}$) (Muller *et al.*, 1994) were purchased from B&K Universal Ltd. BALB/c and CB17 *nu/nu* mice were purchased from Harlan Olac. Mice were bred and maintained in the Centre for Infectious Diseases Animal Unit, College of Medicine & Veterinary Medicine, University of Edinburgh, UK, in specific-pathogen-free and environmentally enriched conditions with food and water supplied *ad libitum*. All breeding and experimental studies were agreed by the University of Edinburgh Ethical Review Committee and were carried out under the authority of a UK Home Office licence.

Infection of mice. Experimental infection of mice was carried out at 4–6 weeks of age. Mice were inoculated intraperitoneally with 0.1 ml PBS with 0.75 % BSA (PBSA) containing 5×10^3 p.f.u. SFV or intracranially with 20 µl PBSA containing 10^3 p.f.u. virus or with PBSA alone. Mice were checked twice daily and euthanized on reaching previously defined clinical end points considered to be indicative of fatal disease; these included: paralysis in two or more limbs; inability to move, feed or drink; incontinence; breathing difficulties; and seizures. Mice to be sampled were deeply anaesthetised with halothane and perfused with PBS through the left cardiac ventricle; brains were removed, divided bilaterally down the midline and either placed in RNA*later* for RNA analysis, snap frozen on dry ice for virus titration or immersion fixed in 10 % phosphate-buffered formal saline for histopathological study.

RNA extraction and quantitative PCR. RNA was extracted from frozen cell-culture pellets or tissue samples stored in RNA*later* using Qiagen kits according to the manufacturer's instructions; the RNeasy Lipid kit was used for brain samples. Extracted RNA was stored at −80 °C. The quality of the extracted RNA was determined using an Agilent 2100 Bioanalyser and the RNA 6000 Nano assay. High-quality RNA samples were reverse transcribed using Superscript II RNase H reverse transcriptase. Samples to be directly compared were reverse transcribed at the same time using the same master mix (all reagents were from Invitrogen). The reaction mixture had a final volume of 20 µl and contained 1 µl oligo(dT)$_{12–18}$ primer, 5 µg RNA template, 1 µl 10 mM dNTPs and DNase/RNase-free water to a volume of 12 µl. The mixture was heated for 5 min at 65 °C. Next, 4 µl 5× First-strand buffer, 2 µl 0.1 M DTT and 1 µl RNasin recombinant RNase inhibitor were added. Reactions were incubated at 42 °C for 2 min and 1 µl reverse transcriptase was added. The reactions were incubated at 42 °C for 1 h. The enzyme was inactivated by incubation for 15 min at 70 °C. The cDNA was stored at −20 °C.

Levels of viral RNA and IFN transcripts were determined by real-time quantitative (Q)PCR. Test samples and standards were assayed in triplicate. QPCR was performed using a FastStart DNA Master SYBR Green I kit (Roche). Briefly, in a total volume of 20 µl (made up in RNase-free water), reaction mixes contained: 50 pM primers, 40 mM dNTPs, 10× buffer plus 2 mM $MgCl_2$, SYBR Green (diluted 1 : 20 000; Biogene), 5 U FastStart *Taq* (Roche Applied Science) and 2 µl cDNA. Tubes were heated to 94 °C for 5 min and 40 cycles of 94 °C for 20 s, 62 °C for 20 s and 72 °C for 20 s were carried out on a RotorGene 3000 (Corbett Research). As a positive control for SFV, an *in vitro* transcript from the pGEM1-SFV cDNA plasmid containing the structural genes of SFV was transcribed using a Promega RiboMax kit. Serial dilutions of this plasmid were used to produce a standard curve for quantification of the PCR amplicons and thus the virus RNA. Brain samples were normalized to levels of β-actin transcripts (Brown *et al.*, 2003). Sequences of the primers used in the assay were as follows: IFN-α: 5′-AGGACAGGAAGGATTTTGGA-3′ and 5′-GCTGCTGATGGAGGTCATT-3′ (degenerate primers based on IFN-α_4; McKimmie & Fazakerley, 2005); SFV E1: 5′-CGCATCAC-CTTCTTTTGTG-3′ and 5′-CCAGACCACCCGAGATTTT-3′; IFN-β: 5′-CACAGCCCTCTCCAT CAACT-3′ and 5′-GCATCTTCTCCGTC-ATCTCC-3′; β-actin: 5′-CGTTGACATCCGTAAAGACC-3′ and 5′-CTGGAAGGTGGACAGTGAG-3′.

***In situ* hybridization.** To observe virus distribution in the brain, after immersion fixation in 10 % phosphate-buffered formal saline, half brains were embedded in paraffin and 5 µm sections cut onto poly-L-lysine-coated (Sigma) or Biobond-coated (British BioCell International) glass slides. Riboprobes were transcribed *in vitro* with T7 polymerase (using a Riboprobe Gemini kit; Promega) from *Hin*cII-linearized pGEM1-SFV. As a control, some sections were hybridized with a riboprobe to the P1 region of the unrelated Theiler's virus. Probes were hydrolysed in 0.04 M $NaHCO_3$ for 30 min at 60 °C prior to use. *In situ* hybridization with ^{35}S-labelled riboprobes was carried out as described previously (Fazakerley *et al.*, 1993). Autoradiographic images of sections hybridized with ^{35}S-labelled riboprobes were produced by exposure of air-dried sections to Hyperfilm βmax (Amersham). Sections were subsequently dipped in photographic emulsion (LM-1, diluted with 0.66 M ammonium acetate; Amersham) and exposed, usually for 7 days, at 4 °C.

Histopathology. Immunostaining to detect SFV-infected cells in paraffin-embedded tissues sections was performed as described previously (Fazakerley *et al.*, 2006). Tissues to be studied for the distribution of eGFP-positive cells were fixed in 10 % phosphate-buffered formal saline overnight and examined on a Zeiss fluorescent stereomicroscope with a GFP filter before cryopreserving by sequential passage through 5, 10 and 25 % sucrose in PBS. After freezing in OCT, 12–14 µm sections were cut onto poly-L-lysine-coated glass slides using a cryomicrotome. Sections were stained with propidium iodide to visualize cell nuclei or were lightly stained with diaminobenzidine to allow visualization of the tissue structure (this preserved the eGFP signal better than conventional stains such as haematoxylin).

RESULTS

SFV A7(74) but not SFV4 is efficiently neuroinvasive in adult mice, and brain infection induces type I IFN gene expression

Following intraperitoneal inoculation, SFV A7(74) has previously been demonstrated to be efficiently and consistently neuroinvasive (Fazakerley *et al.*, 1993; Pusztai *et al.*, 1971). SFV4 is neuroinvasive if given intranasally (Glasgow *et al.*, 1991). The neuroinvasive efficiency of SFV4 following intraperitoneal infection has not been studied in detail. To determine whether SFV4 is naturally neuroinvasive following intraperitoneal inoculation and to determine whether SFV neuroinvasion activates the type I IFN system, 4–5-week-old BALB/c mice were inoculated intraperitoneally with 5000 p.f.u. SFV A7(74) or SFV4. At days 3 and 7 post-inoculation (p.i.), five mice from each group were exsanguinated under terminal anaesthesia, perfused through the left cardiac ventricle with PBS to remove any remaining blood in the circulatory system, and the brains removed and assayed for infectious virus and IFN gene transcripts. Levels of infectious virus were assayed by standard plaque assay. Levels of IFN transcripts were assayed by QPCR. QPCR was used in preference to

assaying functional IFN as RNA levels are less likely to be affected by levels of blood-derived material, particularly as SFV A7(74) is known to disrupt the integrity of the blood–brain barrier (Parsons & Webb, 1982).

At 3 and 7 days p.i., all (10/10) mice infected with SFV A7(74) had infectious virus and IFN-α gene transcripts detectable in the brain (Table 1), demonstrating that the type I IFN system was activated in response to neuroinvasion by this strain of the virus. The levels of infectious virus and the induced levels of IFN-α transcripts showed considerable variation between individual mice. For the virus titres, this was consistent with previous studies (Fazakerley *et al.*, 1993). Presumably, variation resulted from temporal and spatial differences in virus neuroinvasion among individual mice. Interestingly, for individual mice there was a very strong correlation (r^2=0.98) between levels of virus RNA and levels of IFN transcripts (Fig. 1a); the higher the brain virus titre, the higher the level of IFN transcripts. Presumably, the greater the number of virus-infected cells, the greater the number of cells producing IFN.

In contrast to SFV A7(74) infection, intraperitoneal infection with SFV4 resulted in only one of the five mice at day 3 and none of the five mice at day 7 p.i. having detectable infectious brain virus. Intraperitoneal infection with SFV4 was repeated with nine mice per group with similar results; only two had infectious virus in the brain at day 3 and only one had infectious virus at day 7 p.i. In this second experiment, the mean titre of the three virus-positive brains was 2.3 $\log_{10}$ p.f.u. g^{-1}. It was concluded that SFV4 is poorly neuroinvasive, with only 21 % of mice (3/14) demonstrating neuroinvasion at day 3 p.i.

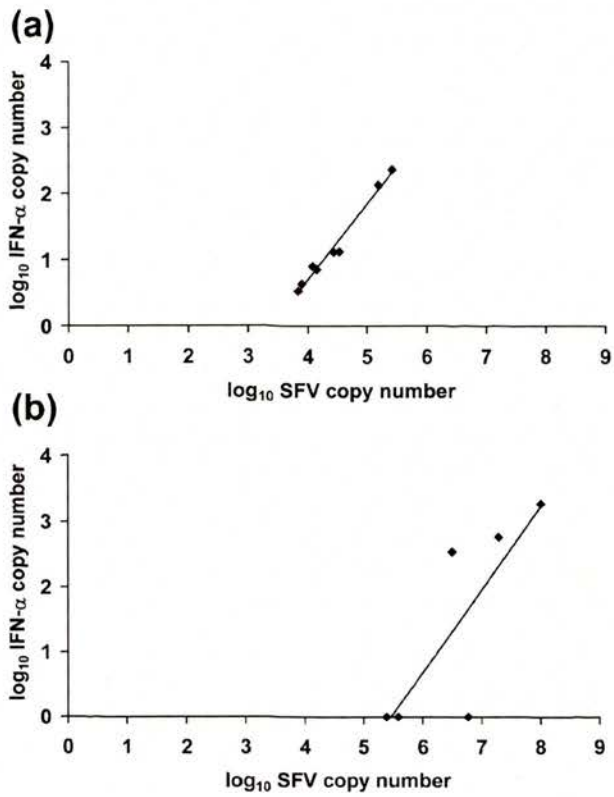

Fig. 1. Correlation between the levels of SFV RNA and IFN-α transcripts in adult (4–5-week-old BALB/c) mouse brains. (a) Intraperitoneal inoculation with SFV A7(74), sampled at 3 and 7 days p.i. r^2=0.98. (b) Intracerebral inoculation with SFV4, sampled between 12 and 40 h p.i. r^2=0.64. Points indicate the levels of transcripts determined by QPCR in individual mice; all values are normalized to those of β-actin and are given as copy number per 10^5 copies of β-actin.

Direct intracerebral inoculation of SFV4 results in widespread brain infection and activation of IFN gene expression

Following intracerebral inoculation, SFV4 replicates efficiently in the CNS and produces a widespread infection (Fazakerley *et al.*, 2002). To determine whether this infection activates IFN gene transcription, SFV4 was inoculated intracerebrally into six 4–5-week-old BALB/c mice. Two mice were each sampled at 12, 24 and 40 h p.i. Infectious brain virus titres were detectable in all mice at all time points. IFN-α gene transcripts were detectable in three

Table 1. Levels of infectious virus and IFN-α transcripts in the brains of BALB/c and BALB/c *nu/nu* mice at 3, 7 and 140 days p.i. following intraperitoneal inoculation with 5000 p.f.u. SFV A7(74)

Results are the mean values from at least four individual mouse brains. Virus titres were determined by standard plaque assay on BHK-21 cells and are given as $\log_{10}$ p.f.u. (g brain)$^{-1}$. IFN-α gene transcripts were measured by QPCR and are given as the mean fold increase (MFI) relative to uninfected brain tissue (which was given a value of 1 and was effectively zero, the limit of detection of the assay).

Days p.i.	BALB/c mice			CB-17 *nu/nu* mice		
	No. of mice positive for virus	Brain virus $\log_{10}$ p.f.u. g^{-1}	Brain IFN transcripts MFI (SEM)	No. of mice positive for virus	Brain virus $\log_{10}$ p.f.u. g^{-1}	Brain IFN transcripts MFI (SEM)
3	5/5	2.8	7 (6.5)	5/5	3.1	12 (4)
7	5/5	3.9	19 (6)	5/5	4.6	255 (140)
140	0/5	<1.4	0	5/5	4.2	13 (10)

out of six mice, with a mean titre of $10^{2.9}$ copies per 10^5 copies of β-actin (Fig. 1b). SFV4 thus had no deficit in its ability to replicate in the brain and this replication activated IFN-α gene expression.

IFN gene transcription in the brain continues during persistent infection

In mice with severe combined immunodeficiency (SCID) or athymic *nu/nu* mice, SFV A7(74) establishes a persistent infection of the brain; athymic *nu/nu* mice survive this infection longer than SCID mice (Amor & Webb, 1986; Fazakerley & Webb, 1987). To determine whether the brain IFN response remained activated during persistent infection, CB17 *nu/nu* mice were inoculated intraperitoneally with 5000 p.f.u. SFV A7(74), exsanguinated, perfused and the brains assayed at 3, 7 and 140 days p.i. Infectious virus and IFN transcripts were detectable in all mice at all three time points (Table 1).

Type I IFN is required for protection against SFV A7(74)

To determine whether the type I IFN system is required to protect adult mice against intraperitoneal infection with SFV, groups of ten 129/Sv(ev) mice lacking the α-chain of the IFN-α/β receptor (IFNAR-$1^{-/-}$) (Muller *et al.*, 1994) and IFN-competent 129/Sv(ev) mice were inoculated intraperitoneally with 5000 p.f.u. SFV A7(74) or SFV4 and monitored for clinical disease. All 129/Sv(ev) mice inoculated with SFV4 or A7(74) survived without clinical signs for the 10 days studied. SFV4 virus is transcribed from a molecular clone derived from the SFV prototype virus, a virus closely related to SFV L10. Both prototype and L10 are virulent, even at low doses, in adult mice (Bradish *et al.*, 1971). It was surprising, therefore, that inoculation of 5000 p.f.u. SFV4 intraperitoneally was avirulent in 129/Sv(ev) mice. For comparison, a group of ten 129/Sv(ev) mice were inoculated intraperitoneally with 5000 p.f.u. SFV L10 virus. These mice all died or reached clinically defined terminal end points on day 3. It was concluded that, relative to virulent L10 virus, SFV4 has an attenuated phenotype when given intraperitoneally. In contrast to the survival of 129/Sv(ev) mice, all IFNAR-$1^{-/-}$ mice inoculated with SFV A7(74) or SFV4 died or reached clinically defined terminal end points within 3 days. The fact that SFV4 and SFV A7(74) are rapidly virulent in IFNAR-$1^{-/-}$ mice but not in IFN-competent mice demonstrated that type I IFN strongly and successfully suppresses these strains of this virus.

Type I IFN in the brain controls viral infection of meningeal and ependymal cells but is not responsible for the restricted infection of neurons

Given that SFV A7(74) is efficiently neuroinvasive and neurotropic and that infection with this strain of virus is restricted in mature neurons of the adult mouse brain (Fazakerley *et al.*, 1993) and that brain infection is associated with an IFN response (Fig. 1a), it was postulated that mortality in the IFNAR-$1^{-/-}$ mice was due to widespread encephalitis. To determine the role of the type I IFN response during brain infection, IFNAR-$1^{-/-}$ and 129/Sv(ev) mice were inoculated intraperitoneally with 5000 p.f.u. SFV A7(74) and the distribution of virus-infected cells in the brain was visualized by *in situ* hybridization at 16 and 40 h p.i. (Fig. 2). The IFNAR-$1^{-/-}$ mice had moderate or substantial clinical signs, but no or only small foci of virus-infected cells in the brains (Fig. 2). This low level of infection was inconsistent with the clinical signs, indicating that the mice were unlikely to succumb to this infection due to events in the brain. To observe the tropism and spread of A7(74) virus in the brain and to determine whether the type I IFN response was required for the restriction of SFV A7(74) replication in neurons, mice were inoculated directly intracerebrally. In both 129/Sv(ev) and IFNAR-$1^{-/-}$ mice, virus-positive cells were observed predominantly in the major white matter tracts such as the corpus callosum and the internal capsule (Fig. 2); this confirmed the distribution observed previously with direct intracerebral inoculation of A7(74) virus in wt mice (Fazakerley *et al.*, 2006). In the IFNAR-$1^{-/-}$ but not the 129/Sv(ev) mice, many virus-positive cells were observed in the meninges and in ependymal cells lining the ventricles, demonstrating that IFN normally protects these cells (Fig. 3). However, the extent of neuronal infection was no different between the two mouse strains. In both mouse strains, infection of neurons was confined to a few cells around the white matter tracts or to small foci scattered around the brain. In the IFNAR-$1^{-/-}$ mice, infection did not spread from the cells in the extensively infected white matter tracts, meninges and ependyma to adjacent neuronal populations (Figs 2 and 3). It was concluded that the restricted replication of A7(74) virus in the neurons of the adult mouse brain does not require an intact type I IFN system.

Absence of a type I IFN response demonstrates the tissues and cell types permissive for SFV infection

Given that mortality in the IFNAR-$1^{-/-}$ mice was not related to widespread CNS infection, the course of extraneural infection was determined. Groups of 129/Sv(ev) and IFNAR-$1^{-/-}$ mice were inoculated intraperitoneally with 5000 p.f.u. SFV A7(74) or SFV4 with an eGFP marker gene inserted into the structural protein open reading frame (SFV4-steGFP). Three mice were sampled from each group of mice at days 1 and 2 p.i. Blood samples were taken for virus titration and samples of tissues from several different organ systems were studied by microscopy. Tissues from the SFV A7(74)-infected mice were processed for paraffin histology, cut into 5 μm sections and immunostained to visualize virus-infected cells (Fig. 3). Tissues from SFV4-steGFP-infected mice were fixed, cut into 12–14 μm sections on a cryomicrotome and studied

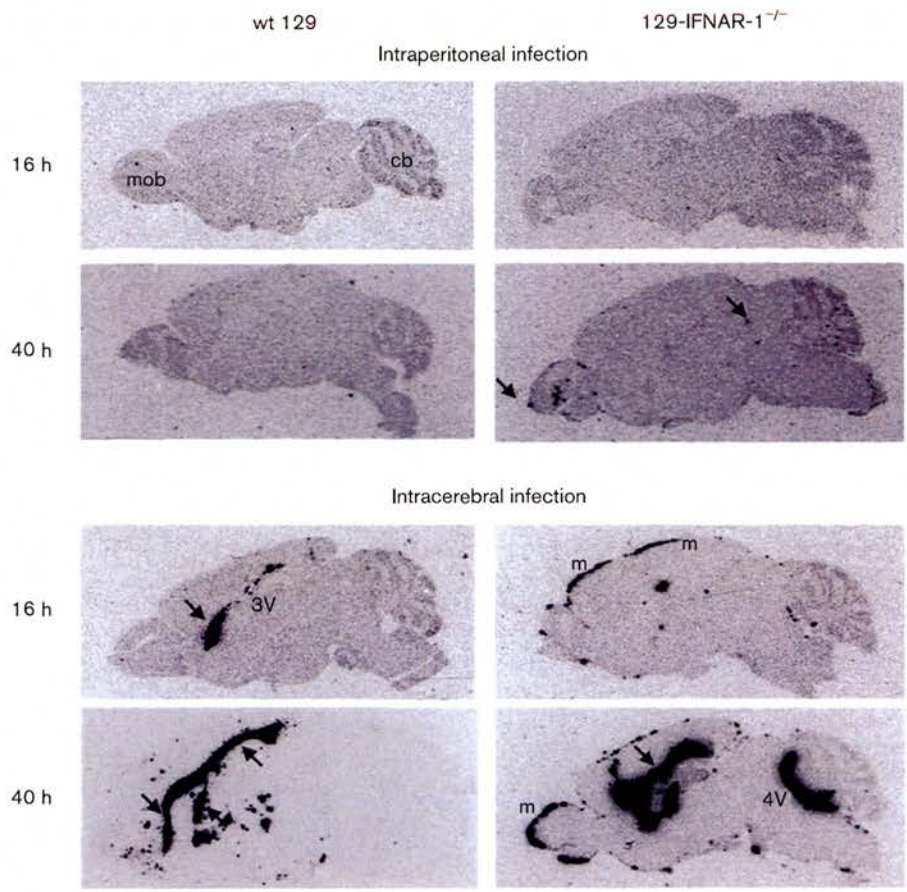

Fig. 2. Representative autoradiographic images illustrating the distribution of virus RNA-positive cells (black) in parasagittal sections of the brains of wt 129/Sv(ev) or IFNAR-1$^{-/-}$ mice 16 or 40 h after intraperitoneal or intracerebral inoculation of SFV A7(74). *In situ* hybridization using a negative-sense ^{35}S-labelled riboprobe complementary to the viral genomic RNA. For each of three mice sampled at each time point, three sections from each of three areas of the brain were studied; the images shown are representative of each group of mice. All brains are in the same orientation; the main olfactory bulb (mob) and the cerebellum (cb) demonstrate the rostro-caudal orientation. Following intraperitoneal inoculation, no virus-positive cells were observed at 16 h and only rare virus-positive cells were observed at 40 h (arrows); the mice sampled at 40 h had clear signs of infection including a hunched posture, piloerection, weight loss, inactivity and tremor. Following intracerebral inoculation in both 129/Sv(ev) and IFNAR-1$^{-/-}$ mice, virus-infected cells were present in the major white matter tracts of the corpus callosum and the internal capsule (arrows). In addition in IFNAR-1$^{-/-}$ mice, ependymal cells surrounding the third and fourth ventricles (3V and 4V, respectively) and meningeal cells (m) were also positive for virus (see also Fig. 3a–c).

on a Zeiss confocal microscope (Fig. 4). At 1 day p.i., the mean (n=3) blood virus titres were $10^{9.2}$ and $10^{8.5}$ $\log_{10}$ p.f.u. ml^{-1} in IFNAR-1$^{-/-}$ mice and $10^{7.8}$ and $10^{4.4}$ $\log_{10}$ p.f.u. ml^{-1} in 129/Sv(ev) mice for SFV A7(74) and SFV4, respectively. In SFV-infected 129/Sv(ev) mice, despite examination of many sections from many tissues including brain, lung, liver, kidney, heart, spleen, small intestine, pancreas, skeletal and smooth muscle, virus-infected cells were observed only rarely, most frequently in the exocrine pancreas. In stark contrast, infected cells were readily observed in all of these tissues in IFNAR-1$^{-/-}$ mice, demonstrating the power of the type I IFN system to curtail virus infection. No differences in tropism were observed between the two viruses in IFNAR-1$^{-/-}$ mice. Most tissues studied showed a selective cellular tropism (Figs 3 and 4 and Table 2). For example, cells of the exocrine but not the endocrine pancreas were heavily infected; many cells in the heart valves but only relatively few cells in the myocardium were infected; many cells of the marginal zone of the spleen, most probably macrophages were infected, as were lymphocytes in the white pulp; adipose tissue showed the most extensive infection; other infected cells included hepatocytes, smooth muscle cells, cells of the kidney glomeruli and cells in the lung. The difference in the extent of infection between mice with and without a type I IFN system dramatically illustrated the power of this system to limit the spread of this virus. In the absence of an intact IFN system, the true tropism and the potential

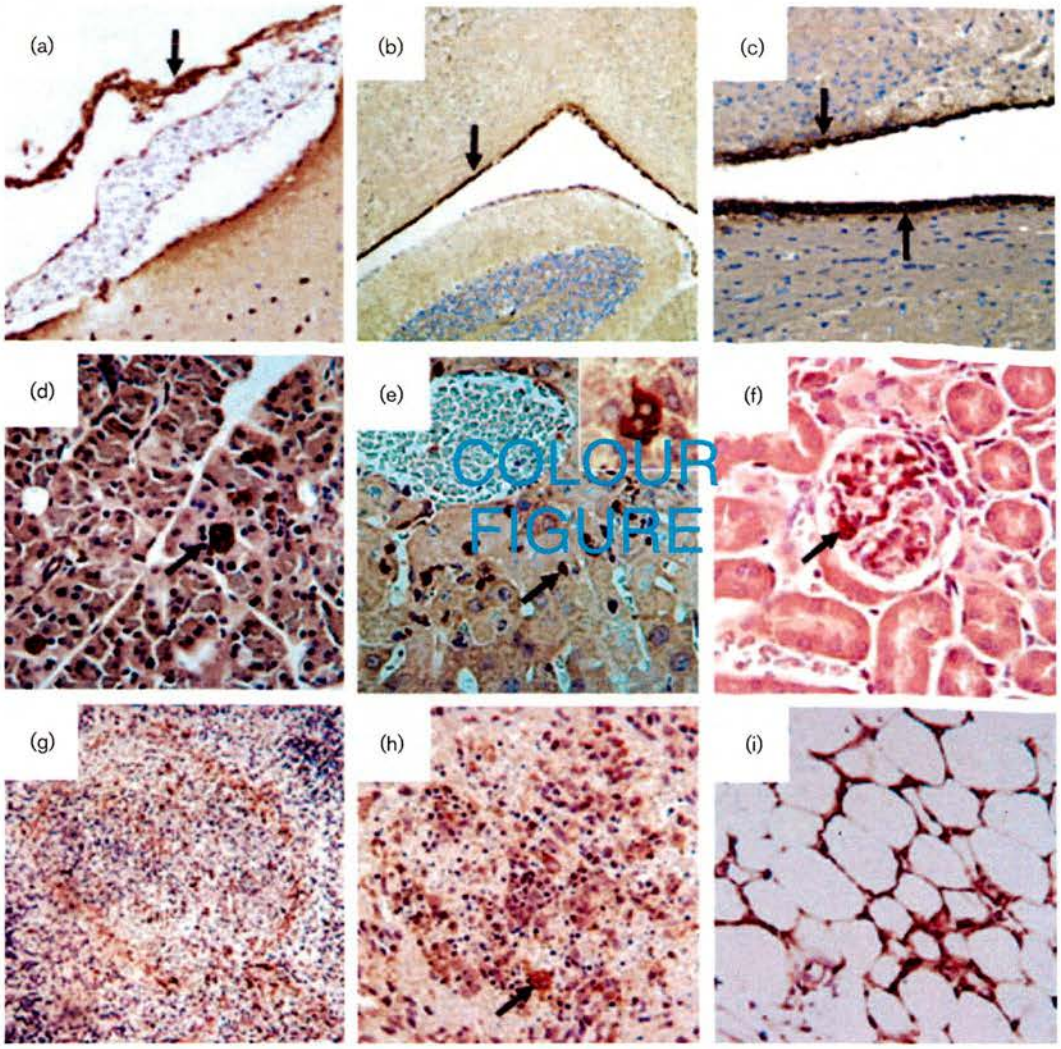

Fig. 3. Immunostaining (brown) for virus structural proteins in SFV A7(74)-infected IFNAR-1$^{-/-}$ mice. (a) Infection of the meninges (arrow). (b) Infection of the ependymal cells of the fourth ventricle is apparent as a continuous line of immunostained cells lining the ventricle. (c) High-power view of infected ependymal cells lining the lateral ventricle. Note that in (b) and (c) (see also Fig. 2) there has been very little spread of the infection to the cells of the underlying brain parenchyma. (d) Virus infection (arrow) of scattered acinar cells of the exocrine pancreas. (e) Virus-infected hepatocytes (arrow) in the liver. (f) Infected cells (example indicated by arrow) in a glomerulus in the kidney. (g) Low-power image of the spleen; the circular distribution of infected cells in the marginal zone between the white pulp (inner) and the red pulp (outer) is apparent. (h) High-power image of the spleen; it is evident that many cells in the white pulp are also infected (example indicated by arrow) and that many cells in this area have pycnotic nuclei indicative of cell death. (j) Widespread infection of cell bodies in adipocyte tissue (unstained white areas are the fat vacuoles).

of this virus for rapid and widespread infection were revealed.

DISCUSSION

Previous studies in the early days of IFN research showed that intraperitoneal inoculation of adult mice with SFV A7(74) induced IFN activity in the blood and that crude preparations of IFN protected mice against virulent strains of SFV (Bradish *et al.*, 1975; Bradish & Titmuss, 1981; Finter, 1966; Smillie *et al.*, 1973). The first description of IFNAR-1$^{-/-}$ mice noted that SFV was rapidly fatal in these mice but the strain of SFV used was not stated (Muller *et al.*, 1994). Here, we have shown that both the nominally avirulent SFV A7(74) and the increasingly used SFV4 are both virulent in IFNAR-1$^{-/-}$ mice and that, in mice with an intact type I IFN system, both viruses induce IFN gene expression in the brain with levels of IFN-α gene transcripts directly proportional to those of viral RNA: the more viral

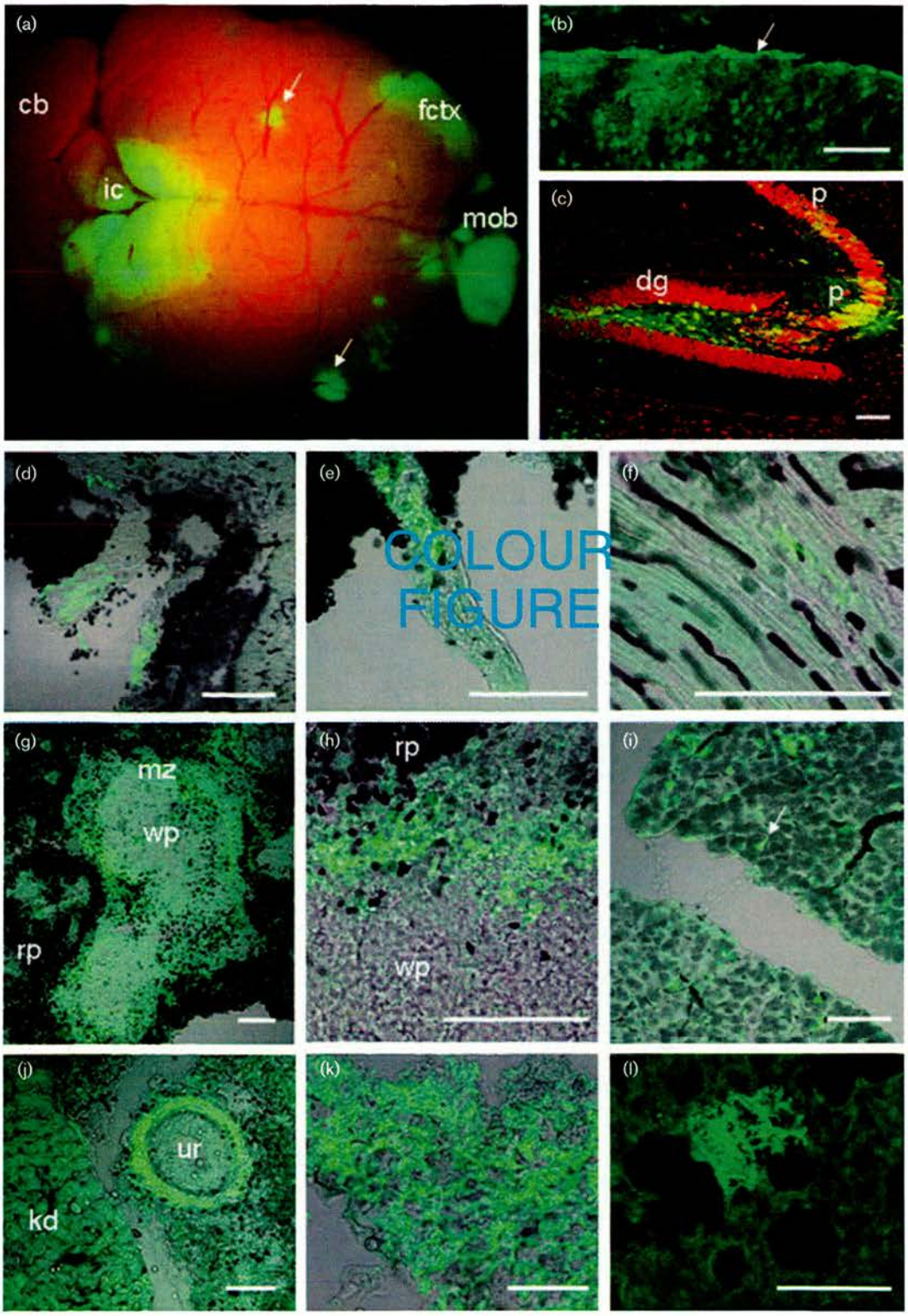

RNA, the more IFN transcripts. Other studies have shown that the type I IFN system is activated in the brain in response to inoculation of poly I:C and to infection with viruses including rabies virus, Theiler's virus, La Crosse virus, simian immunodeficiency virus and lymphocytic choriomeningitis virus (Barber *et al.*, 2004; Delhaye *et al.*, 2006; Johnson *et al.*, 2006; Prehaud *et al.*, 2005; Roberts *et al.*, 2004). In the present study, our novel QPCR approach demonstrated for the first time that the IFN gene expression response is proportional to the viral RNA load.

Fig. 4. Distribution of SFV4 in selected tissues of IFNAR-1$^{-/-}$ mice as visualized by expression (green) of an eGFP marker gene expressed as part of the virus structural polyprotein. For tissue sections (b)–(l), the images are representative of at least nine sections from at least three different areas of each tissue type from at least two mice. In many tissues, areas of infection were apparent, even upon gross examination, as shown for the brain in (a) where areas of infection are present in the inferior colliculi (ic), the frontal cortex (fctx) and the main olfactory bulb (mob); the cerebellum (cb) is marked to facilitate orientation. Some foci of infection appeared to be associated with blood vessels (examples indicated by arrows); however, this was difficult to determine without knowing the depth of tissue imaged). Sections from this brain demonstrated infection of meningeal cells (b; cf. Fig. 2) and several neuronal populations as shown, for example in (c) for pyramidal neurons in the hippocampus (p) and cells in the hilus of the dentate gyrus (dg); red propidium iodide staining of cell nuclei allowed visualization of the neuroanatomy. The sections shown in (d)–(k) were lightly stained with diaminobenzidine to allow visualization of the tissue structure; red blood cells appeared black. In the heart (d–f), strikingly there was consistent infection of cells in the heart valves (d, e) but only small foci of infected cells in the myocardium (f). In the spleen (g, h), infected cells were principally in the marginal zones (mz) between the red pulp (rp) and white pulp (wp), areas know to contain many macrophages and dendritic cells. In the pancreas (i), many isolated scattered acinar cells were infected (example indicated by arrow) in the exocrine pancreas; infection of cells of the endocrine pancreas was never observed. In the kidney (kd) (j), many cell types including cells in the glomeruli and tubule cells were infected; the smooth muscle cell layers surrounding the ureter (ur) were heavily infected. One of the most widely infected cell types was adipose tissue (k). Foci of infection were apparent in the lung (l). Bars, 100 μm.

In culture, CNS cells including neurons and glial cells have been observed to activate the type I IFN system (McKimmie & Fazakerley, 2005; Prehaud *et al.*, 2005). Intrathecal synthesis of IFNs and IFN-activated protein expression have also been demonstrated in patients with CNS virus infections (Dussaix *et al.*, 1985; Ogata *et al.*, 2004).

The type I IFN system has been shown to protect mice against the spread of other viruses in the CNS including Theiler's virus, Bunyamwera virus, Dugbe virus, Hantaan virus, influenza A virus, vesicular stomatitis virus, lymphocytic choriomeningitis virus, Sindbis virus and Venezuelan equine encephalitis virus (Boyd *et al.*, 2006; Bridgen *et al.*, 2001; Fiette *et al.*, 1995; Garcia-Sastre *et al.*, 1998; Grieder & Vogel, 1999; Koerner *et al.*, 2007; Muller *et al.*, 1994; Ryman *et al.*, 2000; Wichmann *et al.*, 2002). Few studies have detailed the CNS cell types protected by this IFN response. As documented previously, SFV A7(74) is efficiently neuroinvasive, but in the adult mouse brain it is restricted in its ability to replicate in and spread between mature neurons (Fazakerley *et al.*, 1993, 2006; Oliver & Fazakerley, 1998; Pusztai *et al.*, 1971). Mouse neurons, both in culture and in the adult mouse brain, can respond to IFNs (Ousman *et al.*, 2005; Wang & Campbell, 2005; Wang *et al.*, 2002; Ward & Massa, 1995). This response could underlie the restricted replication of SFV A7(74) in neurons. Here, however, we showed that this restricted replication is not mediated by type I IFN responses; A7(74) replication in mature neurons remained restricted, even in the absence of type I IFN responses. Type I IFN responses did however control replication of SFV A7(74) in meningeal and ependymal cells, as these cells were infected only rarely in wt mice. Type I IFN responses have also been shown to protect ependymal cells from measles virus, meningeal cells from Sindbis virus and oligodendrocyte, ependymal and choroid plexus cells from Theiler's virus infections (Fiette *et al.*, 1995; Mrkic *et al.*, 1998; Ryman *et al.*, 2000). Given that, in the absence of type I IFN responses, SFV A7(74) does not establish a widespread infection of the brain parenchyma, other factors must be operating to restrict replication of this virus in mature neurons. We have previously suggested that the restricted

Table 2. Cell types infected by SFV A7(74) and SFV4 in IFNAR-1$^{-/-}$ mice

SFV A7(74)-infected cells were determined by immunostaining and SFV4-steGFP-infected cells were detected by fluorescence. Cell types were determined by morphology and location within tissues. The same cell types were found to be infected by SFV A7(74) and SFV4.

Organ	Cell types infected
Brain	Neurons, oligodendrocytes, ependymal cells, meningeal cells but not astrocytes
Heart	Cells in the valves and occasional cells in the myocardium
Lung	Alveolar lining cells
Liver	Hepatocytes and occasional kupffer cells
Pancreas	Acinar cells in the exocrine pancreas but not cells in the endocrine pancreas
Kidney	Cells in the glomeruli and tubule cells
Adipose	Widespread infection
Muscle	Occasional skeletal muscle fibres and particularly smooth muscle
Spleen	Cells in the marginal zone (macrophages?)

replication of A7(74) in the mature neurons of the adult mouse brain is linked to neuronal differentiation and, in particular, to the availability of freshly synthesized intracellular membranes and their constituent lipids (Oliver & Fazakerley, 1998; Oliver *et al.*, 1997; Scallan & Fazakerley, 1999).

We have shown that, although type I IFN does not contribute to the restricted phenotype of SFV A7(74) in adult brain neurons, it is essential to prevent virus spread in extraneural tissues. Several other viruses, including avirulent strains of the related alphavirus Sindbis virus, which, like SFV A7(74), produces subclinical or even unapparent infection, also establish widespread infections in IFNAR-1$^{-/-}$ mice (Bray, 2001; Mrkic *et al.*, 1998; Muller *et al.*, 1994; Ryman *et al.*, 2000). In the case of SFV4 and SFV A7(74), infection was observed in multiple tissues with a similar extent of infection and tropism for both viruses. Whether SFV tropism is determined by entry or post-entry events is unclear. The receptor for this virus and its cellular distribution remain unknown. In the absence of an IFN response, the cell types with the greatest degree of infection were the acinar cells of the exocrine pancreas and adipocytes. To enable their secretion of large amounts of digestive enzymes, pancreatic acinar cells contain large amounts of rough endoplasmic reticulum and have a highly vesiculated cytoplasm. Similarly, adipocytes contain many vacuoles and have a highly developed lipid metabolism. Extensive replication of SFV A7(74) in these cell types would be consistent with a requirement for lipids and freshly synthesized membranes, as suggested for neurons. In the absence of the IFN response, infection of heart valves was consistently observed and was more extensive than infection of other parts of the heart. This could have resulted from a greater exposure of the valves to the high titres of virus in the blood or alternatively from an increased susceptibility of this tissue to infection. In mice, enteroviruses have been shown to preferentially infect valve tissues and some patients with chronic rheumatic heart disease have evidence of enterovirus replication in valve tissue (Burch *et al.*, 1966; Li *et al.*, 2002). In the spleens of IFNAR-1$^{-/-}$ mice, SFV was predominantly observed in cells of the marginal zone, most likely macrophages or dendritic cells. A similar distribution was observed in IFNAR-1$^{-/-}$ mice infected with Sindbis virus where these cells were shown to be cells of the macrophage/dendritic cell lineage (Ryman *et al.*, 2000).

Many RNA viruses antagonize IFN responses (Haller *et al.*, 2006). Viruses, even strains of the same virus, also differ in their susceptibility to the actions of IFN. The virulent L10 strain of SFV is less sensitive to IFN than the avirulent V42 strain (Deuber & Pavlovic, 2007). That SFV A7(74) and SFV4 infections are much more widespread in IFNAR-1$^{-/-}$ mice demonstrates the power of the type I IFN system to control these strains; however it does not preclude the possibility that SFV and other alphaviruses also antagonize IFN responses (Breakwell *et al.*, 2007; Fazakerley *et al.*, 2002; Frolov, 2004; Garmashova *et al.*, 2007). Antagonism of the IFN response is unlikely to be absolute; the timing and the magnitude of IFN induction, action and suppression relative to the rate of virus replication are likely to determine the extent of virus spread. What is clear is that, in the mouse, the IFN response to SFV A7(74) and SFV4 is sufficient to severely curtail the spread of these viruses in many tissue systems.

ACKNOWLEDGEMENTS

This study was supported by funding from the European Union SFVECTORS project (www.sfvectors.ed.ac.uk) and the Medical Research Council (G0000288).

REFERENCES

Aguilar, P. V., Paessler, S., Carrara, A. S., Baron, S., Poast, J., Wang, E., Moncayo, A. C., Anishchenko, M., Watts, D. & other authors (2005). Variation in interferon sensitivity and induction among strains of eastern equine encephalitis virus. *J Virol* **79**, 11300–11310.

Allsopp, T. E. & Fazakerley, J. K. (2000). Altruistic cell suicide and the specialized case of the virus-infected nervous system. *Trends Neurosci* **23**, 284–290.

Amor, S. & Webb, H. E. (1986). Use of *N*-acetylethyleneimine (AEI) for the inactivation of Semliki Forest virus in vitro. *J Med Virol* **19**, 367–376.

Barber, S. A., Herbst, D. S., Bullock, B. T., Gama, L. & Clements, J. E. (2004). Innate immune responses and control of acute simian immunodeficiency virus replication in the central nervous system. *J Neurovirol* **10** (*Suppl. 1*), 15–20.

Boyd, A., Fazakerley, J. K. & Bridgen, A. (2006). Pathogenesis of Dugbe virus infection in wild-type and interferon-deficient mice. *J Gen Virol* **87**, 2005–2009.

Bradish, C. J. & Titmuss, D. (1981). The effects of interferon and double-stranded RNA upon the virus–host interaction: studies with togavirus strains in mice. *J Gen Virol* **53**, 21–30.

Bradish, C. J., Allner, K. & Maber, H. B. (1971). The virulence of original and derived strains of Semliki Forest virus for mice, guinea-pigs and rabbits. *J Gen Virol* **12**, 141–160.

Bradish, C. J., Allner, K. & Fitzgeorge, R. (1975). Immunomodification and the expression of virulence in mice by defined strains of Semliki Forest virus: the effects of cyclophosphamide. *J Gen Virol* **28**, 225–237.

Bray, M. (2001). The role of the type I interferon response in the resistance of mice to filovirus infection. *J Gen Virol* **82**, 1365–1373.

Breakwell, L., Dosenovic, P., Karlsson Hedestam, G. B., D'Amato, M., Liljeström, P., Fazakerley, J. & McInerney, G. M. (2007). Semliki Forest virus non-structural protein 2 is involved in the suppression of the type I interferon response. *J Virol* **81**, 8677–8684.Medline

Bridgen, A., Weber, F., Fazakerley, J. K. & Elliott, R. M. (2001). Bunyamwera bunyavirus nonstructural protein NSs is a nonessential gene product that contributes to viral pathogenesis. *Proc Natl Acad Sci U S A* **98**, 664–669.

Brown, A. R., Webb, J., Rebus, S., Walker, R., Williams, A. & Fazakerley, J. K. (2003). Inducible cytokine gene expression in the brain in the ME7/CV mouse model of scrapie is highly restricted, is at a strikingly low level relative to the degree of gliosis and occurs only late in disease. *J Gen Virol* **84**, 2605–2611.

Burch, G. E., DePasquale, N. P., Sun, S. C., Mogabgab, W. J. & Hale, A. R. (1966). Endocarditis in mice infected with Coxsackie virus B_4. *Science* **151**, 447–448.

Delhaye, S., Paul, S., Blakqori, G., Minet, M., Weber, F., Staeheli, P. & Michiels, T. (2006). Neurons produce type I interferon during viral encephalitis. *Proc Natl Acad Sci U S A* **103**, 7835–7840.

Deuber, S. A. & Pavlovic, J. (2007). Virulence of a mouse-adapted Semliki Forest virus strain is associated with reduced susceptibility to interferon. *J Gen Virol* **88**, 1952–1959.

Dussaix, E., Lebon, P., Ponsot, G., Huault, G. & Tardieu, M. (1985). Intrathecal synthesis of different α-interferons in patients with various neurological diseases. *Acta Neurol Scand* **71**, 504–509.

Fauconnier, B. (1971). Effect of an anti-interferon serum on experimental viral pathogenicity in vivo. *Pathol Biol (Paris)* **19**, 575–578 (in French)

Fazakerley, J. K. (2004). Semliki Forest virus infection of laboratory mice: a model to study the pathogenesis of viral encephalitis. *Arch Virol Suppl* **18**, 179–190.

Fazakerley, J. K. & Webb, H. E. (1987). Semliki Forest virus-induced, immune-mediated demyelination: adoptive transfer studies and viral persistence in nude mice. *J Gen Virol* **68**, 377–385.

Fazakerley, J. K., Pathak, S., Scallan, M., Amor, S. & Dyson, H. (1993). Replication of the A7(74) strain of Semliki Forest virus is restricted in neurons. *Virology* **195**, 627–637.

Fazakerley, J. K., Boyd, A., Mikkola, M. L. & Kaariainen, L. (2002). A single amino acid change in the nuclear localization sequence of the nsP2 protein affects the neurovirulence of Semliki Forest virus. *J Virol* **76**, 392–396.

Fazakerley, J. K., Cotterill, C. L., Lee, G. & Graham, A. (2006). Virus tropism, distribution, persistence and pathology in the corpus callosum of the Semliki Forest virus-infected mouse brain: a novel system to study virus–oligodendrocyte interactions. *Neuropathol Appl Neurobiol* **32**, 397–409.

Fiette, L., Aubert, C., Muller, U., Huang, S., Aguet, M., Brahic, M. & Bureau, J. F. (1995). Theiler's virus infection of 129sv mice that lack the interferon alpha/beta or interferon gamma receptors. *J Exp Med* **181**, 2069–2076.

Finter, N. B. (1966). Interferon as an antiviral agent in vivo: quantitative and temporal aspects of the protection of mice against Semliki Forest virus. *Br J Exp Pathol* **47**, 361–371.

Frolov, I. (2004). Persistent infection and suppression of host response by alphaviruses. *Arch Virol Suppl* **18**, 139–147.

Garcia-Sastre, A., Durbin, R. K., Zheng, H., Palese, P., Gertner, R., Levy, D. E. & Durbin, J. E. (1998). The role of interferon in influenza virus tissue tropism. *J Virol* **72**, 8550–8558.

Garmashova, N., Gorchakov, R., Volkova, E., Paessler, S., Frolova, E. & Frolov, I. (2007). The Old World and New World alphaviruses use different virus-specific proteins for induction of transcriptional shutoff. *J Virol* **81**, 2472–2484.

Glasgow, G. M., Sheahan, B. J., Atkins, G. J., Wahlberg, J. M., Salminen, A. & Liljeström, P. (1991). Two mutations in the envelope glycoprotein E2 of Semliki Forest virus affecting the maturation and entry patterns of the virus alter pathogenicity for mice. *Virology* **185**, 741–748.

Glasgow, G. M., Mcgee, M. M., Sheahan, B. J. & Atkins, G. J. (1997). Death mechanisms in cultured cells infected by Semliki Forest virus. *J Gen Virol* **78**, 1559–1563.

Grieder, F. B. & Vogel, S. N. (1999). Role of interferon and interferon regulatory factors in early protection against Venezuelan equine encephalitis virus infection. *Virology* **257**, 106–118.

Haller, O., Kochs, G. & Weber, F. (2006). The interferon response circuit: induction and suppression by pathogenic viruses. *Virology* **344**, 119–130.

Hwang, S. Y., Hertzog, P. J., Holland, K. A., Sumarsono, S. H., Tymms, M. J., Hamilton, J. A., Whitty, G., Bertoncello, I. & Kola, I. (1995). A null mutation in the gene encoding a type I interferon receptor component eliminates antiproliferative and antiviral responses to interferons α and β and alters macrophage responses. *Proc Natl Acad Sci U S A* **92**, 11284–11288.

Johnson, N., McKimmie, C. S., Mansfield, K. L., Wakeley, P. R., Brookes, S. M., Fazakerley, J. K. & Fooks, A. R. (2006). Lyssavirus infection activates interferon gene expression in the brain. *J Gen Virol* **87**, 2663–2667.

Karlsson, G. B. & Liljeström, P. (2004). Delivery and expression of heterologous genes in mammalian cells using self-replicating alphavirus vectors. *Methods Mol Biol* **246**, 543–557.

Koerner, I., Kochs, G., Kalinke, U., Weiss, S. & Staeheli, P. (2007). Protective role of beta interferon in host defense against influenza A virus. *J Virol* **81**, 2025–2030.

Li, Y., Pan, Z., Ji, Y., Peng, T., Archard, L. C. & Zhang, H. (2002). Enterovirus replication in valvular tissue from patients with chronic rheumatic heart disease. *Eur Heart J* **23**, 567–573.

Liljeström, P. & Garoff, H. (1991). A new generation of animal cell expression vectors based on the Semliki Forest virus replicon. *Biotechnology (N Y)* **9**, 1356–1361.

Mathiot, C. C., Grimaud, G., Garry, P., Bouquety, J. C., Mada, A., Daguisy, A. M. & Georges, A. J. (1990). An outbreak of human Semliki Forest virus infections in Central African Republic. *Am J Trop Med Hyg* **42**, 386–393.

McIntosh, B. M., Brookworth, C. & Kokernot, R. H. (1961). Isolation of Semliki Forest virus from *Aedes* (*Aedimorphus*) *argenteopunctatus* (Theobald) collected in Portuguese East Africa. *Trans R Soc Trop Med Hyg* **55**, 192.

McKimmie, C. S. & Fazakerley, J. K. (2005). In response to pathogens, glial cells dynamically and differentially regulate Toll-like receptor gene expression. *J Neuroimmunol* **169**, 116–125.

Mrkic, B., Pavlovic, J., Rulicke, T., Volpe, P., Buchholz, C. J., Hourcade, D., Atkinson, J. P., Aguzzi, A. & Cattaneo, R. (1998). Measles virus spread and pathogenesis in genetically modified mice. *J Virol* **72**, 7420–7427.

Muller, U., Steinhoff, U., Reis, L., Hemmi, S., Pavlovic, J., Zinkernagel, R. M. & Aguet, M. (1994). Functional role of type I and type II interferons in antiviral defense. *Science* **264**, 1918–1921.

Ogata, S., Ogata, A., Schneider-Schaulies, S. & Schneider-Schaulies, J. (2004). Expression of the interferon-α/β-inducible MxA protein in brain lesions of subacute sclerosing panencephalitis. *J Neurol Sci* **223**, 113–119.

Oliver, K. R. & Fazakerley, J. K. (1998). Transneuronal spread of Semliki Forest virus in the developing mouse olfactory system is determined by neuronal maturity. *Neuroscience* **82**, 867–877.

Oliver, K. R., Scallan, M. F., Dyson, H. & Fazakerley, J. K. (1997). Susceptibility to a neurotropic virus and its changing distribution in the developing brain is a function of CNS maturity. *J Neurovirol* **3**, 38–48.

Ousman, S. S., Wang, J. & Campbell, I. L. (2005). Differential regulation of interferon regulatory factor (IRF)-7 and IRF-9 gene expression in the central nervous system during viral infection. *J Virol* **79**, 7514–7527.

Parsons, L. M. & Webb, H. E. (1982). Blood brain barrier disturbance and immunoglobulin G levels in the cerebrospinal fluid of the mouse following peripheral infection with the demyelinating strain of Semliki Forest virus. *J Neurol Sci* **57**, 307–318.

Prehaud, C., Megret, F., Lafage, M. & Lafon, M. (2005). Virus infection switches TLR-3-positive human neurons to become strong producers of beta interferon. *J Virol* **79**, 12893–12904.

Pusztai, R., Gould, E. & Smith, H. (1971). Infection pattern in mice of an avirulent and virulent strain of Semliki Forest virus. *Br J Exp Pathol* **52**, 669–677.

Roberts, E. S., Burudi, E. M., Flynn, C., Madden, L. J., Roinick, K. L., Watry, D. D., Zandonatti, M. A., Taffe, M. A. & Fox, H. S. (2004). Acute SIV infection of the brain leads to upregulation of IL6 and interferon-regulated genes: expression patterns throughout disease progression and impact on neuroAIDS. *J Neuroimmunol* **157**, 81–92.

Ryman, K. D., Klimstra, W. B., Nguyen, K. B., Biron, C. A. & Johnston, R. E. (2000). Alpha/beta interferon protects adult mice from fatal Sindbis virus infection and is an important determinant of cell and tissue tropism. *J Virol* **74**, 3366–3378.

Scallan, M. F. & Fazakerley, J. K. (1999). Aurothiolates enhance the replication of Semliki Forest virus in the CNS and the exocrine pancreas. *J Neurovirol* **5**, 392–400.

Scallan, M. F., Allsopp, T. E. & Fazakerley, J. K. (1997). *bcl-2* acts early to restrict Semliki Forest virus replication and delays virus-induced programmed cell death. *J Virol* **71**, 1583–1590.

Schuffenecker, I., Iteman, I., Michault, A., Murri, S., Frangeul, L., Vaney, M. C., Lavenir, R., Pardigon, N., Reynes, J. M. & other authors (2006). Genome microevolution of chikungunya viruses causing the Indian Ocean outbreak. *PLoS Med* **3**, e263.

Seamer, J., Randles, W. J. & Fitzgeorge, R. (1967). The course of Semliki Forest virus infection in mice. *Br J Exp Pathol* **48**, 395–402.

Smerdou, C. & Liljeström, P. (1999). Two-helper RNA system for production of recombinant Semliki Forest virus particles. *J Virol* **73**, 1092–1098.

Smillie, J., Pusztai, R. & Smith, H. (1973). Studies on the influence of host defence mechanisms on infection of mice with an avirulent or virulent strain of Semliki Forest virus. *Br J Exp Pathol* **54**, 260–266.

Smithburn, K. C. & Haddow, W. J. (1944). Semliki Forest virus. I. Isolation and pathogenic properties. *J Immunol* **49**, 141–145.

Thomas, J. M., Klimstra, W. B., Ryman, K. D. & Heidner, H. W. (2003). Sindbis virus vectors designed to express a foreign protein as a cleavable component of the viral structural polyprotein. *J Virol* **77**, 5598–5606.

Tuittila, M. T., Santagati, M. G., Roytta, M., Maatta, J. A. & Hinkkanen, A. E. (2000). Replicase complex genes of Semliki Forest virus confer lethal neurovirulence. *J Virol* **74**, 4579–4589.

Vaha-Koskela, M. J., Tuittila, M. T., Nygardas, P. T., Nyman, J. K., Ehrengruber, M. U., Renggli, M. & Hinkkanen, A. E. (2003). A novel neurotropic expression vector based on the avirulent A7(74) strain of Semliki Forest virus. *J Neurovirol* **9**, 1–15.

Wang, J. & Campbell, I. L. (2005). Innate STAT1-dependent genomic response of neurons to the antiviral cytokine alpha interferon. *J Virol* **79**, 8295–8302.

Wang, J., Schreiber, R. D. & Campbell, I. L. (2002). STAT1 deficiency unexpectedly and markedly exacerbates the pathophysiological actions of IFN-α in the central nervous system. *Proc Natl Acad Sci U S A* **99**, 16209–16214.

Ward, L. A. & Massa, P. T. (1995). Neuron-specific regulation of major histocompatibility complex class I, interferon-β, and anti-viral state genes. *J Neuroimmunol* **58**, 145–155.

Wichmann, D., Grone, H. J., Frese, M., Pavlovic, J., Anheier, B., Haller, O., Klenk, H. D. & Feldmann, H. (2002). Hantaan virus infection causes an acute neurological disease that is fatal in adult laboratory mice. *J Virol* **76**, 8890–8899.